HAWKE'S BAY
REGIONAL COUNCIL
TE KAUNIHERA Ā-ROHE O TE MATAU-A-MĀUI

Meeting of the Environment and Integrated Catchments Committee

Date: Wednesday 9 April 2025

Time: 11.00am

Venue: Council Chamber
Hawke's Bay Regional Council
159 Dalton Street
NAPIER

Attachments Excluded From Agenda
available online only

Item	Title		Page
5.	**Te Muriwai o te Whanga plan**		
	Attachment 1:	Te muriwai o te whanga plan	2
	Attachment 2:	HBRC's Te muriwai o te whanga action plan	71
6.	**The source, transport, and fate of sediment into Hawke Bay and the impact of Cyclone Gabrielle**		
	Attachment 1:	Conroy Ted Thesis - The Sediment, River Plume, and Inner Shelf Variability in a Bay with Multiple Fluvial Inputs	77
7.	**Effectiveness of Trees for Landslide mitigation**		
	Attachment 1:	Report of findings - Assessing the effectiveness of trees for landslide mitigation in Hawke's Bay 2024	195
8.	**Ahuriri Regional Park**		
	Attachment 3:	Appendix 2 ARP - Draft Masterplan - March 2025	226
10.	**Connectivity of landslides to waterways**		
	Attachment 1:	Regional Shallow Landslide	250
	Attachment 2:	Uawa Catchment Working Group Hui 6 Transition Advisory Group	273

Te Muriwai o Te Whanga
The Plan

2024 | Te Komiti Muriwai o Te Whanga

Te Komiti Muriwai o Te Whanga

Mana Ahuriri Trust 2024 I 2

"It is the vision of hapū that when they look over Te Pamū (the farm) and the wider Ahuriri Estuary that their eyes meet the sight of blooming kōwhai lining the main channel, and the streams, and waterways that flow into it.

This will be a sign that the mauri of Te Whanganui-a-Orotu is restored."

Te Komiti Muriwai o Te Whanga

Mihi

Acknowledgements

Tēnā koutou e ngā kaitiaki o Te Whanganui-a-Orotu.

Ko koutou e pupuri tonu nei ki te mauri ora o ngā uri e noho kāinga ana ki Ahuriri nei. Tēnei te tuku mihi ki a koutou.

Te Komiti Muriwai o Te Whanga has committed to upholding the mana of Te Whanganui-a-Orotu through the development of this plan. What is evident is the depth of this commitment across our many partners and stakeholders in the Hawke's Bay region in ensuring Te Whanganui-a-Orotu is treated, managed and cared for beyond the present day needs towards a thriving natural environment for many generations to come.

This kaupapa has been shared with whānau and partners from the Te-Matau-a-Māui region and we wish to acknowledge their time and energy towards this mahi. We would like to acknowledge in particular, the following organisations that participated in wānanga and hui towards the development of this plan.

Te Komiti Muriwai o Te Whanga Members

- Mana Ahuriri Trust (MAT)
- Department of Conservation (DOC)
- Napier City Council (NCC)
- Hawke's Bay Regional Council (HBRC)
- Hastings District Council (HDC)

Wider Interested Entities

- Ahuriri Estuary Protection Society (AEPS)
- Ahuriri Regional Park
- Ahuriri Tributaries Catchment Group (ATCG)
- Ahuriri Catchment Group
- Forest and Bird
- Hōhepa
- Pāmu
- Tai Whenua o Te Whanganui ā Orotu
- Maungahararu-Tangitu Trust
- Ngati Pārau Hapū Trust
- Ngāti Hinepare
- Ngāti Maahu
- Ngāti Matepū
- Ngāti Pārau
- Ngāi Tawhao
- Ngāti Tū
- Ngāi Te Ruruku

"This plan reflects our collective commitment to being kaitiaki and safeguarding the environmental, cultural and historical values of this wāhi taonga"

Te Kaha Hawaikirangi
Chair
Te Komiti Muriwai o Te Whanga

He Kōrero Matua

Foreword

Tēnā tātou katoa

On behalf of Te Komiti Muriwai (Te Komiti) and Mana Ahuriri Trust, Te Komiti presents the Te Muriwai o Te Whanga Plan, a legislative masterplan born from the Ahuriri Hapū Claims Settlement Act 2021.

Te Whanganui-a-Orotu is a wāhi taonga in Mana Ahuriri's Takiwā which represents the important history of our tūpuna/ancestors. Te Whanganui-a-Orotu the "great harbour of Orotu" is a site of profound cultural and historical importance. Named after Te Orotu, a descendant of Māhu Tapoanui, it once thrived with abundant resources. However mid-19th-century land sales and the 1931 earthquake led to its degradation.

The Waitangi Tribunal Claim in 1988 initiated our journey to restore the estuary's mana. In 2016 Mana Ahuriri Trust was established culminating in the 2021 settlement. This settlement recognised the estuary's significance and established Te Komiti Muriwai o Te Whanga for its management and protection.

As we embark on this journey to provide for our mokopuna/future generations we acknowledge the invaluable contributions of local authorities and community stakeholders and the 7 Ahuriri Hapū included in the redress; Ngāti Hinepare Ngāti Māhu Ngāti Matepū Ngāti Pārau (which includes Ngāi Tahu Ahi) Ngāi Tāwhao Ngāti Tū and Ngāi Te Ruruku. Part B of the cultural redress acknowledged that the Crown recognised the role of the Hapū as the Kaitiaki of Te Muriwai o Te Whanga.

Our aspiration for this plan is to encourage a thriving healthy estuary that supports diverse ecosystems, whakapapa/lineage and community well-being. Mana Ahuriri prioritises te taiao and the wellbeing of our wai/waters and biodiversity, as we know that it will have significant and long-lasting benefits for our mokopuna. We want to see Te Whanga live up to the whakatauki:

Ko rua te paia ko Te Whanga. He kainga tō te ata. He kainga ka awatea. He kainga ka ahiahi. The Whanga is the storehouse that never closes. A meal in the morning. A meal at noon. A meal in the evening.

While we acknowledge that in the past this meant the abundance of kai, for our whānau today it represents sustenance for our people in terms of kai, environmental, economic, social, spiritual, historical and cultural wellbeing.

We urge all stakeholders and partners - government bodies, private sector entities, communities and individuals—to join us in implementing this master plan. The collective responsibility and commitment of all parties are crucial to achieving our shared objectives. We are confident that together we can overcome the challenges we face and enhance the well-being and sustainability of Te Whanganui-a-Orotu.

In conclusion, the Te Muriwai o Te Whanga Plan is a transformative blueprint for the future. Its successful implementation will shape a positive legacy fostering environmental health, cultural integrity and community resilience. We extend our heartfelt thanks to everyone involved in the planning process and look forward to the collaborative efforts ahead.

He Whakarāpopototanga
Summary

Te Horopaki (Context)

- Ahuriri Hapū, Ngāti Pāhauwera, and Maungaharuru–Tangitū, as Treaty settlement entities, share **profound whakapapa connections to Te Whanganui-a-Orotu, the Ahuriri Estuary.** For Ahuriri Hapū, this estuary is culturally and spiritually significant, representing a crucial aspect of their identity.
- As Pākeha began to colonise Te Matau-a-Māui, much of the land surrounding Te Whanga was unfairly sold, or stolen. **In 1860, the Crown developed the estuary for a harbour, disturbing wildlife and exploiting resources**, diminishing the overall health of the estuary.
- The processes of drainage and reclamation after the 1931 Earthquake, combined with the diversion of the Tūtaekurī River outlet to the sea, reduced Te Whanganui-a-Orotu to a narrow tidal channel.
- In March of 2022 Ahuriri Hapū settled their Treaty of Waitangi Claim. The settlement legislation established a permanent estuary co-governance committee, Te Komiti Muriwai o Te Whanga (Te Komiti), to **safeguard and enrich Te Muriwai o Te Whanga (Ahuriri Estuary and its catchment areas) for present and future generations.**
- Te Komiti is chaired by Mana Ahuriri Trust and comprises representatives from the DOC, HBRC, NCC, and HDC. Te Komiti oversees and coordinates management efforts for the estuary, providing guidance to local authorities and Crown agencies. Additionally, it has developed and will endorse a comprehensive management plan (this document) known as **Te Muriwai o Te Whanga Plan.**

Rautaki (Strategy)

- The vision for Te Muriwai o Te Whanga is *'The health of Te Whanganui-a-Orotu supports environmental, economic, social, spiritual, historical, and cultural value for present and future generations.'* This Rautaki is guided by the whakataukī:

  Ko rua te paia k o Te Whanga.
  He kainga tō te ata. He kainga ka awatea. He kainga ka ahiahi.

  The Whanga is the storehouse that never closes.
  A meal in the morning. A meal at noon. A meal in the evening.

- Te Komiti has core values for itself and all who give regard to the plan. These values are:
  - *Whanaungatanga (Relationships)*
  - *Kaitiakitanga (Guardianship)*
  - *Pono (Integrity)*
  - *Whakapakari (Enhancement)*
  - *Kotahitanga (Unity)*
- Te Komiti has agreed that six pou will be the pillars of this Rautaki and it's subsequent action plan. The base pou that are foundational to all other Te Whanga outcomes, objectives, and initiatives are the pou associated with the taiao: Te Ora o te Wai (Water Health) and Te Mauri o te Taiao (Biodiversity).
- Through achieving the outcomes of these Pou, objectives for Aroā o Te Whanga (Historical / Educational) and Ahurea o te Whenua (Cultural / Spiritual) pou can be achieved. Following these is the achievement of Te Mahi Ohaoha (Economic) and Te Mahi Tūhono a Roopu (Social) pou.
- This Rautaki will support action by Te Komiti partners through the legislated 'levers'. This will be for both regulatory functions through the Resource Management Act and subsequent resource planning documents, and non-regulatory functions through the Local Government Act and subsequent investment planning documents.

He Whakarāpopototanga
Summary

Mahi Tukanga (Process)

- Te Komiti partners have committed to a series of initiatives in line with the Rautaki of Te Muriwai o Te Whanga. These initiatives sit under each Pou in 'focus areas'. Each focus area has a long-term indicator of success. These indicators provide a reference check to ensure current and future mahi continues to achieve the outcomes and overall vision outlined in the Rautaki.
- This initial action plan has 62 initiatives across the six pou.
- Te Komiti also wants to acknowledge the role of interested groups in forming this Plan. These groups have contributed 21 initiatives and will be part of ongoing coordination, monitoring, and evaluation of the Plan through a working group.

Te Anga Whakamua (Moving Forward)

- Te Komiti will publish the Plan and share this within partner organisations, and wider with interested parties. Te Komiti will promote the plan, ensuring resource-management decision makers, potential funding partners, and others as required can give regard to the plan's Rautaki. Te Komiti will also submit on consultations when this has not been the case.
- Te Komiti will work with a technical advisory group and working group to understand how initiatives are contributing to the indicators and outcomes outlined in this Rautaki and Action Plan. These groups will support development of future initiatives required and together with the working group and Te Komiti support monitoring, evaluation, and reviews as appropriate of this plan.

Te Komiti Muriwai o Te Whanga

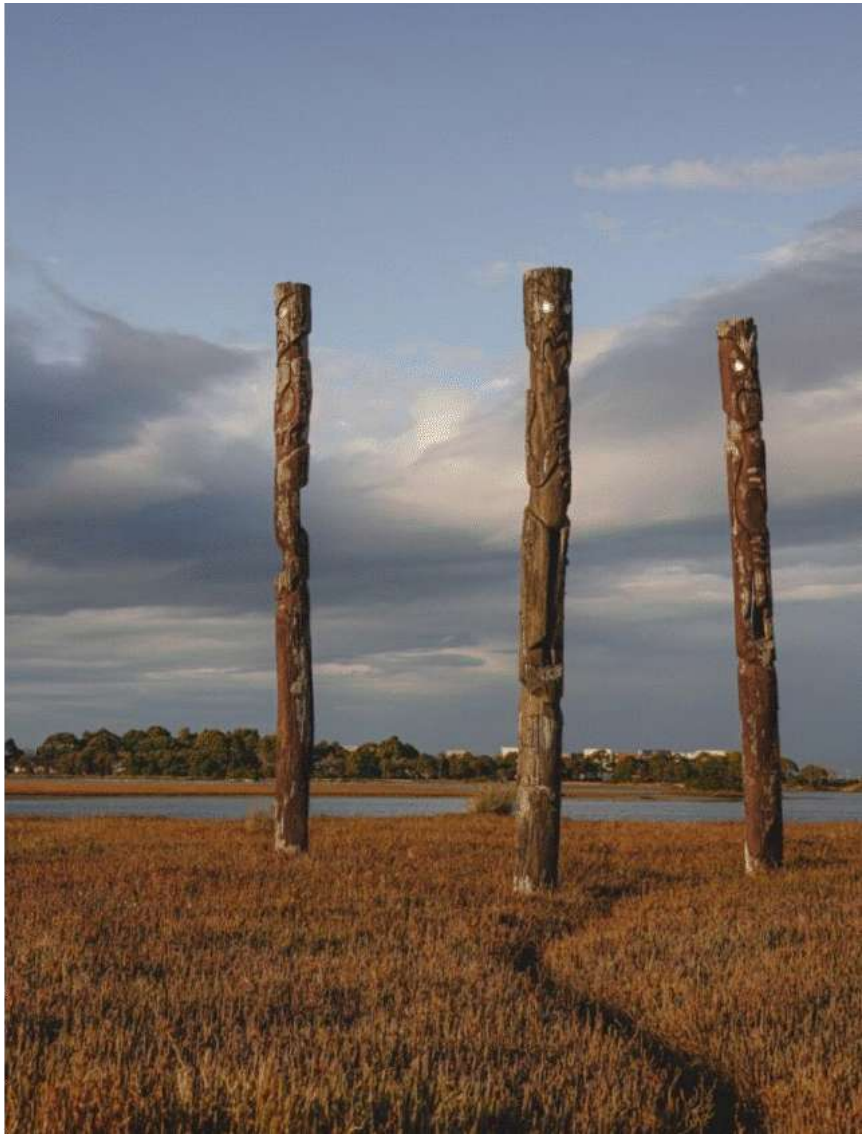

Ngā kupu matua
Key terms

Mahinga Kai (Customary food gathering): Mahinga kai refers to the values and protection of natural resources specific to iwi and their rohe. It means 'to work the food,' encompassing not just gathering but also the ecosystems and habitats involved, along with intergenerational practices and tikanga for production, harvesting, and protection.

Give regard to: The legislative requirement is that the drafting of Regional Plans and District Plans must 'have regard to' the Plan. Therefore, all relevant factors or information must be thoroughly evaluated, though this doesn't necessarily require that they be the deciding factors in the final decisions.

The Plan: Te Komiti Muriwai o Te Whanga Plan is referred to as 'the Plan' throughout this document. This collective document must be given regard to by all decision-makers, including councils when preparing RMA planning documents and assessing resource consent applications, as well as when making decisions under the LGA, in accordance with section 95 and section 96 of the Settlement Act. DoC must have taken it into account when preparing their Conservation Plans and when issuing permits. This document should also guide members of Te Komiti in their decision-making processes.

Te Muriwai o Te Whanga: As defined in the settlement, encompasses both the Ahuriri estuary and its catchment areas. The term "Muriwai" translates directly to "end of water," reflecting the significance and geographical features of the area.

Ahuriri Hapū: The Mana Ahuriri Trust serves as the post settlement governing body for Ahuriri Hapū, which comprises seven hapū based in and around Napier, Hawke's Bay. These hapū include Ngāti Hinepare, Ngāti Māhu, Ngāti Matepū, Ngāti Pārau (including Ngāi Tahu Ahi), Ngāi Tāwhao, Ngāti Tū, and Ngāi Te Ruruku.

Te Whanganui-a-Orotu: Known as the Ahuriri Estuary, holds significant cultural importance to Ahuriri Hapū. In the Deed of Settlement, the Crown acknowledges that Te Whanganui-a-Orotu and its surrounding islands have been cherished taonga of Ahuriri Hapū and continue to be highly valued today. Moreover, the Crown acknowledges Ahuriri Hapū's role as Kaitiaki, or guardians, of Te Muriwai o Te Whanga, encompassing the Ahuriri Estuary and its catchment areas.

Pou: Pillars.

Te Mahi Tūhono a Roopu: Connections to and relationships between partners / friends of Te Whanga. Used in this plan to articulate the Social pou of the Rautaki.

Te Mahi Ohaoha: Work pertaining to growth with an economic focus. Used in this plan to articulate the Economic pou of the Rautaki.

Aroā o Te Whanga: To comprehend or deeply understand Te Whanga. Used in this plan to articulate the Historical / Educational pou of the Rautaki.

Ahurea o te Whenua: Culture that comes from this particular place (Ahuriri). Used in this plan to articulate the Cultural / Spiritual pou of the Rautaki.

Te Mauri o te Taiao: The life force / essence of the environment. Used in this plan to articulate the Biodiverse Ecosystem pou in the Rautaki.

Te Ora o te Wai: The health of the water of Te Whanga. Used in this plan to articulate the Water Health pou of the Rautaki.

Rārangi Take
Contents

Te Komiti Muriwai o Te Whanga

1. Te Horopaki - Context

Overview of Te Whanga 9
History 10 - 13
Te Komiti 14
The Plan 15 - 16
Current and Future States 17 - 18

2. Rautaki - Strategy

What is in the Rautaki and why 20
Rautaki (on a page) 21
Mātaapono - Values 22
Pou - Pillars 23

3. Mahi Tukanga - Action Plan

1. Te Ora o te Wai (water health) 28 - 33
2. Te Mauri o te Taiao (bio-diverse ecosystem) 34 - 36
3. Aroā o Te Whanga (education and awareness) 37 - 39
4. Te Mahi Ohaoha (economic) 40 - 41
5. Te Mahi Tūhono a Roopu (social / partnerships) 42 - 43
6. Ahurea o te Whenua (cultural/spiritual) 43 - 44

4. Appendices

A: Regulatory and Non-Regulatory Levers 47 - 49
B: SO Plan: Statutory legislated area of Te Muriwai o Te Whanga 50 - 51
C: Summary of Pou Indicators 42 - 54
D: Broader Plan 55 - 53

1

Te Horopaki

Context

Te Komiti Muriwai o Te Whanga

Mana Ahuriri Trust 2024 I 9

Map of Te Muriwai o Te Whanga

The map below shows the current impact / value of a range of activities occurring across the different areas of Te Muriwai o Te Whanga

Key:
High: OOO
Medium: OO
Low: O
None: -

Land-based: 🚶
Water-based: 🚙

Lower Estuary
Recreation: OOO (🚙+ 🚶)
Ecological Value: OO
Stormwater Management: OOO
Farming: -

Inner Harbour Area
Recreation: OO (🚶 🚙)
Ecological Value: O
Stormwater Management: O
Farming: -

Upper Estuary
Recreation: O (Eastern 🚶 + 🚙)
Ecological Value: OOO
Stormwater Management: -
Farming: OO

Mid-Estuary
Recreation: O (Northern 🚶)
Ecological Value: OOO
Stormwater Management: OO
Farming: OO

Te Komiti Muriwai o Te Whanga

Mana Ahuriri Trust 2024 I 10

Te Muriwai o Te Whanga

Defining the original landscape

Pre 1840's

Te Whanganui-a-Orotu

- Te Whanganui-a-Orotu, was once a flourishing body of water, supporting an extensive ecosystem. It was protected with mana by the people of the area. Te Whanganui-a-Orotu translates to the 'great harbour of Orotu', symbolising the immense value of mahinga kai.
- It was abundant with shellfish beds and fishing spots, while the rivers and streams teemed with eels and freshwater fish. Recognised as a place of plenty for freshwater fish, shellfish, and birds, it was highly valued as a vital food source in the morning, at noon and in the evening.
- It is named after the ancestor Te Orotu, who was a descendant of the great explorer and ancestor Māhu Tapoanui, who is the very beginning of the Ahuriri Hapū. Te Whanganui-a-Orotu contained islands where Hapū lived and camped while on fishing expeditions, as well as wāhi tapu and urupā.
- The Tūtaekurī River was the most significant source of freshwater into Te Whanga, originating in the Kaweka Ranges and flowing southeast towards the coast. Named after an event 400 years ago, when Ngāti Kahungunu, led by Hikawera, faced starvation in the hills between Waiōhiki and Omāhu. Desperate, Hikawera ordered 70 kurī (dogs) to be sacrificed at Te Umukuri. The river got its name, Tūtaekurī, from the offal (tūtae) thrown into it during this event. This offal or (Tutae) was good for the eco-system ie: eels.

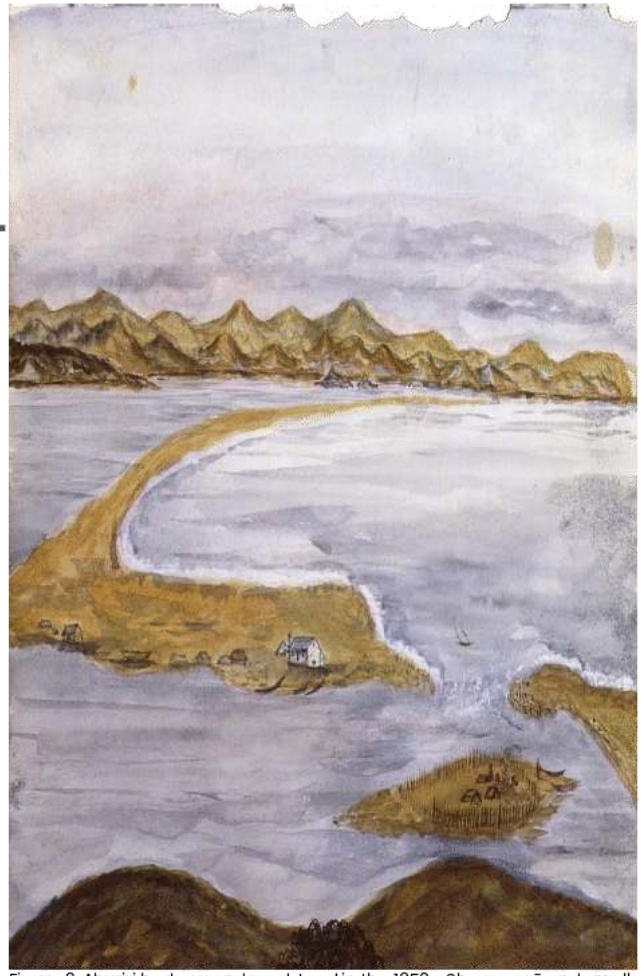

Figure 2: Ahuriri harbour and roadstead in the 1850s. Shows a pā and small Pākehā settlement.

Whakapapa o Te Muriwai o Te Whanga

The significance of Te Whanga and impact of colonisation

Pre 1840+ | 1840 | 1850 - 1930

Cultural Significance

- Ahuriri Hapū, Ngāti Pāhauwera, and Maungaharuru–Tangitū, as Treaty settlement entities, share profound connections to Te Whanganui-a-Orotu, the Ahuriri Estuary. For Ahuriri Hapū, Te Muriwai o Te Whanga is culturally and spiritually significant, representing a crucial aspect of their identity.
- Te Whanga was a source of nourishment for the tangata whenua and embodies the ancestral beginnings of Ahuriri people. The whakapapa of the Ahuriri hapū settlements is woven into their cultural narrative.
- Various hapū, including Ngāti Hinepare, Ngāti Māhu, Ngāti Matepū, Ngāti Pārau (including Ngāi Tahu Ahi), Ngāi Tāwhao, Ngāti Tū, and Ngāi Te Ruruku, have contributed to the historical, cultural, and archaeological significance of Te Whanganui-a-Orotu.

Iwi Settlement of Ahuriri

- Ahuriri hapū lived in settlements around Te Whanganui-a-Orotu and surrounding areas.
- The environment was utilised as a productive natural resource, from farming to horticulture practices. There was enough to share amongst everyone.
- Some Ahuriri Rangatira began to consider the advantages that might arise from the promotion of Pākehā settlement in the Ahuriri district and offered land to the crown for Pākehā settlement. This was the beginning of a catastrophic series of events at the expense of the natural state of the environment.

European Settlers

- In the **1850s**, the Crown negotiated with Ahuriri Māori to buy their land at a low price, promising benefits. They purchased the land in **1851**. This caused tensions among Hawke's Bay Māori, but negotiations continued. In **1860,** the Crown developed the estuary for a harbour, disturbing wildlife and exploiting resources, diminishing the overall health of the estuary.
- Five years later, new land laws allowed individual owners to sell their shares without consent, leading to settlers acquiring a significant amount of Ahuriri hapū land. By **1870** the Crown and private parties had acquired approximately 51,000 acres of approximately 54,000 acres awarded to Ahuriri hapū individuals under the 10-owner rule. The Napier Harbour Board was established in **1874** with no role for Ahuriri hapū. This further impacted the environment by using claimed land for urban and industrial development.

Te Komiti Muriwai o Te Whanga

Mana Ahuriri Trust 2024 I 12

Whakapapa o Te Muriwai o Te Whanga

Impacts of te taiao on Te Whanga

1931

Earthquake

- Until the 1931 Hawke's Bay Earthquake, most of the area was an inland sea from Pandora to Bayview. The earthquake lifted the area 1-2 metres, draining most of the water. This prompted legal complexities and land leasing for drainage and reclamation. This resulted in further residential, industrial, and recreational developments.
- The processes of drainage and reclamation, combined with the diversion of the Tūtaekurī River outlet to the sea, reduced Te Whanganui-a-Orotu (originally approximately 9,500 acres in area) to a narrow tidal channel.

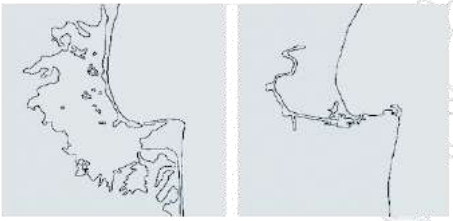

Above: Te Muriwai o Te Whanga before (left) and after (right) the earthquake

1945

WWII

- Ahuriri Māori turned to waged employment, prompting a significant migration to urban areas that gradually eroded the foundations of traditional kāinga and pā communities. Unfortunately, these changes, coupled with the mounting pressures of modern society, led to a decline in the care and preservation of the estuary and its surrounding areas.
- The devastating impacts of the earthquake served as a catalyst, exacerbating the already dire environmental state of the estuary. In particular, the pollution from stormwater and sewage reached its peak during this period.

Whakapapa o Te Muriwai o Te Whanga

Significant events leading towards today

1988 - 2016

Settlement & Mana Restoration

- In **1988** the Waitangi Tribunal Claim was initiated in order to justify breaches of Te Tiriti o Waitangi that the Crown has made and shown Māori to have suffered prejudices as a result.
- In **2009** Mana Ahuriri Incorporated gained the mandated support of the hapū to negotiate a claim.
- In **2010**, the Crown acknowledged the Mana Ahuriri Incorporated mandate for negotiating comprehensive settlement of all Ahuriri hapū historical claims. This recognition led to the signing of an agreement in principle in **2013**, which formed the foundation of the settlement, addressing all historical claims of the seven hapū predating **1992**. The agreement acknowledges Crown breaches of Te Tiriti o Waitangi, resulting in hapū land loss and intergenerational distress. Redress includes a historical account, Crown apology, acknowledgment, and financial, commercial, and cultural redress.

2016 - 2022

Establishment of Te Komiti

- In **2016**, the establishment of the Mana Ahuriri Trust and the initialing of the Ahuriri Hapū Deed of Settlement provided Ahuriri Hapū with mana and control over estuary management and protection.
- In **2019** the Ahuriri hapū claims settlement bill was introduced. The settlement includes $19.5 million worth of financial, commercial, and cultural restitution.
- 3 March **2021** was the official settlement date. The settlement legislation established a permanent estuary committee, Te Komiti Muriwai o Te Whanga, to safeguard and enrich the environmental, economic, social, spiritual, historical, and cultural values of Te Muriwai o Te Whanga (Ahuriri Estuary) for present and future generations.
- The committee is chaired by Mana Ahuriri Trust and comprises representatives from DOC, HBRC, NCC, and HDC. Te Komiti Muriwai o Te Whanga oversees and coordinates management efforts for the estuary, providing guidance to local authorities and Crown agencies. Additionally, it will develop and endorse a comprehensive management plan (this document) known as Te Muriwai o Te Whanga Plan.

2023

Cyclone Gabrielle

- On 13 and 14 February, 2023 Cyclone Gabrielle caused extensive flooding and damage across Hawke's Bay. This event resulted in a period of extreme vulnerability and damage to Ahuriri and the wider area. Te Muriwai o Te Whanga faced consequential change, from sewage contamination, considerable overflow of silt and devastating loss to the ecosystem. The local councils involved in the rehabilitation aimed to focus on reinstatement as opposed to development.

Ngā kaitiaki o Te Whanga
The functions of Te Komiti

The Ahuriri Hapū Claims Settlement Act, section 85 (subsection 1), outlines the functions of the Komiti. These are to provide guidance and co-ordination in the management of Te Muriwai o Te Whanga to local authorities and Crown agencies that perform functions in relation to Te Muriwai o Te Whanga by;

a. promoting a greater understanding of Te Muriwai o Te Whanga and the issues relating to its health and well-being; and
b. advocating on behalf of Te Muriwai o Te Whanga; and
c. providing a forum for the community to express its views on Te Muriwai o Te Whanga and its health and well-being; and
d. identifying the values, vision, objectives, and desired outcomes, and any other matters relevant to Te Muriwai o Te Whanga; and
e. working with stakeholders to gather and collate all data and information relevant to the functions of the Komiti; and
f. monitoring, evaluating, and reporting on matters affecting the ongoing health and well-being of Te Muriwai o Te Whanga; and
g. advising the local authorities and the Director-General on matters pertaining to Te Muriwai o Te Whanga; and
h. communicating to stakeholders matters pertaining to Te Muriwai o Te Whanga; and
i. promoting and seeking opportunities to raise funds and support for the ongoing health and wellbeing of Te Muriwai o Te Whanga; and
j. making recommendations on the integration and coordination of Te Muriwai o Te Whanga management; and
k. preparing and approving the Te Muriwai o Te Whanga Plan; and
l. taking any other action that is considered by Te Komiti Muriwai o Te Whanga to be appropriate to achieve its purpose.

Te Komiti is tasked with several crucial responsibilities aimed at ensuring the health and wellbeing of Te Muriwai o Te Whanga. These functions collectively reflect a comprehensive approach to the sustainable management and protection of Te Muriwai o Te Whanga, involving collaboration with various stakeholders and a focus on community engagement and well-being. In this section, stakeholders means;

- residents of the Hawke's Bay region, Crown agencies, interested parties and businesses with an interest in Te Muriwai o Te Whanga; and
- the local authorities; and
- the Director-General of the Department of Conservation.

Te Komiti is supported by Napier City Council as per Schedule 4 of the Ahuriri Hapū Claims Settlement Act 2021 who undertake their secretariat and technical support functions.

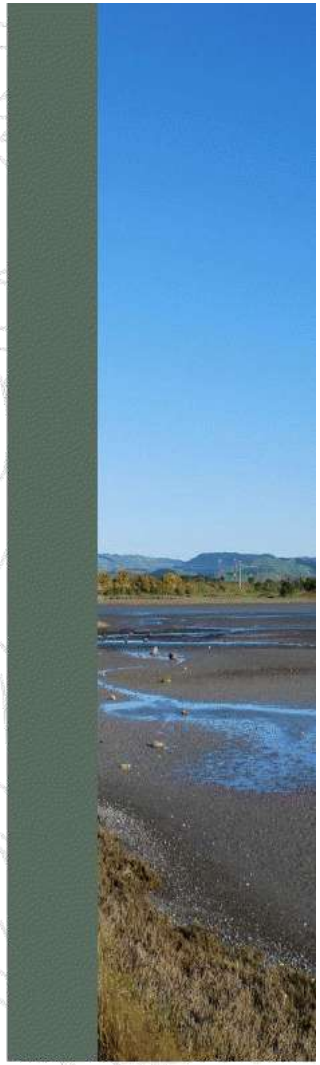

Te Muriwai o Te Whanga Plan

The role of Te Komiti and the Plan

What is a plan?

A plan is used to record and share a collective vision. It articulates a series of steps to deliver this vision. The Te Muriwai o Te Whanga Plan (the Plan) outlines values, objectives, outcomes, indicators, and initiatives required to achieve the desired vision.

What is the purpose of the plan?

This is an overall coordinating plan for the Ahuriri and catchment areas - Te Muriwai o Te Whanga Plan. The scope of the area within the statutory mandate of the plan is outlined in Appendix B.

The purpose of the Plan is to acknowledge the whakapapa and current state of Te Whanga and, with integrated management, propose future initiatives and changes that protect and enhance the environmental, economic, social, spiritual, historical and cultural values of Te Muriwai o Te Whanga for present and future generations.

This initial Plan is a starting point for Te Komiti and other stakeholders to restore the health of Te Whanga as the "storehouse" it once was. The Plan provides both a strategy and associated action plan to guide, promote, and fulfill legislated mechanisms and other activities. The Plan aims to create short, medium and long term change through coordination of activities, associated investment, planning changes, and a comprehensive monitoring, evaluation, and review approach.

How was it developed?

The Plan was developed through collaboration of interested individuals and organisations, while also ensuring compliance with relevant requirements specified in Te Komiti terms of reference for the Plan's development.

How will the plan be achieved?

All partners of Te Komiti are accountable as kaitiaki of Te Muriwai o Te Whanga. How this accountability works in relation to other plans is outlined on the following page in more detail.

All individuals and entities are required to consider, in particular, the values and objectives outlined in the Plan when preparing, reviewing, or approving a conservation management strategy or plan related to Te Muriwai o Te Whanga, or when making decisions under any conservation legislation pertaining to the area.

Te Komiti Muriwai o Te Whanga

How will the plan achieve its vision?

Influence on Resource Management and Local Government Decision-Making

The Plan will be a document that the territorial local authorities (TLA) (HBRC, NCC, and HDC) must give regard to in both their planning instruments, as well as their investment mechanisms (see Appendix A for further detail of how this works). This means, the Te Muriwai o Te Whanga Plan needs to be considered in decision making, consent granting, and policy forming for the relevant TLA depending on the location of the matter.

Regulatory

The Te Muriwai o Te Whanga Plan significantly influences Resource Management Act 1991 planning documents and resource consent decisions. Local authorities must give regard to the plan when preparing or amending regional policy statements, regional plans, or district plans if its contents pertain to resource management issues and if it is the most appropriate means to achieve the Act's purpose.

Any required reports or decisions must explicitly state compliance with the plan. Additionally, when evaluating resource consent applications for activities within Te Muriwai o Te Whanga, authorities must consider the Plan's relevance and necessity in determining the application. Definitions for terms like "policy statement" and "plan" are provided for clarity in the glossary on page 4.

Non-Regulatory

The Plan's relevance extends to local government matters under the Local Government Act 2002, where any local authority making a non-regulatory decision (including funding decisions) under The Act pertaining to Te Muriwai o Te Whanga, needs to have regard to this Plan. This can apply to decision making related (but not limited) to local Asset Management Plans, Ahuriri Catchment Plans, Annual and Long Term Plans.

Other | Conservation

The Plan's influence also extends to conservation matters. Any person or entity must take into account the values and objectives set out here, when preparing conservation management strategies / plans or making decisions under conservation legislation related to Te Muriwai o Te Whanga. The values and objectives are further articulated in the rautaki of this plan.

Current State of Te Taiao o Te Whanga

Understanding where this plan is starting from

To ensure effective planning, it is crucial to have a solid grasp of the current state of the estuary. We have included a high-level overview here. Additionally, the action plan provides a list of current and ongoing initiatives from partners and interested parties, offering insight into the extensive work in place prior to this plan becoming 'live'.

Whenua / Land

- Once a larger lagoon, Te Whanganui-a-Orotu uplifted by over 1.5 metres after an earthquake, and subsequent land reclamation and drainage reduced its size to around 470 hectares. Now a microtidal, well-mixed lagoon amidst Napier City's urban, industrial, and agricultural zones, it spans 4.7 square kilometres, featuring shallow expanses, extensive intertidal areas, and a maximum depth of 2.6 metres in the main tidal channel. Categorised into three sub-estuaries, with the boat harbor near the coast, the western boundary is marked by the Pandora Bridge.
- The Ahuriri Catchment is a landscape shaped by urban, industrial, and agricultural influences. It hosts significant rivers like the Tūtaekurī and Te Waoihinanga which flow along with smaller watercourses like the Taipo Stream. These water sources collectively impact the quantity and quality of water entering the Ahuriri Estuary, underscoring the necessity of understanding the Ahuriri Catchment for effective environmental management and sustainable development in the broader Hawke's Bay area.

Wai / Water

- Elevated sediment levels in Ahuriri and Waitangi Estuaries, with a shift from sandy to muddy sediments due to terrestrial contributions, pose challenges such as reduced light for plants, altered habitats, and potential harm to animals. The Lower Ahuriri comprises predominantly medium sands, while high mud levels in Upper Ahuriri and Waitangi impact sensitive organisms, exacerbated by land claim activities binding contaminants to fine sediments. Deforestation, urbanisation, and industrialisation expedite sedimentation, leading to elevated heavy metals in sediments.
- The estuary, characterised by shallow, microtidal conditions, relies on semi-diurnal tides for effective hydrodynamics. Despite minimal freshwater inflows primarily from the Taipo Stream and a 10:1 saltwater to freshwater ratio, over 70% of Napier's stormwater runoff enters the estuary, compromising water quality with untreated sediment and contaminants, including excessive phosphorus and nitrogen levels. The presence of fan worms further exacerbates challenges.

Mauri / Biodiversity

- The Ahuriri Estuary is a vital wetland supporting 29 fish species and over 70 water bird species of particular significance are the critically endangered Bittern and the flounder and cockle species, with the lower estuary serving as a known nursery for yellow belly flounder. Recognised nationally for its wildlife and fisheries habitat, it showcases the region's unique geological processes. Despite human modifications, it maintains diverse habitats and ecological communities.
- Five smaller wetlands within the complex further enhance its ecological value. The estuary serves as a crucial refuge for a wide array of species. Additionally, hosting thirty-three recorded invertebrate species, the estuary biodiversity underscores its significance as a habitat for various regional species.

Future Impacts

Climate change and human impact will further affect Te Taiao

Future drivers	Expected implications	
Rise in sea level	• **Inundation:** Rising sea and ground water levels can lead to the inundation of estuarine habitats, submerging wetlands, marshes, and tidal flats. Existing stop banks along the outfall channel have been built to protect the adjacent land areas. • **Erosion:** Increased water levels can accelerate coastal erosion, reshaping the estuary and potentially leading to the loss of land.	• **Salinity changes:** Higher sea levels can push saltwater further upstream into estuaries, altering the salinity balance and affecting the freshwater and it's species. • **Loss of wetland:** Rising sea levels and increased rainfall/storm surges can cause the loss of vital wetland habitats affecting many species.
Temperature increases	• **Water Temperature:** Increased sea level temperatures can affect the water temperature within estuaries, influencing the metabolism, reproduction, and distribution of aquatic species.	• **Air Temperature:** Increased air temperatures can alter the estuarine environment and contribute to heat stress on local flora and fauna.
Change in rainfall patterns	• **Increased rainfall:** More intense and frequent storms can lead to greater runoff and flooding, increasing sediment and pollutant loads in estuaries, putting added pressure on stormwater catchments.	• **Drought:** Reduced freshwater input during droughts can increase estuarine salinity and alter the species habitats.
Biodiversity shifts	• **Species Migration:** Changes in temperature and salinity can cause shifts in species distributions, with some species moving to more suitable habitats and others potentially facing local extinction.	• **Invasive Species:** Altered conditions can make estuaries more susceptible to invasive species, which can outcompete native species and disrupt ecosystems.
Increased urban pressure	• **Coastal development:** Infrastructure development can further stress estuarine environments leading to habitat loss and increased pollution.	• **More visitors:** An increase in foot traffic to the estuary can expect to have various impacts including; economic benefits from an increase tourism revenue, education opportunities from greater public awareness, more pollution from littering and wildlife disturbance.

2

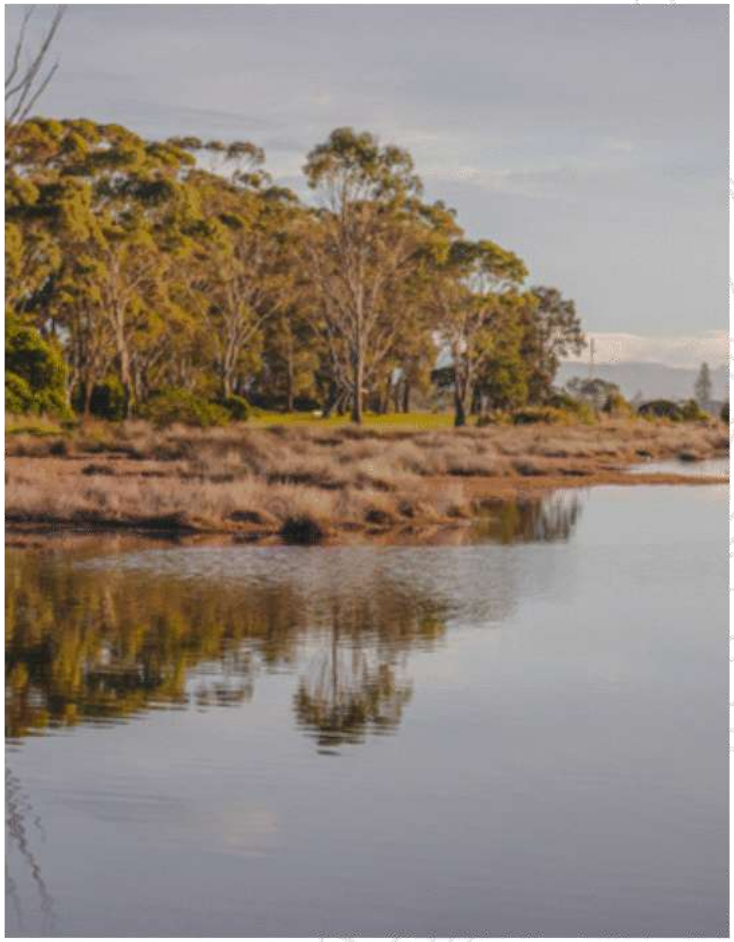

He Rautaki

Strategy

Where has this Plan Rautaki come from?

The Ahuriri Claims Settlement Act outlines a set of functions of Te Komiti, and includes their role in **identifying the values, vision, objectives, and desired outcomes, and any other matters relevant to Te Muriwai o Te Whanga**.

This first section of the Plan, the strategy, accomplishes this through acknowledging past mahi for Te Whanga while understanding this is a new opportunity to achieve intergenerational outcomes for Te Taiao, our seven Hapū and other Hapū interests.

The following nine elements of the strategy rely on each other. The **vision** is the guiding aspiration of Te Komiti for Te Whanga. The **values** are how Te Komiti and its partners will be guided through the decisions they have to make for Te Whanga. The **whakataukī** shares wisdom of the past and future for Te Whanga.

Then the action part of the strategy outlines six **Pou** which together support the vision for Te Whanga. Each Pou has a desired **outcome** - an aspiration for that element of Te Whanga. Each Pou also has an **objective**, which outlines how the objective will be achieved and is supported by a series of **indicators** and **initiatives** that articulate distinct actions to be undertaken.

Vision

Following an initial wānanga, members of Te Komiti agreed upon a vision that successfully encapsulated the motive behind this Plan. This vision serves as a guiding statement that outlines the long-term aspirations and desired future statement of Te Muriwai o Te Whanga.

Values

Partners within Te Komiti collaborated to create a collection of values that effectively illustrate the ways of working for Te Whanga. These values were built from the individual values of each partner of Te Komiti and refined through a series of wānanga. These values will be used to guide Te Komiti and partners in their work for Te Whanga.

Whakataukī

A whakataukī shares a concept that is used to inspire, guide, and share wisdom. In this context, the whakataukī acknowledges the aspirations for Te Muriwai o Te Whanga and the wisdom passed down from whakapapa that protected the area.

Pou

Through research to development of the Plan, Te Komiti identified six key areas of focus. These areas, known as the Pou of the Plan, serve as pillars of our work. While each Pou provides individual focus, their collective strength is essential to realise the vision for Te Whanga.

Outcomes

The desired outcomes outline the aspiration for each Pou in line with the overall vision for Te Whanga. They define the measure of success and what will be considered positive outcomes as we achieve the objectives and initiatives of each Pou. These outcomes were developed through wānanga.

Objectives

The objectives are aligned to each Pou and outcome. They outline the specific way in which the outcome for each Pou will be achieved. These objectives were developed via wānanga.

Focus Areas and Indicators

Within each Pou sits a number of focus areas that indicate commonality between initiatives. Each focus area has a related long-term indicator which shows the desired level of achievement for initiatives collectively in that focus area.

Initiatives

The initiatives are key actions that are already or will be undertaken to achieve the desired outcome and meet the objectives under each Pou. Initiatives were developed through background research, understanding of partners work programmes, and engagement with involved and affected parties.

Further detail on each Pou, its outcomes, objectives, focus areas, indicators, and initiatives is outlined in Section Three (Action Plan) of this Plan.

Te Muriwai o Te Whanga Strategy | Rautaki on a Page

Whāinga | Vision

The health of Te Whanganui-a-Orotu supports environmental, economic, social, spiritual, historical, and cultural value for present and future generations.

Whakataukī

Ko rua te paia ko Te Whanga. He kainga tō te ata. He kainga ka awatea. He kainga ka ahiahi.

The Whanga is the storehouse that never closes. A meal in the morning. A meal at noon. A meal in the evening

Mātāpono | Values

Whanaungatanga
Relationships

Kaitiakitanga
Guardianship

Pono
Integrity

Whakapakari
Enhancement

Kotahitanga
Unity

Detailed articulation of what Te Komiti means by each of the values is included on the following page.

Pou | Pillars

'Our priority for Te Whanga is its mauri through our wai and taiao pou, all other pou are enabled by this'

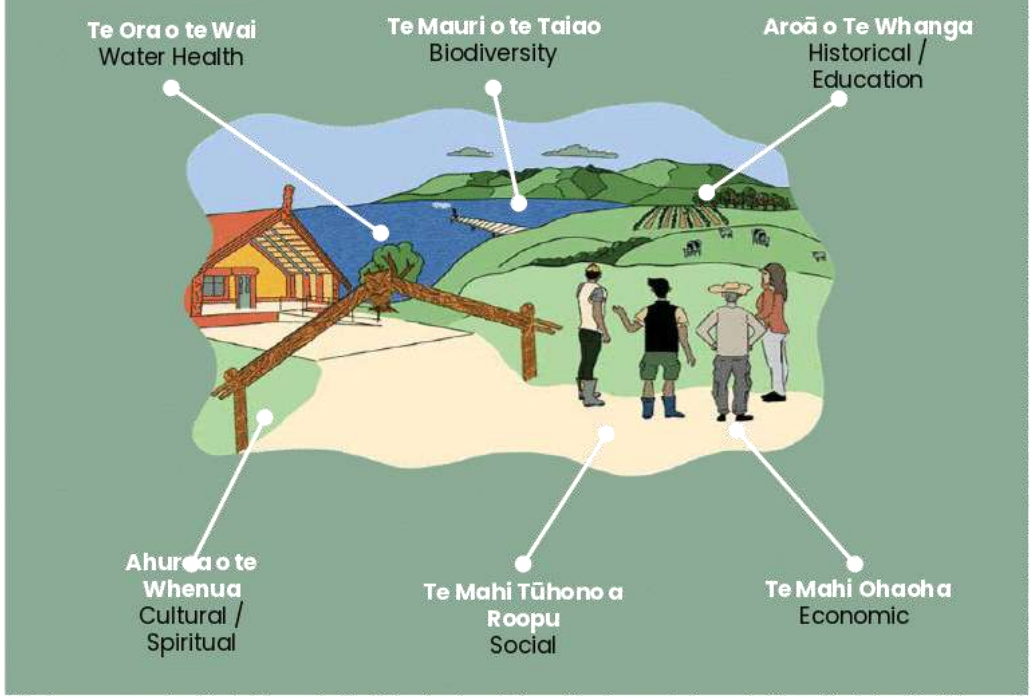

Detailed articulation of what each of the Pou means, the hierarchy Te Komiti intends for them, and their outcomes and objectives within the Plan is included on Page 23.

Te Muriwai o Te Whanga Strategy

Ngā Mātāpono | Values

This plan is values-driven and values based, ensuring that any work undertaken relative to Te Whanganui-a-Orotu is an embodiment of these values. The values and how they are enacted, are articulated below.

Whanaungatanga	Grounded in whakapapa, whanaungatanga fosters enduring intergenerational relationships and partnerships by connecting people, whenua, water, and wildlife, ensuring an understood and shared heritage to effectively inform aspirations for the future of Te Whanganui-a-Orotu.
Kaitiakitanga	Kaitiakitanga embodies an inherent obligation of guardianship, care, and respect, promoting enduring commitment to protect and enhance our environment, empowering communities through active participation and the application and appropriate use of mātauranga Māori for future generations.
Pono	Pono embodies integrity and the commitment to do it right, do it right now, and do it with consistency, ensuring that decisions align with hapū values and are informed to achieve meaningful outcomes throughout the journey.
Whakapakari	Whakapakari emphasises the enhancement, nurturing, and growth of our environment and communities. Respecting and restoring what is given, ensuring no further harm to the environment is undertaken, and making decisions that create a better future for our mokopuna.
Kotahitanga	Kotahitanga embodies unity and collective action, driven by a shared vision and shared outcomes, where responsibility and ownership are embraced together with purpose, fostering positive progress while upholding the mana motuhake of Mana Whenua.

Te Komiti Muriwai o Te Whanga

Te Muriwai o Te Whanga Strategy | Ngā Pou o te Rautaki

5. Te Mahi Tūhono a Roopu

Social

All stakeholders unite to improve Te Whanga, making it a hub for community betterment through activities like kai, exercise and recreation.

Kotahitanga. Ensure alignment and collaboration between all stakeholders, fostering strategic partnerships aimed at enhancing and improving the well-being of Te Whanga.

6. Te Mahi Ohaoha

Economic

Receive value through sustainable practices and use of the estuary to promote further growth for whānau, hāpu, and wider community

All stakeholders engage in sustainable practices and responsible use of the estuary. Mana Ahuriri is a leader in eco tourism.

3. Aroā o Te Whanga

Historical / Educational

Our taonga is acknowledged, promoted and understanding of it shared with the Ahuriri people.

To promote a greater understanding of Te Muriwai o Te Whanga and the issues relating to its health and well-being, and archaeological sites.

4. Ahurea o te Whenua

Cultural / Spiritual

The cultural and spiritual identity of Te Whanga and the wider catchment are enhanced in order to support the connection between people and land.

Enhance a community that recognises the cultural significance of the estuary through prioritising tikanga and mātauranga Māori which includes upholding the mana of local sites of significance / wāhi tapu.

Taiao / Environmental

1. Te Ora o te Wai

Water Health

The water in the estuary is in optimal health.

To give effect to Te Ora o te Wai to improve water quality through management of stormwater and other sources of pollution.

2. Te Mauri o te Taiao

Biodiversity

The estuary is a flourishing ecosystem that supports resilient biodiversity.

Tautoko development of current and reintroduced species in Te Whanga by restoring their habitats and eradicating competing and introduced pests, weeds, and disease.

The taiao is the base of the mana of Te Whanga, emphasising a priority within the Plan.
The te taiao pou underpin all other pou, for without the mauri of our Whanga taiao, no other pou can be achieved.

Definitions for each Pou Name are provided in the Key Terms on Page 4

Te Komiti Muriwai o Te Whanga

Mana Ahuriri Trust 2024 I 24

3

Mahi Tukanga

Action Plan

Te Komiti Muriwai o Te Whanga

Mana Ahuriri Trust 2024 I 25

How to read this Action Plan and who contributed

Unlocking the key components of the Plan

Based on the values and vision of Te Komiti, this section summarises what organisations have already committed to or anticipate doing under the Plan. This Action Plan will evolve over time as initiatives are completed, evaluated, evolved, or added. The action Plan is structure by the six Pou of the Rautaki and aims to meet the objective and outcome articulated for each one. It will do this by:

- **Focus Area:** These are the key areas of mahi identified under each pou that the initiatives will focus around.
- **Indicators:** Each focus area has a related long-term indicator which shows the desired level of achievement for initiatives collectively in that focus area.
- **Initiatives:** These are the detailed actions that are recommended to take place to advance estuary restoration within each of these focussed outcomes and Pou. Following the action lists: who is involved, timeframe, associated interdependencies, funding, and regulation requirements.

Please note: All initiatives are subject to change by the individual organisation in line with their planning processes and operating environment. This Action Plan is a snapshot at this point in time (June 2024).

The structure of how the Action Plan is laid out is presented below with definitions to support understanding of how to read the following pages.

The following partners and interested groups contributed initiatives to the Plan:

- Mana Ahuriri Trust (MAT);
- Department of Conservation (DOC);
- Hawke's Bay Regional Council (HBRC);
- Napier City Council (NCC);
- Pāmu;
- Ahuriri Tributaries Catchment Group Trust (ATCGT);
- Ahuriri Estuary Protection Society (AEPS);
- and Forest and Bird.

Hastings District Council did not have relevant initiatives at the time this was initially formed, however, conveyed their full commitment and participation in the plan.

Summary Dashboards are provided on pages 26 and 27

1. Te Ora o te Wai is on pages 28 to 33
2. Te Mauri o te Taiao is on pages 34 to 36
3. Aroā o Te Whanga is on pages 37 to 39
4. Te Mahi Ohaoha is on pages 40 to 41
5. Te Mahi Tūhono a Roopu is on pages 42 to 43
6. Ahurea o te Whenua is on pages 44 to 45

Pou Objective / Pou Outcome							
Indicator	**Focus Area**	**Initiative**	**Status**	**Start Date**	**End date**	**Lead**	**Partners**
Long-term indicator of success	*Area of focus within the Pou (linked to the long-term indicator)*	*Name and description of the initiative: what it is and what will be delivered*	*What is the current status; not yet started, ongoing (BAU - business as usual), underway, or complete.*	*Anticipated start date*	*Anticipated end date*	*Who is responsible for leading the initiative*	*Who is partnering with the lead on the initiative*

Overview of Pou and Initiatives by Lead

Across the six Pou, lead organisations have focused on areas within their mandates.

		MAT	NCC	HBRC	DOC	Interested Parties
Total number:	**64**	**14**	**13**	**9**	**7**	**21**
Te Ora o te Wai		1	10	7		6
Te Mauri o te Taiao		3		2	4	3
Aroā o Te Whanga		3			1	7
Te Mahi Ohaoha		3				1
Te Mahi Tūhono a Roopu		2	2		1	1
Ahurea o te Whenua		2	1		1	3

Note: The total number of initiatives in this dashboard exceeds the overall count of 62 because two initiatives have co-leads.

Overview of High-Level Sequencing of Initiatives

Across the six Pou there are 62 initiatives

While the majority of initiatives are underway, a number are yet to commence, or are yet to be confirmed. The following table shows the high-level sequencing of initiatives within each Pou as of 30 June 2024.

	Total	Are underway	Are completed	Are ongoing	Not yet started	Are to be confirmed
Total number:	**62**	**32**	**2**	**19**	**8**	**1**
Te Ora o te Wai	23	18	2	3		
Te Mauri o te Taiao	12	7		3	2	
Aroā o Te Whanga	11	1		8	2	
Te Mahi Ohaoha	4	2		1		1
Te Mahi Tūhono a Roopu	5	1		3	1	
Ahurea o te Whenua	7	3		1	3	

1. Te Ora o te Wai - Water Health

Summary

Pou Outcome: The water in the estuary is in optimal health.

Pou Objective: To give effect to Te Ora o te Wai to improve water quality through management of stormwater and other sources of pollution.

Indicators of success

There are six indicators within this Pou linked to eight focus areas.

Indicators	Relevant focus areas
Stormwater, including potential contaminants such as wastewater from network overflows or other sources, is either diverted or treated to ensure it does not negatively impact the water health of Te Whanga	1.1 Stormwater diversion and treatment
There is a strong understanding of potential pollutants in the stormwater going into the estuary at all times	1.2 Stormwater quality monitoring
Tributaries in the catchment have plans in place to manage the risks of negatively impacting Te Whanga	1.3 Catchment management
A baseline of water and related environment quantity and quality is collectively formed	1.4 Water and related environment quality monitoring and testing
Water quality is improved through fit for purpose solutions in the catchment	1.5 Water quality enforcement and compliance 1.6 Water quality environmental health and restoration 1.7 Water quality planning
Environmental restoration is routinely undertaken with the support of the community	1.8 Community engagement and cleanup

Initiatives

There are 23 initiatives from three lead organisations and eight partners.

Te Ora o te Wai reflects a deep understanding of the interconnectedness between the well-being of water and the vitality of life. Water holds great significance, not only as a physical resource but also as a spiritual and cultural entity. The concept emphasises the importance of restoring and maintaining the health and purity of water sources, recognising that the wellbeing of water directly influences the wellbeing of all living things that depend on it. It encapsulates a holistic approach to kaitiakitanga, promoting the sustainable use and protection of water resources for the benefit of present and future generations.

This pou focuses on all the aspects that relate to water quality, including the impact of historic land use changes, sediment transport, urban stormwater management and the aspect of kai and nourishment from Te Whanga.

1. Te Ora o te Wai - Water Health

Action Plan

Pou Outcome: The water in the estuary is in optimal health.

Pou Objective: To give effect to Te Ora o te Wai to improve water quality through management of stormwater and other sources of pollution.

Indicator	Focus area	Initiative	Status	Start date	End date	Lead	Partners
Stormwater is either diverted or treated so that it does not negatively impact the water health of Te Whanga	1.1 Stormwater diversion and treatment	**1.1a Lagoon farm stormwater project.** Stormwater treatment and flood storage diversion.	Underway	2024	2030+	NCC	HBRC, MAT
		1.1b Thames/Tyne stormwater consent implementation and working group. Stormwater Working Group meetings are intended to have representation from those interacting with and contributing to stormwater quality affecting Thames-Tyne waterways and the Ahuriri Estuary. NCC's stormwater resource consent expires next year. A programme is needed to continue monitoring to capture long-term trends and look towards further optioneering and implementation of treatment options.	Underway	Ongoing	Ongoing	NCC	HBRC, MAT, Te Taiwhenua ō Te Whanganui-a-Orotu, Te Komiti, Catchment Collectives, Stormwater working group, industry owners, residential groups, stakeholder groups.
		1.1c Stormwater reserve property encroachment. Removing property encroachment within storm water reserves,	Underway	2024	Ongoing	NCC	
There is a strong understanding of potential pollutants in the stormwater going into the estuary at all times	1.2 Stormwater quality monitoring	**1.2a Water quality stations**. Permanent water quality stations at strategic locations throughout stormwater network. Automating spill gate operations (to prevent contamination into the estuary) are being investigated.	Underway	2024	Ongoing	NCC	HBRC, storm- water working group
		1.2b Cultural monitoring. Annual Purimu, Onehunga, and lagoon farm stormwater discharge cultural monitoring.	Underway	2024	2025	MAT	NCC
		1.2c Westshore tidal gates. Continuation of the 3-year joint monitoring program with HBRC on waterways feeding the discharge to inform budget priorities, identify contaminant sources, and meet resource consent requirements under Westshore tidal gates consent conditions. Additionally, consider end-of-line treatment solutions, stormwater education requirements, and establish a Collaborative Stormwater Working Group that serves beyond compliance purposes.	Underway	Ongoing	Ongoing	NCC	HBRC, MAT, Te Taiwhenua ō Te Whanganui-a-Orotu, Te Komiti, Catchment Collectives, Stormwater working group, industry owners, residential groups, stakeholder groups.

1. Te Ora o te Wai - Water Health

Action Plan

Pou Outcome: The water in the estuary is in optimal health.

Pou Objective: To give effect to Te Ora o te Wai to improve water quality through management of stormwater and other sources of pollution.

Indicator	Focus area	Initiative	Status	Start date	End date	Lead	Partners
Tributaries in the catchment have plans in place to manage the risks of negatively impacting Te Whanga	1.3 Catchment management	**1.3a Freshwater farm plans.** The Plan is relevant to landholders of the 1,000 small blocks that surround the estuary. We anticipate that the landowners commit to activities such as excluding stock from waterways, riparian planting, planting steep slopes, establishing small wetlands. This will help to reduce sediment runoff and support resilience of the catchment in future storm events.	Underway	Ongoing	Ongoing	ATCGT	HBRC and NZ Landcare Trust A2E.
		1.3b Ahuriri catchment/Flood control scheme. Improved flood resilience for Napier residential areas through design of ARP. Particularly with regard to management of the Taipo stream.	Underway	2024	2030+	NCC (Submitted by HBRC)	HBRC, MAT, wider community
		1.3c Proposed Plan Change 9 – TANK. The Tūtaekurī, Ahuriri, Ngaruroro and Karamū (TANK) Plan change introduces new provisions to manage the land and waterways of the Tūtaekurī, Ahuriri, Ngaruroro and Karamū (TANK) catchments. The Plan includes objectives for how to manage the water bodies in the catchments and the policies and rules needed to achieve the objectives.	Underway	2020	Ongoing	HBRC	NCC, HBRC, Te Komiti, Catchment Group, landowners, industry and stakeholders .
		1.3D Erosion Control Scheme. Hawke's Bay Regional Councils Erosion Control Scheme is there to help landowners across the region tackle erosion issues by using tools such as fencing, land retirement and non-commercial tree planting to help keep soil on hillslopes and out of water ways.	Ongoing (BAU)	Ongoing	2028	HBRC & landowners	

1. Te Ora o te Wai - Water Health

Action Plan

Pou Outcome: The water in the estuary is in optimal health.

Pou Objective: To give effect to Te Ora o te Wai to improve water quality through management of stormwater and other sources of pollution.

Indicator	Focus area	Initiative	Status	Start date	End date	Lead	Partners
A baseline of water and related environment quantity and quality is collectively formed.	1.4 Water and related environment quality monitoring and testing	**1.4a eDNA testing of water ways.** Form an analysis of the progress from testing (part of the sustainable centre in Hawke's Bay/Hastings). AEPS wants to find where species are spawning to then create protection for the species. The outcome is to create a protection programme, based on where they are spawning, and build fencing / planting.	Underway	2024	2024	AEPS and Wai Connection, Farmer, ATCGT	DOC
		1.4b Rainfall water monitoring. Rainfall event monitoring linked with Ahuriri Farm Pump Discharge Consent, will be conducted four times a year within the first two years of the consent commencement, along with bi-monthly water monitoring upstream of the pump at the discharge point when the pump is operational. A baseline monitoring report will be submitted on the Council at the end of the two-year period.	Not yet Started	2025	2035 (or as long as consent is granted)	Pāmu (occupier of Ahuriri farm)	
		1.4c Reducing sediment in the streams. We have commissioned PDP consultancy to carry out a range of tests to establish the current condition of the streams around the estuary. This will form a baseline to measure the impact of our activities. We have also carried out an eDNA testing programme supported by the Environmental Protection Agency "Wai Tuwhera o te Taiao" and are working with Wai Connection to continue this testing programme.	Underway	2024	TBC	ATCGT	PDP consulting and the Environmental Protection Agency
		1.4d Reporting of any environmental hazards/concerns. Take photos of any notable occurrences in the environment, such as slips, and send them to NCC Environmental Solutions team.	Ongoing (BAU)	Ongoing	Ongoing	AEPS	NCC, HBRC
		1.4d State of the environment monitoring. Monitoring of estuary ecology (infauna, fish, habitat, eDNA), estuary sediment quality (nutrients, metals, grain size, accumulation rate), stream water quality (nutrients, suspended sediment, E.coli), stream ecology (habitat, macroinvertebrates, fish, eDNA).	Underway	Ongoing	Ongoing	HBRC	

1. Te Ora o te Wai - Water Health

Action Plan

Pou Outcome: The water in the estuary is in optimal health.

Pou Objective: To give effect to Te Ora o te Wai to improve water quality through management of stormwater and other sources of pollution.

Indicator	Focus area	Initiative	Status	Start date	End date	Lead	Partners
continued: **A baseline of water and related environment quantity and quality is collectively formed.**	Continued: 1.4 Water and related environment quality monitoring and testing	**1.4h Ecological health assessments.** Multiple different methods to assess estuary health (Bayesian Network model, different health indices, susceptibility to eutrophication).	Complete			HBRC	
		1.4i Hydrodynamic model of estuary. Creation of a hydrological and constituent model of the Ahuriri Estuary to facilitate the understanding and management of environmental flows within the catchment. This model will also help to improve the water quality and ecological functions of both the catchment and the estuary.	Complete			HBRC	
		1.4j Baseline water and Environment. Creation of a comprehensive Catchment baseline monitoring project across all the tributaries in the Ahuriri Catchment. This analysis was completed by PDP environmental consultants. This project monitored 13 sites across the Ahuriri catchment, dry weather and first flush sediment and water testing including Rapid Habitat Assessments.	Complete			Ahuriri tributaries catchment group trust.	

1. Te Ora o te Wai - Water Health

Action Plan

Pou Outcome: The water in the estuary is in optimal health.

Pou Objective: To give effect to Te Ora o te Wai to improve water quality through management of stormwater and other sources of pollution.

Indicator	Focus area	Initiative	Status	Start date	End date	Lead	Partners
Water quality is improved through fit for purpose solutions in the catchment	1.5 Water quality enforcement and compliance	**1.5a Stormwater Bylaw enforcement.** NCC are able to follow up on any breaches of the stormwater bylaw to ensure only rain is discharged to the stormwater network. If non-complying discharges are found, NCC is going to provide enforcement to ensure this doesn't happen again as well as improving the quality of the discharge.	Underway	2024	Ongoing	NCC	
	1.6 Water quality environmental health and restoration	**1.6a Post-Cyclone Environmental Health Inter-agency Working Group**. Have worked on silt management, air quality, fresh water quality, shell fish etc.	Underway	2024	Ongoing	NCC and joint initiative	MAT, NCC, HBRC, HDC, CHBDC, Te Whatu Ora, FENZ, NIWA , MPI, MfE etc
		1.6b Seagrass Initiative. Investigate and implement methods of restoring seagrass beds in Te Whanga. This involves sourcing seagrass from other parts of Hawke's Bay to restore habitat in parts of the estuary where it's been lost.	Underway	Ongoing	Ongoing	NCC and MAT joint initiative	MAT, HBRC, DOC, biodiversity HB, EIT, National Aquarium, Sustainable HB
	1.7 Water quality planning	**1.7a Water quality masterplan - Estuary and tributaries.**	Underway	2024	2025	NCC	MAT, HBRC, DOC
Environmental restoration is routinely undertaken with the support of the community	1.8 Community engagement and cleanup	**1.8a Monthly litter clean up.** Start at Pandora pond and work around the estuary. A couple of hours on the second Sunday of every month. NCC collects big black rubbish sacks and provides all other resources in support of the clean up.	Ongoing (BAU)	Ongoing	Ongoing	AEPS	NCC

2. Te Mauri o te Taiao - Biodiversity

Summary

Pou Outcome: The estuary is a flourishing ecosystem that supports resilient biodiversity.

Pou Objective: Tautoko development of current and reintroduced species in the Whanga by restoring their habitats and eradicating competing and introduced pests, weeds, and disease.

Indicators of success

There are two indicators within this Pou linked to three focus areas:

Indicators	Relevant focus areas
Invasive species, pests and diseases have been addressed or are actively managed	2.1 Managing pests and invasive species
Habitats supporting biodiversity have been restored to an acceptable level	2.2 Kaitiaki 2.3 Restoration and planting

Initiatives

There are 12 initiatives from four lead organisations and five partners.

The estuary faces health and biodiversity degradation, requiring urgent conservation, habitat protection, and climate change mitigation. However, challenges such as development constraints, natural hazards, and climate change effects complicate these efforts. Ecology and biodiversity are important for estuaries as they provide essential ecosystem services, support species interactions, enhance resilience to environmental stressors, and serve as indicators of environmental health, cultural value, and recreational opportunities for communities.

This pou focusses on two large components of biodiversity at the Ahuriri Estuary including: Eradication of invasive species, and restoration of habitats to support existing species.

The action plan for this Pou is outlined in detail on the following page.

2. Te Mauri o te Taiao - Biodiversity

Summary

Pou Outcome: The estuary is a flourishing ecosystem that supports resilient biodiversity.

Pou Objective: Tautoko development of current and reintroduced species in the Whanga by restoring their habitats and eradicating competing and introduced pests, weeds, and disease.

Indicator	Focus area	Initiative	Status	Start date	End date	Lead	Partners
Invasive species, pests and diseases have been addressed or are actively managed	2.1 Managing pests and invasive species	**2.1a Predator Control.** Predator control to suppress introduced species that impact on threatened wildlife.	Underway	2024	Ongoing	DOC for Public Conservation Land	Volunteers, community groups, MAT
		2.1b Servicing and maintaining traps, bait stations etc. Support the community in delivering animal pest control to areas of high biodiversity value.	Ongoing (BAU)	Ongoing	Ongoing	HBRC	Te Taiwhenua o Te Whanganui a Orotu and other members of the public
		2.1c Pest control activites. Monitoring and analysing primary data collection or tag along with NCC.	Onoging (BAU)	Ongoing	Ongoing	MAT	NCC
		2.1d Tubeworms. Tubeworm is an invasive species that blocks waterways, it is manually removed to maintain waterways, eradication is highly unlikely.	Underway	2024	Ongoing	DOC	HBRC
		2.1e Weeds. Terrestrial and aquatic weed management.	Underway	2024	Ongoing	DOC for Public Conservation Land	Volunteers and community groups
		2.1f Staffled surveillance and Service Delivery. Apple of Sodom, White Edged Nightshade, Chilean Needle Grass.	Ongoing (BAU)	Ongoing	Ongoing	HBRC	Relevant landowners, relevant landowners, affected landowners

2. Te Mauri o te Taiao - Biodiversity

Summary

Pou Outcome: The estuary is a flourishing ecosystem that supports resilient biodiversity.

Pou Objective: Tautoko development of current and reintroduced species in the Whanga by restoring their habitats and eradicating competing and introduced pests, weeds, and disease.

Indicator	Focus area	Initiative	Status	Start date	End date	Lead	Partners
Habitats supporting biodiversity have been restored to an acceptable level	2.2 Kaitiaki	**2.2a Research of at risk indigenous species- Māori musk (Thyridia repens).** A subgroup of AEPS is organising the work to protect the plant. Aiming to create a display area.	Underway	Ongoing	2026	AEPS	DOC, HBRC
		2.2b Taonga species. Creating a habitat to reintroduce and protect taonga species i.e inanga spawning. ATCGT are working with APS and a local landowner to identify a salt water "wedge" in the Ahuriri lagoon where inanga breeding has historically been found. The intention is to protect this area.	Underway	Ongoing	2026	MAT	ATCGT & AEPS
		2.2c Kaitiaki rangers. Whānau task with specific kaitiakitanga functions.	Underway	Ongoing	Ongoing	MAT	
	2.3 Restoration and planting	**2.3a Landscape planting plan.** (Linked with Ahuriri Farm Pump Discharge consent) Planting for the water channels in Ahuriri Farm.	Not yet started	2025	2035+	Pāmu	Input from Maungaharuru-Tangitu, MAT, Ngati Parau and DOC.
		2.3b Planting of Kākābeak. We will encourage the planting of Kakabeak varieties native to Hawke's Bay in partnership with 'The Urban Kakabeak Project'.	Not yet started	2024	TBC	ATCGT	The Urban Kākābeak Project
		2.3c Environmental maintenance. General track and site maintenance, including cutting and spraying grass, and removing fallen dead trees.	Underway	Ongoing	Ongoing	DOC	

3. Aroā o Te Whanga - Historical & Education

Summary

Pou Outcome: Our taonga is acknowledged, promoted and understanding of it is shared with the Ahuriri people.

Pou Objective: To promote a greater understanding of Te Muriwai o Te Whanga and the issues relating to its health and well-being, and archaeological sites.

Indicators of success

There are 2 indicators within this Pou linked to 3 Focus areas:

Indicators	Relevant focus areas
Public knowledge on the environment, human impact, and conservation efforts is increased. The Whakapapa and history of Te Muriwai o Te Whanga is widely understood	3.1 Public engagement and education 3.2 Community outreach and events 3.3 Sharing our connection to Te Muriwai o Te Whanga

Initiatives

There are 11 initiatives from 2 lead organisations and 2 partners.

Te Whanganui-a-Orotu is a significant identifier of Ahuriri. Many people connect and identify with this body of water. It must be recognised that those who had initial and enduring contact and interaction with Te Whanganui-a-Orotu over many generations, are the primary kaitiaki. There is a depth and breadth generational mātauranga that ought to be adhered to and upheld alongside western scientific models of understanding and care of the estuary. Our taonga needs to be acknowledged, promoted and understanding of it shared with Ahuriri people

This pou focuses on enhancing Te Komiti's profile towards being a world leading example of partnership that emphasises Mātaraunga Māori in its' inherent ability to uplift the quality of our local ecosystems. It aims to foster education and connection of whānau to the land with Mātauranga Māori being key to resource use in conflict contexts.

The action plan for this Pou is outlined in detail on the following page.

3. Aroā o Te Whanga - Historical & Education

Action Plan

Pou Outcome: Our taonga is acknowledged, promoted and understanding of it is shared with the Ahuriri people.
Pou Objective: To promote a greater understanding of Te Muriwai o Te Whanga and the issues relating to its health and well-being, and archaeological sites.

Indicator	Focus area	Initiative	Status	Start date	End date	Lead	Partners
Public knowledge on the environment, human impact, and conservation efforts is increased.	3.1 Public engagement and education	**3.1a Protection of endangered birds through engagement and signage.** Talk to people and explain that the birds are present. We hope to put signs up soon to protect the area.	Ongoing (BAU)	Ongoing	Ongoing	AEPS	DOC, Forest and Bird, Police
		3.1b Twice yearly public viewing and talk of Godwit Migration. Opportunity to go on a guided walk with an expert to view the Godwits during spring and Autumn (all equipment provided).	Ongoing (BAU)	Ongoing	Ongoing	AEPS and BirdsNZ	Forest and Bird, Save the Dotterels
		3.1c Take schools groups twice a year to the estuary. Working alongside schools to educate students about the wildlife and ecosystem within and around the estuary.	Ongoing (BAU)	Ongoing	Ongoing	AEPS	Local schools
		3.1d Spread awareness about the estuary as a wildlife refuge. Focus on youth and incorporate appropriate signage.	Not yet started	2024	Ongoing	Forest and Bird	
	3.2 Community outreach and events	**3.2a Speakers/picnic to inform the public about the estuary.** Picnic in summer and indoors event in winter.	Ongoing (BAU)	Ongoing	Ongoing	AEPS	.
		3.2b Running community seminars. Six community seminars have been held on a range of topics, including cyclone recovery and resilience, eDNA testing and findings, history of Te Whanganui a Orotu both pre and post-Earthquake. Additionally, there was a field visit to the Holts family farm to showcase a QE2 covenant example of excellence in native planting, and 'Right Plant, Right Place' field event with Plant Hawke's Bay. Over 40 residents and partners attended each event, including local experts from Councils, Mana Ahuriri, Farmer support, Future Farming Trust, Environmental Protection Authority and Ministry of Primary Industries.	Ongoing (BAU)	2024	Ongoing	ATCGT	
		3.2c Compliance. Presence to educate public about the rare birds and designated areas: non-dog areas and dog-on-lead areas.	Underway	Ongoing	Ongoing	DOC	NCC

3. Aroā o Te Whanga - Historical & Education

Action Plan

Pou Outcome: Our taonga is acknowledged, promoted and understanding of it is shared with the Ahuriri people.
Pou Objective: To promote a greater understanding of Te Muriwai o Te Whanga and the issues relating to its health and well-being, and archaeological sites.

Indicator	Focus area	Initiative	Status	Start date	End date	Lead	Partners
The Whakapapa and history of Te Muriwai o Te Whanga is widely understood	3.3 Sharing our connection to Te Muriwai o Te Whanga	**3.3a Hāpu wānanga.** Series of wānanga to inform whānau on environmental matters and seek input for future direction.	Ongoing (BAU)	2024	Ongoing	MAT	All
		3.3b Whakapapa. Our connection to te taiao.	Ongoing (BAU)	2024	Ongoing	MAT	All
		3.3c Storytelling. Sharing stories on te taiao.	Ongoing (BAU)	2024	Ongoing	MAT	All
		3.3d Mapping. We will map remaining examples of native forest and bushland in the catchment to research and record the historical uses. Where possible, we will re-establish these trees and plants for future generations.	Not yet started	TBC	TBC	ATCGT	All

4. Te Mahi Ohaoha - Economic

Summary

Pou Outcome: Receive value through sustainable practices and use of the estuary to promote further growth for whānau, hāpu, and the wider community.

Pou Objective: All stakeholders engage in sustainable practices and responsible use of the estuary. Mana Ahuriri is a leader in eco tourism.

Indicators of success

There are 2 indicators (TBC) within this Pou linked to 2 Focus areas:

Indicators	Relevant focus areas
TBC	4.1 Infrastructure investment
TBC	4.2 Economic development

Initiatives
There are 4 initiatives from 2 lead organisations and 3+ partners.

Te Whanga is a 'crown jewel' that is a natural resource with the ability to provide an interconnected future. Restoring the health of Te Whanga can create opportunities for economic growth, education, cultural connection and recreational use.

Ko rua te paia ko Te Whanga, He kainga tō te ata, He kainga ka awatea, He kainga ka ahiahi.

Te Whanga is the storehouse that never closes, A meal in the morning, A meal at noon. A meal in the evening

This pou ensures that through sustainable development Te Whanga can be a source of not only kai, but economic prosperity, housing, recreation and more.

The action plan for this Pou is outlined in detail on the following page.

4. Te Mahi Ohaoha - Economic

Action Plan

Pou Outcome: Receive value through sustainable practices and use of the estuary to promote further growth for whānau, hāpu, and the wider community.

Pou Objective: All stakeholders engage in sustainable practices and responsible use of the estuary. Mana Ahuriri is a leader in eco tourism.

Indicator	Focus area	Initiative	Status	Start date	End date	Lead	Partners
TBC	4.1 Infrastructure investment	**4.1a Airport.** Invest in the HB airport to grow economic base.	Underway	TBC	TBC	MAT	
		4.1b State Highway. TREC constructions on East Coast highway.	Ongoing (BAU)	TBC	TBC	Waka Kotahi	Kiwi Rail, stakeholders, contractors
TBC	4.2 Economic development	**4.1a TBC.** Te Komiti envisions that sustainable economic use of the estuary for tourism could be an option in the future.	TBC	TBC	TBC	MAT	
		4.1b Future Development strategy. Aspirations for housing, Ecologically Sensitive Business Hub, upgrades to airport, solar farm, and enhancement to Te Whanga.	Underway	TBC	TBC	MAT	Land Transfer Act (LTA) and Crown

5. Te Mahi Tūhono a Roopu - Social

Summary

Pou Outcome: All stakeholders unite to improve Te Whanga, making it a hub for community betterment through activities like kai, exercise and recreation.

Pou Objective: He waka eke noa. Ensure alignment and collaboration between all stakeholders, fostering strategic partnerships aimed at enhancing and improving the well-being of Te Whanga.

Indicators of success

There are 2 indicators within this Pou linked to 3 Focus areas:

Indicators	Relevant focus areas
The estuary supports a range of recreational options for the community in a sustainable way	5.1 Recreational activities 5.2 Infrastructure
People in the catchment are connected and collaborate with programmes and plans	5.3 Community engagement and support

Initiatives

There are 5 initiatives from 4 lead organisations and 6+ partners.

Our partners play a vital role in supporting us to achieve our vision. This pou ensures we focus on growing genuine partnership with all of our key stakeholders, including ngā hapū o Ahuriri, Napier City Council, Hawke's Bay Regional Council, Hastings District Council, Te Papa Atawhai (Department of Conservation), the wider Ahuriri community, and other key partners. Mana whenua and local government are aligned and working in partnership for the betterment of Te Whanga.

He waka eke noa

This pou is to ensure alignment and collaboration between mana whenua and local government, fostering a strategic partnership aimed at enhancing and improving the well-being of Te Whanga.

The action plan for this Pou is outlined in detail on the following page.

5. Te Mahi Tūhono a Roopu - Social

Action Plan

Pou Outcome: All stakeholders unite to improve Te Whanga, making it a hub for community betterment through activities like kai, exercise and recreation.

Pou Objective: He waka eke noa. Ensure alignment and collaboration between all stakeholders, fostering strategic partnerships aimed at enhancing and improving the well-being of the Whanga.

Indicator	Focus area	Initiatives	Status	Start date	End Date	Lead	Partners
The estuary supports a range of recreational options for the community in a sustainable way	5.1 Recreational activities	**5.1a Water sports hub (waka ama, Napier sailing club, fishing club).** Relocate waka ama into pandora pond, waka ama to continue to grow at estuary. Includes infrastructure changes and information centre/signs.	Ongoing (BAU)	Ongoing	Ongoing	NCC and MAT	Community groups
		5.1b Triathlon events (iron Māori and world triathlon series). Aim to have the swim located at pandora pond again.	Ongoing (BAU)	Ongoing	Ongoing	MAT	Community groups and organisers of the event
	5.2 Infrastructure	**5.2a Ahuriri Regional Park**	Underway	2024	2030+	NCC	HBRC, MAT, HB airport, DOC, wider community
		5.2b Boardwalk review. Review structural integrity and need for boardwalks, consider removal or replacements.	Not yet started	2024	2027	DOC	TBC
People in the catchment are connected and collaborate with programmes and plans	5.3 Community engagement and support	**5.3a Ongoing community engagement/ support.** Work to engage our community and promote interest and excitement in the potential of the Ahuriri environment. In due course, community members will be able to share their knowledge and enthusiasm amongst their neighbours and build on the positive community spirit.	Ongoing (BAU)	Ongoing	Ongoing	ATCGT	All

6. Ahurea o te Whenua - Cultural & Spiritual

Summary

Pou Outcome: The cultural and spiritual identity of Te Whanga and the wider catchment are enhanced in order to support the connection between people and land.

Pou Objective: Enhance a community that recognises the cultural significance of the estuary through prioritising tikanga and mātauranga Māori which includes upholding the mana of local sites of significance / wāhi tapu.

Indicators of success

There are 3 indicators within this Pou linked to 3 Focus areas:

Indicators	Relevant focus areas
There are designated areas for cultural practice and preservation (including mātauranga Māori informed practices relative to Te Whanga)	6.1 Cultural practices
Māori have visible representation in relevant locations and forums for the benefit of Te Whanga	6.2 Cultural representation
Monitoring of items of cultural importance is occurring	6.3 Cultural monitoring

Initiatives

There are 7 initiatives from 7 lead organisations and 7 partners.

Developing the cultural and spiritual identity of Te Whanga and its catchment is pivotal for fostering a strong bond between the community and the land. By embracing and preserving traditional practices, stories, and rituals, this initiative not only deepens a sense of belonging but also instills a collective commitment to sustainable stewardship, aligning with principles of kaitiakitanga and promoting a resilient and culturally rich community.

The purpose of this pou is to enhance a community that recognises the cultural significance of the estuary through prioritising tikanga and upholding mataurangа Māori.

The action plan for this Pou is outlined in detail on the following page.

6. Ahurea o te Whenua - Cultural & Spiritual

Action Plan

Pou Outcome: The cultural and spiritual identity of Te Whanga and the wider catchment are enhanced in order to support the connection between people and land.

Pou Objective: Enhance a community that recognises the cultural significance of the estuary through prioritising tikanga and mātauranga Māori which includes upholding the mana of local sites of significance / wāhi tapu.

Indicator	Focus area	Initiatives	Status	Start date	End date	Lead	Partners
There are designated areas for cultural practice and preservation (including mātauranga Māori informed practices relative to Te Whanga)	6.1 Cultural practices	**6.1a Koura trapping.** Mana Ahuriri has expressed an interest to demonstrate traditional Koura trapping practices in the Wharerangi stream. This will particularly be targeted at local tamariki.	Not yet started	TBC	TBC	ATCGT	MAT
		6.1b Māori historical use of plants. Provide information leaflets to our residents who take up our Mini Freshwater Environment Plan Initiative on the Māori medicinal or cultural uses of plants found in Hawke's Bay.	Not yet started	TBC	TBC	ATCGT	MAT
		6.1c Create a place to participate in tikanga. Baptism, tangihanga, pūre, karakia, etc	Not yet started	TBC	TBC	MAT	
		6.1d. Rāhui. Under guidance of Kahui Kaumātua, place a Rāhui when water quality poses a threat to human health or the health of the ecosystem, including instances where human activities or invasive species are harming water quality. A Rāhui may also be placed following a tangihanga (funeral) or for other cultural reasons, to protect the Wairua of the environment.	underway	ongoing	ongoing	MAT	NCC
Māori have visible representation in relevant locations and forums for the benefit of Te Whanga	6.2 Cultural representation	**6.2a Estuary Pou replacement.** Replacement of six pou in the estuary with new pou in improved locations.	Underway	2024	2025	DOC (Submitted by MAT)	NCC, MAT
		6.2b National iwi chairs. Pou taiao - iwi response to environmental matters.	Ongoing	Ongoing	Ongoing	MAT	

6. Ahurea o te Whenua - Cultural & Spiritual

Action Plan

Pou Outcome: The cultural and spiritual identity of Te Whanga and the wider catchment are enhanced in order to support the connection between people and land.

Pou Objective: Enhance a community that recognises the cultural significance of the estuary through prioritising tikanga and mātauranga Māori which includes upholding the mana of local sites of significance / wāhi tapu.

Indicator	Focus area	Initiatives	Status	Start date	End date	Lead	Partners
Monitoring of items of cultural importance is occurring	6.3 Cultural monitoring	**6.3a Cultural monitoring programme.** Under consent conditions, four cultural monitoring programmes are underway to ensure health and wellbeing of taiao and māhinga kai are protected.	Underway	2024	Ongoing	NCC	HBRC, MAT
		6.3b Mahinga Kai cultural monitoring program. (Linked with Ahuriri Farm Pump Discharge consent) Focus on shellfish – monitoring to start within 3 months of the commencement, annual report prepared and submitted to councils.	Not Yet Started	2025	2035+	Pāmu	Hapu

Appendices

A: Regulatory / Non-Regulatory Levers

B: Summary of Pou Indicators

C: SO Plan

D: Broader Initiatives

A: Regulatory / Non-Regulatory Levers

Regulatory Levers

Regulation Resource Management Act

The planning committees of NCC, HBRC, and HDC and their staff must have regard to the Plan.

The HB Conservation board must taken into account the objectives and values of the plan as they develop, deliver and make decisions on the HB Conservation Management strategy.

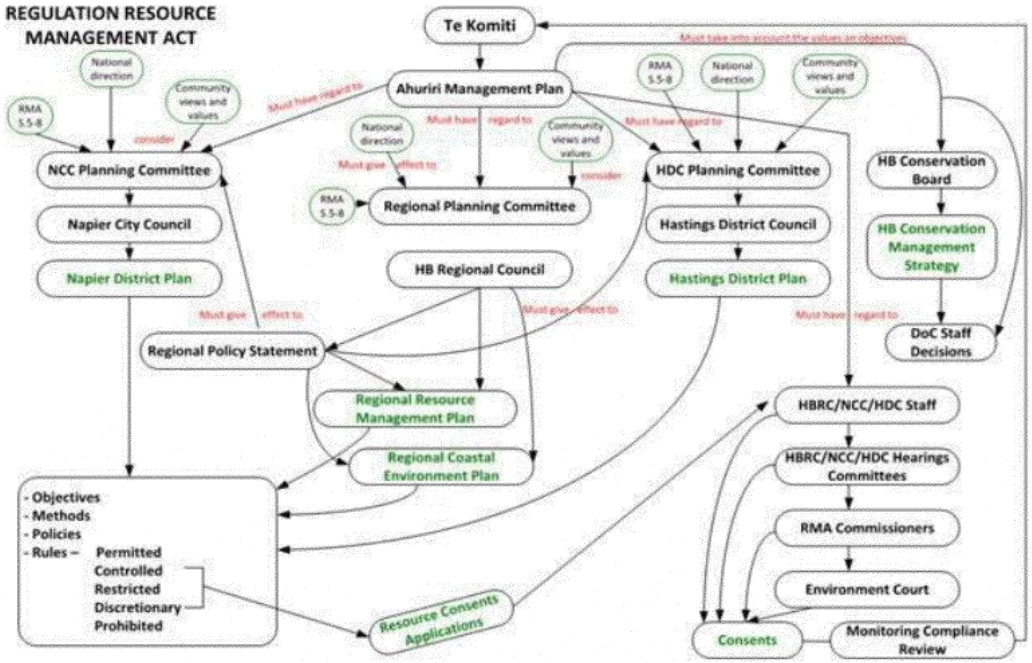

Note: This diagram is indicative only for illustrative purposes.

Investment (Non-Regulatory) Levers

Non-Regulatory Local Government Act

The involved councils; Napier City Council (NCC), Hawke's Bay Regional Council (HBRC), and Hastings District Council (HDC) must all have regard to the Plan.

This requirement extends to their Long Term Plans (LTPs), annual plans, and asset management plans, all of which must have regard to the Plan. This will influence decision-making in the respective areas.

Te Komiti will a) ensure each organisation understands how they can have regard to the Plan in their own planning processes and will b) submit on consultations and in hearings if consultations are not aligned to this Rautaki.

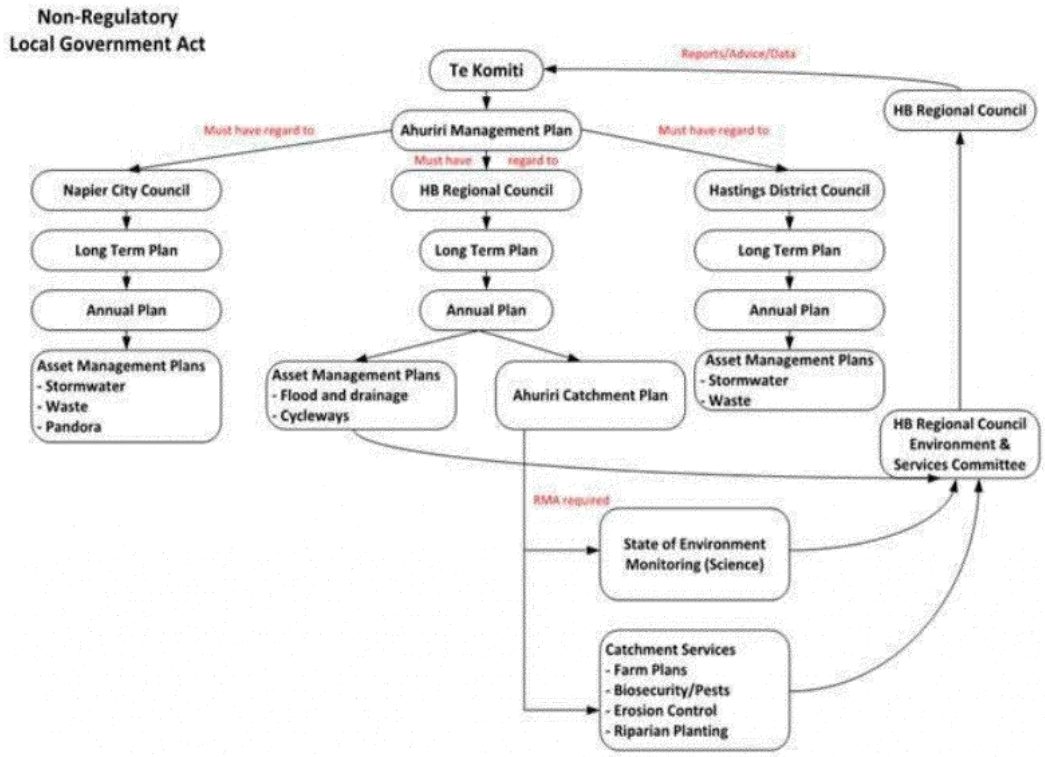

Note: This diagram is indicative only for illustrative purposes.

B: SO Plan

Te Muriwai o Te Whanga

Catchment SO 486367

Statutory Definition of Te Muriwai o Te Whanga: Ahuriri Estuary and catchment areas

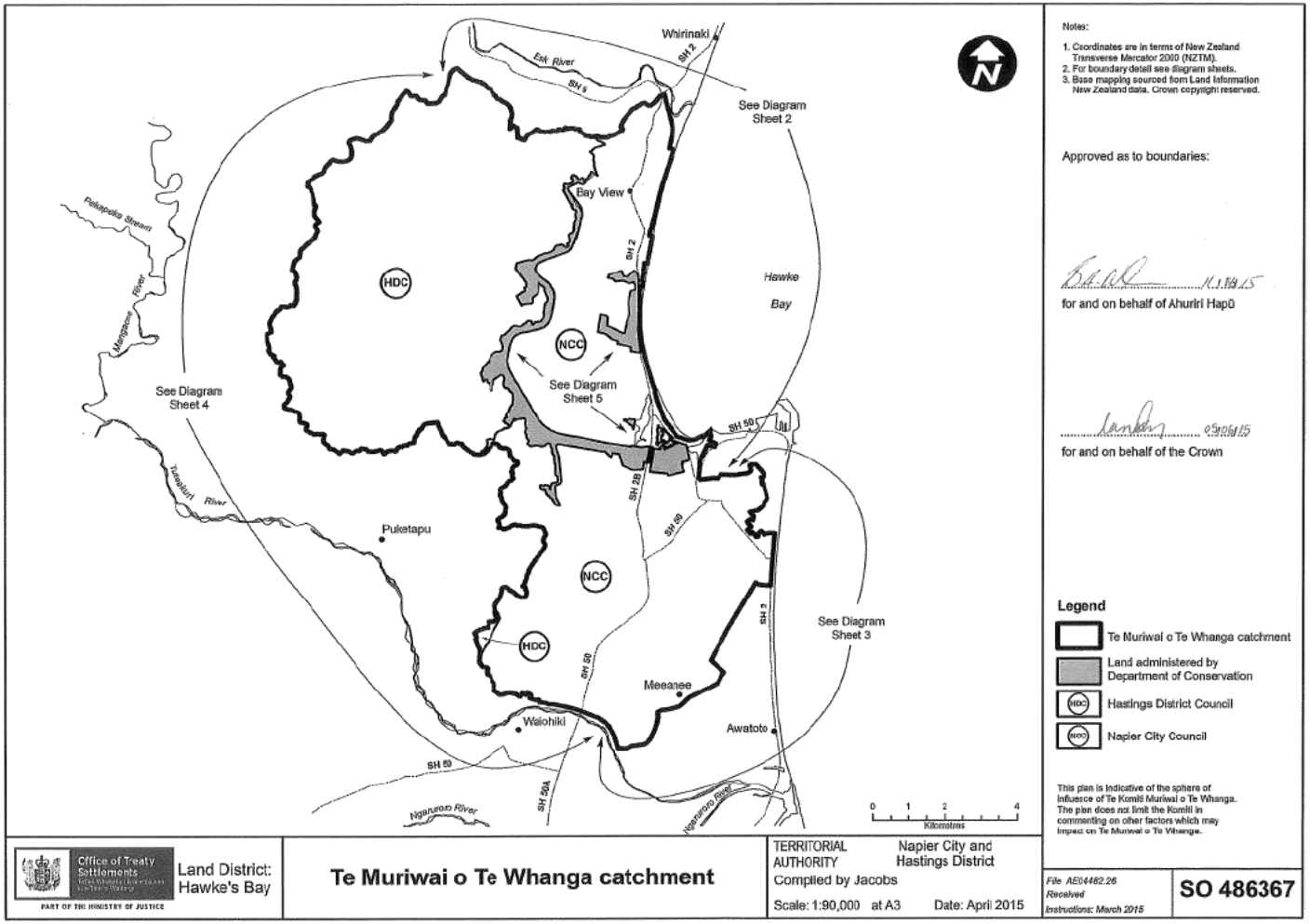

Te Komiti Muriwai o Te Whanga

C: Summary of Indicators

Summary of Indicators 1/2

Pou	Indicators
Te Ora o te Wai	Stormwater is either diverted or treated so that it does not negatively impact the water health of Te Whanga
	There is a strong understanding of potential pollutants in the stormwater going into the estuary at all times
	Tributaries in the catchment have plans in place to manage the risks of negatively impacting Te Whanga
	A baseline of water and related environment quantity and quality is collectively formed
	Water quality is improved through fit for purpose solutions in the catchment
	Environmental restoration is routinely undertaken with the support of the community
Te Mauri o te Taiao	Invasive species, pests and diseases have been addressed or are actively managed
	Habitats supporting biodiversity have been restored to an acceptable level
Aroā o Te Whanga	Public knowledge on the environment, human impact, and conservation efforts is increased.
	The Whakapapa and history of Te Muriwai o Te Whanga is widely understood

Summary of Indicators 2/2

Pou	Indicators
Te Mahi Ohaoha	TBC
	TBC
Te Mahi Tūhono a Roopu	The estuary supports a range of recreational options for the community in a sustainable way
	People in the catchment are connected and collaborate with programmes and plans
Ahurea o te Whenua	There are designated areas for cultural practice and preservation (including mātauranga Māori informed practices relative to Te Whanga)
	Māori have visible representation in relevant locations and forums for the benefit of Te Whanga
	Monitoring of items of cultural importance is occurring

D: Broader initiatives plan

Includes initiative submitted that were not intended for the Plan.

Te Ora o te Wai - Water Health

Broader Plan

Focus area	Initiatives	Status	Start date	End date	Lead	Partners
Storm water	**Bay View Ocean Outfall.** A pump station and ocean outfall will direct stormwater from Esk Hills and Bay View directly to the ocean, instead of routing it through the Onehunga Pump Station, which typically charges to the estuary.	Not yet started	2030+	2030+	NCC	HBRC
	Guppy Road and Harold Holt stormwater pump station upgrades. Pump station and pipe upgrades to remove bottlenecks in the network to prevent wet weather overflows into the stormwater network.	Underway	2024	2029	NCC	HBRC
	3 Waters Masterplan. Revisiting each of the 3 waters masterplans, along with the overarching masterplan, to ensure the strategic management, planning of networks, and modelling are up to date.	Underway	2024	2026	NCC	
	Statutory acknowledgment. CIA on stormwater and discharge into stormwater.	Ongoing (BAU)	Ongoing	Ongoing	MAT	NCC, HBRC, Developers
	Drainage and Flood Management Scheme (Heretaunga Plains Flood Control Scheme). Management of Stormwater: Area 1: Meeanee/Napier/Puketapu Drainage area.	Ongoing (BAU)	Ongoing	Ongoing	HBRC	NCC
	Reducing erosion in upper catchments to avoid sediment in lower catchments. Reducing erosion in upper catchments to avoid sediment in lower catchments.	Ongoing (BAU)	Ongoing	Ongoing	HBRC	HDC, DOC, private land owners/managers, ATCGT
	Northern Ahuriri Estuary Stopbank Maintenance.	Underway	Ongoing	Ongoing	HBRC	

Te Ora o te Wai - Water Health

Broader Plan

Focus area	Initiatives	Status	Start date	End date	Lead	Partners
Stormwater	**Environmental Management Plan for high risk sites.** Identifying high risk industries to see if they pose a risk to waterways. Helping them create an environmental management plan, and enforce their implementation. Ahuriri is next to be investigated and Pandora to be revisited.	Underway	Ongoing	Ongoing	HBRC, NCC	Pollutant Response
	Royal society catalyst. Novel biological and chemical methods to identify stormwater pollutants.	Ongoing (BAU)	Ongoing	2025	Royal catalyst	MAT, NCC
	MAT taiao plan. Strategic plan to support operations in the taiao for Mana Ahuriri.	Underway	2024	2024	MAT	Poipoia
	Proposed District Plan. Introduction of new provisions in the PDP that require on-site treatment on large car parks and state highways.	Underway	2025	2027	NCC	
Water quality	**Shellfish quality relating to Ocean Outfall.** Research programme looking into the effect of the ocean outfall on toxin levels in shellfish.	Underway	2024	2028	NCC	HBRC, MAT, DOC
	Stormwater By-law review.	Underway	2024	2025	NCC	
	Sediment and erosion programme. Monitoring and enforcement of all development sites across Napier. Conditions relating to earthworks require enforcement.	Underway	2024	Ongoing	NCC	MAT, HBRC

Te Ora o te Wai - Water Health

Broader Plan

Focus area	Initiatives	Status	Start date	End date	Lead	Partners
Water quality	**Sustainable seas.** Initiative to identify models and methodologies to better inform coastal monitoring and management across aotearoa. Ahuriri estuary as a selected case study.	Underway	Ongoing	2025	MFE	MAT
	Water Supply Master Plan. Supply of freshwater to homes and businesses.	Underway	Ongoing	2025	NCC	
Other	**Taiao and tikanga committees.** MAT board oversight on taiao and tikanga.	Ongoing (BAU)	Ongoing	Ongoing	MAT	
	Farm environment plan. Linked with Ahuriri Farm Pump Discharge consent	Underway	2024	2035	Pāmu	
	Landscape planting plan. Planting for the water channels in Ahuriri Farm.	Not yet started	2024	2034	Pāmu	Input from Maungaharuru-Tangitū, Mana Ahuriri Trust, Ngati Pārau and DOC.
	Kotahi plan. Collaborate on the Kotahi plan to ensure better outcomes for Taiao.				HBRC	MAT, other PSGE's

Te Mauri o te Taiao - Biodiversity

Broader Plan

Focus area	Initiatives	Status	Start date	End date	Lead	Partners
Restore Habitats	**Fish passage.** Passages on pump stations and tidal gates.	Ongoing (BAU)	Ongoing	Ongoing	NCC	MAT, HBRC
	Protection and Enhancement Programme. This fund aims to deliver high-value environmental outcomes on a catchment/sub-catchment scale, such as improved water quality, riparian protection, biodiversity enhancement, and wetland development.	Ongoing (BAU)	Ongoing	Ongoing	HBRC	Landholders, Iwi, QEII, Nga Whenua Rahui, DOC, Catchment and Community Groups, Biodiversity Hawke's Bay.
	Priority Ecosystem Programme. This programme was initiated in the 2018-2028 LTP and is focused on preventing the extinction of the remaining high biodiversity remnants in Hawke's Bay.	Ongoing (BAU)	Ongoing	Ongoing	HBRC	Landholders, Iwi, QEII, Nga Whenua Rahui, DOC, Catchment and Community Groups, Biodiversity Hawke's Bay.
	Retiring grazing leases. We are reviewing current lease agreements with DOC to transition these into regenerative wetland.	Underway	2024	2025	DOC	MAT, Taiwhenua o Te Whanganui o Orotu, lessee
	Taonga species. Identify taonga species and give detail to quality, quantity etc.	Ongoing (BAU)	Ongoing	Ongoing	MAT	NCC

Aroā o Te Whanga - Historical & Education

Broader Plan

Focus area	Initiatives	Status	Start date	End date	Lead	Partners
Increase awareness of history, environment, and conservation to the public	**Dual language signage.** Appropriate Māori names of our sites, roads, waters, whenua and maunga.	Not yet started	2024	Ongoing	NCC, DOC,	MAT
	Sites of significance. Recording of sites of significance in council plans.	Ongoing (BAU)	2024	2024	TLA's	MAT, Crown
	Curriculum. Local stories incorporated in local curriculum.	Not yet started	2025	Ongoing	Ministry of Education	MAT
	Update Estuary Signage. Update names on current signage on the estuary. Also review design and concept.	Not Yet started	2024	2024	DOCs	MAT, Te Komiti, NCC, HB tourism, HBRC
	Bridge wrapping. To raise the awareness of the connection between what goes down the drain enters our river, estuaries and oceans.	Complete	2024	2024	NCC	Te Komiti

Te Mahi Ohaoha - Economic

Broader Plan

Focus area	Initiatives	Status	Start date	End date	Lead	Partners
Transport infrastructure to support access	**Northern Ahuriri Estuary Stopbank Maintenance.** Mana Ahuriri, HB Airport, Pāmu, NCC, HBRC discussion on Stopbank Maintenance and inclusion into HBRC run scheme.	Underway	Ongoing	Ongoing	HBRC	MAT, HB Airport, Pamu, NCC, HBRC
	Maintaining critical Infrastructure. Provision of strategic life line resilience.	Ongoing (BAU)	Ongoing	Ongoing	NZTA	HBRC Regional transport Plan

Te Mahi Tūhono a Roopu - Social

Broader Plan

Focus area	Initiatives	Status	Start date	End date	Lead	Partners
Recreational facilities and infrastructure	**Ahuriri rock pools.** Community initiative to build rock pool down Hardinge road. Provide coastal protection.	Underway	Ongoing	Ongoing	NCC	MAT, Ahuriri Rock Pool Development
	Hawke's Bay Cycle Trails including Great Rides (Water Ride). Ongoing development & maintenance of Hawke's Bay Cycle Trails including Great Rides (Water Ride).	Ongoing (BAU)	Ongoing	Ongoing	HBRC	NCC
	Iway cycle trail network. Ongoing development and maintenance of Iway cycle network.	Ongoing (BAU)	Ongoing	Ongoing	NCC, HDC	HBRC, cycling advocacy groups, wider public
	Bird watching. 2-3 bird watching platforms beside Water Ride cycle trail in Ahuriri Regional Park.	Ongoing (BAU)	Ongoing	Ongoing	Asset Ownership TBC	HBRC, DOC
	Sports field irrigation project. Currently an approach to irrigation of sportsfield, with reliance on water from network. Limits on how much water can be taken.	Not yet started	2024	2025	NCC	
Other	**Tourism opportunities.** World class environmental eco-tourism attraction.	Not yet started	2024	Ongoing	MAT	NCC, HBRC

Ahurea o te Whenua - Cultural & Spiritual

Broader Plan

Focus area	Initiatives	Status	Start date	End date	Lead	Partners
Cultural preservation and practice (including mātauranga Māori informed practices relative to Te Whanga	**Waka Ama Hub.** Provision of purpose-built facilities for waka storage at Humber St. Reserve.	Underway	2024	Ongoing	NCC	MAT
	Whakapapa research. Identify sites of significance, ancestral stories, etc.	Ongoing (BAU)	Ongoing	Ongoing	MAT	NCC
Partnering with mana whenua on initiatives	**Taiao unit.** PSGE collaboration in RMA matters.	Ongoing (BAU)	Ongoing	Ongoing	MAT	Te Kahui Ohanga

Ngā mihi nui

2024 | Te Komiti Muriwai o Te Whanga

Te Muriwai o Te Whanga Plan

The Te Muriwai o Te Whanga Plan significantly influences RMA planning documents and resource consent decisions. Local authorities must give regard to the plan when preparing or amending regional policy statements, regional plans, or district plans if its contents pertain to resource management issues and if it is the most appropriate means to achieve the Act's purpose. Settlement Act Section

Any required reports or decisions must explicitly state compliance with the plan. Additionally, when evaluating resource consent applications for activities within Te Muriwai o Te Whanga, authorities must consider the Plan's relevance and necessity in determining the application. Settlement Act Section

The Plan's relevance extends to local government matters under the Local Government Act 2002, where any local authority making a non-regulatory decision (including funding decisions) under The Act pertaining to Te Muriwai o Te Whanga, needs to have regard to this Plan. This can apply to decision making related (but not limited) to local Asset Management Plans, Ahuriri Catchment Plans, Annual and Long-Term Plans. Settlement Act Section

Action Plan – HBRC as lead agency

Te Ora o te Wai - Water Health							
Indicator	**Focus area**	**Initiative**	**Status**	**Start date**	**End date**	**Partners**	**Who at HBRC**
Tributaries in the catchment have plans in place to manage the risks of negatively impacting Te Whanga	1.3 Catchment management	1.3c Proposed Plan Change 9 - TANK. The Tūtaekurī, Ahuriri, Ngaruroro and Karamū (TANK) Plan change introduces new provisions to manage the land and waterways of the Tūtaekurī, Ahuriri, Ngaruroro and Karamū (TANK) catchments. The Plan includes objectives for how to manage the water bodies in the catchments and the policies and rules needed to achieve the objectives	Underway	2020	Ongoing	NCC, Te Komiti, Catchment Group, landowners, industry and stakeholders	Policy and Planning
		1.3d Erosion Control Scheme. Hawke's Bay Regional Councils Erosion Control Scheme is there to help landowners across the region tackle erosion issues by using tools such as fencing, land retirement and non-commercial tree planting to help keep soil on hillslopes and out of water ways	Ongoing (BAU)	Ongoing	2028	Landowners	ICM
A baseline of water and related environment quantity and quality is collectively formed.	1.4 Water and related environment quality monitoring and testing	1.4d State of the environment monitoring. Monitoring of estuary ecology (infauna, fish, habitat, eDNA), estuary sediment quality (nutrients, metals, grain size, accumulation rate), stream water quality (nutrients, suspended sediment, E.coli), stream ecology (habitat, macroinvertebrates, fish, eDNA).	Underway	Ongoing	Ongoing		Science
		1.4h Ecological health assessments. Multiple different methods to assess estuary health (Bayesian Network model, different health indices, susceptibility to eutrophication).	Complete				Science
		1.4i Hydrodynamic model of estuary. Creation of a hydrological and constituent model of the Ahuriri Estuary to facilitate the understanding and management of environmental flows within	Complete				Science

		the catchment. This model will also help to improve the water quality and ecological functions of both the catchment and the estuary					
Te Mauri o te Taiao - Biodiversity							
Indicator	**Focus area**	**Initiative**	**Status**	**Start date**	**End date**	**Partners**	**Who at HBRC**
Invasive species, pests and diseases have been addressed or are actively managed	2.1 Managing pests and invasive species	2.1b Servicing and maintaining traps, bait stations etc. Support the community in delivering animal pest control to areas of high biodiversity value.	Ongoing (BAU)	Ongoing	Ongoing	Te Taiwhenua o Te Whanganui a Orotu and other members of the public	Biodiversity/Biosecurity
		2.1f Staff led surveillance and Service Delivery. Apple of Sodom, White Edged Nightshade, Chilean Needle Grass.	Ongoing (BAU)	Ongoing	Ongoing	Relevant landowners, relevant landowners, affected landowners	Biodiversity/Biosecurity

Action Plan – HBRC as partner agency

Te Ora o te Wai - Water Health								
Indicator	**Focus area**	**Initiative**	**Status**	**Start date**	**End date**	**Lead**	**Partners**	**Who at HBRC**
Stormwater is either diverted or treated so that it does not negatively impact the water health of Te Whanga	1.1 Stormwater diversion and treatment	1.1a Lagoon farm stormwater project. Stormwater treatment and flood storage diversion	Underway	2024	2030+	NCC	MAT	
		1.1b Thames/Tyne stormwater consent implementation and working group. Stormwater Working Group meetings are intended to have representation from those interacting with and contributing to stormwater quality affecting Thames-Tyne waterways and the Ahuriri Estuary. NCC's stormwater resource consent expires next year. A programme is needed to continue monitoring to capture long-term trends and look towards further optioneering and implementation of treatment options.	Underway	Ongoing	Ongoing	NCC	MAT, Te Taiwhenua ō Te Whanganui-a-Orotu, Te Komiti, Catchment Collectives, Stormwater working group, industry owners, residential groups, stakeholder groups	
There is a strong understanding of potential pollutants in the stormwater going into the estuary at all times	1.2 Stormwater quality monitoring	1.2a Water quality stations. Permanent water quality stations at strategic locations throughout stormwater network. Automating spill gate operations (to prevent contamination into the estuary) are being investigated.	Underway	2024	Ongoing	NCC	Storm-water working group	
		1.2c Westshore tidal gates. Continuation of the 3-year joint monitoring program with HBRC on waterways feeding the discharge to inform budget priorities, identify contaminant sources, and meet resource consent requirements under Westshore tidal gates consent conditions. Additionally, consider end-of-line treatment solutions, stormwater education requirements, and establish a Collaborative Stormwater	Underway	Ongoing	Ongoing	NCC	MAT, Te Taiwhenua ō Te Whanganui-a-Orotu, Te Komiti, Catchment Collectives, Stormwater working group, industry owners, residential groups, stakeholder groups	

		Working Group that serves beyond compliance purposes.						
Tributaries in the catchment have plans in place to manage the risks of negatively impacting Te Whanga	1.3 Catchment management	1.3a Freshwater farm plans. The Plan is relevant to landholders of the 1,000 small blocks that surround the estuary. We anticipate that the landowners commit to activities such as excluding stock from waterways, riparian planting, planting steep slopes, establishing small wetlands. This will help to reduce sediment runoff and support resilience of the catchment in future storm events.	Underway	Ongoing	Ongoing	ATCGT	NZ Landcare Trust A2E	
		1.3b Ahuriri catchment/Flood control scheme. Improved flood resilience for Napier residential areas through design of ARP. Particularly with regard to management of the Taipo stream.	Underway	2024	2030+	NCC	MAT, wider community	
A baseline of water and related environment quantity and quality is collectively formed.	1.4 Water and related environment quality monitoring and testing	1.4d Reporting of any environmental hazards/concerns. Take photos of any notable occurrences in the environment, such as slips, and send them to NCC Environmental Solutions team.	Ongoing (BAU)	Ongoing	Ongoing	AEPS	NCC	
Water quality is improved through fit for purpose solutions in the catchment	1.6 Water quality environmental health and restoration	1.6a Post-Cyclone Environmental Health Inter-Agency Working Group. Have worked on silt management, air quality, freshwater quality, shellfish etc.	Underway	2024	Ongoing	NCC and joint initiative	MAT, NCC, HDC, CHBDC, Te Whatu Ora, FENZ, NIWA , MPI, MfE etc	
		1.6b Seagrass Initiative. Investigate and implement methods of restoring seagrass beds in Te Whanga. This involves sourcing seagrass from other parts of Hawke's Bay to restore habitat in parts of the estuary where it's been lost.	Underway	Ongoing	Ongoing	NCC and MAT joint initiative	MAT, DOC, biodiversity HB, EIT, National Aquarium, Sustainable HB	Science
	1.7 Water quality planning	1.7a Water quality masterplan - Estuary and tributaries.	Underway	2024	2025	NCC	MAT, DOC	
Te Mauri o te Taiao - Biodiversity								
Indicator	**Focus area**	**Initiative**	**Status**	**Start date**	**End date**	**Lead**	**Partners**	**Who at HBRC**
Invasive species, pests and diseases have been addressed or are actively managed	2.1 Managing pests and invasive species	2.1d Tubeworms. Tubeworm is an invasive species that blocks waterways, it is manually removed to maintain waterways, eradication is highly unlikely	Underway	2024	Ongoing	DOC	Te Taiwhenua o Te Whanganui a Orotu and other members of the public	Science
Habitats supporting biodiversity have been restored to an acceptable level	2.2 Kaitiaki	2.2a Research of at risk indigenous species- Māori musk (Thyridia repens). A subgroup of AEPS is organising the work to protect the plant. Aiming to create a display area.	Underway	Ongoing	2026	AEPS	DOC	Science
Te Mahi Tūhono a Roopu - Social								
Indicator	**Focus area**	**Initiative**	**Status**	**Start date**	**End date**	**Lead**	**Partners**	**Who at HBRC**
The estuary supports a range of recreational options for the	5.2 Infrastructure	5.2a Ahuriri Regional Park	Underway	2024	2030+	NCC	MAT, HB airport, DOC, wider community	

community in a sustainable way								
Ahurea o te Whenua - Cultural & Spiritual								
Indicator	**Focus area**	**Initiative**	**Status**	**Start date**	**End date**	**Lead**	**Partners**	**Who at HBRC**
Monitoring of items of cultural importance is occurring	6.3 Cultural monitoring	6.3a Cultural monitoring programme. Under consent conditions, four cultural monitoring programmes are underway to ensure health and wellbeing of taiao and māhinga kai are protected.	Underway	2024	Ongoing	NCC	MAT	

THE UNIVERSITY OF WAIKATO Te Whare Wānanga o Waikato Research Commons

https://researchcommons.waikato.ac.nz/

Research Commons at the University of Waikato

Copyright Statement:

The digital copy of this thesis is protected by the Copyright Act 1994 (New Zealand).

The thesis may be consulted by you, provided you comply with the provisions of the Act and the following conditions of use:

- Any use you make of these documents or images must be for research or private study purposes only, and you may not make them available to any other person.
- Authors control the copyright of their thesis. You will recognise the author's right to be identified as the author of the thesis, and due acknowledgement will be made to the author where appropriate.
- You will obtain the author's permission before publishing any material from the thesis.

The Sediment, River Plume, and Inner Shelf Variability in a Bay with Multiple Fluvial Inputs

A thesis

submitted in fulfilment

of the requirements for the degree

of

Doctor of Philosophy in Earth Science

at

The University of Waikato

by

TED CONROY

THE UNIVERSITY OF
WAIKATO
Te Whare Wānanga o Waikato

2024

2

Abstract

Small mountainous rivers deliver considerable sediment loading to the coastal ocean and play a disproportionate role in marine sediment deposition globally. Discharge in these rivers is often driven by short episodic events and they typically deliver sediment to energetic coastal environments where in-situ observations of cross-shelf sediment transport are spatially limited and are difficult to maintain over representative periods of time. How these river plumes respond to environmental conditions, and where sediment is initially deposited from the river plumes are essential to understanding long-term sediment transport and deposition patterns in the coastal ocean. This thesis explores this problem using three approaches applied to Hawke Bay (Aotearoa New Zealand) and its river plumes: remote sensing (paper 1), large-scale numerical modelling (paper 2) and high resolution in situ observations at one of the river mouths (the Tukituki River) (paper 3).

Using ocean colour remote sensing to determine the length scales of sediment transport from small mountainous river plumes

Satellite ocean colour records now extend >20 years and have the potential to facilitate spatially-explicit, long-term studies of suspended sediment variability in river plumes in many coastal regions of the world. In this work, I developed a local algorithm for total suspended sediment (TSS) concentration and applied it to the daily MODIS ocean colour record to characterize river plume dynamics, determine their drivers, and identify likely sediment deposition sites in Hawke Bay, Aotearoa New Zealand. This natural embayment, located in a temperate region, is an energetic coastal environment receiving sediments inputs from multiple small mountainous rivers, making it an ideal test site for this study. Our analysis revealed that the river plume length scales were found to be 2–8 km, varying with river size and river discharge. Waves driving sediment resuspension also contributed to the observed concentration signal. Wind was an important factor determining the plume directionality.

Circulation and cross-shelf sediment fluxes in an energetic bay with multiple small mountainous rivers

Understanding the source to sink transport of sediment from rivers into the coastal ocean is a key process that has implications for marine ecology and land and river management. In locations with multiple rivers that have episodic, high intensity discharge events, the response to inner shelf conditions and the transit of sediment is a highly relevant issue both in Aotearoa New Zealand and for small mountainous river systems worldwide. In this chapter, a three dimensional, realistic numerical

ocean model that couples hydrodynamics and waves is used to simulate these patterns in Hawke Bay, Aotearoa New Zealand over multi-year time scales. The developed model is well validated with a broad range of oceanographic data, and is used to characterise the understudied circulation in Hawke Bay, the river plume dynamics, and the resulting cross-shelf sediment flux. The mean circulation and stratification largely influenced by buoyancy input, with river plumes and coastal currents commonly present in the nearshore. Wind was found to be a key driver of plume transport and mixing. Both event time scale and multi-year sediment deposition and erosion patterns were detailed throughout the Bay, finding that longer term deposition primarily occurs in depths greater than 40 m, due to persistent wave resuspension of sediment.

The variability of cross-shelf flows offshore of a small mountainous river

The response of a river plume circulation, stratification, and mixing to common inner shelf forcings ultimately impacts the cross-shelf flux of terrestrial material. In particular, for small mountainous river systems, the magnitudes of river discharge can be high, the coastal ocean receiving environment can be energetic with strong wind and large wave conditions, and the spatial scales are typically smaller than classic river plume studies have presented. In this chapter, an in-situ dataset of density and circulation throughout the water column was collected offshore of the Tukituki River in Aotearoa New Zealand. This dataset captured a broad range of environmental conditions that was uniquely situated in the near-field river plume for a large portion of the deployment. This chapter characterised the response to varying wind conditions on river plume vertical structure, finding that upwelling winds, along with offshore winds, the latter which has not been studied in detail prior, can drive the largest cross-shelf fluxes in the surface layer. This chapter additionally highlighted the importance of inlet morphology for setting the river plume directionality, and the implications for cross-shelf sediment transport.

5

Acknowledgements

This thesis would not have been possible without the unrelenting support, positivity, and help of Karin Bryan. Cedric Fichot was instrumental in developing my knowledge of remote sensing and working with satellite data. Thank you to Joe O'Callaghan for the continual advice regarding physical processes in river plumes and the inner shelf. Thank you to Hayden Moffitt at Ocean Adventures for being an amazing boat captain, wealth of maritime and local knowledge, and being nice to me when I got seasick. A huge thank you to Ben Roche for helping with the instrument deployment, that was a massive undertaking that wouldn't have been possible without your help. Thank you to Moritz Lehmann for the advice on how to use the hyperspectral radiometer. Thank you to Becky Shanahan and Jose Beya for the advice throughout the project regarding Hawke Bay. Lastly, thank you to my family for the support.

Table of Contents

Chapter 1: Introduction *14*

1.1 Introduction to thesis **14**

1.2 Inner shelf and river plume circulation **15**

1.3 Sediment transport from rivers into the coastal ocean **17**

1.4 Ocean colour remote sensing **18**

1.5 Study site **19**

1.5.1 Site description 19
1.5.2 Oceanographic description 20
1.5.3 Sediment characterisation 23

1.6 Research objectives and approach **25**

Chapter 2: Using ocean colour remote sensing to determine the length scales of sediment transport from small mountainous river plumes *26*

2.1 Introduction **28**

2.2 Regional setting: Hawke Bay **29**

2.3 Methods **31**

2.3.1 Satellite ocean colour data 31
2.3.2 In-situ data 32
2.3.3 Additional data sources 33
2.3.4 Analysis methods 34

2.4. Results and discussion **34**

2.4.1 On the Rrs-TSS relationship in Hawke Bay 34
2.4.2 River discharge and TSS concentrations 35
2.4.2 Temporal variability of TSS 36
2.4.3 High-TSS events in the Bay 39
2.4.4 Typical spatial variability of TSS 42
2.4.5 Length scales of TSS concentrations in river plumes 43
2.4.6 Plume directionality 46
2.4.7 Relation between TSS and forcing mechanisms 48
2.4.8 Length scales of plume transport 51

2.5. Conclusion **52**

Chapter 3: Circulation and cross-shelf sediment fluxes in an energetic bay with multiple small mountainous rivers *54*

3.1 Introduction **56**

3.2 Background **56**

3.2.1. Regional setting: Hawke Bay 56
3.2.2. River plume and inner shelf flows 57

3.3 Methods **58**
3.3.1 Numerical model 58
3.3.2. Grids and bathymetry 59
3.3.3. Sediment characteristics 60
3.3.4. Observational data 63
3.3.5 Model skill metrics 64
3.3.6 River plume analysis methods 64

3.4. Results **64**
3.4.1. Model evaluation and overview 64
3.4.2. Density and circulation patterns in Hawke Bay 71
3.4.3. River plume variability 75
3.4.4. Sediment flux 78
3.4.2. Influence of waves on hydrodynamics 82

3.5 Discussion **84**
3.5.1 Sediment transport from small mountainous rivers 84
3.5.2. Limitations and future work 85

3.6. Conclusion **85**

Chapter 4: The variability of cross-shelf flows offshore of a small mountainous river ***86***

4.1 Introduction **88**

4.2 Background **88**
4.2.1 Inner shelf and river plume circulation 88
4.2.2 Response of river plume and inner shelf to wind forcing 89
4.2.3 Hawke Bay and Tukituki River 89

4.3 Methods **91**
4.3.1 Instrument Deployment 91
4.3.2 Additional Data Sources 92

4.4 Results **92**
4.4.1 Overview of collected data 92
4.4.2 Inlet morphology and plume spatial variability 95
4.4.3 Variability with environmental conditions 97
4.4.4 Relation between wind and circulation 97
4.4.5 Plume mixing 98

4.5 Discussion **99**
4.5.1 Characterizing the wind response 100
4.5.2 Mixing response 101
4.5.3 Cross-shore sediment transport 101
4.5.4 Scale dependence of river plume 103

4.6 Conclusion **103**

Chapter 5: General Conclusions ***105***

5.1 Main findings of thesis **106**

5.2 Limitations of current work **109**

5.3 Relevance of thesis **110**

References *111*

List of Figures

Figure 1.1 The Tukituki River in Hawkes Bay, Aotearoa New Zealand, during a flood event.....14
Figure 1.2 Spatial overview of the study site. The left plot shows the bathymetry (m) of the North Island of Aotearoa New Zealand.....15
Figure 1.3 Schematic of river plume dynamical regions. The schematic includes the near field, mid-field, and far field regions.....16
Figure 1.4 Schematic of the typical sediment transport pathway for marine dispersal dominated river systems.....17
Figure 1.1 Satellite imagery of suspended sediment in Hawke Bay.....19
Figure 1.6 Boundary currents around Aotearoa New Zealand.....21
Figure 1.7 The estimated circulation of Hawke Bay from Ridgeway and Stanton (1969).....22
Figure 1.8 The estimated circulation in the southern Hawke Bay region from White (1994).....22
Figure 1.9 The locations of sediment samples and bed characteristics as measured by Pantin (1966).....23
Figure 1.10 The merged and interpolated bed sediment characteristics in Hawke Bay.....24
Figure 1.11 Summary reconstructions of past sediment deposition and transport pathways.....24
Figure 2.1 Overview of the study area and locations of data collection.....30
Figure 2.2 The measured remote sensing reflectance, TSS, and the empirical regression between remote sensing reflectance and TSS.....32
Figure 2.3 Box and whisker plot of the river discharge and remotely sensed TSS for each river.....36
Figure 2.4 Time series of environmental conditions in Hawke Bay from 2000 to 2021.....37
Figure 2.5 The timeseries of remotely sensed TSS for the major rivers in Hawke Bay.....38
Figure 2.6 Monthly means of TSS (mg l^{-1}) over the entire MODIS record.....39
Figure 2.7 Example of a river discharge event in the winter of 2017 from June 15 to August 15.....40
Figure 2.8 Example of elevated TSS due to wind and waves from February to March of 2006.....41
Figure 2.9 The percentages of occurrence for a range of TSS values.....42
Figure 2.10 The estimated locations, transit distances, and depths of likely initial sediment deposition from two methods.....44
Figure 2.11 The river plume directionality and relation with wind direction.....47
Figure 2.12 Average composites of remotely sensed TSS (mg l^{-1}) for various environmental conditions.....49
Figure 2.13 The coefficient of determination (r^2) between remotely sensed TSS and forcing mechanisms.....50
Figure 2.14 The spatial relationship between bed stress and likely initials sediment depositional areas.....51

Figure 3.1 Overview of the Hawke Bay region, data sources, and COAWST model grid.....60
Figure 3.2 Bed sediment grain size percentages interpolated to the model grid.....62
Figure 3.3 Timeseries of environmental conditions and modelled parameters.....65
Figure 3.4 The comparison of wave statistics with modelled and observed values.....66
Figure 3.5 Model/data comparisons from inner shelf mooring HAWQi.....67
Figure 3.6 Comparisons of wind roses with observed and modelled values.....68
Figure 3.7 Model/data comparison of glider data, collected in April 2019.....69
Figure 3.8 Comparison between model surface sediment concentration (SSC) and SSC derived from MODIS.....70
Figure 3.9 Select days of MODIS SSC (top row) and model SSC (bottom row) for a range of conditions.....71
Figure 3.10 Seasonal averages of surface salinity (top row), the surface to bed salinity vertical stratification (second from top row), surface temperature (third row), and the surface to bed vertical temperature stratification (fourth row).....72
Figure 3.11 Seasonal averages of circulation in Hawke Bay.....73
Figure 3.12 Inner shelf circulation timeseries for the year of 2018.....74
Figure 3.13 Description of river discharge events in the period of 2017-2019 for the largest rivers that enter Hawke Bay.....75
Figure 3.14 River plume salinity contour boundary heat maps for each river.....76
Figure 3.15 River discharge event plume statistical descriptions.....77
Figure 3.16 Modelled SSC concentrations for differing sediment sizes and locations in the water column.....79
Figure 3.17 Timeseries of sediment fluxes in Bay.....80
Figure 3.18 Long term bathymetry change (cm) at the end of the model run.....81
Figure 3.19 Grain size changes for the mud size classes.....82
Figure 3.20 Comparison between ROMS and Coupled ROMS/SWAN runs using average seasonal values.....83
Figure 3.21 Timeseries offshore of the Wairoa River that compares the coupled ROMS/SWAN model with the ROMS only run over a select period in 2018.....84
Figure 4.1 Areal overview of Hawkes Bay, Aotearoa New Zealand.....90
Figure 4.2 Timeseries of collected data offshore of the Tukituki River from July 12 (day 1) to August 24, 2022.....93
Figure 4.3 Satellite imagery focused on the Tukituki River mouth labelled by days of the deployment (red).....95
Figure 4.4 Comparison between periods with varying river inlet configurations.....96
Figure 4.5 Correlation between river plume and environmental conditions.....97
Figure 4.6 Timeseries of mixing related values.....99

Figure 4.7 Average velocity profiles with to respect to wind direction over the entire deployment..100

Figure 4.8 The calculated surface Ekman depth (m) compared with the Richardson number (near-surface), coloured by wind direction.....101

Figure 4.9 Timeseries of suspended sediment concentration and sediment fluxes.....102

Figure 5.3 The mean surface density and circulation from 2017 to 2019.....107

Figure 5.2 The bed sediment deposition from the numerical model (cm) over the period of 2017 to 2019.....108

Figure 5.3 The relation between wind and river plume characteristics throughout Hawke Bay.....110

List of Tables

Table 3.1 Sediment classes and characteristics used in the sediment transport model……...…….62

Table 3.2 Statistics from model/data comparisons…….....……66

Table 4.1 Description of instrumentation used and sampling information for the 2023 deployment offshore of the Tukituki River…….....……..91

Chapter 1: Introduction

1.1 Introduction to thesis

The flux of sediment and terrestrial material to the coastal ocean is linked through river outflows and buoyant river plumes which transit material across the nearshore and inner shelf (e.g. Fig. 1.1). Many rivers in Aotearoa New Zealand yield high suspended sediment concentrations and transit millions of tons of sediment to the coastal ocean annually (Hicks et al. 2011), where flood events typically occur over short time scales related to episodic storm systems (Walsh and Nittrouer 2009). Small mountainous rivers, which have drainage basins less than 10,000 km^2 and are found on active margins with steep coastal topography, in particular transit large amounts of sediment to the coastal ocean relative to their watershed size (Milliman and Syvitski 1992). For example, Aotearoa New Zealand rivers have been estimated to contribute 1.7% of the global sediment flux to the ocean although its land area covers 0.2% of the global land area (Hicks et al. 2011). The delivery of terrestrial sediment into the coastal ocean can cause impacts on the shelf and nearshore ecosystem, such as limiting light penetration and blanketing the benthic environment with fine sediments, ultimately changing the structure and function of these areas (Thrush et al. 2004). Characterizing the sediment pathway from rivers, to transit within river plumes, to deposition on the inner shelf and beyond is important for understanding potential future changes due to land use changes and climate change.

Figure 1.1 The Tukituki River in Hawkes Bay, Aotearoa New Zealand, during a flood event. Image from Hawkes Bay Regional Council.

This work is focused on understanding the circulation and suspended sediment transport from small mountainous rivers to the coastal ocean. The study site is Hawke Bay, in Aotearoa New Zealand (Fig. 1.2), a large bay with multiple rivers that yield a significant flux of terrestrial material to the coastal ocean. There are major knowledge gaps regarding the circulation of Hawke Bay and the transport of fine sediment from rivers to the coastal ocean, with implications to coastal ecosystems. Additionally, the dynamics of small to medium sized rivers with episodic river discharge (that are typically produced by small mountainous rivers) have received less attention than larger rivers with steadier river discharge (Horner-Devine et al. 2015). For a comprehensive understanding of dynamics for these river plumes and impacts to the suspended sediment transport, an assessment of the impacts of common inner shelf processes and environmental conditions is needed at a multitude of temporal and spatial scales. Relevant to this thesis are the topics of inner shelf circulation, river plume dynamics, and suspended sediment transport, each of which are reviewed in this introduction.

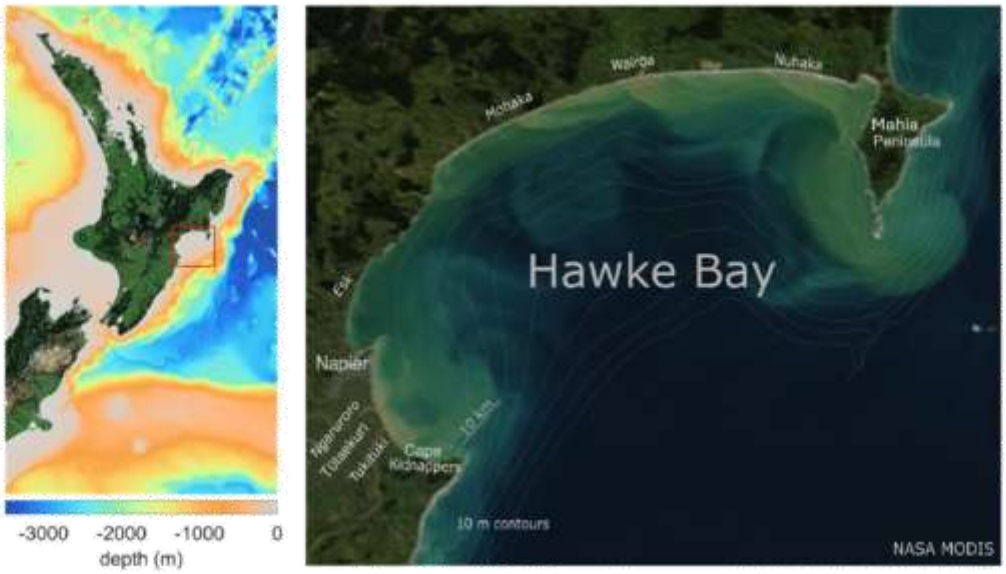

Figure 1.2 Spatial overview of the study site. The left plot shows the bathymetry (m) of the North Island of Aotearoa New Zealand. The red box marks the region of Hawkes Bay. On the right is a satellite image of Hawke Bay, including the names of the major rivers and places throughout the region, and 10 m depth contour lines from 10 to 100 m depth (grey). Image from NASA MODIS.

1.2 Inner shelf and river plume circulation

The currents on the inner shelf are influenced by wind, waves, tide, and offshore forcings (Lentz and Fewings 2012, Kumar et al. 2016). Tides are a key driver of coastal circulation in New Zealand (Stevens et al. 2021) and rotate counter clockwise around the North Island. Wind stress can drive upwelling and downwelling which in turn drive cross-shelf currents, and wave induced currents can drive cross-shelf, vertical and alongshore currents in the nearshore. The additional input of

buoyancy from rivers drives river plume circulations and can create regions of freshwater influence (e.g. O'Callaghan and Stevens 2017).

River plumes are formed due to the input of buoyancy from rivers into the coastal ocean, and are persistent features of Hawke Bay which can be commonly identified from satellite imagery (e.g. Fig. 1.2). River plumes are the initial transport mechanism for sediment and other terrestrial material from land to the coastal ocean, and the currents associated with river plumes can greatly alter coastal circulation patterns (Horner-Devine et al. 2015). The plume dynamics are dependent on the outflow strength of the river, the intensity of stratification, and mixing processes which act to slow the river plume and dilute the river plume water. A river plume can be characterised by three regions, which are the near field, mid-field, and far field (Fig. 1.3; Horner-Devine et al. 2015, Hetland 2005).

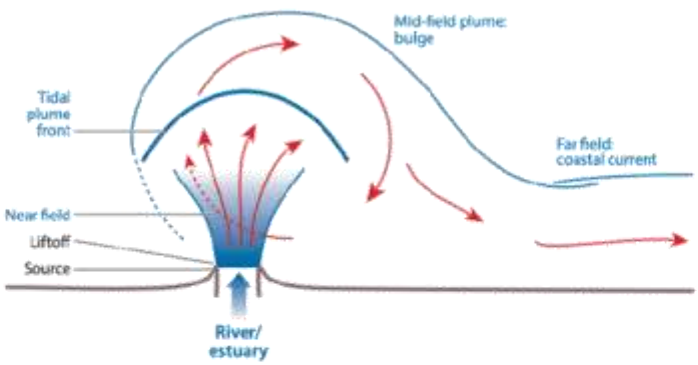

Figure 1.3 Schematic of river plume dynamical regions. The schematic includes the near field, mid-field, and far field regions. Figure is sourced from Horner-Devine et al. (2015).

In the near field region, transport is dictated by the outflow momentum at the river mouth and behaves as a jet, being slowed down by shear mixing at the base of the plume (Fig. 1.3). A near field plume will occur if the flow becomes supercritical at the mouth of the river. In the mid-field region, other processes become important as the momentum flux decreases due to shear driven mixing. The density contrast between the fresh and ocean water produces lateral spreading at the rate of the internal wave speed, and local winds can create surface currents which transport the freshwater as well as provide vertical mixing if the Ekman layer depth is greater than the plume depth. In the far field plume, winds become the dominant mixing and transport mechanism, as well as other inner shelf currents and the Coriolis force which can drive rotation and the formation of a coastal current (Fig. 1.3).

Upwelling winds that are directed alongshore have been shown to enhance the cross-shore river plume transport and thin the plume, while downwelling winds have been shown to inhibit the cross-shore transport and thicken the plume vertically (Fong and Geyer 2001). The role of cross-shelf winds has received less attention, as cross-shore transport related to Ekman dynamics is expected to

be more important. However, Hunter et al. (2010) noted the relation between direct cross-shore wind and associated cross-shore plume transport in the Hudson River plume, and Kakoulaki et al. (2014) similarly showed direct relations between wind and plume directions for wind speeds greater than 4 m s^{-1}. These studies showed that smaller scales plumes are likely more susceptible to cross-shelf winds than larger river plumes such as the Columbia River (e.g. Hickey et al. 2010).

1.3 Sediment transport from rivers into the coastal ocean

The transport of sediment from rivers into the ocean is dependent on the plume circulation and sediment characteristics (Geyer et al. 2004), and the dispersal and deposition of sediment is largely dependent on the characteristics of the coastal ocean receiving environment and plume circulation (Wright and Nittrouer 1995). For example, Walsh and Nittrouer (2009) classify varying types of dispersal settings, with the *marine dispersal dominated* setting most relevant for small mountainous rivers in New Zealand (as studied here). Small mountainous rivers are characterised by steep coastal mountain ranges that generally drain into energetic coastal oceans and have episodic discharge events, and make up a large portion of the sediment transported into the ocean globally (Milliman and Syvitski 1992). In these systems, buoyant river plumes advect suspended sediment horizontally until it falls out of the plume into a region with sufficient bottom stress to be resuspended and further transported at depth to longer-term depositional areas (Fig. 1.4). Rivers that fit the *marine dispersal dominated* category include the Eel River (Geyer et al. 2000), the Po River (Harris et al. 2008), and the Waipaoa River in Poverty Bay (Kuehl et al. 2016).

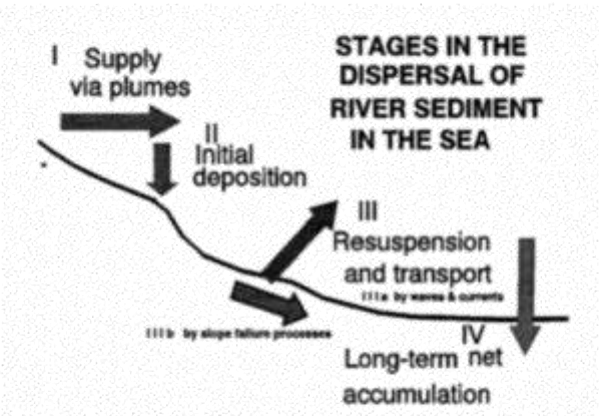

Figure 1.4 Schematic of the typical sediment transport pathway for marine dispersal dominated river systems. Figure is sourced from Wright and Nittrouer (2009).

The sediment settling velocity is a function of the grain diameter and density of the sediment. This is complicated by the aggregation of fine particles, termed flocculation, where smaller particles aggregate to form larger flocs. Flocs can have order of magnitude increases in settling velocity which can greatly influence how far sediment can be transported from river plumes (Geyer et al. 2000). The

flocculation process is thought to be dependent on sediment composition, turbulence intensity, the chemical interaction with salt water, and the organic compounds that aggregate particles together (Geyer et al. 2004). Coarser sediments such as sand will be deposited near the inlet mouth and would produce a delta offshore of the inlet in the absence of wave activity. Flocs have also been shown to be deposited in close proximity to the river inlet due to their high settling velocity (Milligan et al. 2007; Warrick et al 2008). Average plume trajectories have been shown to coincide with fine sediment depositional areas for marine dispersal dominated rivers (Wright and Nittrouer 1995).

For example, offshore of the Waipaoa River in Poverty Bay, aggregate and coarser particles were found to settle in the embayment and slightly offshore, while finer sediment is more dispersive along the continental shelf (Moriarity et al. 2015). Some sediment was found to be stored in long-term mud deposition areas located at bathymetric low points, but a majority would be resuspended by wave orbital currents in the thin wave boundary layer, which can reach concentrations high enough to form turbidity currents that transport sediment further offshore (Traykovski et al. 2000, Hale and Ogsten 2015). If river flood events co-occurred with significant waves, sediment was likely transported offshore immediately, but if they did not co-occur, sediment could be stored temporarily in Poverty Bay and on the continental shelf (Bever et al. 2011, Moriarity et al. 2015). In Poverty Bay, Kniskern et al. (2010) used isotopic dating to show that muddy sediments are stored ephemerally between 30-50 m, and that longer-term deposition was found offshore at 80-120 m. Due to the proximity to Hawke Bay and similar environment, similar aspects are expected to be found in Hawke Bay, although these processes have not yet been assessed for the region.

1.4 Ocean colour remote sensing

Satellites routinely image the surface of the coastal ocean, providing ocean colour data with sufficient spatial resolution to resolve features such as river plumes. Satellite ocean colour datasets now allow for long time scales (> 20 years) to be studied, and the observed ocean colour directly relates to the surface suspended sediment concentration (Kirk 1994), allowing estimates of the suspended sediment concentration in river plumes to be analysed over time. These snapshots of surface sediment characteristics have much higher spatial coverage than would be possible observationally, but lack vertical information and have time resolution of one day or greater.

Satellites measure the spectrum of the water leaving radiance $L_w(\lambda)$, which corresponds with the Inherent Optical Properties (IOPs) of the water, including non-algal particles (including sediment), chlorophyll, coloured dissolved organic matter, and water itself, which can scatter and absorb light, and together attenuate light through the water column (Kirk 1994). To account for changes in downwelling light, normalized reflectances such as the remote sensing reflectance $R_{rs}(\lambda) = L_w/E_d$, where E_d is the downwelling irradiance at the sea surface, are used to obtain information about the IOPs, as these are independent of the ambient light field (Kirk 1994).

Estimates of the Suspended Sediment Concentration (SSC) from R_{rs} measurements can be approximated analytically, or from empirical relations determined from global datasets or locally collected data (Basdurak et al. 2020). Many studies have estimated the sediment concentration in river plumes and coastal settings from satellite imagery (Many et al. 2018, Aurin et al. 2013, Constantin et al. 2018), where Total Suspended Solids (TSS) or SSC is commonly estimated from wavelengths in the red or near-infrared portion of the spectrum. These studies have determined seasonal SSC patterns and related spatial SSC variability to variations in river discharge and wind variability (Pawlowicz et al. 2017; Constantin et al. 2018), indicating that satellite ocean colour data provides a useful tool for investigating surface SSC variability in river plumes over long time scales.

1.5 Study site

1.5.1 Site description

Hawke Bay is a large southeast facing embayment on the east coast of the North Island of Aotearoa New Zealand, extending from the Mahia Peninsula southward to Cape Kidnappers (Fig. 1.2). The bay is ~80 km long, and has 9 significant rivers that discharge into the bay. The rivers have a relatively high combined average sediment flux of 11 million tonnes per year (Hicks et al. 2011). Limited oceanographic work has been conducted to understand the circulation, sediment transport and depositional patterns that occur in the Bay (Stevens et al. 2021). River plumes with elevated suspended sediment concentrations are common features of the Bay (Fig. 1.5), which have not been studied in detail for the entire Hawke Bay prior to in this thesis.

Figure 1.5 Satellite imagery of suspended sediment in Hawke Bay. The left image shows Hawke Bay and the right image shows the Wairoa River plume during a flood event. Image data is from Sentinel-2 (European Space Agency).

The continental shelf offshore of the Bay is broad and gently sloping, in comparison to the shelf to the north and south of the Bay, and extends to the Hikurangi subduction zone offshore. The

region is highly geologically active with complex uplift patterns (Komar 2010) and steep coastal mountains, including the Huiarau, Kaweka, and Ruahine Ranges. The coastal mountains are sedimentary with mainly sandstone and mudstone layers. The sediment delivered to the southern portion of the bay is generally mesozoic greywacke with other conglomerates, sandstones and mudstones, and the sediment delivered to the northern portion of the bay is primarily tertiary sandstone (Komar 2010). The issue of sedimentation in the Bay has likely been exacerbated since human settlement in the area, as the conversion from native forest to pasture land has been shown to increase the sediment yield by a factor of four in the region (Eyles and Fahey 2006).

1.5.2 Oceanographic description

The Hawkes Bay region is subject to predominantly southwest winds and is subject to highly variable and sporadic precipitation that can occur throughout the year (Chappell 2013). The rainfall patterns in the region are highly linked to the direction in which storms approach the region. Occasional cyclone events typically approach from the east to northeast and have the potential to transport significant amounts of precipitation to the region. The Bay is susceptible to strong wind and wave forcing at times. The average significant wave height recorded off Napier was 1.2 m, but high wave events can be from 2.5–3.5 m, and the largest events are greater than 8 m (Komar 2010). Waves on average approach from the east-southeast, are larger in winter, and wave heights in the bay can be variable for a given swell due to wave refraction. Waves create longshore currents that are important for sediment transport and beach erosion in the southern bay (Komar 2010). The spring tidal range is 1.9 m and during neap is 1.2 m as measured at the Napier Port.

There are two dominate currents that flow offshore of the Bay: the warmer and saltier East Cape current from the north and the cooler and fresher Wairarapa coastal current from the south (Fig. 1.6; Kerry et al. 2023; Stevens et al. 2021); the latter being a mixture of the Southland and D'Urville water masses that are generally mixed between the two islands (Chiswell 2002). Chiswell (2002) showed that water from the Wairarapa coastal current is commonly advected into Hawke Bay by studying the propagation of temperature signals northward into the Bay.

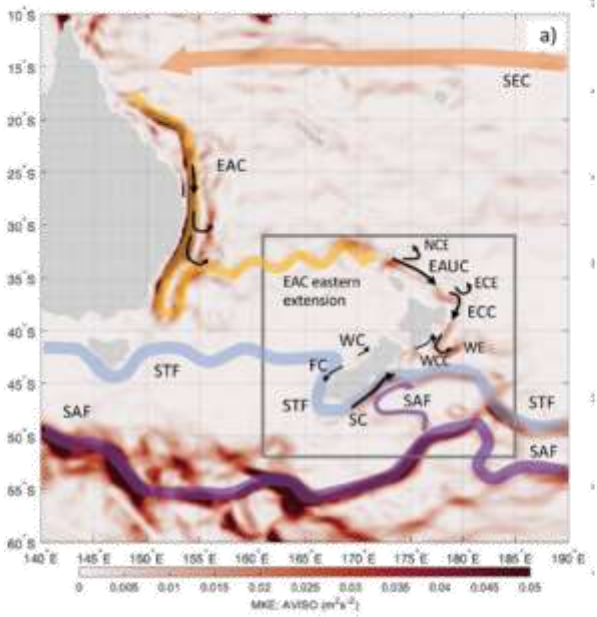

Figure 1.6 Boundary currents around Aotearoa New Zealand. Of particular interest is the East Cape Current (ECC), Wairarapa Coastal Current (WCC), and Wairarapa Eddy (WE). The colour scale refers to the mean kinetic energy ($m^2 s^{-1}$). Figure is sourced from Kerry et al. (2023).

The circulation pattern in Hawke Bay has been sporadically studied in the past 60 years. Ridgeway (1960) used Lagrangian drift cards deployed from an airplane and documented where the cards ended up on local beaches. Vectors were then drawn between the drop location and the beach where the card was found, to conclude that the general circulation pattern in the bay is an inflow into the center of the bay and then a divergence toward the north and south from there. Ridgeway and Stanton (1969) drew a similar conclusion by measuring the density at an instance throughout the Bay and hypothesizing a potential circulation pattern from the density observations (Fig. 1.7).

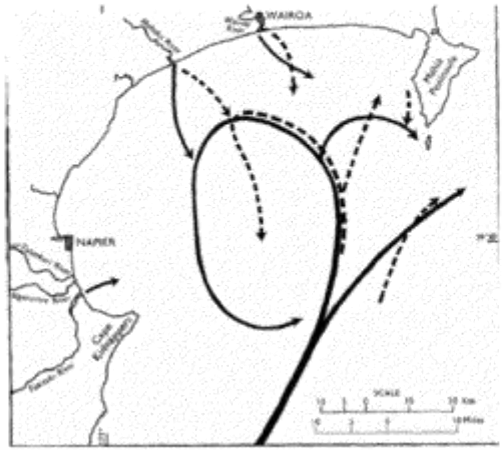

Figure 1.7 The estimated circulation of Hawke Bay from Ridgeway and Stanton (1969). Figure is sourced from Ridgeway and Stanton (1969).

White (1994) conducted a detailed study of suspended sediment and circulation patterns in the southern region of Hawke Bay, observing highly stratified river plumes, sediment resuspension from waves in non-riverine regions, and sharp salinity gradients in the rivers. General circulation patterns for the southern region of Hawke Bay were estimated (Fig. 1.8), showing nearshore flows commonly northward while outside of the nearshore the flow was commonly southward directed towards Cape Kidnappers. These past studies of the circulation may have characterized general patterns of the Hawke Bay circulation, but given the limited time periods of observations it is likely that key elements to the circulation and water column structure may vary from these generalisations.

Figure 1.8 The estimated circulation in the southern Hawke Bay region from White (1994). Figure is sourced from White (1994).

1.5.3 Sediment characterisation

The sediment characteristics in the Bay follow common continental shelf sedimentary patterns, with coarse sand on beaches and muddy areas becoming progressively dominant with distance offshore. There are also several gravel zones and rock reefs in the Bay, as described below. Pantin (1966) comprehensively sampled and described the bed sediment characteristics in the Bay (Fig. 1.9), observing that coarse beach sand (with the median grain size (d_{50}) around 250 µm) persists for a relatively short distance offshore until fine sand becomes the dominant sand size in the Bay (in the range of 63–150 µm, and from 100–125 µm; Marshall 1929, Pantin 1966, Hume 1989, White 1994). Muddy regions offshore were recorded to have silt/clay to sand ratios of typically 70/30.

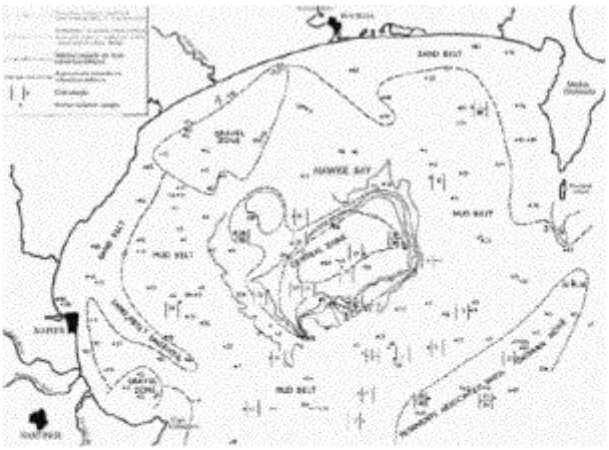

Figure 1.9 The locations of sediment samples and bed characteristics as measured by Pantin (1966). Figure is sourced from Pantin (1966).

Gravel is found along numerous beaches of the Bay, including at the inlets of the major rivers, and a few offshore regions such as offshore of the Mohaka River (Pantin 1966). Grain sizes at the bed of the Tukituki River near the inlet and up to 1.5 km upriver from the inlet range from 4–32 mm, with the average d_{50} 16 mm. Rocky reefs areas in the Bay include the Pania reefs, Wairoa Hard, Clive Hard, and offshore of the Mahia Peninsula. A region in the middle of the Bay contains coarse sediment mixed with little mud. Pantin (1966) hypothesized that stronger bed stress may be found at this location due to the inflow of offshore currents into this area. The compiled bed sediment datasets (data from Bostock et al. 2019 and Hawkes Bay Regional Council) show similar patterns to the description from Pantin (1966) with additional spatial variable variability resolved by more recent sediment samples. Sand is found in the nearshore region, with mud offshore of ~20–30 m depth, and gravel/reefs found at few locations throughout the Bay (Fig. 1.10).

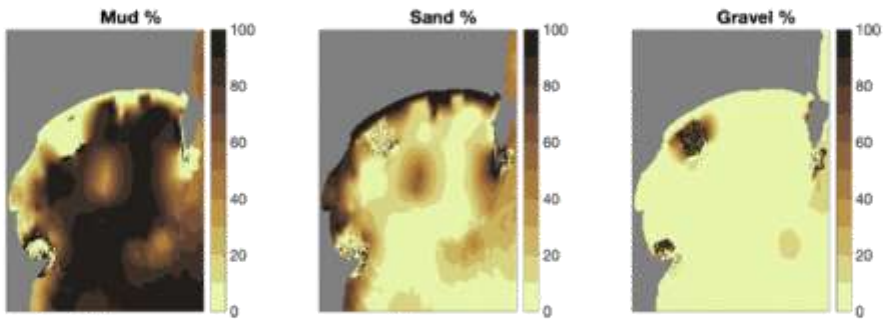

Figure 1.10 The merged and interpolated bed sediment characteristics in Hawke Bay. The data sets includes data from Pantin (1966), Bostock et al. (2019), and data from Hawkes Bay Regional Council. The gravel class includes rocky reef areas.

Estimates of sedimentation rates from carbon dating have been made from Pantin (1966) and sediment thicknesses have been mapped from seismic data (Paquet et al. 2009). Pantin (1966) measured a maximum depositional rate of 0.23 cm per year and more typically rates of ~0.07 cm per year in other muddy regions. From a geophysical analysis, Paquet et al. (2009) mapped estimates of geographic, depositional, and hypothesised sediment transport pathways for 20,000 and 7,200 years ago (Fig. 1.11a,b). The most recent period analysed by Paquet et al. (2009) displays depositional zones offshore of the Ngaruroro, Tūtaekurī, and Tukituki Rivers as well as offshore of the Wairoa River, with limited deposition occurring at Kidnappers and Lachlan Ridges (Fig. 1.11b). These studies provide a basic description of likely sedimentation in the Hawke Bay, but further detailed investigation is needed to determine the present day sedimentation regime in Hawke Bay.

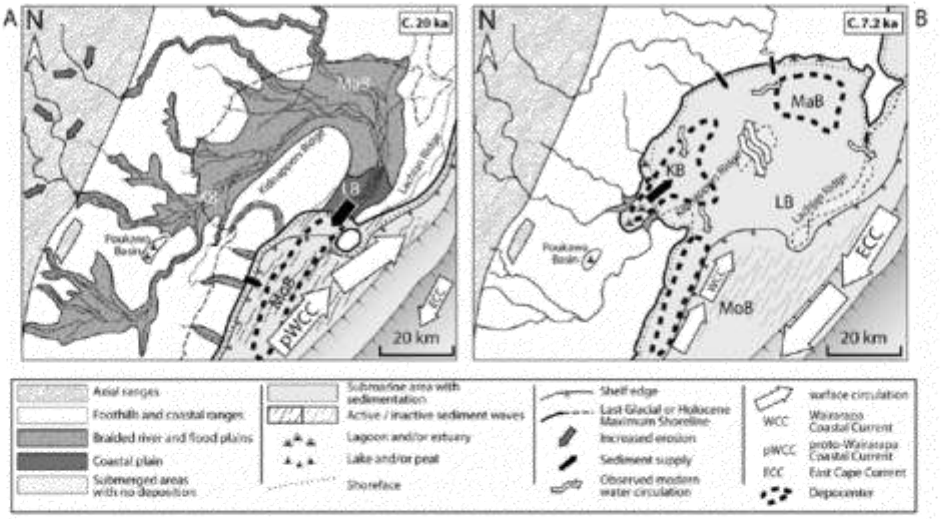

Figure 1.11 Summary reconstructions of past sediment deposition and transport pathways. Figure is sourced from Paquet et al. (2009).

1.6 Research objectives and approach

The overarching aim of this thesis is to detail the controls on the coastal dynamics of small mountainous river plumes and associated cross-shelf suspended sediment transport. Specifically, the characteristic scales of suspended sediment in river plumes over long time scales will be determined from satellite remote sensing, the fundamental drivers of variability will be assessed using a calibrated numerical model, and finally to document river plume dynamics in high temporal resolution through a mooring deployment offshore of a small mountainous river. This thesis sets out to determine the how environmental conditions impact river plume dynamics and sediment transport in an energetic coastal ocean, particularly for smaller rivers than have been mostly focused on in prior research.

The aims work together to cover a range of temporal and spatial scales and show how those scales interact to respond to varying environmental conditions. These aims were studied in the case study system of Hawke Bay, Aotearoa New Zealand, a semi-enclosed bay with four significant small mountainous rivers that discharge into the Bay. Together, the research presented in this thesis provides a comprehensive description of the circulation and sediment transport in Hawke Bay as well as insights pertaining to small mountainous river systems worldwide. Hawke Bay is a natural laboratory for studying small mountainous rivers.

This thesis is separated into three components that use different methods to investigate varying spatiotemporal scales and processes regarding circulation and sediment transport in Hawke Bay. Chapter 2 uses satellite ocean colour data to document the surface SSC variability in Hawke Bay for over 20 years. Chapter 3 utilises a realistic numerical ocean model developed for Hawke Bay that simulates the three dimensional circulation and sediment transport in Hawke Bay. Chapter 4 uses a mooring dataset that was collected offshore of one of the main rivers in Hawke Bay that recorded river plume circulation and the response to environmental forcing in high detail.

The following Chapters 2–4 are formatted as individual manuscripts that will be submitted to peer reviewed journals and Chapter 5 is a conclusion and summary of the thesis. The main chapters include:

- **Chapter 2**: Using ocean colour remote sensing to determine the length scales of sediment transport from small mountainous river plumes.
- **Chapter 3**: Circulation and cross-shelf sediment fluxes in an energetic bay with multiple small mountainous rivers
- **Chapter 4**: The variability of cross-shelf flows offshore of a small mountainous river

Chapter 2: Using ocean colour remote sensing to determine the length scales of sediment transport from small mountainous river plumes

Contribution of Authors

Chapter 2 presents the article "Using ocean colour remote sensing to determine the length scales of sediment transport from small mountainous river plumes" which will be submitted to the journal *Remote Sensing of Environment* for review. Ted Conroy conceptualized the study, performed all field work and data analysis, and wrote the article. Karin R. Bryan provided feedback, supervision, and editing of the article throughout the process. Cedric G. Fichot provided assistance with the conceptualization, interpretation, and editing of the article.

2.1 Introduction

Relative to the size of their watersheds, small mountainous rivers deliver disproportionally large amounts of sediment, nutrients, terrigenous organic matter, and pollutants to the coastal ocean (Milliman and Syvitski 1992). These systems are generally located on active margins with steep coastal mountain ranges and are driven by weather systems characterized by fast, episodic storm events (typically 1–3-day duration) that quickly deliver freshwater and sediment to the ocean. Suspended sediment transport within these river plumes is complex and has important implications for long-term sediment deposition (Geyer et al. 2004, Hetland and Hsu 2013). It also plays an important ecological and biogeochemical role through its effects on water column turbidity and its supply of particulate matter to the benthos (McKee et al. 2004).

Small mountainous rivers typically flow into an energetic coastal ocean influenced by wave-driven currents that can resuspend deposited sediment (Wright and Nittrouer 1995). Studies have shown that transport to long-term sediment depositional sites in these systems occurs in multiple deposition-resuspension steps following the initial gravitational settling from the river plume (Geyer et al. 2000, Hill et al. 2000, Milligan et al. 2007, Bever et al. 2011, Hale and Ogsten 2015). In these systems, which are classified as marine dispersal dominated (Walsh and Nittrouer 2009), the length scales of the primary sediment deposition are generally shorter than the length scale of the inner-shelf zone, where fine grain sediment can be resuspended. Wave-driven currents can then initiate gravity flows that transport sediment offshore to longer term depositional areas (Traykovski et al. 2000). Plume dynamics, which are characterized by a strong near-field jet and mediated by various factors influencing mid-field and far-field plume dispersal (Hetland and Hsu 2013, Horner-Devine et al. 2015), are critical because they determine where sediment initially falls from the plume.

Characterizing plume dynamics from marine dispersal dominated rivers is therefore critical to understand sediment deposition patterns. Previous studies have shown the initial depositional site is generally within a few kilometers to a few tens of kilometers from the river mouth, as is the case for the Eel River (Geyer et al. 2000), the Columbia River (Wright and Nittrouer 1995), and the Po River (Harris et al. 2008) These observations suggested that aggregation (flocculation) increases the effective settling velocity of particles, given that the length scale would be much longer (e.g., tens of kilometers) based on unaggregated-particle Stokes settling velocity and the observed horizontal transport. In-situ measurements of sediment transport in these systems are difficult to obtain due to the highly energetic environment and dynamic nature of the plumes, and often prevent long temporal observational records of sediment deposition from mountainous river plumes.

Satellite remote sensing of ocean colour is being increasingly used to estimate suspended sediment concentrations in surface coastal waters, using the strong relationship existing between the optical backscattering coefficient of particles and water remote-sensing reflectance in the red and

near-infrared spectral domains (Kirk 1994; Nechad et al. 2016). The long record of satellite ocean colour data (> 20 years) can now facilitate detailed studies of suspended sediment dynamics in nearshore systems. For instance, recent work using satellite ocean colour have documented suspended sediment variability in river plumes, including the characterization of spatial patterns, and the assessing variability with discharge and environmental conditions (Pawlowicz et al. 2017, Saldias et al. 2012, Gangloff et al. 2017, Many et al. 2018, Zhang et al., 2020). However, few studies have used these ocean colour records to provide more specific information about sediment transport and initial deposition patterns from rivers to the coastal ocean.

Here, using Hawke Bay in Aotearoa New Zealand as an ideal test site, we demonstrate how these >20-years records of ocean colour data can be used to document detailed spatiotemporal patterns of mountainous river plumes and determine the length scales of sediment deposition from these rivers in the coastal ocean. Ocean colour data from MODIS, in combination with an empirical relation for Total Suspended Solids (TSS), provided daily snapshots of river plume variability. We analysed the plumes of three mountainous rivers flowing into Hawke Bay, a large energetic coastal embayment in New Zealand. The temporal variability of TSS is investigated and compared with the environmental conditions, and the spatial gradient of the TSS in the plumes is used to gain new insights about the initial deposition sites of sediments from river plumes. The relative controls of river discharge, wave forcing, and wind forcing are compared and related to river plume length scales and their relative importance for river plume trajectories.

2.2 Regional setting: Hawke Bay

Hawke Bay is a 40-by-80-km embayment located on the North Island of Aotearoa New Zealand (Fig. 2.1). The Bay is on the eastern coast and faces south toward the Pacific Ocean and is exposed to significant swell from the Southern Ocean. Hawke Bay is located inshore of the Hikurangi margin, and is bordered by steep, highly erodible coastal mountain ranges, where median annual rainfall rates are around 2 m or higher (Chappell 2013). The four largest rivers discharging to the Bay are the 1) Wairoa River, 2) Mohaka River, 3) the combination of the Ngaruroro, Tūtaekurī, and Mokotūāraro Rivers which merge near the river inlet (here denoted as the Ngaruroro/Tūtaekurī as they are the main contributors), and 4) the Tukituki River (Fig. 2.1). The focus of this work is on these larger rivers, although other rivers such as the Esk and Nuhaka Rivers (Fig. 2.1) can create noticeable river plumes. The river inlet morphology is highly variable in time, as some of the river inlets close during the dry season while the larger river inlets generally remain open year-round. The inlet widths of the 4 rivers generally range from 50–200 m, and a submerged ebb-tidal delta will commonly form offshore of the inlets. These types of inlets are commonly found in micro-tidal regimes on wave-dominated coasts (McSweeney et al. 2017). The flow from the inlet to the coastal ocean is strongly modulated by both tidal currents and the river discharge, and the rivers have generally short (few km

to flood tide only) salinity intrusions, except for the Wairoa River, which can have a salinity intrusion exceeding 10 km in the dry season (K. Bryan, unpublished data).

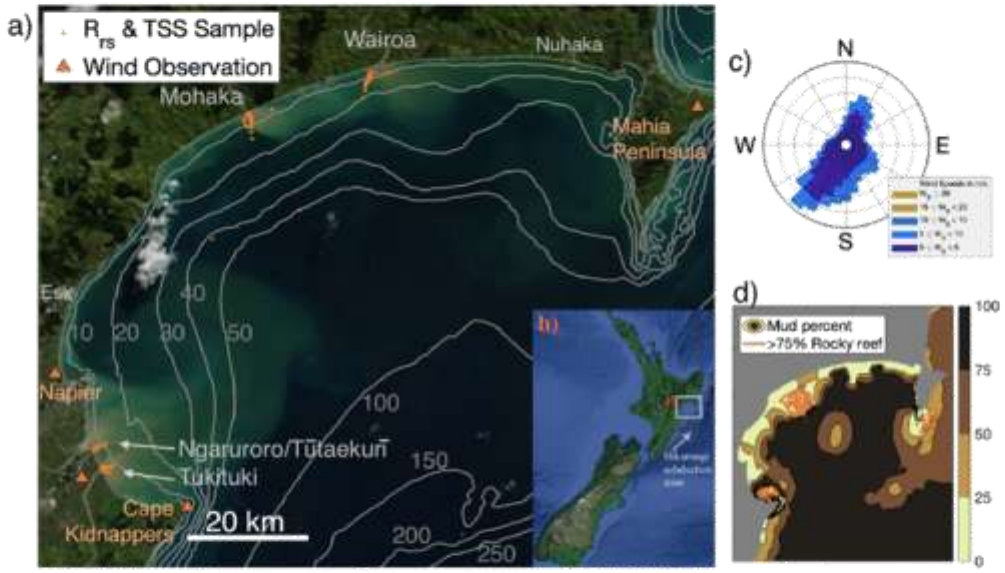

Figure 2.1 a) Map of Hawke Bay, Aotearoa New Zealand. The location of the Bay in Aotearoa is shown in b) in the red box (image from Google Earth). Sample locations are shown in orange and bathymetric contours (m) are plotted in grey. The true colour image is from NASA MODIS. Red triangles and text show meteorological stations where wind data is used. The main rivers flowing into the Bay are labelled in grey and places are labelled in orange. c) Wind rose from the Napier Airport meteorological station showing the frequency occurrences of wind magnitude (m s^{-1}) and direction over the period of this study from 2000-2021. d) The percent mud throughout the Bay and the areas of rocky reef (coloured red).

The bathymetry of the Bay is generally smooth with a gentle slope that extends to the continental slope and the Hikurangi subduction zone (Fig. 2.1). The seafloor composition in the Bay is muddy/fine-sand nearshore, and sandy/mud (ranging from 1–50% sand) offshore of the ~20 m isobath, but varies spatially (Pantin 1966, Bostock et al. 2019). Large sedimentary cliffs (> 100 m) line a significant portion of the coastline of the Bay, which are prone to landslides and erosion into the Bay. Estimates of sediment accumulation in the Bay range from 0.1 cm yr^{-1} in muddy areas of the Bay and up to 0.3 cm yr^{-1} in two main depositional areas (Pantin 1966, Paquet et al. 2009). The Bay is susceptible to strong wind and wave forcing. The average significant wave height recorded off Napier is 1.2 m, but although it typically reaches 2.5–3.5 m during high wave events, it can also reach > 8 m in extreme cases (Komar 2010). Waves approach on average from the east-southeast and are generally larger in the austral winter (Godoi et al. 2016). When rainfall events coincide with high-wave events, sediment is more likely to be transported to long-term depositional areas than when rainfall events

occur during calm conditions (Bever et al. 2011). The southern portion of the Bay experiences wind on average from the SW, as seen at the Napier airport weather station (Fig. 2.1), although winds from the NE, S, and SE are also common. In the northern portion of the Bay, SW winds are also common, but NE and E winds are more common than in the Southern Bay (Fig. 2.1; Chappell 2013).

Hawke Bay is microtidal, with a spring tidal range of 1.9 m, and neap tidal range of 1.2 m (as measured at the Napier Port). Current patterns in the Bay are not well studied. The prevailing notion of the mean currents is inflow at the center of the Bay from the South producing a pair of semi-persistent cyclonic and anticyclonic eddies from west to east (Stevens et al. 2021), which are likely influenced by the offshore boundary currents. The East Auckland Current predominately flows offshore of the Bay in the summer months, flowing from North to SE, carrying subtropical warmer, saltier water, while the Wairarapa Coastal Current, flowing from the South, carries cooler fresher water into the Bay (Stevens et al. 2021).

2.3 Methods

2.3.1 Satellite ocean colour data

Satellite ocean colour data from MODIS Aqua and Terra was used as the source of remote sensing reflectance (R_{rs}) data. Level 1A MODIS files were obtained from the NASA Ocean Colour website (https://oceancolour.gsfc.nasa.gov) and were atmospherically corrected and processed to level 3 with the SeaDas OCSSW multi-level processor. The atmospheric correction was modified from the default *l2gen* parameters to suit the commonly turbid water in the study area. Specifically, the dark-pixel atmospheric correction used the 748 and 859-nm bands, the iterative correction was turned off, the cloud detection method used the 2130-nm band with a threshold of 0.018 (following Aurin et al. 2013), the pixel saturation flag was turned off, and the straylight flag was turned off in order to retain pixels directly adjacent to the coast due to the small scale of the river plumes. These changes to the default *l2gen* settings allow for higher reflectance values to be processed, although it led to an increase in noise due to glint and a higher return of negative reflectance values in open-ocean waters (e.g. Feng et al. 2018). Pixels were processed at the nadir resolution of 250 m for the 645 nm band, and gaps in the data due to off-nadir image collection were filled by successive runs of the processing algorithm using larger interpolation stencils.

For each day, either an Aqua or Terra image was selected based on the number of cloud-free pixels in the Bay, given differences between the two sensors have been shown to be acceptable for this type of study (Dogglioti et al. 2016). Negative reflectance values were removed. All images were visually inspected for data quality, and where cloud remnants from the OCSSW processing were evident in pixels, these pixels were manually removed. Usable data existed for most of the Bay for about 40% of the entire MODIS record. The atmospherically corrected MODIS R_{rs} was compared

with in-situ R_{rs} (described below) for a limited number of matchups that occurred during two separate days of cloud-free sampling, collected within 3 hours of image collection.

2.3.2 In-situ data

Concurrent hyperspectral radiometry and water samples for TSS (n = 65) were taken at multiple locations in the Bay (Fig. 2.1) to facilitate the development of a local TSS algorithm applicable to MODIS. Typically, the data and samples were collected along cross-shelf transects off the major rivers' entrances following discharge events. A Seabird Scientific HyperOCR hyperspectral radiometer was deployed from a boat on a floating platform measuring downwelling irradiance ($E_d(0+)$), and water-leaving radiance (L_w) above the water surface using the skylight-blocked approach (Lee et al., 2013) over the spectral range of 350–800 nm at 3.3 nm resolution. For each sample, the boat was anchored to sample a consistent region of the river plume, and the HyperOCR sampled for two minutes at 3 Hz and then averaged over the sample duration. While data recorded, a 1 L bottle sample was taken at the sea surface for the TSS measurement. The remote-sensing reflectance was calculated as $R_{rs} = L_w/E_d(0)$ (Fig. 2.2a) and was corrected for self-shading using the method of Yu et al. (2021). The full data set can be accessed through the GLORIA database (Lehmann et al. 2023).

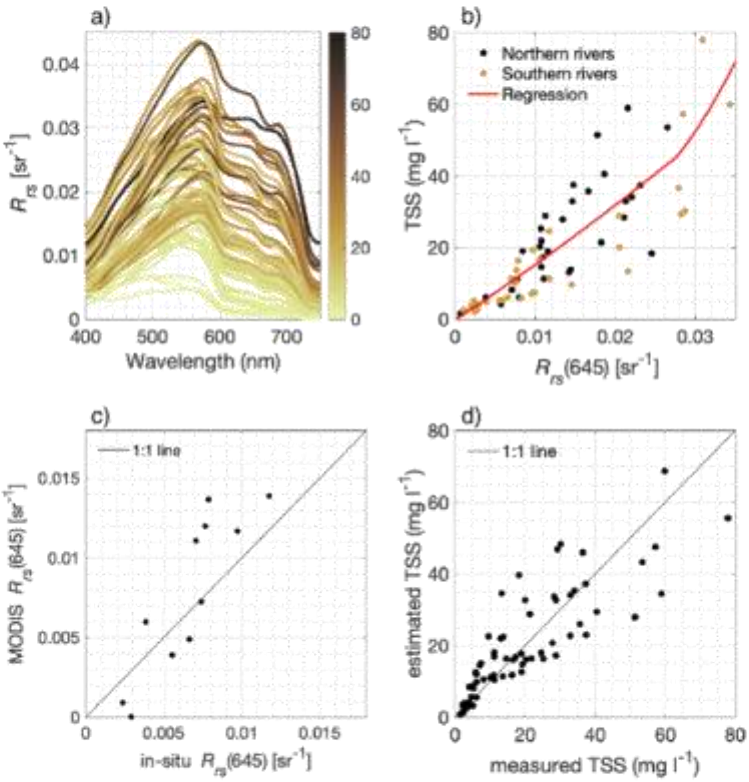

Figure 2.2 The measured remote sensing reflectance, TSS, and the empirical regression between remote sensing reflectance and TSS. a) R_{rs} (sr^{-1}) spectra coloured by co-located TSS (mg l^{-1}). Locations of samples are shown on the map in Fig. 1. b) Piecewise quadratic and exponential regression between in-situ R_{rs} (using MODIS 645 nm spectral response function, c) comparison of in-situ R_{rs} at 645 nm with co-located MODIS derived R_{rs} at 645 nm after the atmospheric correction, d) the evaluation of the regression compared with the observed values of TSS (mg l^{-1}).

The MODIS red band (centered on 645 nm) was used for an empirical relation to estimate TSS (Fig. 2.2b). The hyperspectral R_{rs} data were weight-averaged to match the MODIS 645 nm spectral response (denoted as R_{rs} (645)), then a piecewise quadratic and exponential regression was fit to the TSS data

$$TSS = 5984R_{rs}^2(645) + 1480R_{rs}(645) - 0.2438 \qquad \text{for } R_{rs}(645) < 0.0274\ sr^{-1}$$

$$TSS = 7.863exp(63.2R_{rs}(645)) \qquad \text{for } R_{rs}\,(645) \geq 0.0274\ sr^{-1} \ (2.1).$$

2.3.3 Additional data sources

River flow data were collected by the Hawkes Bay Regional Council for the four rivers at 15-minute intervals (https://www.hbrc.govt.nz/environment/river-levels/). Concurrent river suspended sediment and river flow data for the Wairoa, Mohaka, and Tūtaekurī/Ngaruroro Rivers (but not the Tukituki River) were sourced from Hicks et al. (2011), where concurrent measurements of river flow and cross sectionally averaged suspended sediment concentration were made. The data were used to fit a power-law regression model between discharge and TSS for the Wairoa, Mohaka, and Tūtaekurī/Ngaruroro Rivers. Wind data were sourced from four stations positioned across the Bay (Fig. 2.1), where hourly wind speed and direction were recorded, maintained by NIWA and Hawkes Bay Regional Council.

Modelled wave height, period, and direction were sourced from a wave hindcast model of Aotearoa New Zealand (Albuquerque et al. 2021) which extends until the end of 2019. The wave model grid has a 9-km resolution in the study area which captures the Bay's geometry and wave shadowing effects from the headlands of the Bay. The wave model output was interpolated to the MODIS grid, using nearest values for the extrapolation to locations outside of the wave model grid. Wave bed shear stress was calculated as $\tau = 0.5\rho f_w u_b^2$, where ρ is the water density, and the wave friction factor f_w was calculated as $f_w = 1.39(A/z_0)^{-0.52}$ (Soulsby 1997). The wave orbital velocity was calculated as $u_b = \frac{\pi H}{t}\sinh(kh)$ and the wave orbital amplitude as $A = H/2\sinh(kh)$, where linear wave theory was used to compute the wavenumber k, and the bottom roughness was calculated as $z_0 = d_{50}/12$. The median grain size d_{50} was sourced from a compiled sediment bed data set from Bostock et al. (2019) merged with samples collected by Hawkes Bay Regional Council (293 in total)

as well as seafloor classification data obtained from sonar. The bed sediment percent mud (grain size less than 63 μm) and rocky reef data were interpolated to cover the Bay (Fig. 2.1).

2.3.4 Analysis methods

For the major rivers in the Bay, a time series of TSS was extracted by finding the maximum TSS value within a 1 km radius of the general region of the river mouth, which was to account for the change in river inlet position over time, and the lateral advection of the plume by waves and currents. Each value was manually checked to make sure an appropriate pixel was selected. Additionally, for each major river in the Bay, the plume centerline, defined as the path that would follow the dominant along-plume velocity (and create a local maximum of TSS), was computed to quantify the horizontal scale of each plume, given that the plumes can have complicated geometries. To calculate the plume centerline for each river, the TSS field was smoothed to reduce spatial noise. Next, starting at the maximum TSS value near the river mouth, the centerline was computed by following the local maximum in the TSS until either the 2 mg l^{-1} value was reached, or the sign of the gradient along the transect changed from negative to positive. Each plume centerline was quality-checked and manually drawn if necessary. A majority of the transects needed to be manually altered, typically due to noisy or missing data. Only transects displaying an unambiguous TSS plume were retained, which excluded days with small plumes comprised of few pixels (250–500 m) or which showed elevated TSS from wave resuspension or advection from other locations such as alongshore coastal currents.

2.4. Results and discussion

2.4.1 On the Rrs-TSS relationship in Hawke Bay

Although significant scatter remained, the empirical regression of TSS on $R_{rs}(645)$ captured the general relationship between the two variables and facilitated the retrieval of reasonably accurate TSS concentrations (r^2=0.71, RMSE=9.16 mg l^{-1}, MAPE=33.53%; Fig. 2.2b,d). A quadratic regression captured the TSS variability relatively well at low TSS, but an exponential fit captured it better at high TSS values. This exponential fit represented the relationship between these two variables for high *Rrs*(645) values (> 0.0274 sr^{-1}) because *Rrs*(645) becomes less sensitive to changes in TSS as TSS concentration increases. Here, the algorithm was developed using in-situ data covering a TSS concentration range of <1 to 78 mg l^{-1}.

Although the TSS concentrations in the Hawkes Bay rivers can reach > 1000 mg l^{-1} during high-discharge events (Hicks et al. 2011), almost all *Rrs*(645) values derived from the satellite ocean colour imagery were < 0.047 sr^{-1} (corresponding to estimated TSS concentration of ~150 mg l^{-1}), and the vast majority of them were < 0.037 sr^{-1} (corresponding to estimated TSS concentrations of < 80 mg l^{-1}). The comparison of the in-situ R_{rs} with MODIS derived R_{rs} at 645 nm (Fig. 2.3c) shows moderate ability in replicating the observed values (r^2=0.56, RMSE=0.0040 sr^{-1}).

The higher scatter observed in the *Rrs*(645)-TSS relationship at higher TSS values (Fig. 2.2b) was likely the result of several factors. The northern and southern rivers exhibited different relationships (Fig. 2.2b) likely in part because of differences in sediment characteristics (e.g., particle size, organic carbon content). Differences in sediment characteristics including particle size, shape, and mineral composition directly influences the specific backscattering coefficient of the sediment, which can directly impact the relation between R_{rs} and TSS (Kirk 1994). These differences among rivers are likely due to varying geological characteristics of source sediment from the Northern region of the Bay (Tertiary sandstone) compared to the Southern region (Mesozoic sandstones; Pantin 1966). Additionally, elevated and variables concentrations of phytoplankton and chromophoric dissolved organic matter (CDOM), which can vary independently from non-algal suspended particles, can also impact *Rrs*(645) and create scatter in the *Rrs*(645)-TSS relationship (Kirk 1994). Although differences in the *Rrs*(645)-TSS relationship exist between rivers, a single algorithm/relationship was derived here from the collated data set to avoid creating any artificial spatial gradients in the imagery caused by applying region-specific algorithms.

2.4.2 River discharge and TSS concentrations

The daily river discharge (interpolated to the MODIS image collection times) shows that the Wairoa and Mohaka Rivers have the largest median discharge events (Fig. 2.3a), compared with the Tukituki and Ngaruroro/Tūtaekurī Rivers. The mean and 99.9th percentile daily discharge ($m^3 s^{-1}$) are 110 and 2183 (Wairoa River), 71 and 1015 (Mohaka River), 47 and 1241 (Ngaruroro/Tūtaekurī Rivers), and 41 and 1329 (Tukituki River). We note that daily values do not reflect the highest magnitude event discharge due to the typical short event durations.

The remotely sensed TSS offshore of these rivers was found to be of similar magnitude for the three rivers investigated (Fig. 2.3b), with mean values (in mg l^{-1}) of 21 (Wairoa), 24 (Mohaka), and 23 (Tukituki). The estimated mean TSS in the rivers from rating curves (in mg l^{-1}) yielded 214 (Wairoa) and 114 (Mohaka), while the 99th percentile values reach concentrations of 2518 and 1036 mg l^{-1} for the Wairoa and Mohaka Rivers respectively. The difference in magnitude between the estimated river TSS and remote sensing derived offshore TSS indicate that substantial dilution of the suspended sediment concentration occurs offshore of the river inlet or that the empirical relation for TSS used here underestimates the higher range of TSS.

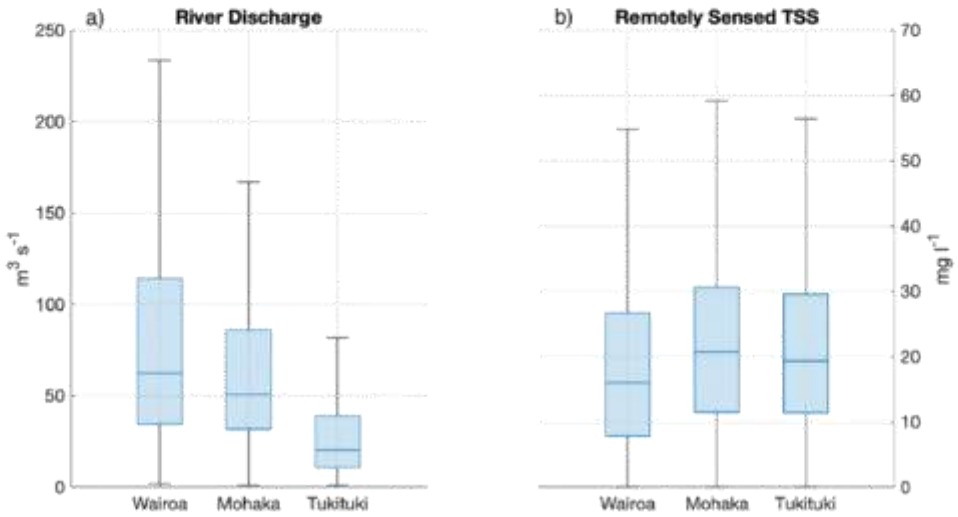

Figure 2.3 Box and whisker plot of the river discharge and remotely sensed TSS for each river. a) The daily river discharge ($m^3 s^{-1}$) for each river, and b) box and whisker plot of the TSS ($mg\ l^{-1}$) offshore of each river derived from MODIS.

2.4.2 Temporal variability of TSS

The TSS averaged over the nearshore coastal waters of Hawke Bay (0–10 m depth range, Fig. 2.4c) has a strong seasonal cycle with persistently elevated values (~15 $mg\ l^{-1}$) in the austral winter, when background total discharge into the Bay is around 300–400 $m^3 s^{-1}$ (Fig. 2.4a), and during discharge events when the total discharge into the Bay is from 500 to >2000 $m^3 s^{-1}$ and the nearshore averaged TSS can reach values from 15–30 $mg\ l^{-1}$. The significant wave height follows a similar seasonal pattern to the river discharge (Fig. 2.4b), commonly co-occurring with discharge events, with generally larger heights (1–3 m) during the winter, generally occurring predominately from the S as well as from the E/NE, and generally smaller heights in the summer (Fig. 2.4b). During the summer, the TSS generally drops to values in the 0–5 $mg\ l^{-1}$ range when the discharge drops substantially, although sizeable rainfall events can occur during summer when storms and tropical cyclones impact the region (Chappell 2013), which can also produce large easterly swells.

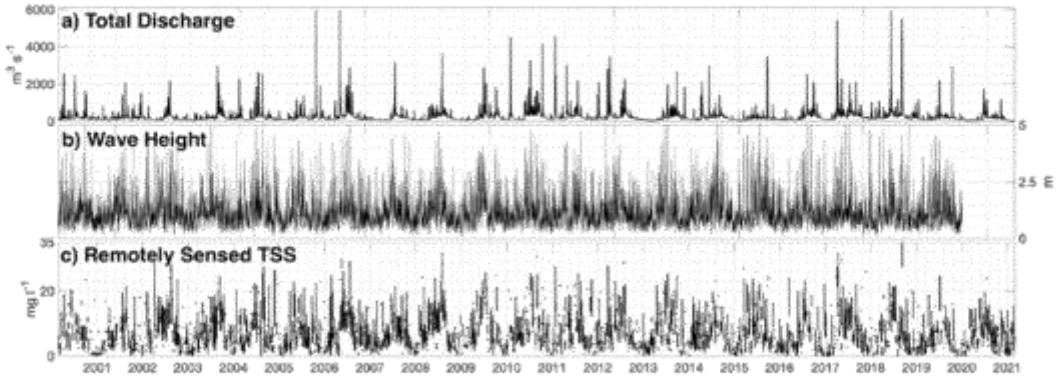

Figure 2.4 Time series of environmental conditions in Hawke Bay from 2000 to 2021. a) The summed river discharge from the four main rivers in Hawkes Bay, b) time series of the significant wave height (m) in the northern part of the Bay offshore of the Mohaka River, derived from the wave model hindcast of Alburqurque et al. (2021) which terminates in 2019, and c) time series of remote sensing derived TSS (mg l^{-1}) averaged between 0-10 m depth in the Bay. The TSS is plotted such that lines connect data points when there are consecutive data points, otherwise individual data points are shown.

Remotely sensed TSS concentrations near the outflow of major rivers is often elevated due to the riverine flux of sediment into the Bay. Near the river mouths TSS concentrations can reach ~150 mg l^{-1} (Fig. 2.5b, d, f). For the major rivers in the Bay, large discharge events are the main contributors to the total annual flux (Fig. 2.5a, c, e, g), as is common for small mountainous river systems (Milliman and Syvitski 1992). The Wairoa River has the largest flux, followed by the Mohaka River. The Ngaruroro/Tūtaekurī and Tukituki rivers export roughly similar amounts of sediment (not shown). Due to the proximity of the rivers, the sediment fluxes to the Bay from different rivers commonly co-occur. However, the fluxes for all rivers display strong interannual variability, which is driven by a small number of large discharge events as indicated by the stepwise nature of the fluxes. Discharge events for all rivers are generally short (1–3 day durations) and the corresponding TSS signal from remote sensing has short lag times (0–1 days).

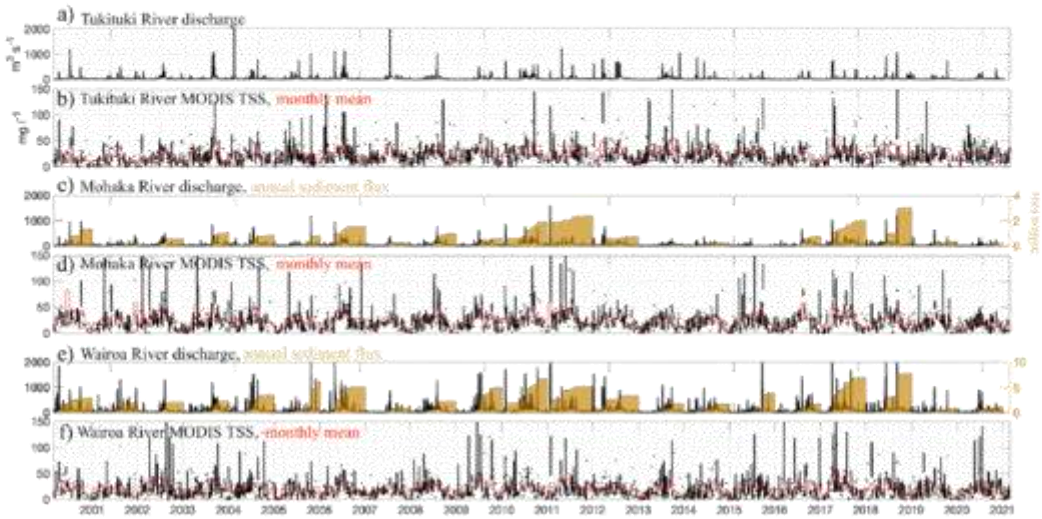

Figure 2.5 The timeseries of remotely sensed TSS for the major rivers in Hawke Bay. a) Timeseries of river discharge ($m^3 s^{-1}$), river suspended sediment flux estimated from regressions for river TSS (right axis) in accumulated millions of tons annually (panels a, c, and e). The MODIS derived TSS ($mg\ l^{-1}$) is shown for each river in panels b, d, and f, along with monthly averages of TSS in red. The TSS is plotted such that lines connect data points when there are consecutive data points, otherwise individual data points are shown.

The monthly averaged values of TSS for each main river (red lines in Fig. 2.5) show a clear seasonal cycle, which is more apparent for the larger rivers (Mohaka and Wairoa). Interannual variability is present in all the signals, caused by a range of interannual variability in the river discharge and subsequently the sediment flux for all the rivers. Monthly averages of TSS (Fig. 2.6) show a clear seasonal signal in the intensity of TSS both around the main river areas and on the continental shelf. In the summer months, average TSS values around the river mouths are around 5–10 $mg\ l^{-1}$, as well as in the Southern part of the Bay near Cape Kidnappers. Persistent elevated TSS can be seen directly north of Cape Kidnappers, a region with large sedimentary cliffs adjacent to the shoreline that are prone to erosion. Some of the elevated values in the area may also be due to the river discharge from the Maraetotara River, which has a much smaller discharge regime than the Tukituki River. In the peak of the winter, average TSS values around river mouths are elevated to values between 20–25 $mg\ l^{-1}$, and the entire shelf inshore of 50 m has average values around 5 $mg\ l^{-1}$.

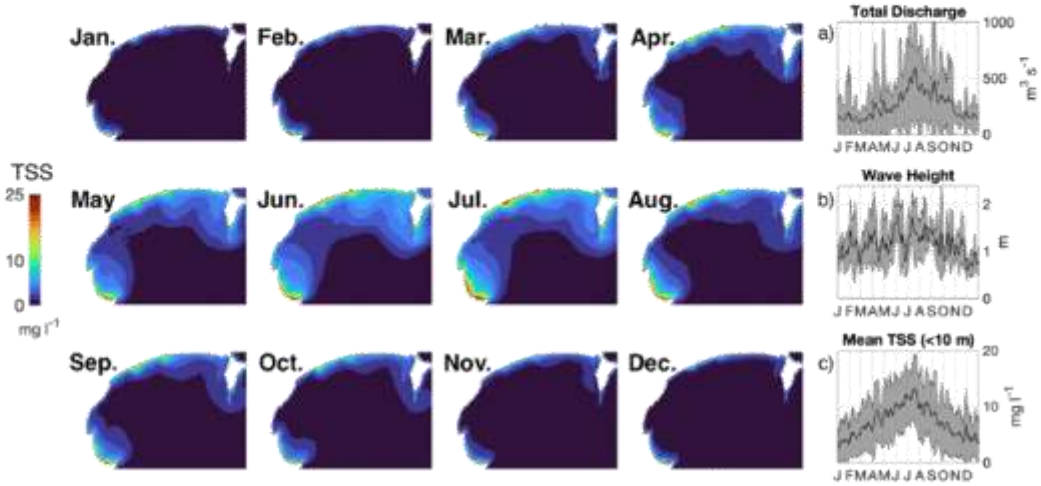

Figure 2.6 Monthly means of TSS (mg l^{-1}) over the entire MODIS record. The panels on the right show weekly moving means of annual variability (black line) and one standard deviation (shading) for a) total river discharge (m^3 s^{-1}), b) significant wave height offshore of the Mohaka River (m), and c) the spatially averaged TSS in 0–10 m depths in the Bay.

The time-series of TSS offshore of rivers (Fig. 2.5) shows that river discharge at seasonal and event timescales appear to be the dominant signal driving the TSS variability of the Bay. For each river, the TSS time series partitioned into the annual, monthly, and higher frequency components is used to determine the linear relationship with the total TSS time series. The annual component of the TSS, averaged over the four main rivers, comprises 2.8 % of the variance, the monthly component comprises 22 % of the variance, and the remainder (the total minus the annual and monthly—the event-driven component) comprises 70 % of the variance. Similarly, the cumulative sediment flux into the Bay generally occurs in a small number of discrete events every year (Fig. 2.5). Although the TSS from remote sensing also shows that most of the signal is from discrete events, the time scales of TSS in the Bay reflects other processes related to river plume dynamics, sediment resuspension, as well as clouds during large storm events causing missing data.

2.4.3 High-TSS events in the Bay

An example of a discharge and wave event is shown in Fig. 2.7 for June through August of 2017. The first snapshot (Fig. 2.7c) shows moderate TSS values in the nearshore of the Bay, where the TSS reaches 30–40 mg l^{-1} offshore of the major rivers, likely caused by a moderate discharge event the day prior. Wind of around 9 m s^{-1} from the E during this time likely caused northward deflection of the Mohaka and Wairoa River plumes, while transport in the Southern Bay is directed offshore and to the north. The TSS transects for each river plume (if distinct plumes are present) are

plotted as black lines on the map view plot, and the TSS values are shown in the plot below each map view plot, plotted as the distance in km from the river mouth. Panel d shows a slight increase in discharge from the Wairoa River, causing the initial TSS in the transect to reach above 50 mg l^{-1} then abruptly drop within 2 km of the river mouth. These days both show the plume from the Wairoa River traveling up the coast where the TSS transect extends much further than the other rivers. An elevated TSS region from the Wairoa River is also visible after a moderate discharge event with S to SW winds (Fig. 2.7d), again causing transport upcoast for all rivers.

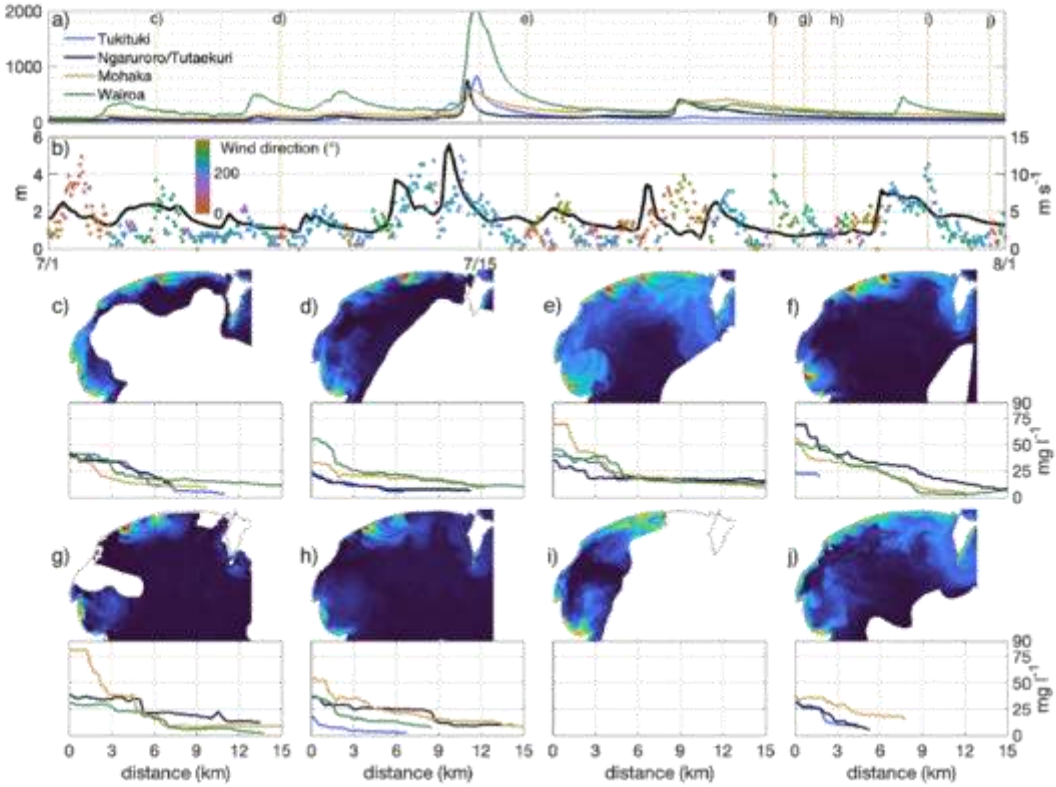

Figure 2.7 Example of a river discharge event in the winter of 2017 from June 15 to August 15. A time series of forcing variables is shown including a) river flow ($m^3 s^{-1}$) for the main rivers, b) significant wave height (m) in black on the left axis and the wind speed and direction (coloured) on the right axis. The gold lines marking the times of TSS (mg l^{-1}) panels numerically listed in a). Transects of TSS along plume centrelines are shown in the lower right for each corresponding day for each river plume, unless no clearly defined plume was observed for that river or day. The scale bar for the TSS map view plots is shown in the lower right (range 0–50 mg l^{-1}).

A large storm event occurred on July 15, and a MODIS image was acquired two days after (Fig. 2.7e). During the storm event, wind speeds exceeded 10 m s^{-1} from the SW, the significant wave height exceeded 5 m, the Wairoa River discharge reached 2100 $m^3 s^{-1}$, and the other rivers discharges exceeded 500 $m^3 s^{-1}$. The TSS offshore of the rivers were elevated until ~6 km from the river mouths

and large areas of the Bay showed increased TSS as compared with the other days during this period, potentially due to the large wave and high winds over the previous two days. Another discharge event occurred (~400 $m^3 s^{-1}$) on July 22, followed by a MODIS image collected on July 24 (Fig. 2.7f) with westerly winds causing plumes to be directed offshore and to the left. With the river discharge still elevated, the wind direction then shifted from N to NE to E, causing plume directions to shift accordingly. A southerly wind event (> 10 m s^{-1}; Fig. 2.7i) with a significant wave height of ~3 m occurred on July 28 which caused widespread increased TSS in the northern region of the Bay, and increased TSS advected northward from Cape Kidnappers. Likely remnant increased TSS from this wind event is then observed two days later (Fig. 2.7j).

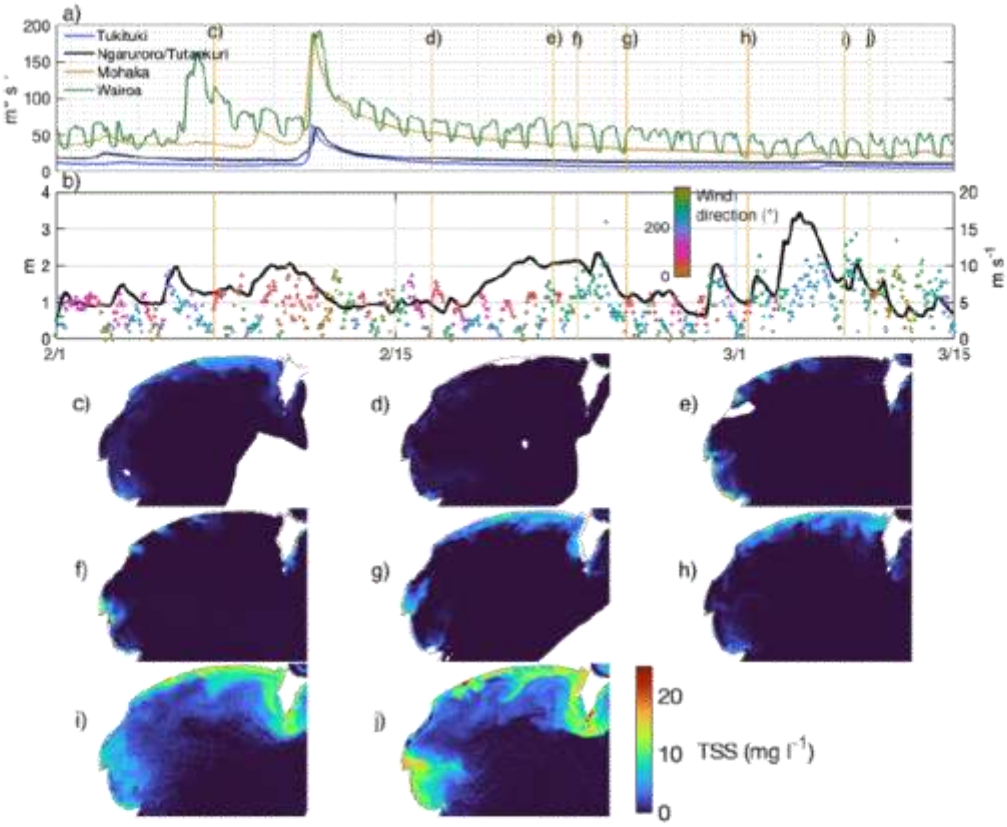

Figure 2.8 Example of elevated TSS due to wind and waves from February to March of 2006. A time series of forcing variables is shown including a) river flow ($m^3 s^{-1}$) for the main rivers, b) significant wave height (m) in black on the left axis and the wind speed and direction (coloured) on the right axis, with the panels showing TSS (mg l^{-1}) at the numeric labels plotted in a).

At other times, moderate to high TSS values are found after significant wave or wind events without substantial river discharge occurring, indicating resuspension of sediment from the inner

shelf. For example, Fig. 2.8 shows a period from February to March of 2006 with two small discharge events with moderate surface TSS expression, followed by periods of moderate to large waves (from 2 to 3.7 m significant wave height) and a wind event. Panel c shows the remnants of the discharge event from the Wairoa River (peaked at 170 $m^3 s^{-1}$) and SW wind which caused upcoast transport towards the Mahia Peninsula, while panel d shows a return to low magnitudes of TSS in the Bay, as river discharge magnitudes further drop. Panels e-h show a period with increased wave heights greater around 2 m and regions of increased TSS in depths less than 20 m. On March 4, a 3.7 m wave event occurred along with moderate SW winds, and on March 5 the TSS in the Bay is greatly increased compared to background conditions, with TSS of 5–15 mg l^{-1} throughout most of the Bay. The day after, the wind speed increased to around 15 m s^{-1} from the E, and the TSS substantially increased, particularly in the Southern region of the Bay, advecting material offshore in the Southern region of the Bay and northward around the Mahia Peninsula in the Northern region of the Bay.

2.4.4 Typical spatial variability of TSS

The average spatial variability of TSS in the Bay is revealed by the percentage of time that the remotely sensed TSS concentration was above a threshold value, relative to the number of observations available at each pixel. Here, these percentages were computed for the 5, 15, and 45 mg l^{-1} thresholds (Fig. 2.9). In all cases, the most frequent occurrences were near the inlets of the main rivers, with the Mohaka and Wairoa Rivers exhibiting prominent half-circular regions of higher occurrence for both the 5 and 15 mg l^{-1} intervals (Fig. 2.9a-b). The 50% occurrence for 5 mg l^{-1} for these two rivers extended roughly 2.5 km from the inlet. The same 50% occurrence contours for the Tukituki and Ngaruroro/Tūtaekurī Rivers merged to form a continuous band roughly 2.5 km wide. The contours widen at Cape Kidnappers to 3.75 km from the shoreline, potentially due to enhanced sediment supply to the nearshore from cliff erosion and wave resuspension.

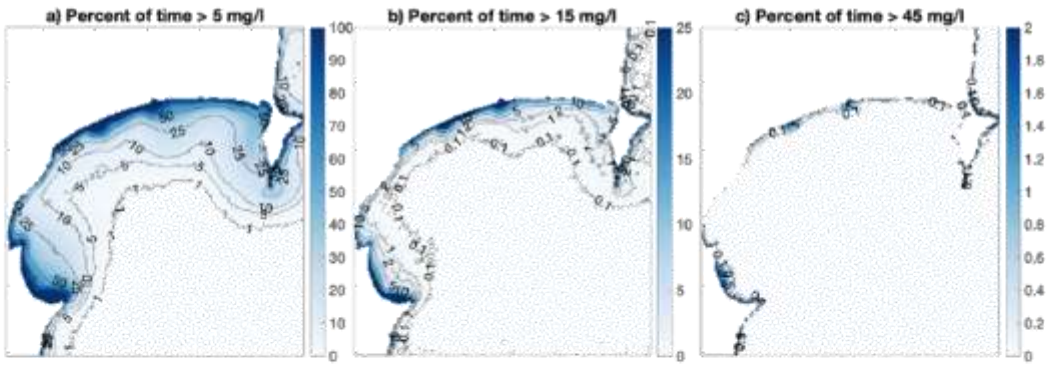

Figure 2.9 The percentages of occurrence for a range of TSS values. a) 5, b) 15, and c) 45 mg l^{-1} is shown for each pixel in the bay. The percentage was computed using the number of days that each pixel had available data.

The contours for the 15 mg l^{-1} threshold (Fig. 2.9b) follow similar spatial patterns as the 5 mg l^{-1} threshold. However, they are greatly reduced in areal extent for the 45 mg l^{-1} threshold (Fig. 2.9c), where high values are restricted to areas directly adjacent to the river inlets. For example, the 1% occurrence of the greater than 45 mg l^{-1} contour was located 2, 0.9, 2.5, and 1.5 km from the shoreline for the Wairoa, Mohaka, Ngaruroro/Tūtaekurī, and Tukituki rivers. For the rest of the coastline, the contours are typically 250 m offshore or not present.

2.4.5 Length scales of TSS concentrations in river plumes

The remotely sensed TSS can be used to infer the extent of the offshore transport in the surface layer. This can be altered by ambient subsurface currents and bed stresses which can prevent bed deposition. However, determining the length scales of the initial step of offshore transport is a key step for understanding the sediment transport to long-term depositional areas, determining regions of increased turbidity in the water column, and for assessing the health of benthic communities. Length scales of cross-shelf transport are dependent on the plume velocity to advect sediment, the plume thickness, and the sediment setting velocity. For example, Geyer et al. (2004) defined a general length scale of sediment deposition from a river plume as $L = uh/w_s$, where u is a characteristic along plume velocity (neglecting lateral advection), h is the plume thickness, and w_s is the settling velocity.

To quantify the length scales of initial deposition, the daily TSS transects for three of the rivers are used and two different length scale metrics are defined, including the e–folding distance (the distance following the transect until 37% of the initial TSS) and the distance to the 5 mg l^{-1} value. We note that not every TSS transect may reach the thresholds for an e–folding value or reach 5 mg l^{-1}. The e–folding distance is dependent on the gradient of TSS along the plume, which is controlled by

sediment advection and fallout from the plume. The 5 mg l^{-1} length scale is additionally used as a general outer boundary value of the river plume.

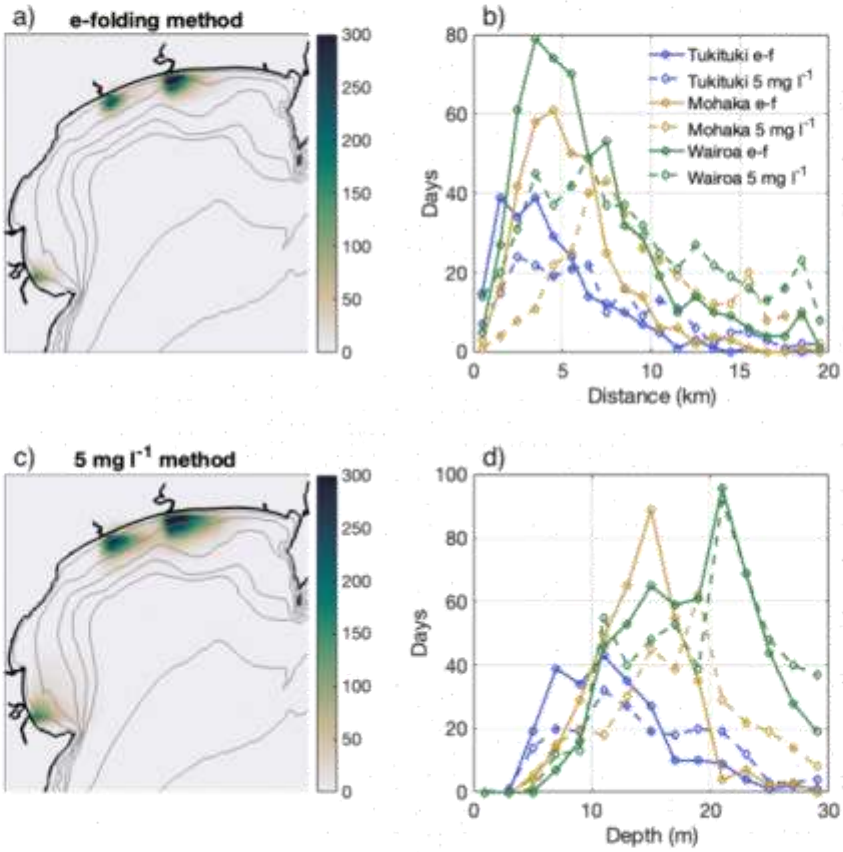

Figure 2.10 The estimated locations, transit distances, and depths of likely initial sediment deposition from two methods. a) The number of occurrences on a 1 km grid on e–folding locations computed for the Tukituki, Mohaka, and Wairoa Rivers. b) Histogram counts of the e–folding distance of TSS for along plume centerline transects for each river. The solid lines are the e–folding metric (named e-f), and the dashed lines are the distance of the 5 mg l^{-1} TSS value. c) The number of occurrences on a 1 km grid on 5 mg l^{-1} locations computed for the Tukituki, Mohaka, and Wairoa Rivers. d) Histogram counts of the depth corresponding to each location for each river. The solid lines are the e–folding metric, and the dashed lines are the distance of the 5 mg l^{-1} TSS value.

For each major river where a TSS plume was clearly identified, the distance from the edge of the river mouth inlet to the e–folding location and depth at that location, as well as the distances and depths to the 5 mg l^{-1} value (dashed lines), are shown in Fig. 2.10b,e. In general, the larger rivers have greater distances that extend further offshore to deeper depths, and the 5 mg l^{-1} metric is generally further offshore and deeper than the e–folding metric. Spatially, the southern rivers e–folding

locations are mostly inshore of the 10 m isobath clustered around the rivers (Fig. 2.10a). In contrast, the locations are inshore of the 20 m isobath for the Mohaka River, and even further offshore for the Wairoa River (Fig. 2.10a). The e–folding locations for the Tukituki River is well distributed in all directions from the river mouth while the northern rivers are mostly distributed directly offshore and down coast (in the direction of Kelvin wave propagation) from the river mouths. In comparison to the e–folding locations, the locations of the 5 mg l^{-1} value (Fig. 2.10d) show similar patterns but with more instances found, and generally exacerbated patterns that reflect the ending location of the transect.

The e–folding distance for all rivers has broad distributions with most transects having distances from 2–6 km, with a peak for the Wairoa and Mohaka Rivers around 3–4 km and 2–3 km for the Tukituki River (Fig. 2.10b). The histogram for all rivers shows a tail with distances greater than 10 km extending to 20 km, with more instances found for the Wairoa and Mohaka Rivers. The distances to the 5 mg l^{-1} value are slightly shifted to further distances but follow similar patterns. The similarities between the two metrics likely reflect commonly occurring TSS values offshore of the river mouths (10–15 mg l^{-1}) that would give e–folding values around 5 mg l^{-1}. The peak depths of the e–folding locations are deepest for the Wairoa River (21 m), followed by the Mohaka River (15 m) and the Tukituki River (11 m), which reflect a combination of the traversed distance offshore and the bathymetry offshore of the river. The initial transect TSS value shows weak linear relations with daily river discharge (r^2 from 0.1–0.2), and the e–folding distance displays higher scatter (r^2~0.025) than the distance to the 5 mg l^{-1} value (r^2~0.21) when related to daily river discharge. This likely signifies that the e–folding distance metric and TSS gradients are also controlled by other hydrodynamic and sediment processes, while the distance to the 5 mg l^{-1} is more related to advection related to river discharge.

Using general settling velocities for clay (0.01 mm s^{-1}), fine silt (0.1 mm s^{-1}), and aggregated particles or coarse silt (1 mm s^{-1}), along with plume velocities ranging 0.2–1 m s^{-1} and plume thicknesses ranging 0.5–4 m (Geyer et al. 2004), we can estimate the distances over which different sediment sizes are advected offshore before exiting the plume layer. Clay particles can be advected over tens to >100 km because of their low settling velocity, whereas fine silt particles travel anywhere between a few to a few tens of km. Particles with settling velocities of 1 mm s^{-1} likely travel a few km at the most. Aggregated particles have been shown to be deposited proximity to the river inlet due to their high settling velocity (Milligan et al. 2007, Warrick et al 2008). These results imply that the bulk of suspended sediment falls out of plumes within roughly 5 km from the river inlet and that the bulk settling velocities are 0.1 mm s^{-1} or higher. The furthest distances found here (>10 km) are likely dominated by particles with low settling velocities (~0.01 mm s^{-1}). However, without additional data to constrain the hydrodynamics of the river plumes, it is not possible to further constrain estimates of settling velocities.

2.4.6 Plume directionality

The direction of the river plume has important implications for determining which processes are most important for sediment dispersal in Hawke Bay. The main processes important for directing river plume transport in addition to the river momentum and buoyancy forcing are the Coriolis force (steering the plume down coast and northward in the direction of Kelvin wave propagation), wind driven currents, including upwelling and downwelling processes that can modify the plume structure (Horner–Devine et al. 2015), the inlet configuration (Geyer et al. 2000), and tidal modulation (Basdurak et al. 2020). If the length of the plume is greater than the baroclinic Rossby radius of deformation, which is on the order of 10 km for typical conditions, the Coriolis force is more likely to steer the plume towards the left and create a buoyancy-driven coastal current, and in the absence of other forcing with steady discharge, a recirculating bulge can form (Horner–Devine et al. 2015).

The river plume directionality was classified as spreading either down coast (northward), up coast (southward), or offshore, by classifying the location of the end location of the TSS transect in three 60° windows extending from each river mouth (Fig. 2.11a). Both the Mohaka and Wairoa Rivers plumes were predominately directed down coast ~65% of the recorded times, with less occurrences directly offshore (29%), and a small percentage of times the plumes directed up coast (<10%). In contrast, the plumes from the Tukituki and Ngaruroro/Tūtaekurī (not shown) Rivers predominately were directed offshore (52%), with comparable instances (~25%) directed either up or down coast. The dominant plume directions can also be seen in the locations of the TSS transect points (Fig. 2.10c).

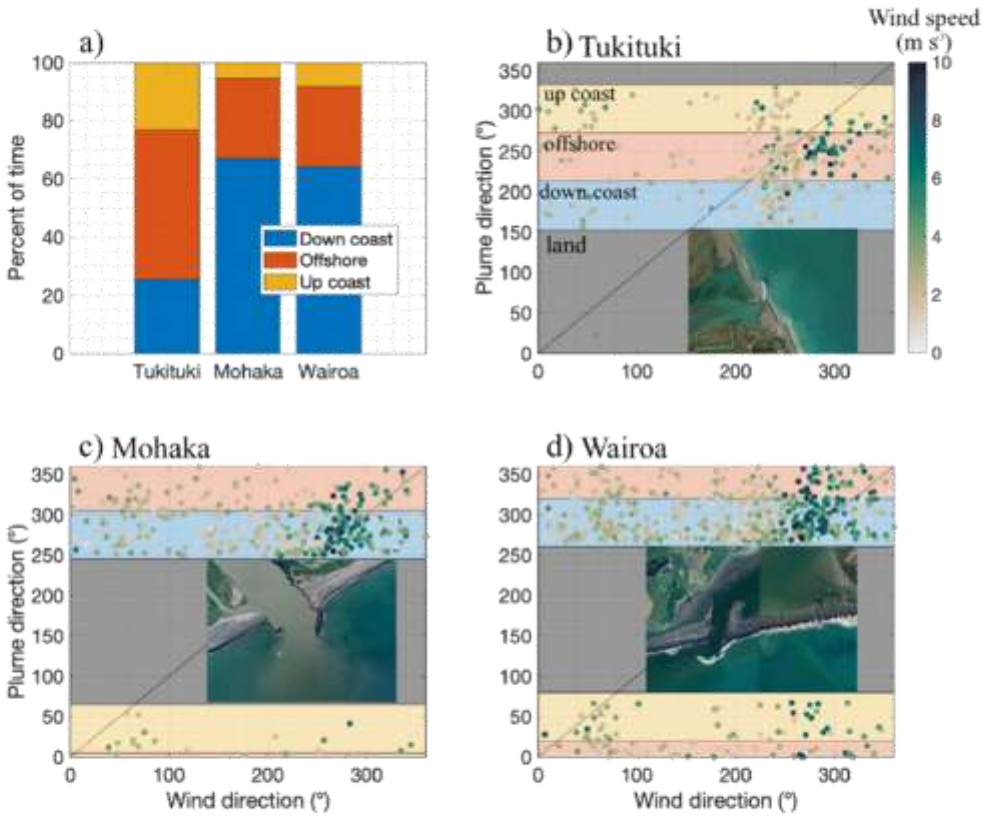

Figure 2.11 The river plume directionality and relation with wind direction. a) Plume directionality of each TSS transect for each river, in 60-degree sections offshore of the coastline at each river, computed using the location of the end point of the TSS transect. Down coast is oriented northward and up coast southward. b–d) Wind direction and speed (m s^{-1}) from the nearest wind station, averaged over the previous six hours to satellite image collection compared with plume direction for the Tukituki, Mohaka, and Wairoa Rivers. The grey shading represents the land boundary for each river, and the coloured shading corresponds to the colours from a). The coastline orientation is shown by Google Earth images at each of the river mouths.

Using the plume directions for each river, the angle of the river plume from the river mouth to the end of the TSS transect was computed and compared with the wind speed and direction (Fig. 2.11b–d) from the nearest weather station, where the wind speed and direction was averaged over the 6-hour period prior to satellite image collection. Downwelling winds from the SE to W (for the southern and northern regions of the Bay respectively) would be expected to vertically thicken and horizontally compress the plume along the coastline, while upwelling winds (NW to E) would be expected to thin and expand the plume in the cross-shore direction (Fong and Geyer 2001).

In general, the plume directions show weak linear relations with wind direction, with lighter winds showing more scatter than higher wind speeds. For the Tukituki River when wind speed is >5

m s^{-1}, a linear response is shifted such that the river plume is typically directed ~30° to the left of the wind direction, predominately during W–SW winds where the plume is directed offshore. For the Mohaka and Wairoa Rivers, the strongest winds came from the W–SW, where most of the correlation between wind direction and plume direction is found, with lighter winds from other directions showing higher scatter. Relatively few instances of higher wind speeds for wind directions other than W–SW were observed for the available plume transects.

These results indicate that the river-plume directionalities are sensitive to the predominant W–SW winds, which typically exhibited greater wind speeds. High scatter and low wind speeds for other wind directions limit the understanding of the plume response for those conditions. In the Merrimack River plume, Kakoulaki et al. (2014) found that the plume responded to wind speeds greater than 4 m s^{-1}, comparable to the speed threshold observed here. However, Kakoulaki et al. (2014) shows that the plume direction was typically offset from the wind direction by 45° due to Coriolis deflection. The Tukituki River displays a leftward shift related to wind direction but there is too much scatter for the Mohaka and Wairoa River plumes to discern any relation.

Other processes not considered here that likely influence plume trajectories include the inlet configuration, which for the Eel River was found to be important for setting the initial direction of the near–field plume (Geyer et al. 2000). The inlets in Hawke Bay can form complex morphologies which direct the near–field plume either up or down coast (e.g. Fig. 2.11b–d). Tidal motions have been shown to influence small discharge plume direction to either down coast or up coast depending on the tidal stage (Basdurak et al. 2020).

2.4.7 Relation between TSS and forcing mechanisms

Although the river forcing is likely the dominant driver of TSS variability, other processes including resuspension from wave bed shear stress and wind driven currents are likely important for resuspending sediment, potentially mixing to the surface layer, and advecting sediment throughout the Bay (e.g., Fig. 2.8).To illustrate this, the average TSS values are computed for varying forcing conditions (Fig. 2.12), including wind speed (averaged over the previous six hours), total river discharge into the Bay (the maximum value over the previous two days) and the significant wave height (averaged over the previous day). Additionally, for the wave height averages, days were selected on whether the total river discharge was greater than 500 m^3s over the previous 7 days.

The averaged composites show that river discharge is a key factor in the magnitude of TSS variability adjacent to the rivers and the inner shelf in general. Roughly half of the wave events greater than 2.5 m co–occur with elevated river discharge, leading to higher TSS during times of a past discharge event than without. However, wave events during low discharge also show elevated TSS in the northern nearshore region of the Bay as well as the Cape Kidnappers region, indicating

that wave resuspension alone is an important driver of TSS variability. Additionally, broad regions of the Bay show elevated mean TSS concentrations (~15 mg l^{-1}). For more moderate wave events (1–2.5 m), there is noticeably lower TSS away from river mouths, although elevated values are still seen around Cape Kidnappers. The TSS shows a slight increase in relation to increased wind speeds, but no clear pattern is apparent.

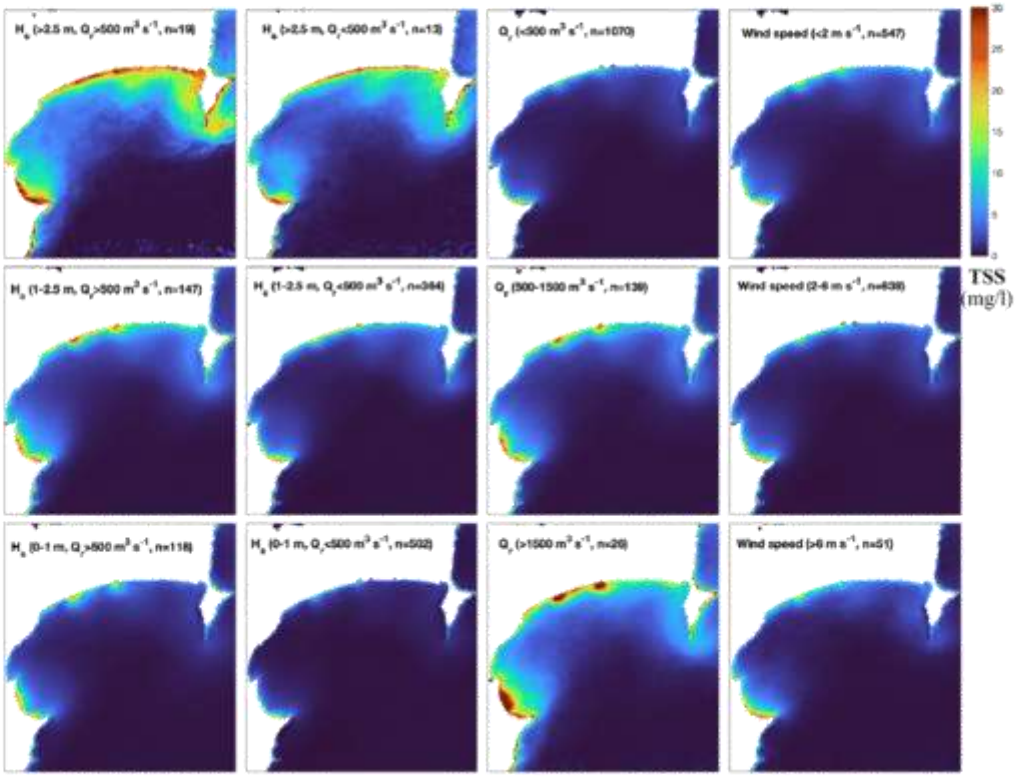

Figure 2.12 Average composites of remotely sensed TSS (mg l^{-1}) for various environmental conditions. The number of days averaged is shown for each plot. The left column averages wave conditions (using the 24-hour average significant wave height prior to image collection) when a greater than 500 m^3 s peak total discharge flowed into the Bay over the previous 7 days, and the middle–left column shows the same wave height ranges but when the total discharge did not reach a 500 m^3 s peak over the previous 7 days. The middle right column shows averaged days in total river discharge ranges (using the maximum value over the previous two days). The right column shows the averaged days under varying wind speed values (using averages over the previous 6 hours) measured from Napier Airport.

To estimate the relative contributions of forcing mechanisms with the surface TSS for each location on the MODIS grid, we use linear regression against three primary drivers (Fig. 2.13) including: 1) combined freshwater discharge into the Bay, 2) wind speed from the nearest wind

station averaged over six hours prior to image capture, and 3) bed stress due to waves. The linear regression (where significance levels are greater than 0.05) shows the river discharge is the dominant driver of TSS variability (Fig. 2.13a), particularly offshore of the Tukituki and Ngaruroro/Tūtaekurī rivers where the r^2 value is around 0.5 extending about 10 km offshore of the river inlet. Offshore of the Mohaka and Wairoa Rivers, high coefficients of determination of around 0.4 are found, and a broad portion of the Bay inshore of the 50 m isobath has elevated r^2 values of around 0.25. The linear correlation with the wave bed stress (Fig. 2.13b) has a broad region of moderate correlation with r^2 values greater than 0.2 for areas less than 50 m deep, and with higher correlations outside of regions of high correlation with the river forcing. The correlation with the wind speed is low throughout the entire Bay (Fig. 2.13c). However, the linear regression does not account for the temporal history of the TSS, as well as the expected nonlinearity in the relation between the bed shear stress and sediment resuspension.

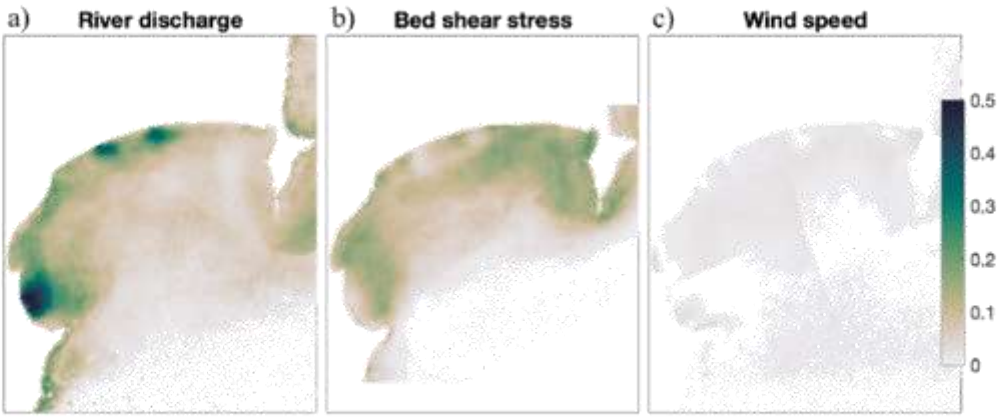

Figure 2.13 The coefficient of determination (r^2) between remotely sensed TSS and forcing mechanisms. The r^2 value for each pixel is based on the linear regression of TSS with a) the combined river discharge into the Bay, b) the wave bed shear stress, and c) the wind speed from the nearest wind station. The scale bar corresponds to all plots and only r^2 values where significance levels are greater than 0.05 are shown.

The bed stress due to waves, computed from modelled wave statistics, shows the wave climate of the Bay is often large enough to resuspend fine sediment that is deposited from the rivers (Fig. 2.14). The rivers predominately transport suspended sediment from clay to coarse silt sizes. Therefore, general critical erosion thresholds of 0.05 N m^{-2} for a fine silt sized particle (Fig. 2.14a) and 0.1 N m^{-2} for a coarse silt (Fig. 2.14b) are used here to gauge the frequency of exceedance (as the percentage of time) of the critical shear stresses for sediment deposited from the rivers. The bed stress exceedances show spatial variability associated with variable bottom roughness, as there are multiple rocky zones within the Bay (Fig. 2.1), as well as due to wave shadowing from the geometry of the Bay. The rocky zones within the Bay have persistently high enough shear stress values to resuspend

any material that was deposited there. Inshore of 30 m depth, roughly half of the time fine silt will be able to be resuspended. Coarse silt can be resuspended approximately a quarter of the time. Offshore of 50 m depth, fine sediment is likely resuspended for the largest wave events.

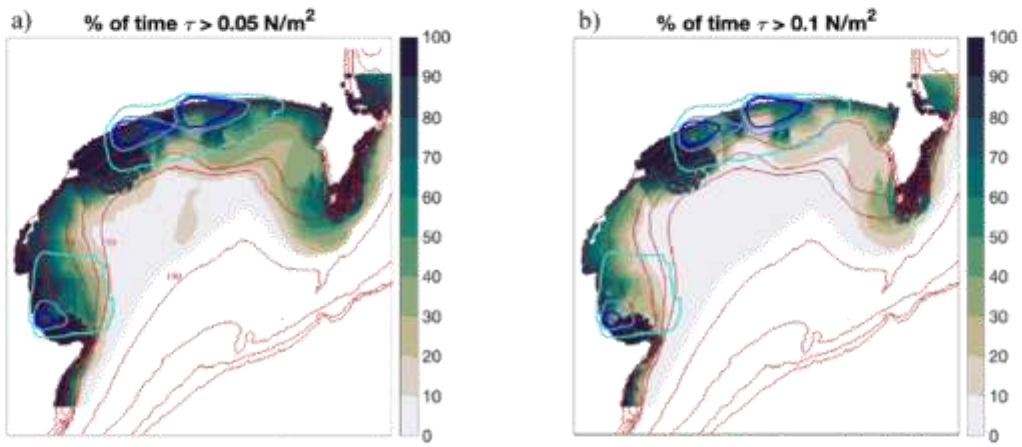

Figure 2.14 The spatial relationship between bed stress and surface transport regions. a) The percentage of time (evaluated at the time of image collection) of exceeding 0.05 N m^{-2} and b) 0.1 N m^{-1}. Bathymetry contours are shown in red and labelled on a). The blue to turquoise lines represents the contours of 100, 50, and 5 occurrences of the 5 mg l^{-1} TSS value (as seen in Fig. 10c) which was computed on a 1 km grid.

In the regions of likely initial deposition, here using the locations of the 5 mg l^{-1} TSS (Fig. 2.10c) transect points for occurrence values of 5, 50, and 100 (Fig. 2.14), shear stress exceedances for the fine and coarse silts are frequent, particularly for the higher occurrences (blue lines). However, this simple comparison does not consider the complexities of sediment erosion, including sediment consolidation, cohesion, and aggregation (Grabowski et al. 2011), and only provides a speculation into subsurface processes.

2.4.8 Length scales of plume transport

The derived length scales of likely sediment deposition found in this work largely corroborate prior studies of marine dispersal dominated river systems (Walsh and Nittrouer 2009), with relatively short length scales of surface transport that are typically further transported subsurface by processes that are not captured by satellite remote sensing. We found that the depths of the e–folding locations are typically shallow enough for material to be suspended upon common wave events, but more work is needed in Hawke Bay to further document these processes. For example, in the Waipaoa River (just north of Hawke Bay), the aggregate and coarser particles settle in the bay and slightly offshore (<7 km offshore), while finer sediment is more dispersive (Moriarity et al. 2015). Some sediment was found to be stored in long-term mud deposition areas located at bathymetric low points, but a majority

would be resuspended by wave orbital currents in the thin wave boundary layer, which can reach concentrations high enough to form hyperpycnal currents transporting sediment offshore (Hale and Ogsten 2015). If river flood events co–occurred with significant waves, sediment was likely transported offshore immediately, but if they did not co–occur, sediment would be stored temporarily in the bay and on the shelf (Bever et al. 2011, Moriarity et al. 2015). Kniskern et al. (2010) used isotopic dating to show that muddy sediments are stored ephemerally between 30–50 m, and that longer term deposition was found offshore at 80–120 m. Similar subsurface processes likely occur in Hawke Bay, and more detailed measurements are needed to investigate how initial surface transport relates to long term sediment transport and deposition in Hawke Bay.

2.5. Conclusion

Using a twenty-year record of satellite ocean colour data, we assessed the spatial and temporal variability of suspended sediment concentration offshore of several small mountainous rivers. The use of satellite remote sensing, here combined with an empirical regression for TSS based on in-situ data, allowed for an unprecedented number of discharge events to be captured for multiple rivers as compared with traditional in-situ measurements of river plume sediment transport. Longer temporal records enabled a full range of discharge events, wave, and wind conditions to be captured. TSS offshore of the main rivers in the Bay showed strong seasonal cycles related to seasonal changes in river discharge, but that the majority of the TSS variance offshore of rivers occurred at timescales shorter than seasonal. Although there were interannual differences in sediment flux into the Bay, typical of small mountainous river systems due to the importance of individual events, the interannual TSS variations from remote sensing were small in comparison. This is likely due to the short time scale of the events, which may not be captured due to cloudiness from remote sensing. The empirical algorithm used here was well suited for general conditions (0–80 mg l^{-1}) but may not accurately estimate the higher range of TSS values possible during the largest discharge events.

The use of remote sensing allowed detailed spatial information of three separate river plumes to be tracked over time. We found that river plumes spatial extents are highly related to the river discharge magnitude, which sets the outflow velocity, buoyancy, and sediment concentration of the river plume. Rivers with larger freshwater fluxes have a larger corresponding inner-shelf footprint of persistent TSS conditions. Plume length scales were defined using the distance to the 5 mg l^{-1} TSS value as well as a metric based on the TSS gradient (e–folding distance of TSS) along the plume centerline. Length scales of the TSS plume extent (to the 5 mg l^{-1} value) were most commonly between 2–8 km offshore, with the larger rivers (Wairoa and Mohaka Rivers) having further distances. The e–folding distance was shorter, with peak values ranging 2–6 km. The transport distances and depths were consistent with the previously established notion that coarser particles settle from the plume in the range of a few km from the river mouth, with the bulk of sediment typically

falling from the plume within ~6 km, while finer particles can be transported further offshore greater than 10 km. The prevailing wind direction relative coastline orientation were important for the observed river plume transport directions.

In Hawke Bay, the dominant contributor of the TSS signal was river discharge followed by waves. Waves were shown to cause elevated surface TSS even during low river discharge. Wind was not as important of a driver for TSS signals at the surface of the Bay but was important for advecting river plumes. Further work in Hawke Bay should address subsurface processes to better understand how surface sediment transport in river plumes, and the patterns that can be detected from satellite remote sensing, is related to long-term sediment deposition. Future satellite remote sensing work of small mountainous river plumes will benefit from using datasets with higher accuracy TSS retrievals at high TSS, higher resolution imagery particularly in the near-field plume and coupling with in–situ data of plume circulation can lead to new insights about sediment deposition and settling from river plumes.

Chapter 3: Circulation and cross-shelf sediment fluxes in an energetic bay with multiple small mountainous rivers

Contribution of Authors

Chapter 3 presents the article "Circulation and cross-shelf sediment fluxes in an energetic bay with multiple small mountainous rivers" which will be submitted to the journal *Continental Shelf Research* for review. Ted Conroy conceptualized the study, performed all numerical modelling, data analysis, and wrote the article. Karin R. Bryan provided feedback, supervision, and editing of the article throughout the process. Joe O'Callaghan provided assistance with the interpretation, and editing of the article.

3.1 Introduction

The delivery of terrestrial sediment into the coastal ocean can cause impacts on the shelf and nearshore ecosystem, such as limiting light penetration and blanketing the benthic environment with fine sediments, ultimately changing the structure and function of these areas (Thrush et al. 2004). Sediment stressors are particularly relevant for coastal oceans that receive river discharge from small mountainous river systems, where high levels of sediment can be transited quickly to the coastal ocean (Walsh and Nittrouer 2009). In such cases, the longer-term fate of the material is dependent on inner shelf processes which can redistribute sediment across the shelf (Geyer et al. 2000).

In this study, we characterize the inner shelf circulation and cross-shelf sediment transport response of an embayment with multiple small mountainous rivers that is exposed to an energetic coastal ocean using a numerical model. The study is focused on Hawke Bay, Aotearoa New Zealand, where little oceanographic information is available, and the region is highly susceptible to devastating storm events, such as Cyclone Gabrielle in 2023 and Cyclone Bola in 1978. The region has steep deforested catchments and erodible soils that have the potential to cause widespread ecological damage to the near shore and shelf seabed during such events. A three-dimensional hydrodynamic sediment transport model is verified against observational data and used to explore the relative importance of environmental drivers in determining sediment fluxes throughout the Bay. This study sets out to describe the circulation patterns in Hawke Bay comprehensively for the first time, as well as investigating how environmental conditions impact small mountainous river plumes and cross-shelf sediment transport.

3.2 Background

3.2.1. Regional setting: Hawke Bay

Hawke Bay is a large southeast facing embayment, roughly 40 by 80 km, on the east coast of the North Island, extending from the Mahia Peninsula in the North to Cape Kidnappers (Fig. 3.1). The continental shelf offshore of the bay is relatively broad and gently sloping compared with the narrower shelf north and south of the Bay. Steep coastal mountains combined with high rainfall rates produce significant episodic river discharge events that transport on average 11 million tons (MT) of suspended sediment to the Bay each year (Hicks et al. 2011).

The Bay is susceptible to strong wind and wave forcing at times. The average significant wave height recorded off Napier was 1.2 m, but high wave events can be from 2.5 – 3.5 m, and the largest events are greater than 8 m (Komar 2010). Waves on average approach from the east-southeast, are larger in winter, and wave heights in the bay can be spatially variable for a given swell due to wave refraction. Waves create longshore currents that are important for sediment transport and beach erosion in the southern Bay (Komar 2010). The spring tidal range is ~1.9 m and neap are ~1.2

m as measured at the Napier Port. Current patterns in the Bay have received limited investigation, but early work suggests general current patterns of inflow at the Bay center and outflow at each headland (Ridgeway and Stanton 1969) as well as the presence of expansive freshwater plumes (Bradford et al. 1976).

There are two dominate currents that flow offshore of the Bay: the warmer and saltier East Cape Current (ECC) that flows from the north and the cooler and fresher Wairarapa Coastal Current (WCC) from the south (Stevens et al. 2021). Chiswell (2002) showed that water from the WCC can be advected into Hawke Bay. Kerry et al. (2023) studied the offshore circulation in much higher detail than has been done previously and showed that for mean conditions the WCC flows northward on shelf slope offshore of the Bay until roughly 1 km depth about 100 km from shore, where then the ECC predominately takes over with southward transport. The transport displays seasonal variability with larger southward ECC transport in summer (Kerry et al. 2023).

3.2.2. River plume and inner shelf flows

Transport of sediment within a river plume is dependent on the sediment characteristics, which determine the downward settling velocity, as well as the lateral advection which transports sediment particles horizontally (Geyer et al. 2000). The plume dynamics are dependent on the river velocity at the inlet mouth, the density contrast between the outflowing water and ambient ocean water, the barotropic pressure gradient, and ambient currents created by the wind or offshore currents (Horner-Devine et al. 2015; Hetland 2005). In the near-field region, the transport is dictated by the outflow momentum at the river mouth and behaves as a jet, being slowed down by shear mixing at the base of the plume. During discharge events, the freshwater will generally detach from the bottom at the mouth of the river inlet.

In the mid-field region, other processes become important. The density contrast between the fresh and ocean water produces lateral spreading at the rate of the internal wave speed (Horner-Devine et al. 2015). Local winds can create surface currents which transport the freshwater, as well as provide vertical mixing if the Ekman layer depth is greater than the plume depth. Upwelling winds have been shown to elongate the plume offshore, while downwelling winds tend to trap fresh water near the coast (Fong and Geyer 2001). If the length of the plume is greater than the baroclinic Rossby radius of deformation, the Coriolis force can steer the plume towards the left and create a buoyant coastal current, and if other processes are absent, a recirculating bulge can form (Horner-Devine et al. 2015). The ambient currents on the inner shelf are influenced by waves (surface and internal), wind, tidal forcing, and offshore flows such as boundary currents and submesoscale flows (Lentz and Fewings 2012; Kumar et al. 2016; Wu et al. 2020). Wind driven upwelling and downwelling flows can initiate cross-shelf and vertical velocities, and wave induced currents can drive cross-shelf, vertical and alongshore currents in the nearshore (Lentz and Fewings, 2012).

Wave current interaction offshore of the inlet and wave breaking near the inlet mouth can significantly alter the plume structure and currents (Wright et al. 1980) and create strong vertical velocities in the inlet region. Wright et al. (1980) documented enhanced deposition near the river inlet due to wave breaking. The geometry of the inlet and existence of a shoal or submerged delta also play key roles in the momentum structure of the inlet region (Olabarrieta et al. 2011). However, the influence of these processes on sediment transport has not been studied in detail, and understanding the role of these complexities in controlling zones of sediment deposition is essential to successful management of these stressors.

3.3 Methods

3.3.1 Numerical model

To simulate hydrodynamics and sediment transport in Hawke Bay, the Coupled Ocean-Atmosphere-Wave-Sediment Transport (COAWST) modelling system (Warner et al. 2008) was used. From the COAWST system, we utilized the coupling of the Regional Ocean Modelling System (ROMS), with Simulating WAves Nearshore (SWAN) and the community sediment transport model. ROMS is a three-dimensional, hydrostatic, finite difference numerical model that approximates the Reynolds averaged Navier-Stokes equations on a structured grid (Haidvogel et al. 2008). ROMS is commonly used in inner shelf settings (e.g. Suanda et al. 2018, Kumar et al. 2016). SWAN is a spectral wave model that solves the spectral density evolution equation (Booij et al. 1999) and includes refraction, shoaling, and dissipation. Atmospheric forcing to the ROMS is configured using the bulk fluxes formulation with atmospheric model data from the ERA-5 interim hindcast dataset (Hersbach et al. 2020).

The Hawke Bay SWAN model is forced by a wave hindcast of Aotearoa New Zealand waters by Alberqurque et al. (2022), which showed good skill at replicating wave height and period at the local wave buoy located in Napier (Alberqurque et al. 2022). At the model boundaries, spectrally averaged values were used to force SWAN at 2 km increments. SWAN was set up to compute the wave action balance equation in the frequency range of 0.04 to 1 Hz with a resolution of 24 bins in 36 directional bins. Exchange of information between ROMS and SWAN was set to occur every 10 minutes. The vortex force formulation was used to model the effect of waves on current and currents on waves (Kumar et al. 2012), and additionally modelled processes included wave driven mixing and bottom streaming.

At the outer boundary of the coarse domain, ROMS is forced by the momentum and density fields of a realistic hindcast simulation of Aotearoa New Zealand waters (De Souza et al. 2022, Kerry et al. 2023), termed the MOANA hindcast model. The MOANA hindcast model is a 5 km resolution ROMS model that performed well when compared to available sea surface temperature, and showed high skill for water level variability, including sea level set up and set down. The boundary condition

for the coarse grid for the density, velocity, and sea surface height fields use a radiation-nudging condition, allowing information to propagate out the domain, with a strong inflowing nudging time scale and a weak outflowing time scale (1 and 365 days respectively). At the open boundary, the Chapman condition is used for the free surface, the Flather condition for barotropic velocities, and gradient condition for the turbulent kinetic energy.

The MPDATA advection scheme is used horizontally and vertically for all tracers, as it is well-suited for the modelling of areas of large tracer gradients and preserving positive values of salinity and sediment concentration (Smolarkiewicz and Margolin 1998). Bottom roughness was computed as a time dependent function of the sediment grain size. The horizontal diffusivity and viscosity constants were set to 0.01 m^2/s to reduce numerical instability. The k-e turbulence closure model was used with default parameters, and mixing was formulated to occur along geopotential surfaces for tracers and along constant sigma surfaces for momentum.

Freshwater fluxes for most of the rivers that drain into the Bay are measured by the Hawkes Bay Regional Council and recorded at 15-minute intervals (https://www.hbrc.govt.nz/environment/river-levels/). For smaller ungauged rivers, including the Nuhaka, Waihua, and Waikere Rivers, linear scalings based on watershed areas with nearby rivers were used to estimate the discharge. The river freshwater flux entered the domain as a horizontal momentum flux as a point source for all rivers, which was vertically evenly distributed for the upper 20 layers of the water column. The temperature of the river flux for all rivers was set to the measured river temperature from data collected in the Tukituki River at Red bridge (Fig. 3.1). Two model runs were performed from the period of March 2017 to December 2019, one with only ROMS and with two-way ROMS and SWAN coupling. The coupled model is used for all analysis presented, and the ROMS only run is used for comparison to assess how waves impact river plume circulation in Hawke Bay.

3.3.2. Grids and bathymetry

Bathymetry used for the ROMS and SWAN grids are sourced from several datasets, including a 250 m gridded dataset from NIWA, lidar and multi-beam sonar datasets sourced from the Hawkes Bay Regional Council, where multi-beam datasets were focused on hard structure areas in the Bay. All datasets were vertically referenced to mean sea level in the time-period of 2006-2016, then merged and interpolated to the grid. The bathymetry was smoothed to meet the criteria of a maximum stiffness value of 0.2, and the minimum depth was set to -2 m (where positive is downwards). Wetting and drying was used with a minimum critical depth of 40 cm. The model used 22 vertical sigma layers with greater vertical resolution at the surface and bed.

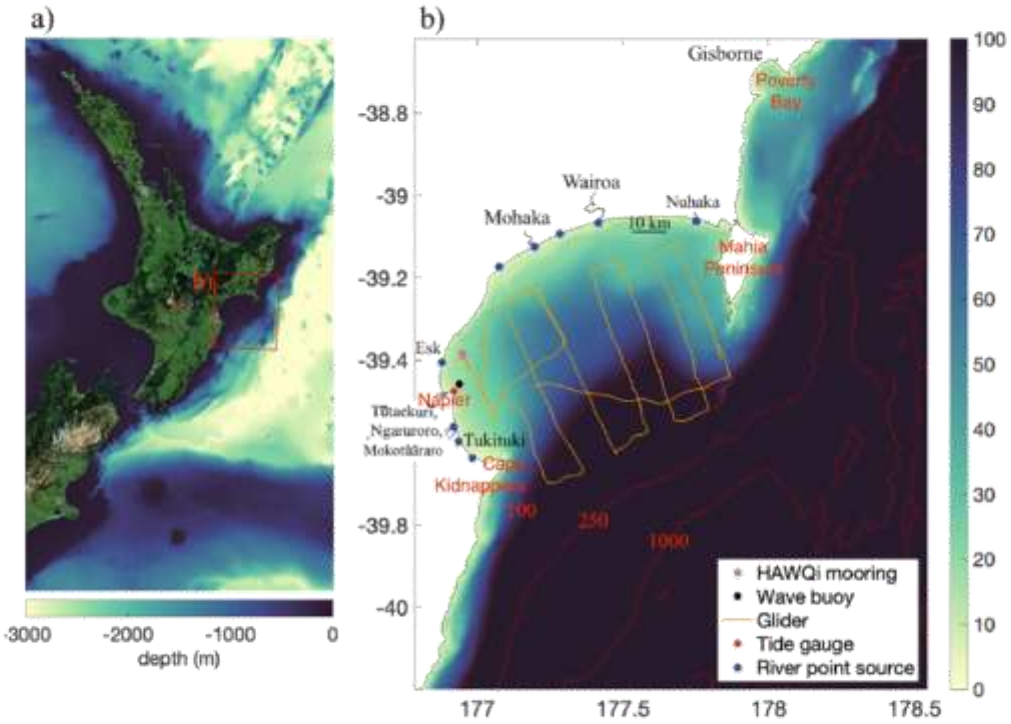

Figure 3.1 Overview of the Hawke Bay region, data sources, and COAWST model grid. a) The bathymetry of the north island of Aotearoa New Zealand (m), with the COAWST model domain shown in red. b) The ROMS and SWAN model domain and bathymetry (m), where the red contour lines show the bathymetry deeper than 100 m. Major rivers are labelled, as well as the data locations used, including the HAWQi mooring, wave buoy, tide gauge, and glider tracks. The blue dots represent freshwater and suspended sediment point sources. A 10 km scale bar is shown in the northern region of the Bay for reference.

The grid expands beyond the continental shelf and tens of kilometers north and south from Hawke Bay to reduce impacts from the boundary on the flow in the Bay (Fig. 3.1). The grid resolution is 500 m. The rivers and river inlets are not resolved by the grid and are implemented as point sources. This approach does not accurately simulate the near field plume, which is dependent on the inlet width, which is typically much narrower than 500 m, as well as estuarine processes which can impact the outflow density and momentum.

3.3.3. Sediment characteristics

Suspended sediment transport is modelled in the Bay by using a fixed number of grain sizes that represent the sediment characteristics in the Bay. The model options used in this work include allowing morphological bed changes, the sediment in the water column contributes to the water

column density, and only suspended transport considered. We use static sediment classes with no cohesive processes such as flocculation or bed consolidation.

The bed sediment grain size is initialized with data sourced from a compilation dataset from NIWA, with samples mainly collected in the 1960s, along with data collected by Hawkes Bay Regional Council in the 2010s, and grain size data collected in the Tukituki River and inlet in 2022 (Atkin, 2022). The sediment characteristics in the Bay follow common continental shelf sedimentary patterns, with coarse sand on beaches and muddy areas becoming progressively dominant with distance offshore. There are also several gravel zones and rock reefs in the Bay, as described below. Pantin (1966) comprehensively sampled and described the bed sediment characteristics in the Bay, observing that coarse beach sand (with the median grain size (d_{50}) around 250 mm) persists for a relatively short distance offshore until fine sand becomes the dominant sand size in the Bay (in the range of 63-150 mm, and around 100-125 mm in general; Marshall 1929, Pantin 1966, Hume 1989, White 1994). Muddy regions offshore were recorded to have silt/clay to sand ratios of typically 70/30.

Gravel is found along the beaches of the southern Bay, including at the inlets of the Ngaruroro/Tūtaekurī and Tukituki Rivers, as well as a few offshore regions such as offshore of the Mohaka River (Pantin 1966, Atkin 2022). Grain sizes at the bed of the Tukituki River near the inlet and up to 1.5 km upriver from the inlet range from 4-32 mm, with the average d_{50} 16 mm. The Mohaka and Wairoa River inlets also have coarse grain beaches with gravel sizes. Hard structure rocky reefs areas in the Bay include the Pania reefs, Wairoa Hard, Clive Hard, and offshore of the Mahia Peninsula. Seafloor classification for these areas has been done using sidescan sonar, which classified sediment types (data from Hawkes Bay Regional Council). We use the derived maps from these surveys to prescribe the sediment bed sediment class for these areas.

Bed grain size distributions have been measured in the Tūtaekurī/Ngaruroro River (average 4% clay, 19% silt, 77% fine sand; Atkin 2022), and the Wairoa River (50% fine sand, 45% silt, and 5% clay; data from Hawkes Bay Regional Council). White (1994) reported suspended d_{50}values from the Tukituki and Ngaruroro/Tūtaekurī rivers with clay sized values around 4 µm for the Tukituki and Ngaruroro/Tūtaekurī Rivers. More recent measurements collected by Hawkes Bay Regional Council in the Tukituki River report bimodal peaks of suspended d_{50} by volume of 15 and 45 µm. Additional measurements for suspended d_{50} taken in 2021 had bimodal peaks of 7 and 34 µm for the Wairoa River, 6 and 25 µm for the Mohaka River, and 13.6 µm for the Tukituki River. A small number (11) of grain size samples were taken in the four main river plumes at various distances offshore had a range of d_{50} values from 3–15 µm.

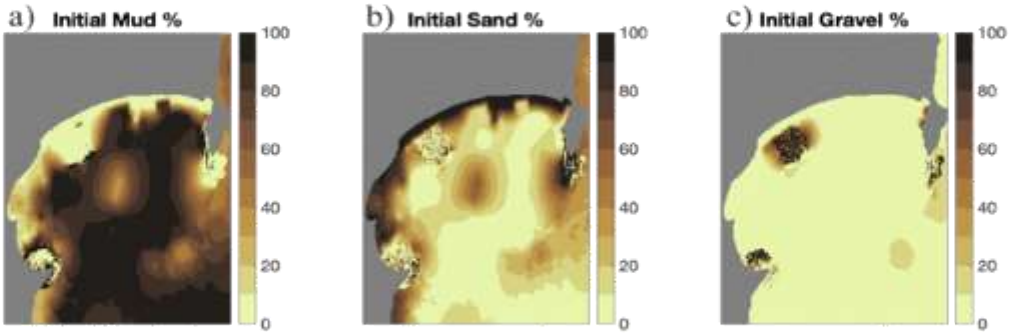

Figure 3.2 Bed sediment grain size percentages interpolated to the model grid. a) Mud, b) sand, and c) gravel sized sediments. These distributions were used to initialize the bed sediment model.

The initial bed composition was based on a spatial interpolation of the bed data to the model grid (Fig. 3.2). For rock areas, we use the gravel class, which will remain immobile for these simulations as only suspended transport is considered. Due to the ubiquitous presence of aggregated particles that have been documented in other river plume studies (Geyer et al. 2004), the lack of measurements that have been made in the region, and the significant influence that the effective settling velocity has on sediment dispersal (e.g. Geyer et al. 2004), we assume that a fraction of the river flux of suspended particles are aggregated and use commonly reported values for the diameter and settling velocity. For the bed sediment fractions, all gravel and rock areas use the gravel class with values measured from the Tukituki River (d_{50}~ 16000 μm), and all sand in waters deeper than 5 m was set to fine sand while shallower than 5 m was set to the medium sand class. In muddy areas the mud percent was distributed as 50% coarse silt, 40% silt, and 10% clay.

Table 3.1 Sediment classes and characteristics used in the sediment transport model. The settling velocity was computed from the Stokes settling velocity and the critical shear stress from the Shields critical stress. The critical shear stress for erosion and deposition were set to the same value.

Sediment class	d_{50} (μm)	Settling velocity (mm/s)	River fraction (%)	Critical shear stress (N/m^2)
Clay	4	0.014	30	0.03
Silt	10	0.1	30	0.05
Flocculated silt and clay	10	1	20	0.05
Coarse silt	50	2	20	0.1
Fine sand	125	10	0	0.145

Medium sand	250	30	0	0.194
Medium pebbles	16000	800	0	12.2

Given the range of observed suspended sediment sizes observed in the Bay, general size values were chosen that were best thought to represent the observed variability in in-situ samples. Sediment settling velocities were calculated based on Stokes settling velocities, and critical Shields shear stress was used for each sediment type. Here the critical shear stress for deposition was set equal to the value for erosion. All sediment densities are set corresponding to the density of greywacke, 2650 kg m^{-3}, and the sediment porosity was set to 0.6 for all classes. The erosion rate for all classes was set to 5×10^{-4} kg/m^2, as was used for a ROMS modelling study directly north of Hawke Bay in Poverty Bay (Bever and Harris 2014). Other options used include that sediment concentration is included in the water column density calculation, and that morphology is active. Cohesive sediment processes such as flocculation and bed consolidation were not modelled. The bed was modelled with 5 bed layers, where a new layer was created upon 10 cm of sediment deposition.

The suspended sediment fluxes from all rivers were estimated based on power-law relationships between SSC and discharge, fit to data measured by Hicks et al. (2011). This data measured discharge and point-values of SSC at a wide range of discharge conditions for the Wairoa, Mohaka, Ngaruroro, Esk, Nuhaka, and Tūtaekurī Rivers.

3.3.4. Observational data

To validate the model performance, we use several different observational data sets that encompass the different aspects of the hydrodynamics in the Bay, including the inner shelf flow and vertical structure, tides, wave propagation, and surface sediment concentration. Water level is measured at the Napier Port, and wave height is measured from a Triaxis wave buoy located directly offshore of the Port (Fig. 3.1). A long-term mooring HAWQi has been deployed by Hawkes Bay Regional Council directly north of the Port in 18 m depth, with three CTDs in the water column and a downward looking ADCP at the surface. For one month in 2019, a Slocum 200 m electric glider was deployed in the Bay and collected 8506 profiles (Fig. 3.1; O'Callaghan 2020). The glider was equipped with a Seabird CTD and additional water quality sensors (additional details described in O'Callaghan 2020). We utilize a derived surface Total Suspended Solids (TSS) dataset sourced from daily MODIS satellite remote sensing imagery that used an empirical algorithm to estimate the TSS (Chapter 2). This dataset gives a 250 m resolution surface TSS snapshot each cloud free day for the entire period considered here.

3.3.5 Model skill metrics

To assess the performance of the COAWST model of Hawke Bay, we compare observed data with the numerical model output and use comparison metrics including the linear regression coefficient, root mean square error, and a skill score. The skill score is defined as

$$SS = 1 - \frac{1}{\sigma_{obs}^2 N}\sum_{i=1}^{N}(x_{obs} - x_{model})^2 \quad (3.1)$$

(Murphy 1988), where s is the standard deviation.

3.3.6 River plume analysis methods

Due to the episodic nature of river discharge events and the varying spatial positioning of river plumes, a set of analysis methods are described that allow for the systematic analysis of river plume properties. River discharge events are identified based on a 50 m^3s^{-1} prominence threshold and the duration of the event is defined as the width of the event at half of the prominence magnitude of the event. This metric generally encompasses the rapid beginning of the event but does not cover the tapering nature of the event, such that the duration metric does not fully account for the nonlinearity of event signals. To identify the time-varying spatial patterns of river plumes, salinity contours are computed and associated with each river through time. At each model output time, each major river plume is characterized spatially based on the surface salinity contoured at the values of 33, 30, and 20 psu which are assigned to a river if present for a given time.

Several metrics are defined to quantify the importance of different processes on plume vertical structure, mixing, and transport direction. As most mixing occurs vertically rather than at plume horizontal boundaries (Horner-Devine et al. 2015), and we are generally interested in mixing processes at the plume interface. The pycnocline depth is defined as the location of the maximum vertical density gradient ($\partial\rho/\partial z$). We designate this location in the water column as the plume interface and calculate stratification and mixing processes at that vertical location. The turbulence production is defined as $P = k_m\left(\frac{\partial u^2}{\partial z} + \frac{\partial v^2}{\partial z}\right)$, where k_m is eddy viscosity. The buoyancy flux is defined as $B = g\beta k_z\frac{\partial s}{\partial z}$, where β is the coefficient of saline contraction and k_z is the salinity diffusivity from the model, is used to determine the intensity of plume mixing.

3.4. Results

3.4.1. Model evaluation and overview

Over the period from 2017–2019, multiple discharge events occurred typically during the winter with event magnitudes surpassing 500 $m^3 s^{-1}$ (Fig. 3.3a). The model shows high skill at reproducing the sea surface height at Napier Port (Fig. 3.3b) as well as the subtidal component of the

sea surface height (Fig. 3.3c). Note that due to the model output frequency of 3-hour intervals, the amplitude as shown in the comparison plot appears smaller than the hourly observed tidal data.

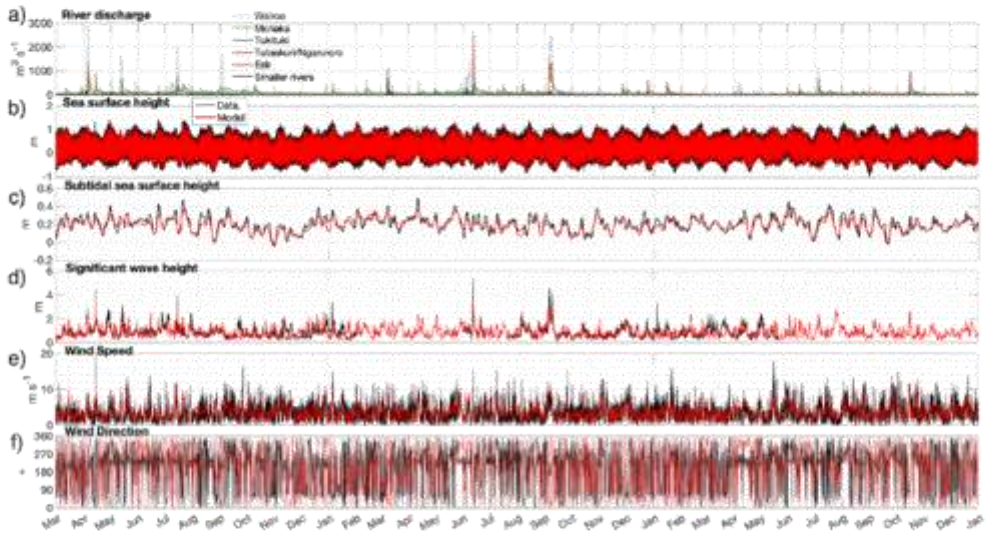

Figure 3.3 Timeseries of environmental conditions and modelled parameters. a) River discharge for main rivers in Hawkes Bay ($m^3 s^{-1}$). b) Sea level (m) measured at Napier Port (black) and modelled (red). c) Tidally filtered sea level (m). d) Significant wave height (m). e) Wind speed comparison ($m s^{-1}$), and f) Wind direction comparison (degrees).

The model simulates the variability of significant wave height (Fig. 3.3d), period, and direction (Fig. 3.4), and captures most events, although with discrepancies for some wave events. In general there is a slight overestimation of wave period in the model, and a slightly broader range of typical wave directions than observed (Fig. 3.4). The location of the wave measurement is affected by substantial shadowing from the headlands at either side of the Bay, resulting in a narrow range of measured swell directions from both the model and observations. The discrepancies of the wave modelling, including not simulating several smaller wave events with heights less than 2.5 m, is likely due to the boundary forcing of the wave model which used spectrally averaged values rather than the full directional spectrum. The wind surface forcing, sourced from the ERA-5 hindcast, reproduces the observed directionality and magnitude of the wind recorded at the Napier Airport (Fig. 3.3e-f) and shows moderate ability to replicate the east/west and north/south wind magnitudes (Table 3.2). Wind roses from Napier Airport show that the model reproduces the dominant wind direction from the SW (Fig. 3.6), but does not simulate a number of NNE wind events that are present in the observed record.

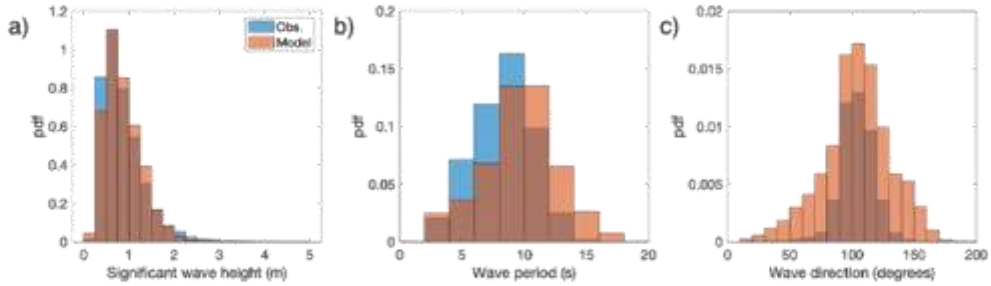

Figure 3.4 The comparison of wave statistics with modelled and observed values. The histograms compare probability density functions of the observed (blue) and modelled (orange) a) significant wave height (m), b) mean wave period (seconds), and c) mean wave direction (degrees) over the three-year model run period.

Table 3.2 Statistics from model/data comparisons. The table includes the linear correlation coefficient (R^2), Skill Score (SS), and Root Mean Squared Error (RMSE).

Data	Location	R^2	SS	RMSE
Sea surface height	Napier Port	0.99	0.98	0.07 m
Subtidal sea surface height	Napier Port	0.89	0.76	0.04 m
Salinity	HAWQi	0.56	0.02	1.4 psu
Temperature 0.5 m depth	HAWQi	0.98	0.95	0.7 degrees
U velocity 2 m depth	HAWQi	0.13	-0.85	0.07 m s^{-1}
V velocity 2 m depth	HAWQi	0.45	-0.03	0.09 m s^{-1}
Significant wave height	Offshore Napier Port	0.53	-0.1	0.44 m
Mean wave period	Offshore Napier Port	0.30	-0.4	3.5 seconds
Wind U velocity	Napier Airport	0.73	0.53	2.3 m s^{-1}
Wind V velocity	Napier Airport	0.75	0.44	2.0 m s^{-1}

At the inner shelf mooring HAWQi, located in 18 m depth, the model reproduces the seasonal and event time scale variations in water column temperature and salinity. Sea surface temperature displays a strong seasonal cycle varying from 10–25° (Fig. 3.5a), also well simulated by the model.

Sharp variations that interrupt seasonal patterns in the model are strongly related to variations in solar forcing, offshore boundary current transport, and wind forcing. Vertical temperature stratification also follows seasonal patterns (Fig. 3.5b), with warmer water overlying cooler water in the summer, punctuated by warming events, and during the winter cooler water typically overlying warmer water in both observations and the model. In contrast, salinity does not show a clear seasonal cycle but shows salinity generally around 35 psu interrupted by periodic changes and discrete events that quickly reduce the salinity (Fig. 3.5c). The model captures most of the drops in salinity, often capturing the general magnitude of the decrease in salinity. Only limited subsurface salinity measurements were recorded during the study period, but comparison with the available data suggests that the model salinity stratification is the correct magnitude (Fig. 3.5d), with background stratification of generally 1 psu or less and maximum difference values around 10 psu.

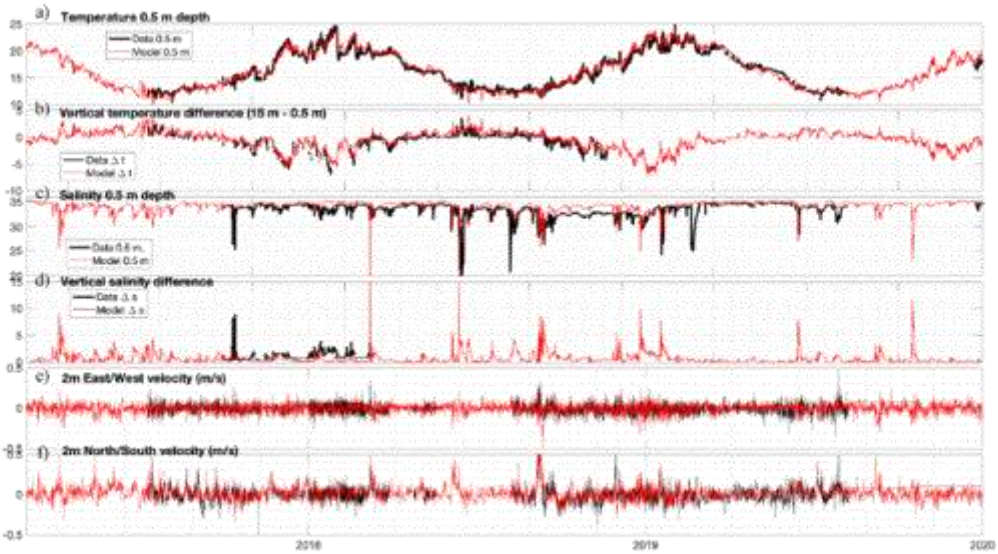

Figure 3.5 Model/data comparisons from inner shelf mooring HAWQi. a) Temperature at 0.5 m below the surface. Observed data is in black and modelled in red. b) Vertical temperature difference (between 15 and 0.5 m below the surface). c) Salinity at 0.5 m below the surface. d) Vertical salinity difference (between 15 and 0.5 m below the surface). e) East/west velocity at 2 m below the surface. f) North/south velocity at 2 m below the surface.

The surface velocity at 2 m from the surface at HAWQi is strongest along-shore (up to 0.5 m s^{-1}) with smaller cross-shore velocity (typically ~0.1 m s^{-1}) in both observations and the model (Fig. 3.5e-f). River discharge events cause the largest fluctuations in alongshore velocity (likely from the nearby Esk River), which causes northward surface flow. Tidal velocities oscillate in a counterclockwise orientation throughout the Bay associated with tidal propagation to the north along the coastline, with flow out of the Bay during ebb and into the Bay during flood. Tidal oscillations are

observed in the cross-shore flow while the along-shore flow is more dependent on river discharge and wind variability, both in observations and in the model.

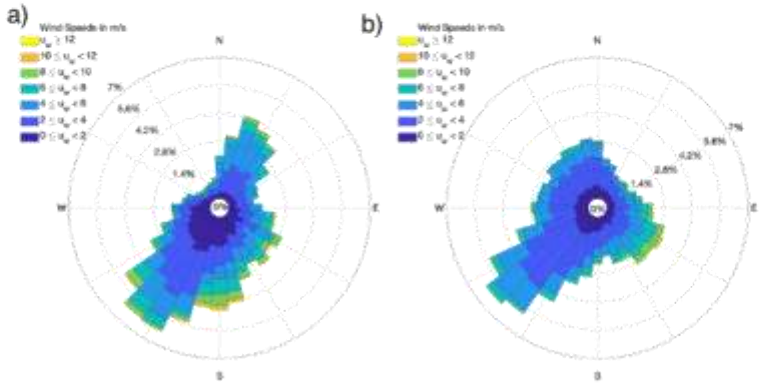

Figure 3.6 Comparisons of wind roses with observed and modelled values. Wind rose from observed data from a) Napier Airport during simulation period, and b) modelled wind at the nearest model location to Napier Airport.

The month-long glider deployment in March 2019 transited the entire inner shelf of the Bay from south to north, extending from ~40 to 150 m water depth (Fig. 3.7f). The glider showed that the upper 50 m of the water column is much warmer and saltier than the underlying water deeper than 50 m. Modelled vertical profiles of temperature generally show similar patterns to the observed structure (Fig. 3.7g), with the model correctly simulating bottom and surface temperature magnitude, but observations show sharper vertical gradients than the model. This can additionally be seen in the comparison of temperature and salinity space (Fig. 3.7e), where the model simulates the correct bounds of temperature and salinity at the highest temperatures near the surface, but at the lower mid and lower water column levels with temperatures below 19° the model shows a narrow band of salinity variability in contrast to the observed values. Importantly however, the model correctly simulates the regions of lower salinity water associated with the glider going shallower towards riverine influenced waters (e.g., times 2 and 4).

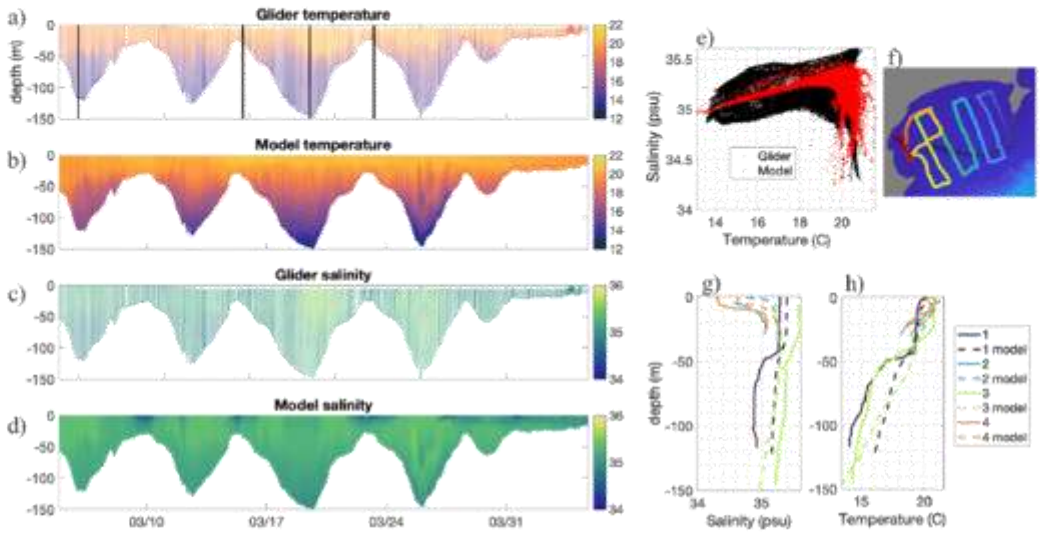

Figure 3.7 Model/data comparison of glider data, collected in April 2019. f) Shows the path of the glider data throughout the Bay (going from blue to red). a-b) show temperature profiles, c-d) show salinity profiles, and e) shows the comparison of observed and modelled temperature/salinity space. g-h) show vertical profiles at select times (shown in a), where the solid line is observed, and the dashed line is modelled.

Satellite derived TSS (from here noted as SSC) is compared with modelled SSC during cloud-free days (Figs. 3.8 and 3.9). The satellite derived SSC dataset shows spatial patterns and gradients of SSC; however, the model likely estimates SSC values below ~70 mg l^{-1} better due to the limited empirical data above this threshold used in the local algorithm (Chapter 2). The SSC from the model was obtained at similar times of MODIS imagery collection (either at 11 AM or 1 PM) for each day, and the model SSC was interpolated to the MODIS grid and no-data locations from MODIS were applied to the model to allow for comparison. The average daily model SSC shows elevated nearshore SSC in the range of 35–50 mg l^{-1} (Fig. 3.8a, while the MODIS derived dataset shows nearshore average SSC values in the range of 10–20 mg l^{-1} (Fig. 3.8b), with the mean daily bias showing the greatest offset near the coast (inshore of 20 m) with values up to 20 mg l^{-1} (Fig. 3.8c), and lower

values (~5 mg l^{-1} throughout the deeper regions of the Bay). The standard deviation of the mean daily bias similarly shows higher offsets near the coast, with highest values around 60 mg l^{-1}.

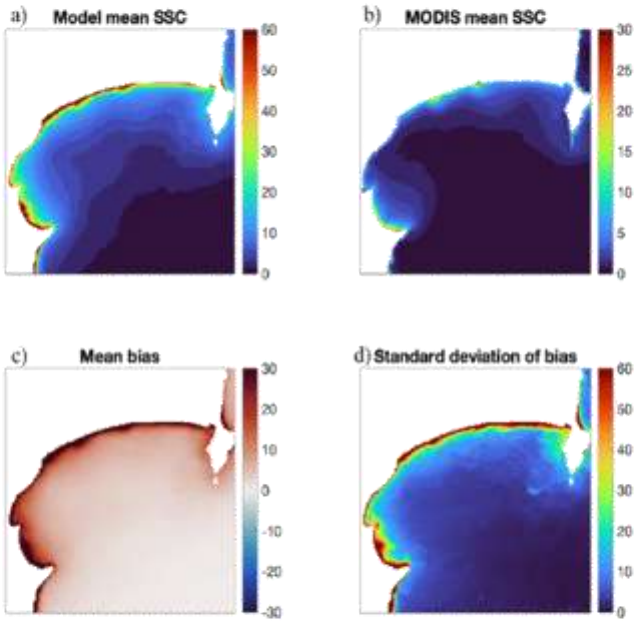

Figure 3.8 Comparison between model surface sediment concentration (SSC) and SSC derived from MODIS. a) daily model averaged SSC (mg l^{-1}). b) daily MODIS averaged SSC (note the change of colour range from a) (mg l^{-1}). c) Average daily bias between MODIS and the model (mg l^{-1}). d) The standard deviation of the daily SSC bias between the model and MODIS (mg l^{-1}).

Daily comparisons are made between MODIS SSC (Fig. 3.9 top rows) and the model SSC (Fig. 3.9 bottom rows) for a selected range of conditions spanning varying magnitudes of discharge events and wave conditions. In general, the model simulates the spatial patterns of SSC and the directionality of river plumes and frontal features that are commonly associated with wind forcing in the Bay. However, the model SSC is much higher than the MODIS SSC, such that the colour range is doubled for all model instances (Fig. 3.9). Qualitatively, spatial patterns for river plumes are similar between the two at each day, with similar directionalities occurring. Exact comparison is difficult due to the differing magnitude of the two, but the model displays circulation-related features found in the remote sensing data, including northward coastal currents (17-Oct-2019), transport associated with Cape Kidnappers (27-Feb-2019), eddying motion of suspended sediment (22-May-2019), and the formation of radial plumes (18-Jul-2018). The SSC estimated from MODIS is likely underestimated (Chapter 2), but the modelled SSC has additional uncertainty associated with the estimation of sediment flux, not well-resolving river inlets or the surfzone, as well as the ratio of sediment sizes that

are present in the rivers, which have a large impact on advection distances of sediment transport within plumes.

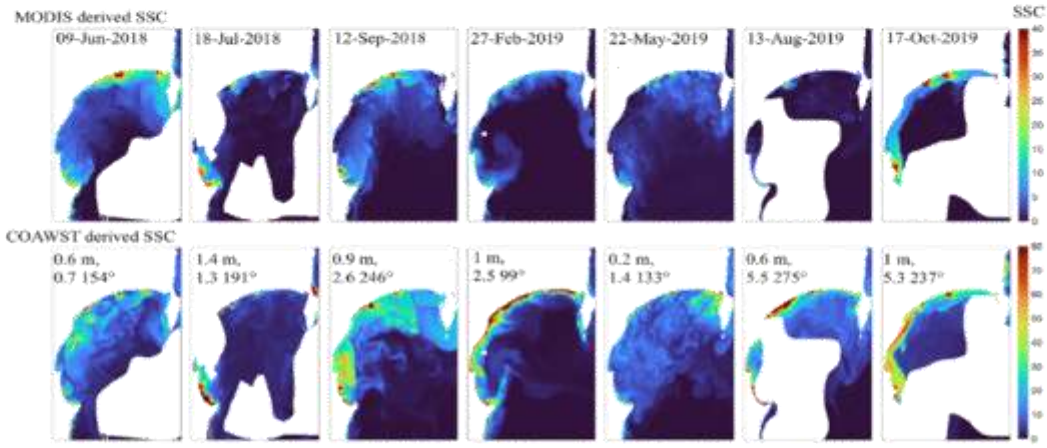

Figure 3.9 Select days of MODIS SSC (top row) and model SSC (bottom row) for a range of conditions (mg l^{-1}). The MODIS SSC colour range goes from 0 to 40, while the model SSC colour range goes from 0 to 80 mg l^{-1}. On the modelled SSC plots, the wave height (m), wind speed (m s^{-1}) and direction averaged in the 6-hour period before image collection are labelled. The gaps in the data correspond to clouds and regions of poor data.

3.4.2. Density and circulation patterns in Hawke Bay

Seasonal averages of key water mass and circulation features are shown over the duration of the 3-year run averaged over 3-month periods (Fig. 3.10, 3.11). Large seasonal changes are associated with varying solar radiation as well as river discharge, the latter results in wintertime low salinity waters (less than 32 psu) over much of the inner shelf in depths less than 30 m and enhanced vertical salinity stratification (greater than 3 psu). These patterns are greatest offshore of the rivers, with average surface salinity less than 30 psu and salinity stratification reaching 8 psu. The inner shelf less in than ~30 m displays pronounced seasonal variations in temperature, with higher warming than offshore in summer and higher cooling than offshore waters in winter. The wintertime cooling nearshore leads to cooler water overlying warmer water. Although the density structure resulting from river plumes, particularly from salinity variability, is a persistent feature of the Bay all year, it is strongest in winter.

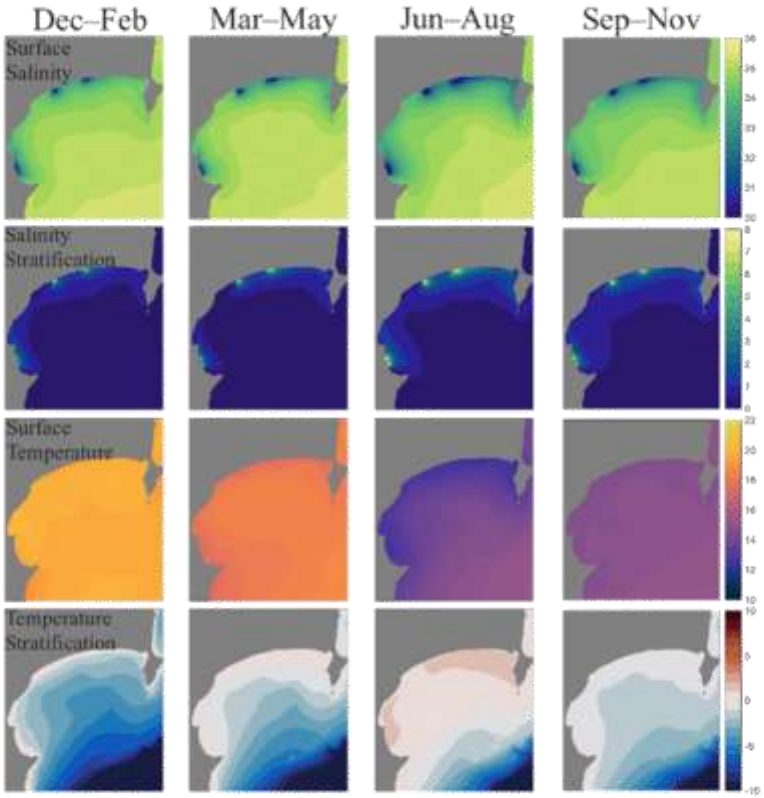

Figure 3.10 Seasonal averages of surface salinity (top row), the surface to bed salinity vertical stratification (second from top row), surface temperature (third row), and the surface to bed vertical temperature stratification (fourth row). Averages are computed over the three-year run time using ROMS average files that were output at monthly intervals.

The average wind direction is most commonly from the SW year-round, which appears to influence surface velocity patterns (Fig. 3.11). The strongest and most persistent surface velocity features are located in regions influenced by river plumes, with outward flow from the river inlets, with average velocity values greater than 0.2 m s^{-1} (Fig. 3.11). The river plumes from the Mohaka and Wairoa Rivers typically flow offshore and to the left, while the Tukituki River typically flows offshore and the Tūtaekurī/Ngaruroro River flows offshore and to the right. Other persistent patterns include flow out of the Northern Bay around the Mahia Peninsula, which during the winter months flows continuously in a coastal current from the Wairoa River along the coast out of the Bay. At the southern end of the Bay, flow also goes out of the Bay, either around Cape Kidnappers or directly offshore of the Bay, with stronger flow in the winter originating from the southern rivers. The middle of the Bay shows much slower surface average velocities (on the order of a few cm s^{-1}), with spatial variability showing eddying motions and recirculation regions with flow into the Bay.

Near bed average velocities are much weaker, with stronger landward flow (~0.025 m s^{-1}) in the winter in depths less than 30 m likely associated with buoyancy driven return currents. Average bed stress values are much larger in winter than summer, associated with seasonal variability in wave height, and are highest in shallower areas and areas with larger bed roughness such as rocky reef areas.

Offshore of the Bay, the Wairarapa Coastal Current (WCC) is a persistent current that flows Northward along the shelf break of the Bay throughout all seasons (Fig. 3.11). The WCC diverges towards the east roughly around Cape Kidnappers. The bottom currents in the region are the strongest offshore of the Bay in the WCC (>0.2 m s^{-1}) which is present year-round. The ECC flows generally southward offshore of the Mahia Peninsula but does not directly flow into Hawke Bay (not shown).

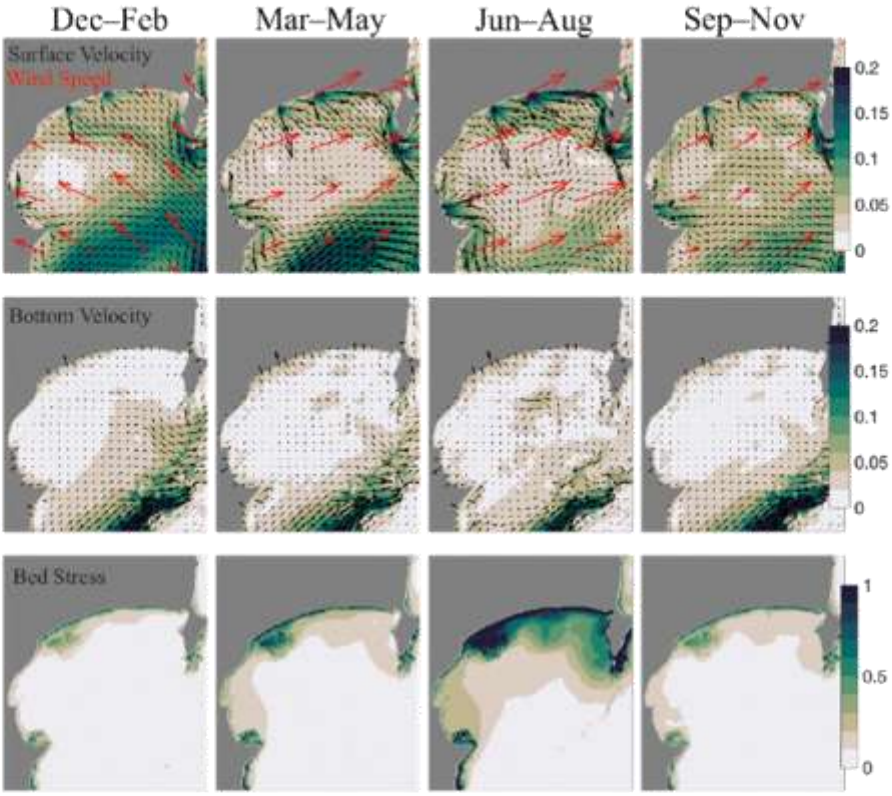

Figure 3.11 Seasonal averages of circulation in Hawke Bay. The plots show the seasonal averages of surface velocity and wind speed (m s^{-1}; top panels), bottom velocity (m s^{-1}; middle panels), and bed stress (N m^{-2}; bottom panels). Averages are computed over the three-year run using ROMS average files that were output at monthly intervals.

To highlight the temporal variability throughout the Bay associated with river plumes, tide, wind, and other inner shelf processes, timeseries of circulation features are shown at 6 locations for the year of 2019 (Fig. 3.12a) at 2 and 10 km from the shoreline, located offshore of the Tūtaekurī/Ngaruroro River (points 1-2), Wairoa River (points 3-4), and a location with no direct river influence (points 5-6). At 2 km offshore of the Wairoa River, the highest stratification occurs within 2 m of the surface, but during discharge events lower density water extends to the bed. At the locations offshore of the rivers, impacts of discharge are noticeable in the surface density and stratification (Fig. 3.12e-f), with similar magnitudes of surface density and stratification occurring offshore of the northern and southern rivers during discharge events. At the locations not directly offshore of a river, impacts from other rivers are seen in the density structure with reduced magnitude and a time lag. In all locations, the seasonal variability of inner shelf water masses is evident, with denser water more common in winter than summer (e.g. Fig. 3.12d).

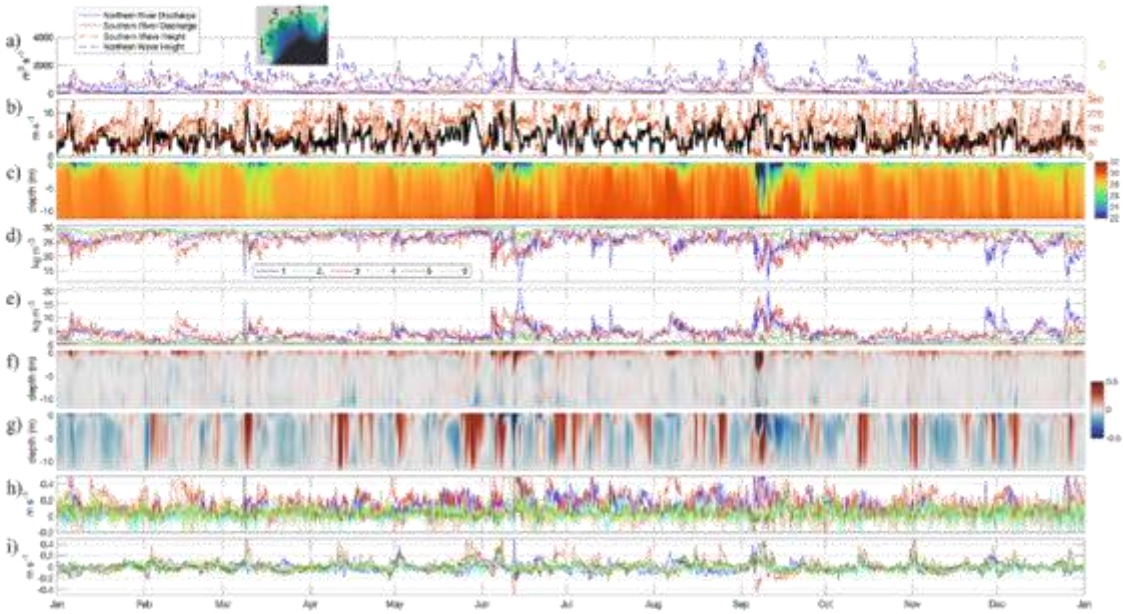

Figure 3.12 Inner shelf circulation timeseries for the year of 2018. The locations are shown in a), which are located 2 and 10 km offshore of the coastline for each region. b) Total river discharge from the southern rivers (red), northern rivers (blue), and northern wave height (dashed blue), and southern wave height (dashed red). c) wind speed and direction near the HAWQi mooring. d) Density of water (values added to 1000, in kg m^3) at point 3, 2 km offshore of the Wairoa River. e) Surface density (kg m^3). f) Density stratification (kg m^3). g) Cross-shore velocity at point 3 (m s^{-1}). h) Cross-shore velocity at point 3 (positive offshore; m s^{-1}). i) Surface cross-shore velocity (m s^{-1}). j) Depth averaged alongshore velocity (positive northward; m s^{-1}).

The cross-shore flow structure 2 km offshore of the Wairoa River (Fig. 3.12g) is predominately baroclinic and shows upper layer seaward flow associated with buoyancy and spreading of the river

plume, and landward flow at depth. At other locations, the surface cross-shore velocity typically flows offshore (Fig. 3.12i), with variation associated with discharge events as well as wind and other forcings. This is in contrast with the alongshore flow structure, which is predominately barotropic and varies with periodic wind events (Fig. 3.12h), except for discharge events which can show alongshore baroclinic structure. The depth averaged alongshore velocity (Fig. 3.12j) generally shows similar responses between locations, with locations 2 km from the coastline showing higher velocities than 10 km offshore. The alongshore directionality shows differences from the northern and southern locations for easterly wind directions due to the orientation of the Bay.

3.4.3. River plume variability

The modelling results show that the density structure and circulation patterns in Hawke Bay are largely influenced by the presence of buoyancy from rivers (Fig. 3.10, 3.11), and modulated by wind and other forcing conditions (Fig. 3.12). The river plumes have been shown to predominately flow northward, likely corresponding to the predominate SW wind direction but are periodically affected by reversals in wind direction. However, the way in which the rivers influence the plume, and consequently the distribution of sediment, depends on the detailed characteristics of the river and event characteristics (Fig. 3.13).

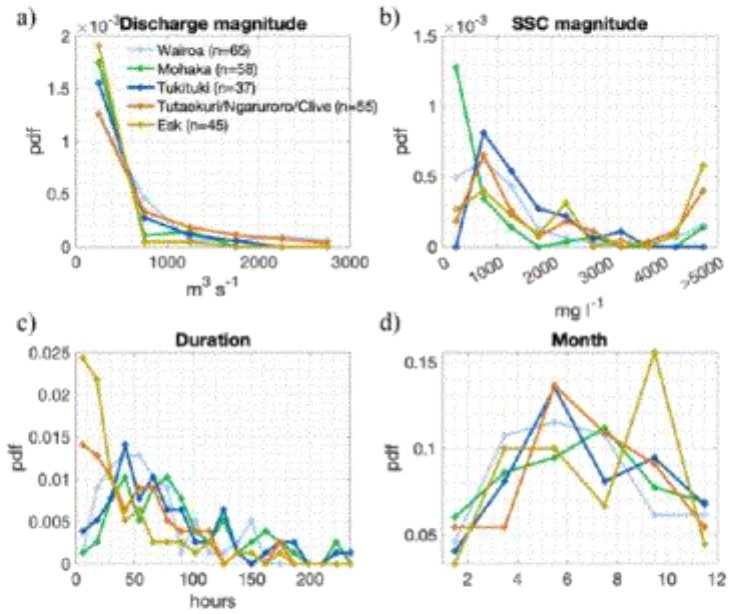

Figure 3.13 Description of river discharge events in the period of 2017-2019 for the largest rivers that enter Hawke Bay. a) The magnitude of each event, b) the magnitude of SSC during the peak discharge, c) the duration in hours, and d) the month of the year that the discharge event occurred in.

In general, larger river discharges were associated with short duration intense events, with the Wairoa and Mohaka rivers experiencing the largest events in terms of discharge while the smaller rivers (Esk and Tūtaekurī/Ngaruroro Rivers) events were associated with the highest SSC values. To demonstrate this, the main rivers discharge events are identified and compared with environmental conditions. Over the three-year period, for the five largest rivers that discharge into the Bay, generally around 50 events were found each, with a higher probability of smaller magnitude discharge events (Fig. 3.13). Most durations were between 0.5–3 days with a number of extended events greater than 100 hours. The SSC during events, in the range of 500 to > 4000 mg l^{-1}, and event durations followed similar patterns between rivers, with a greater number of shorter events with lower SSC (Fig. 3.13c).

The typical spatial patterns of river plumes were assessed through salinity contours compiled through time (Fig. 3.14). These patterns show that the Mohaka and Wairoa Rivers have radial patterns that extend to the left towards the Mahia Peninsula. The Tukituki and Tūtaekurī/Ngaruroro Rivers show expanses that stretch from Cape Kidnappers to north of Napier.

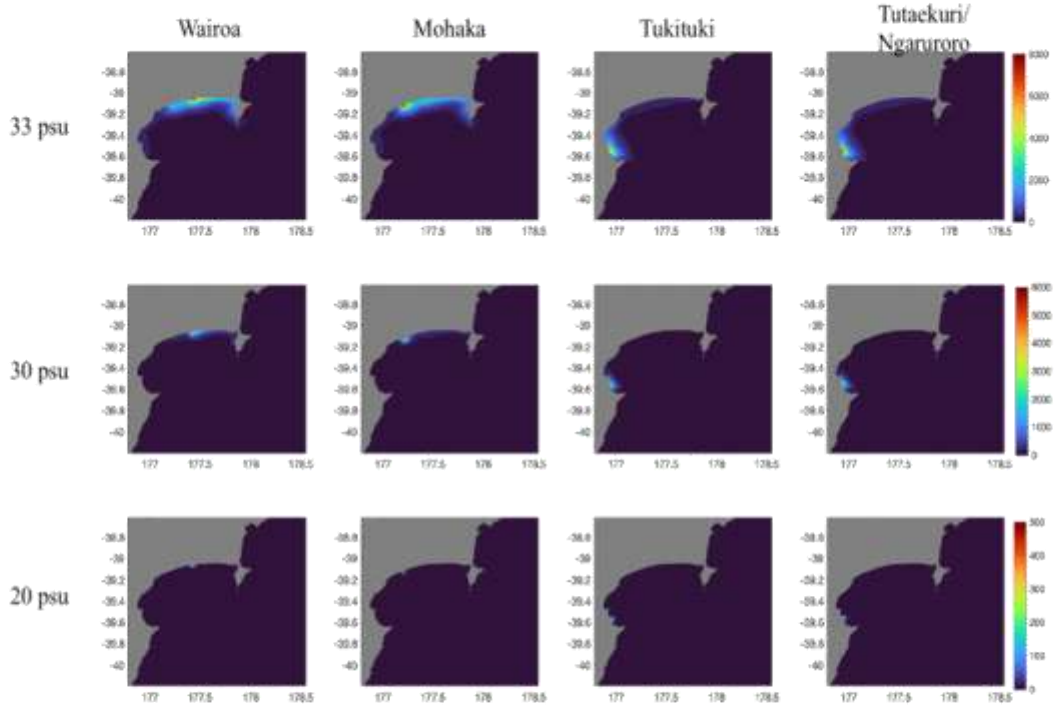

Figure 3.14 River plume salinity contour boundary heat maps for each river. Each column represents a river for 33, 30, and 20 psu contours (rows). The colour scale represents the number of occurrences from 2017-2019 (from the 3-hour model output).

For each discharge event for each river, the river plume characteristics show variability primarily associated with the magnitude of discharge and wind. The river plume characteristics were

computed for each discharge event by averaging the values from the beginning to end of the event, using spatial coordinates from the 30 psu salinity contour (e.g. Fig. 3.14). This value was chosen as it was often present and includes varying regions of the river plume without extending to far-field plume regions such as the 33 psu contours (Fig. 3.14). The plume velocity was averaged between the depth of the pycnocline and the surface. The plume directions were most directed offshore and to the left (traveling northward) for all rivers. The Wairoa River has the highest tendency of leftward directions, which is expected due to the change in coastline orientation with respect to the predominate wind direction. Plume directions show linear relations with wind along and cross-shelf velocity (Fig. 3.15b-c), except for onshore wind, which shows no relation, likely due to the broad area that encompasses the analysis region. Density stratification displays a nonlinear relation with maximal stratification values reached for each river above a threshold discharge (ranging from 300-500 m^3s^{-1}).

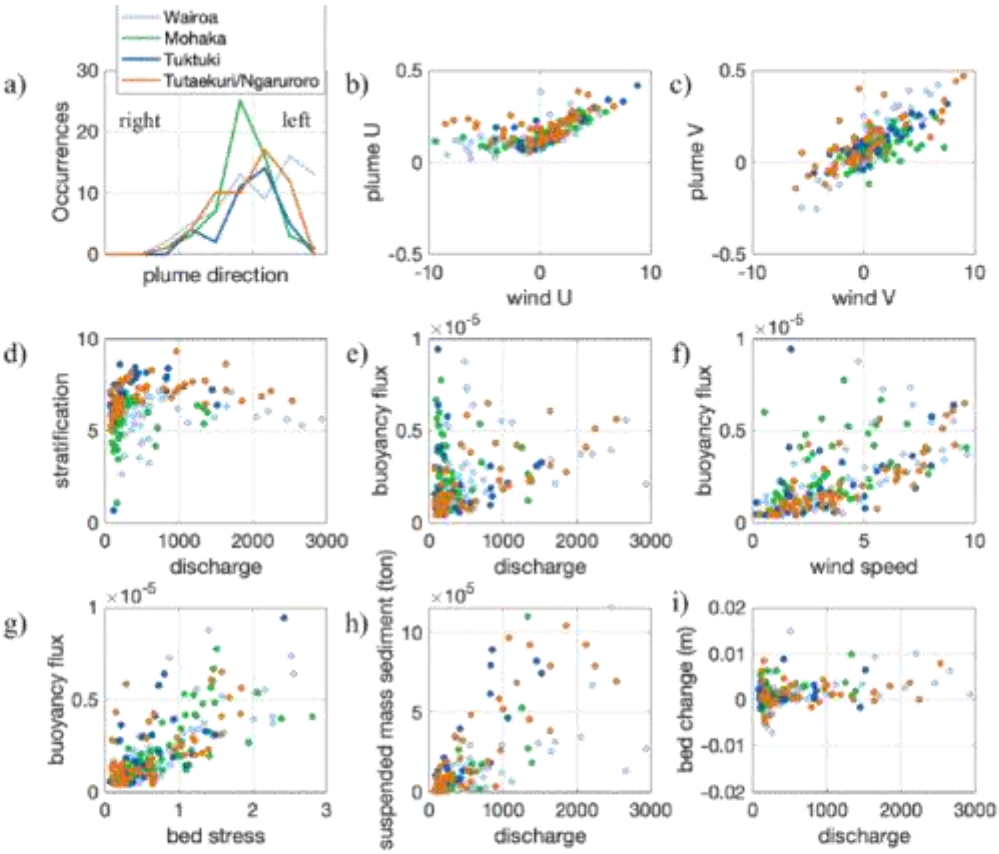

Figure 3.15 River discharge event plume statistical descriptions. Plume values were calculated using spatial averages over the 30 psu salinity contour. a) plume direction (in relation to the shoreline) during discharge event, b) wind and plume cross-shore velocity averaged during discharge event, c) wind and plume alongshore velocity averaged during event, d) surface to bottom density stratification and river discharge averaged over

discharge event, e) the buoyancy flux ($m^2 s^{-3}$) at the pycnocline and river discharge averaged over discharge event, f) the buoyancy flux ($m^2 s^{-3}$) at the pycnocline and wind speed averaged over discharge event, g) the bed stress ($N m^2$) and buoyancy flux ($m^2 s^{-3}$) averaged over discharge events h) the suspended sediment mass (tons) and river discharge averaged over discharge event, and i) the spatial average of bed vertical change (m) and river discharge over discharge event. The spatial bounds of the bed change were determined by the surface locations of the 30 psu contour during the times of the discharge event.

The mixing intensity, shown here by the buoyancy flux at the pycnocline, varies with river discharge (Fig. 3.15f), wind speed (Fig. 3.15g), and bed stress (Fig. 3.15g). Generally, higher discharge initiates higher plume momentum which causes increased shear driven mixing, while wind predominately acts on the mid-field and far-field plume (Horner-Devine et al. 2015). Higher bed stress is typically not associated with increased mixing at the plume base and the correlation could be due to other processes associated with storms. However, tidal mixing originating at the bed has been shown to impact plume interface mixing (Spicer et al. 2021). Further investigation that separates the plumes into different regions would likely show the spatial differences in mixing patterns related to inertial and wind forcing. For discharge events greater than ~200 m^3s^{-1} a positive (accumulated) bed sediment change occurred within the bounds of the 30 psu plume, with average values over the plume area increasing with discharge in the range of roughly 1-10 cm. For discharge events less than ~200 m^3s^{-1}, both erosion and deposition occurred, likely signifying greater wave driven bed changes rather than from fluvial input.

The four rivers showed overall similar responses to conditions with generally similar ranges of velocity, stratification, and buoyancy flux values. Differences between the rivers include slightly higher observed stratification offshore of the Tukituki and Tūtaekurī/Ngaruroro Rivers (~1–2 kg m^{-3} higher) . While the relationship between wind and plume directionalities are linear for all rivers (Fig. 3.15b,c), the coastline orientation varies across the Bay, resulting in differing cross-shore plume directionalities, with the northern river plumes most commonly directed northward and the southern rivers most commonly directed offshore.

3.4.4. Sediment flux

Fluvial sediment is transported seaward by river plumes and can be resuspended by waves and advected to other parts of the Bay. The fluvial sediment flux consists of four size classes (Table 3.1) where the settling velocity is a key factor in determining the horizontal distance of transport from the rivers. Averaged SSC values over the month of July 2019 for each size sediment class show the general patterns of the size class distribution in the Bay (Fig. 3.16). The clay size class with settling velocity of 0.014 mm s^{-1} is broadly dispersed, with low SSC values (~5 mg l^{-1}) extending throughout the entire Bay. The silt size, floc, and coarse silt size classes are concentrated in nearshore waters with the highest values found in waters less than 20 m deep, indicating short transport distances from rivers

(generally less than 2 km). The total surface sediment concentration (Fig. 3.16c) is roughly a magnitude smaller than the bed sediment concentration (Fig. 3.16f) averaged over the period. The bed sediment concentration shows elevated values dispersed offshore of the coastline in comparison to the surface concentration, which is concentrated nearshore, and shows regions of concentrated elevated values in the southern Bay and offshore of the Wairoa and Nuhaka Rivers.

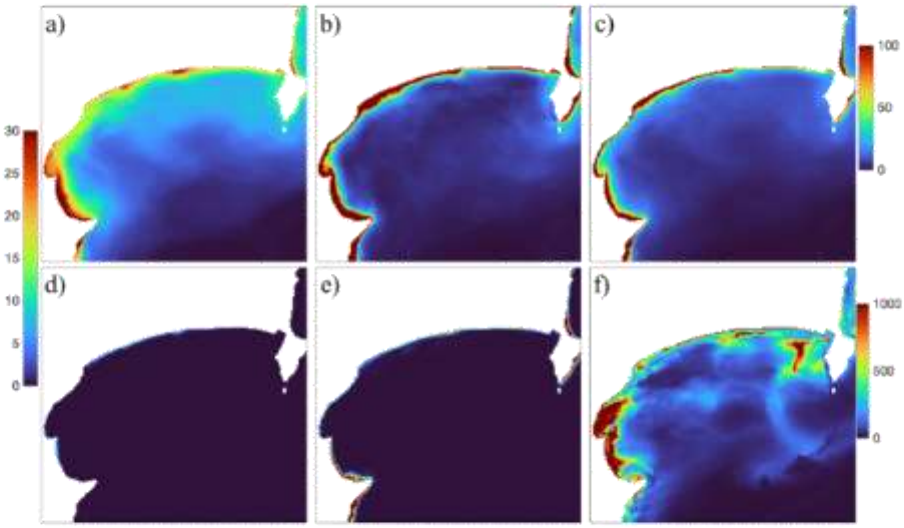

Figure 3.16 Modelled SSC concentrations for differing sediment sizes and locations in the water column. Average SSC concentrations (mg l^{-1}) for the mud sediment size classes (a,b,d,e), and the c) total surface sediment concentration and f) bed sediment concentration, averaged over the month of July 2019. The mud size classes include a) clay, b) silt, d) flocculated, and e) coarse silt. Note that the bed and surface sediment concentration plots have different colour scales.

To further describe sediment transport throughout the Bay, the sediment fluxes are decomposed into change of mass of suspended and bed sediment (Fig. 3.17b), and the mass of the suspended sediment in the Bay is divided into different depth intervals (Fig 3.17c). The estimated sediment fluxes from each of the main rivers ranged between 1–3 million tons of sediment input to the ocean over the three-year period, with the Wairoa River having the largest flux and the other main rivers having similar flux magnitudes between 1–1.5 million tons. Smaller rivers such as the Esk River contribute a relatively small amount to the total flux into the Bay.

The initial model bed displayed continuous erosion for ~5 months, which we classify as an adjustment time for the initial interpolated sediment bed into a state more equilibrated with typical bed stresses. Over the three-year period, about 8 million tons of sediment were input to the Bay from rivers, which is well below the annual average of 11 million tons per year (Hicks et al. 2011). During

normal wave conditions (1-2 m swell), 1–2 million tons of sediment can be in suspension in the Bay (Fig. 3.17b), and during wave and/or river events, >10 million tons can be in suspension in the Bay. The bed mass change is anti-correlated with suspended sediment mass, indicating that most of sediment suspended is sourced from the bed, which is then redistributed throughout the Bay. The flux of sediment mass out of the Bay occurs during periods of bed mass erosion, which is predominately transported northward around the Mahia Peninsula (not shown).

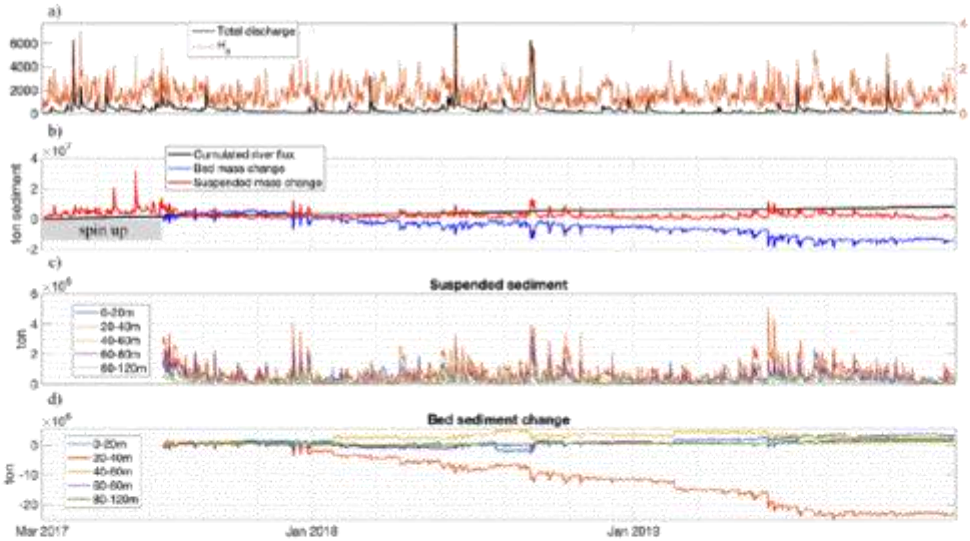

Figure 3.17 Timeseries of sediment fluxes in Bay. a) The significant wave height (orange; m) and total river discharge (black; $m^3 s^{-1}$). b) Tons of sediment separated into the cumulative river flux (black), bed mass change (blue), and suspended sediment mass change (red). d) The integrated bed sediment mass change (tons) at 20 m depth intervals in the Bay.

The largest changes to the bed mass throughout the study period occur in the 20-40 m depth range, with accumulation occurring offshore of 40 m depth, with little change occurring deeper than 80 m (Fig. 3.17d). Most of the suspended mass is found in depths less than 40 m (Fig. 3.17c), and the suspended mass throughout the depths of the Bay vary similarly in time. The relatively high and consistent suspended mass is associated with suspended sediment concentrations on the order of 500-5000 mg l^{-1} when bed stress is elevated, with maximum values around 20,000 mg l^{-1}.

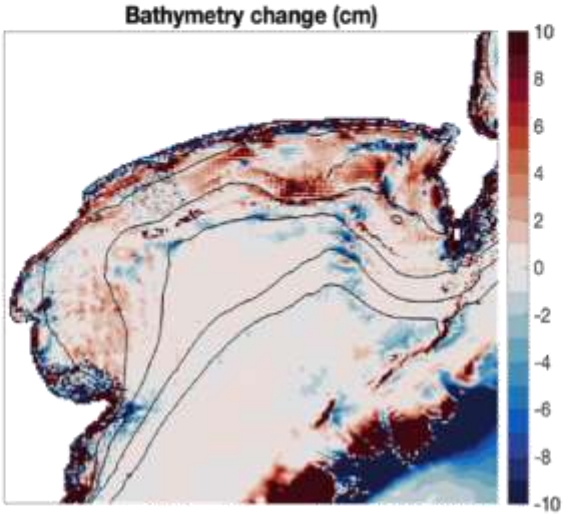

Figure 3.18 Long term bathymetry change (cm) at the end of the model run. The bathymetric contours (black lines) are shown for the 20, 40, 60, 80 and 100 m depths.

Over the three-year period, two general bed change patterns occurred, including 1) an adjustment of bed elevation adjacent to the coastline, and 2) accumulation offshore of 20 m. Erosion occurred adjacent to the coastline with deposition directly offshore on the order of 5-10 cm, and larger changes occurred in the regions of rocky reefs which experience higher bed stress (Fig. 3.18). Accumulation areas are typically between 20-60 m, with the largest region occurring offshore of the Wairoa and Nuhaka Rivers. Changes in bed muddy grain sizes show that all the clay sized material eroded from the shelf (Fig. 3.19i), fine silt eroded from the nearshore except offshore of the Esk River (Fig. 3.19j), which was accumulated in the middle of the Bay. The aggregated material, which did not have initial distribution and was only input from the rivers, shows depositional zones with ~6 km from rivers, generally directly offshore of the Mohaka and Wairoa Rivers, and transported northwards from the southern rivers towards the Esk River (Fig. 3.19k). Coarse silt was removed from the nearshore (Fig. 3.19l) and transported to the middle of the Bay. The model shows that the bed stress in the Bay can consistently suspend bed material, from which the transport is then dependent on the near bed circulation, which was not thoroughly investigated here.

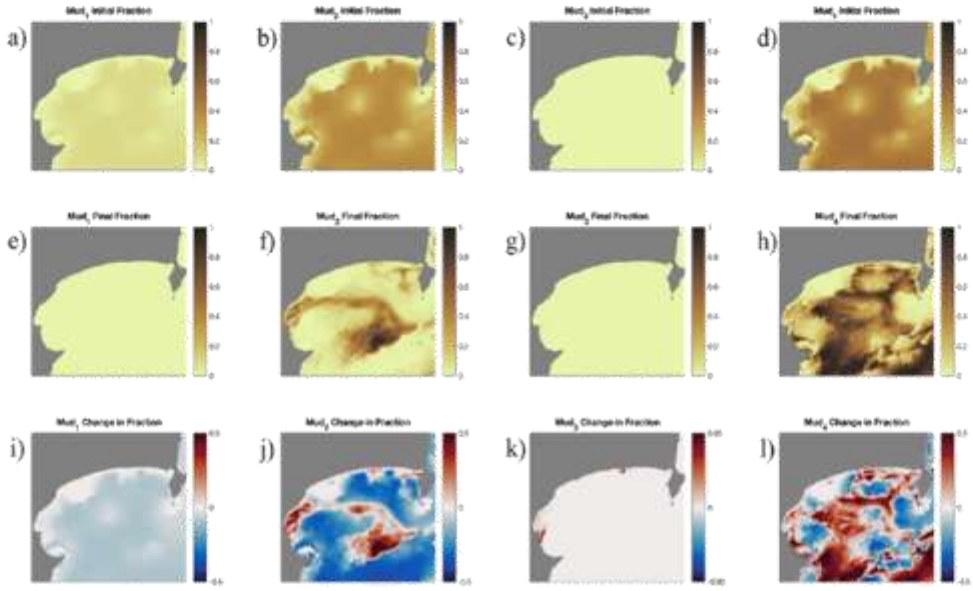

Figure 3.19 Grain size changes for the mud size classes. The plots show the initial fraction (top row), final fraction (middle row), and changes in fraction (bottom row). The grain sizes are found in Table 3.1.

3.4.2. Influence of waves on hydrodynamics

The inclusion of the coupled wave model introduces wave driven currents, impacts to the currents from waves, and altered mixing and bed stress patterns which impact cross-shelf sediment transport (Wright et al. 1980, Geyer et al. 2004) and potentially river plume circulation (e.g. Gerbi et al. 2013). From the three-year simulations, seasonally averaged differences between the ROMS and coupled ROMS/SWAN runs show that the inclusion of wave processes causes higher surface salinity, lower stratification, increased landward near-bed velocity, and complex differences in surface velocity patterns, with plume areas showing reduced speeds and other nearshore areas showing increased speeds (Fig. 3.20). Seasonal differences in velocity patterns are apparent between the two runs. Previous studies comparing ROMS and ROMS/SWAN models have similarly found that coupled simulations show increased surface turbulence injection from wave breaking that leads to reduced plume stratification (Gerbi et al. 2013; Rong et al. 2014; Moghimi et al. 2019). Wave-current interaction at river outflows is expected to alter wave propagation in plume areas (Olabarrieta et al. 2011), and other wave-driven circulation patterns (e.g. Stokes drift) are expected to alter the inner shelf circulation (Moulton et al. 2023).

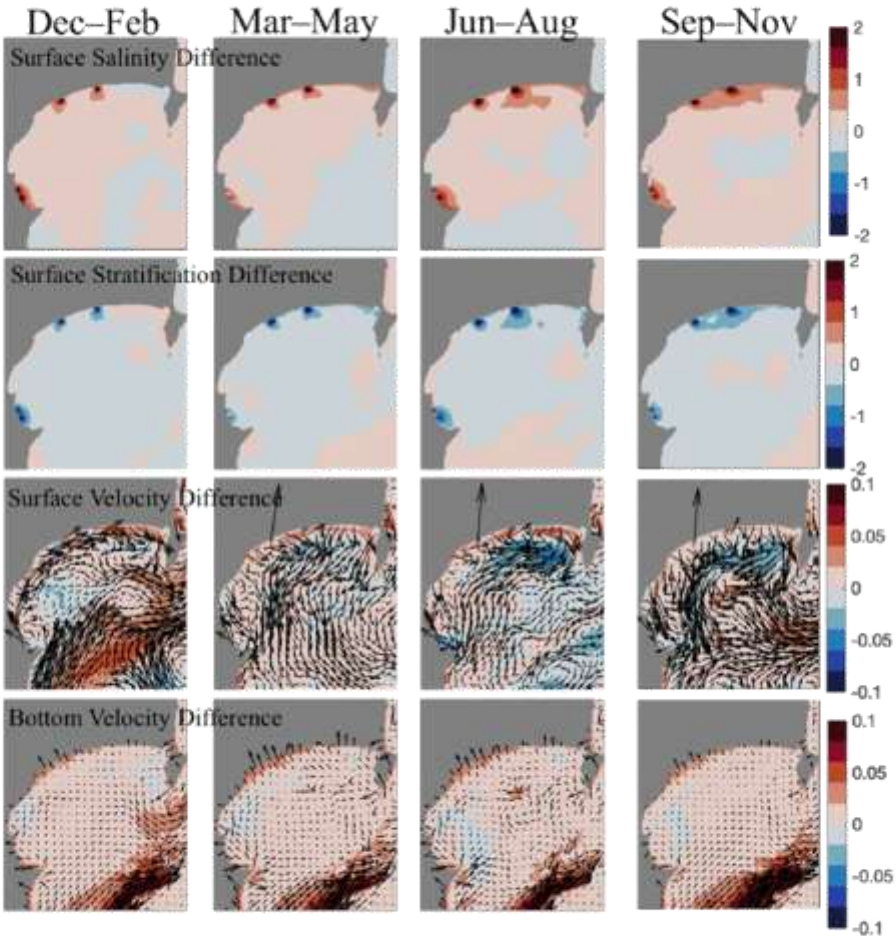

Figure 3.20 Comparison between ROMS and Coupled ROMS/SWAN runs using average seasonal values. Each row shows the surface salinity difference (Coupled – ROMS), salinity stratification difference (calculated as the difference from top to bottom), surface velocity difference, and bottom velocity difference.

The time-varying response to the inclusion of waves is assessed through a timeseries offshore of the Wairoa River which compares the vertical structure of density, velocity, and mixing in relation to varying wave conditions for the ROMS and ROMS/SWAN runs over the winter of 2018 (Fig. 3.21). The inclusion of waves generally reduces the plume thickness and magnitude of stratification (Fig. 3.21b-c). Surface cross-shore velocities show similar variability with typical differences of 0.1 m s^{-1}, with the largest differences occurring during discharge events (Fig. 3.21d). The long-shore velocity differences have greater magnitudes with typical differences of 0.2 m s^{-1} and the coupled run shows higher magnitudes (Fig. 3.21e), particularly during wave events in October and November of 2018. Higher turbulence production is seen in the coupled runs with increased surface and bed values (Fig. 3.21f-g), with typically increased buoyancy fluxes during these same periods (Fig. 3.21h-i). The

most pronounced differences between the two model runs occur during periods of increased buoyancy from rivers due to the proximity of the Wairoa River as well as during wave events. The findings suggest the including waves may additionally impact the flux of suspended sediment from rivers, as impacts to the cross-shore and long-shore currents will impact the initial sediment deposition. Other potential wave driven processes such as Stokes drift are not investigated.

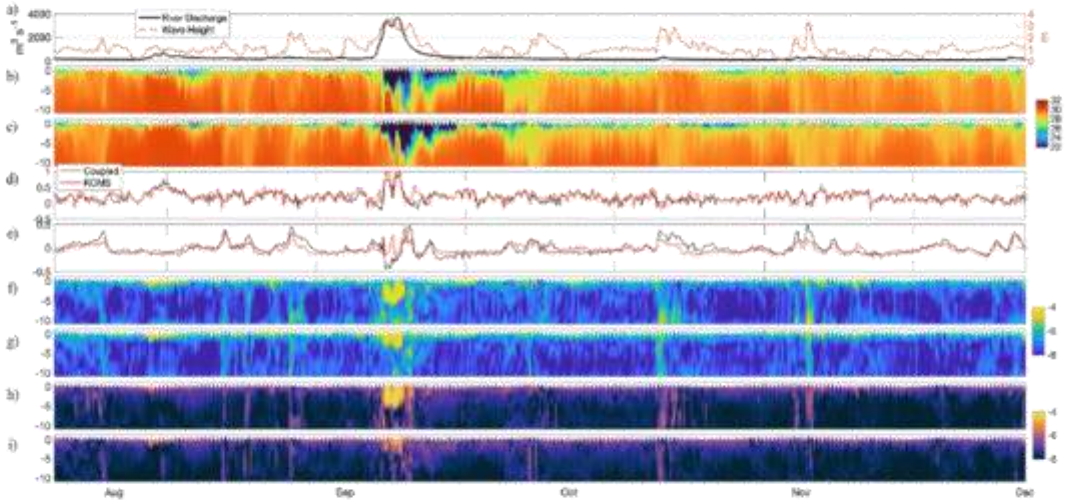

Figure 3.21 Timeseries offshore of the Wairoa River that compares the coupled ROMS/SWAN model with the ROMS only run over a select period in 2018. a) River discharge of the northern rivers (left axis; $m^3 s^{-1}$) and wave height offshore of the Wairoa River (right axis; m). b) Density (plus 1000; kg m^{-3}) offshore of the Wairoa River for the coupled run. c) Density (plus 1000; kg m^{-3}) offshore of the Wairoa River for the ROMS only run. d) Surface cross-shore velocity (m s^{-1}). e) Depth averaged long-shore velocity (m s^{-1}). f) Log of turbulence production for coupled and g) ROMS only. h) Log of buoyancy flux for coupled and i) ROMS only.

3.5 Discussion

3.5.1 Sediment transport from small mountainous rivers

The suspended sediment transport from river plumes was found to be largely dependent on the grain size which sets transport distances, with the majority of riverine sediment being transported distances on the order of kilometers. The erosion of bed mass is caused during elevated wave conditions (greater than ~1.5 m) which allows bottom currents to redistribute sediment. The spatial patterns in the changes in bed sediment generally reflect modifications to pre-existing bed sediment and do not necessarily reflect the transport of recently derived fluvial sediment, as the modelled magnitudes of instantaneous transport in the Bay greatly surpass the riverine flux. These findings are in qualitative agreement with previous works on small mountainous rivers in energetic settings (Geyer et al. 2004; Walsh and Nittrouer 2009; Harris et al. 2008) although specific transport metrics are not investigated here.

3.5.2. Limitations and future work

Further investigations focused specifically on the riverine sediment and near-bed currents would be able to distinguish between riverine sediment transport patterns and bed adjustment to oceanographic conditions in the Bay. The modelling of sediment transport considered here was limited by unknown sediment properties within the Bay as well as model formulations that excluded processes such as flocculation and bed consolidation. Future modelling work in Hawke Bay would be better constrained by additional measurements of the grain size distribution in rivers and identifying the prevalence of flocculated particles, and additionally resolving estuarine processes that would impact river plume dynamics.

3.6. Conclusion

A numerical model of Hawke Bay, Aotearoa New Zealand, performed well when assessed against a range of measurements, and was used to elucidate the general circulation patterns and the transport of suspended sediment from rivers. The model shows that the density structure and inner shelf circulation is heavily influenced by the input of surface buoyancy from multiple rivers, with elevated stratification present in vicinity of the major rivers throughout the year. The average circulation in the Bay reflects localized river plume circulations, superimposed on wind driven patterns and the characteristic pattern of outflow at the northern and southern ends of the Bay. Offshore of the Bay, the Wairarapa Coastal Current is present at the shelf break throughout the year and the East Cape Current can intrude into the Bay during summer months.

The river plumes are mainly influenced by wind once away from the river inlets, which can steer the river plumes and mix the surface fresh layer. The northern rivers on average flow offshore and toward the south, while the southern rivers flow offshore on average, corresponding to the influence of the average wind direction. The four main rivers in the Bay display similar magnitudes of stratification and velocity patterns, with the main difference being the orientation of the coastline in relation to the predominate southwest wind direction which alters plume processes.

The inclusion of surface waves predominantly impacts the resuspension of sediment from the bed as well as turbulent mixing of the water column. The spatial patterns of sediment concentration variability in the Bay validated well against satellite derived estimates, while the magnitude showed large biases likely associated with errors in the satellite derived estimates. Similar to previous studies of small mountainous river systems, the cross-shelf river plume transport of sediment is highly dependent on the settling velocity, with grain sizes larger than coarse silt not able to initially transit farther than a few kilometers. Waves consistently resuspend material, and the long-term sedimentation patterns are largely due to bed sediment redistribution after the sediment has initially settled from river plumes. Waves additionally modify the vertical structure of turbulence, increasing surface mixing and altering river plume circulation.

Chapter 4: The variability of cross-shelf flows offshore of a small mountainous river

Contribution of Authors

Chapter 4 presents the article "The variability of cross-shelf flows offshore of a small mountainous river" which will be submitted to the journal *JGR: Oceans* for review. Ted Conroy conceptualized the study, performed all field work and data analysis, and wrote the article. Karin R. Bryan provided feedback, supervision, and editing of the article throughout the process. Joe O'Callaghan provided assistance with the conceptualization, interpretation, and editing of the article.

4.1 Introduction

The cross-shelf flux of material across the inner shelf is a key parameter for understanding the fate of terrestrial material in the coastal ocean. A detailed understanding of the processes responsible for sediment delivery is particularly relevant for small mountainous rivers, which can yield large discharge magnitudes in episodic events to energetic coastal areas (Wright et al. 1980). Small mountainous river systems deliver disproportionate amounts of sediment to the coastal margin (relative to their catchment size) and are found worldwide on active margins (Milliman and Syvitski 1992). Timescales and magnitudes of the cross-shelf flux are relevant for long-term sediment fluxes, ecological impacts, and the management of coastal areas.

The majority of river plume studies have focused on larger river systems that operate on slower time scales and have spatial scales on the order of 10's of kilometers rather than 100's of meters to kilometers (Horner-Devine et al. 2015), while smaller scale river plumes have received less attention. River plumes from small mountainous river systems generally have narrow inlets with small estuaries, large magnitudes of discharge, and commonly outflow to energetic inner shelf environments (e.g. Geyer et al. 2000, Lemagie and Lerczak 2022). Smaller rivers have been found to be less influenced by rotation (Horner-Devine et al. 2015), although the distinction between river size and the importance of rotation is unclear at present. Smaller river plumes than considered here have been found to be influenced by tidal currents (Basdurak et al. 2020) and wave breaking (Rodriguez et al. 2018).

Using in-situ observations, the coupled inner shelf and river plume response was investigated offshore of a small mountainous river to common shelf forcings, with particular emphasis on the response of the cross-shelf velocity, density, and shear structure. The aim was to quantify the differences that occurred during storm events and varying wind conditions, and from these measurements, infer the ultimate impact on the cross-shelf sediment flux from small mountainous rivers. Observations were collected offshore of the Tukituki River in Hawke Bay, New Zealand, which drains a steep, highly erodible catchment which is regularly subjected to intense rainfall events. We use a number of data sources to quantify plume transport, mixing, and the resultant impact on cross-shelf sediment transport.

4.2 Background

4.2.1 Inner shelf and river plume circulation

River plume dynamics are controlled by the interplay between processes within the river and the currents and stratification in the receiving environment of the shelf. In turn, the currents on the inner shelf are influenced by waves, wind, tide, and regional current patterns (Lentz and Fewings 2012, Kumar et al. 2016). The interplay of processes within the river plume depend on the river

velocity at the inlet mouth, the density contrast between the outflowing water and ambient ocean water, the barotropic pressure gradient, and ambient currents created by the wind or offshore currents (Horner-Devine et al. 2015, Hetland 2005). In the near-field region, transport is generally dictated by the outflow momentum at the river mouth, modulated by tidal forcing (e.g. Basdurak et al. 2020), which transitions into the subcritical mid-field region, where lateral spreading of the plume predominately occurs and wind forcing plays a larger role in directing and mixing the plume, and is the dominant mechanism of vertical mixing in the far-field plume (Horner-Devine et al. 2015). Mixing intensity is typically highest in the near-field region due to high shear values after the plume detaches from the bed.

4.2.2 Response of river plume and inner shelf to wind forcing

The most-studied wind-driven response of river plumes has been found to be upwelling or downwelling Ekman transport (Horner-Devine et al. 2015). Upwelling winds are directed alongshore, flowing with the coast on the left in the southern hemisphere, whereas the opposite conditions cause downwelling. Upwelling winds have been shown to vertically thin and transport river plumes offshore, while downwelling winds have been shown to trap fresh water near the coast and deepen the plume layer while enhancing coastal current formation (Horner-Devine et al. 2015; Fong and Geyer 2001). The plume response to cross-shore winds has received limited attention but a few studies have found that plumes can be advected in the direction the wind is blowing (Hunter et al. 2010, Kakoulaki et al. 2014).

Similarly, inner shelf flows respond to downwelling and upwelling wind forcing with geostrophic flow in the alongshelf direction, and in the cross-shelf direction Ekman transport occurs in the surface layer and a compensating return flow is present in the lower layer. Cross-shore winds can drive sea level set up and circulation in depths less than ~30 m but do not drive alongshore geostrophic flows (Lentz and Fewings 2012). Similarly, cross-shore winds can drive a return flow in the bottom layer. Stratification limits the cross-shelf transport by limiting the Ekman depth, which inhibits penetration of the surface current surface into the water column.

4.2.3 Hawke Bay and Tukituki River

Hawke Bay is a southeast facing embayment (~40 by ~80 km), on the east coast of the North Island of New Zealand, extending from the Mahia Peninsula in the north to Cape Kidnappers (Fig. 4.1). The Bay has a gentle slope that extends to the shelf break outside of the Bay. Steep coastal mountains combined with high average rainfall rates produce significant episodic river discharge events that transport on average 11 million tons of suspended sediment to the Bay each year (Hicks et al. 2011). The Bay is exposed to a strong wave climate from the south (Komar 2010) and has a spring tidal range of 1.9 m.

The Tukituki River is in the southern Hawkes Bay, flowing from a ~2500 km^2 catchment in the Ruahine Range for ~80 km to the Pacific Ocean. The discharge is highly episodic with increased flows in winter but the potential for large events year-round. The largest recorded discharge was 3040 m^3 s^{-1} while typical events occur on the order of 10^2–10^3 m^3 s^{-1} and the mean discharge is 43 m^3 s^{-1}. The annual sediment flux from the Tukituki River is estimated to be around 1 million tons (Hicks et al. 2011). Near the river inlet, the bed is composed of gravel pebbles with gravel beach on each side of the inlet, with fine sand present offshore (White 1994). The inlet morphology is highly variable in spatial position, impacted by flood events and alongshore transport from waves, and can vary from being fully closed to an inlet width of ~300 m. The inlet was surveyed 8 days prior to the instrument deployment where the depth at the inlet was 3.5 m (below mean sea level).

A study describing the sediment and circulation properties of the Tukituki River and surrounding coastal region described the estuary as highly stratified with muddy bed sediment (predominately fine silt), with the main muddy sediment deposits located offshore of the river deeper than ~10 m (White 1994). In the river, the maximum recorded Suspended Sediment Concentration was ~2500 mg l^{-1} (Norris, 2019) and offshore of the river at the bed was around 4000 mg l^{-1} (White 1994). However, the inner shelf processes that guide the river sediment offshore are unknown.

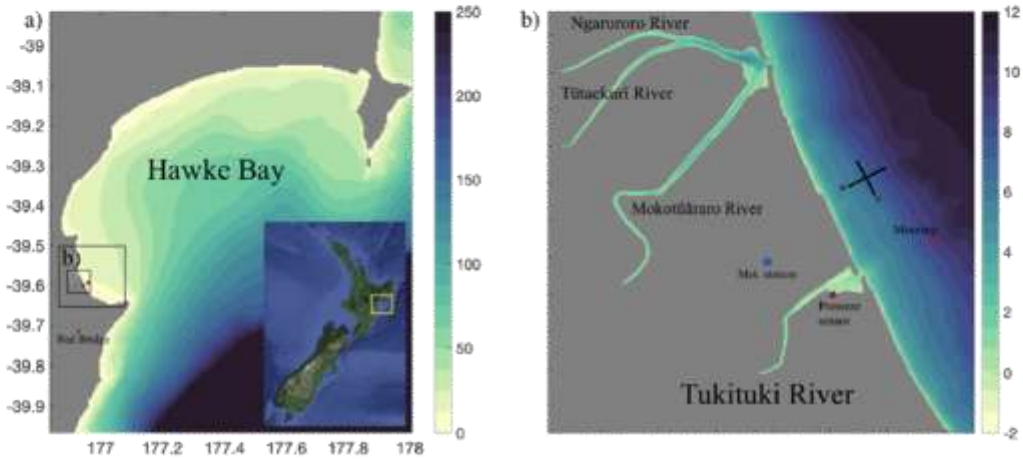

Figure 4.1 Areal overview of Hawkes Bay, Aotearoa New Zealand (shown in inset figure). The bathymetry of Hawke Bay (m) is shown on the left, and a zoomed in view of the Tukituki River area is shown on the right. To the north of the Tukituki River is the river complex of the Ngaruroro, Tūtaekurī, and Mokotūāraro Rivers. On the right image, the black cross represents the rotated coordinate system used in this study.

4.3 Methods

4.3.1 Instrument Deployment

A set of instruments was deployed in the winter of 2022 located 1 km offshore of the mouth of the Tukituki River in 8 m depth, including downward and upward facing bed mounted Acoustic Doppler Current Profilers (ADCPs), five Conductivity, Temperature and Depths Sensors (CTDs), and three Optical Backscatter Sensors (OBSs) (Fig. 4.1). The instruments were deployed for 41 days with varying sampling rates aimed at resolving river plume processes (Table 4.1).

Table 4.1 Description of instrumentation used and sampling information for the 2023 deployment offshore of the Tukituki River. Locations of instruments are shown in Fig. 4.1.

Instrument	Depth	Sampling	Additional info
ADCP (Nortek Signature 1000)	35 cmab looking up	Average 120 seconds every 5 minutes, 5 beam continuous burst 2 Hz. Echosounder continuous sampling	20 cm bins average, 40 cm bins burst, 1 cm bins echosounder
ADCP (Nortek Aquadopp 2 khz)	43 cmab looking down	Burst 8 Hz 2400 times every 1800 sec	25 mm bins
OBS at bed	19.5 cmab	Burst 8 Hz 2400 times every 1800 sec	High range setting
2 OBSs in water column	0.35, 1.7 m below surface	Burst 6 Hz 1024 times every 10 minutes	Auto ranging
2 RBR Concerto CTDs	0.35, 1.7 m below surface	Burst 6 Hz 1024 times every 10 minutes	High salinity bias accounted for with offset
3 Seabird Microcat 37 ODO CTDs	43 cmab, 5 mab, 50 cmbs	Sample every 10 minutes	

The Signature 1000 upward-facing ADCP was processed by removing data with correlation lower than 50% (Nortek Operations Manual for Signature 1000) as well as removing the surface layer. The density measurements show large density fluctuations between 0.35 and 1.7 m from the surface (Fig. 4.2) such that the river plume is typically surface focused with the pycnocline less than 1.7 m from the surface. The quality of ADCP data directly below the water surface was variable over the deployment, which was removed by removing data 25 cm below the surface. The Signature

measured up to 8.9 m above the instrument, while the maximum recorded level above the instrument was 9.5 m, so the near-surface velocity was not observed during several of the largest high tides.

A downward facing Aquadopp ADCP was similarly processed but stopped recording data around July 22 indicating a potential burial of the frame. Echo intensity shows that the bed was normally 17 cm below the Aquadopp sensor, implying a vertical change of 22.5 cm. Whether burial occurred because of sediment deposition or frame sinking is not known. The ADCP velocities were rotated to shore-normal coordinates. The suspended sediment concentration from OBS sensors was estimated using lab calibrations of each of the instruments using sediment sourced from a sediment trap that was located on the ADCP frame.

The two uppermost CTDs were fixed to a surface buoy such that they remained below a constant height from the water surface at 0.35 and 1.7 m below the surface, while the three other CTDs were fixed to the bed at mean heights of 4, 5, and 8.2 m below the surface. The RBR CTDs showed a continuous bias of higher salinity in comparison to the Microcat CTDs throughout the deployment. A fixed salinity bias of 0.24 and 1.48 psu were subtracted from the RBR salinity measurements, as the calibrations on the Microcat CTDs (on loan from NIWA) were more up to date. The suspended sediment concentration from the OBS sensors was estimated by calibrating the backscatter data recorded by the OBS sensors in a tank using bed sediment collected at the location of the instruments.

4.3.2 Additional Data Sources

Data for river discharge and river turbidity were sourced from Hawkes Bay Regional Council at observations station Red Bridge, located 15 km from the river mouth (https://www.hbrc.govt.nz/environment/river-levels/). The river suspended sediment concentration (SSC) was determined from a linear relationship between river turbidity and SSC in samples taken during flood events. Wind speed and direction data were sourced from the Whakatu meteorological station located 3 km inland from the river mouth (data provided by NIWA). Satellite data used here were sourced from Planet Labs and Sentinel-2. Suspended sediments from the Tukituki River contains mostly fine silt (4.3 µm) with mean settling velocities of 0.008 and 0.015 m s^{-1} (White 1994).

4.4 Results

4.4.1 Overview of collected data

Instruments were deployed on July 14 (denoted as day 3) for 41 days, the day after the largest discharge event of the deployment period, where the Tukituki River peak flow was 530 m^3 s^{-1} (Fig. 4.2a). Three additional discharge events occurred during the deployment, including on day 4 (270 m^3 s^{-1}), day 16 (260 m^3 s^{-1}), and day 30 (300 m^3 s^{-1}). During these discharge events, similar magnitudes and timing of freshwater fluxes occurred from the combined outflow of the

Tūtaekurī/Ngaruroro/Mokotūāraro Rivers to the North of the Tukituki River. Smaller discharge events occurred separately for the Ngaruroro/Tūtaekurī/Mokotūāraro Rivers on day 38 (145 $m^3 s^{-1}$) and for the Tukituki River on day 39 (120 $m^3 s^{-1}$). The magnitude of suspended sediment concentration in the Tukituki River had similar patterns to river discharge, with sharp increases to values between 500-2000 mg l^{-1} during discharge events which quickly dropped to values in the range of 20-50 mg l^{-1} during non-events.

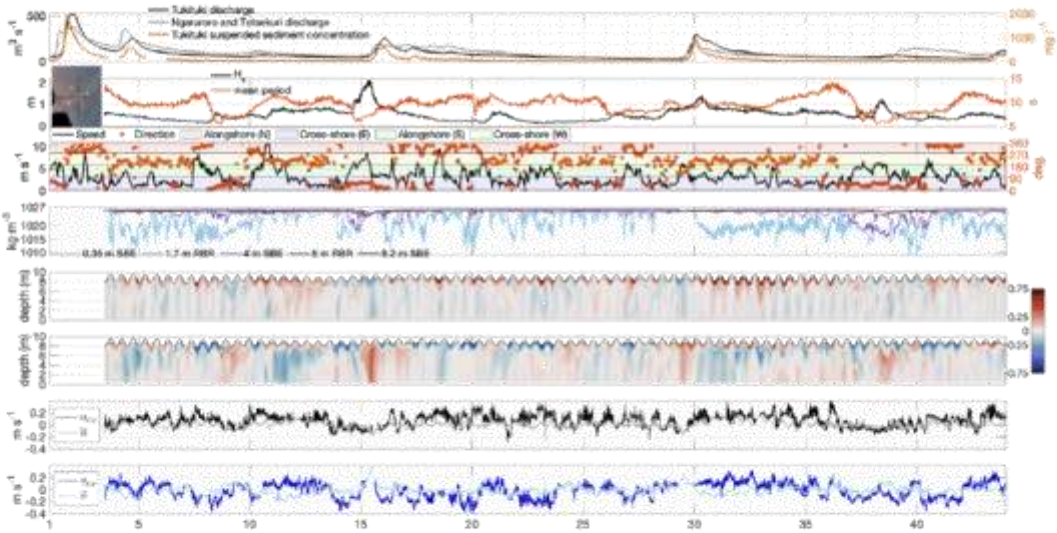

Figure 4.2 Timeseries of collected data offshore of the Tukituki River from July 12 (day 1) to August 24, 2022. a) River discharge ($m^3 s^{-1}$) from the Tukituki River (black), combined Ngaruroro, Tūtaekurī, and Mokotūāraro Rivers (grey), and the suspended sediment concentration (mg l^{-1}) in the Tukituki River (gold; right axis). b) Left inset panel shows the orientation of the coastline with the rotated coordinate system (yellow). The significant wave height (H_s) in m and the mean wave period (s; right axis). c) The wind speed and direction (right axis) measured at Whakatu. The wind direction axis was coloured based on the coastline orientation at the Tukituki River. d) Density (kg m^{-3}) of from CTD measurements throughout the water column. e) Cross-shelf velocity (m s^{-1}) where positive velocity is directed offshore. f) Along-shelf velocity (m s^{-1}) where positive velocity is directed northward. The surface is shown by the black line. g-h) show the cross-shelf and along-shelf exchange and depth averaged velocities (m s^{-1}).

Wave conditions generally followed the temporal variability of river discharge because the storm events were characterized by both catchment rain and offshore wind conditions that generated swell (Fig. 4.2b). Measured values of significant wave height (H_s) ranged from 0.2 to 2.1 m during the deployment and the measured mean period ranged from 5.5 to 14.2 seconds. Three moderate swell events occurred on day 15 (2.1 m), day 30 (1.4 m), and day 38 (1.2 m), with sustained increased heights from days 11-14 and days 30-36. The mean period was low (~7 s) during the first and third

swell events and elevated during the second swell (12 s) with longer period swell generally occurring during lower wave heights.

The wind speed and direction were highly variable, with multiple wind events with wind speeds greater than 5 m s^{-1} occurring over the 41-day deployment period (Fig. 4.2c). The wind direction was classified in relation to the coastline orientation (left panel in Fig. 4.2b and the right axis of Fig. 4.2c), which shows a predominate offshore wind direction (wind from the SW) with periods of onshore wind (from the NE), as well as alongshore wind in both directions. The water column density showed pronounced surface variability at 0.35 m below the surface throughout the deployment (Fig. 4.2d), while 1.7 m below the surface showed a much smaller range of density variability, indicating the plume thickness was generally less than 1.7 m . The time variability of the surface density was linked with the river discharge and tidal variability but shows additional complexity likely related to wind variability and the river inlet geometry (discussed below).

The water column velocity showed a 1–2 m surface layer throughout the deployment with increased speeds (> 0.5 m s^{-1}) during periods of high stratification and tidal oscillations (Fig. 4.2e-f). The velocity fluctuated between two-layer baroclinic flows, unidirectional flow with increased speed at the surface, and barotropic full water column velocity patterns. The cross-shelf velocity was strongest at the surface (0.2–0.8 m s^{-1}) related to the plume circulation, and weaker at depth (0.1–0.2 m s^{-1}) in comparison to the along-shelf velocity (0.1–0.4 m s^{-1}).

Depth averaged velocities ($\bar{u}, \bar{v}$) and the exchange velocities (u_{ex}, v_{ex}), defined as the average velocity from the surface to the first zero crossing at depth (Moulten et al. 2023) are shown in Fig. 4.2g-h. The cross-shelf exchange velocity u_e is primarily positive and is related to the river plume but varies in magnitude between 0.3 and -0.2 m s^{-1}, while the depth averaged cross-shelf velocity varies in range from 0.4 and -0.4 m s^{-1}. Both appear to relate to tidal oscillations and the wind speed and direction. The depth averaged velocities are slower, with $\bar{u}$ showing predominately tidal variability and $\bar{v}$ showing predominantly wind related variability.

To determine which river plume region the observations where in over the deployment, the upper layer Froude number ($Fr = u/\sqrt{g'h}$) was calculated (Hetland 2005), where u is the average cross-shelf velocity in the plume layer, h is the plume depth, and g' is the reduced gravity. In the near-field region, Fr will be maintained to be greater than 1 and the mid field plume region begins where Fr drops below 1 (Horner-Devine et al. 2015). Given that the density measurements were collected at five locations in the water column, and the largest stratification is typically present between the upper two measurement points (Fig. 4.2), the Froude number was calculated assuming the plume depth, defined as the depth of the maximum stratification, was likely between 0.35 and 1.7 m from the water surface. Using a general plume depth of 1 m and the plume velocity averaged in the

upper 1 m, the Froude number was found to be greater than 1 roughly 50% of the deployment, signifying that the mooring location sampled both the near-field and mid-field plume in time.

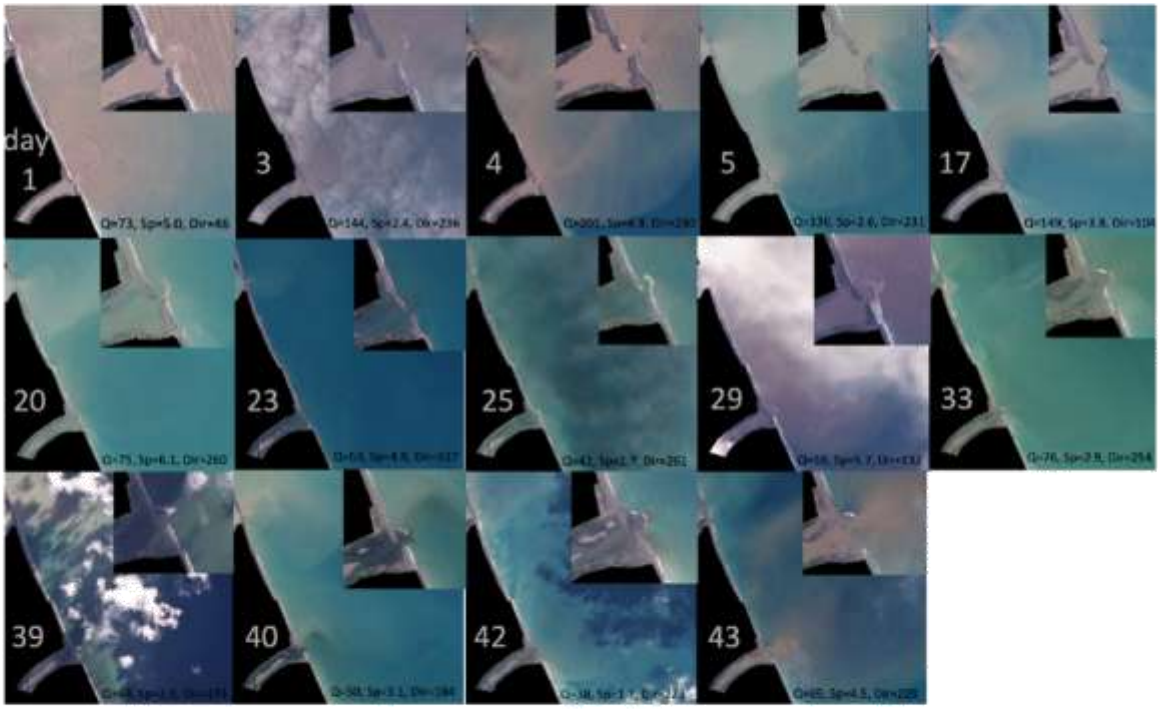

Figure 4.3 Satellite imagery focused on the Tukituki River mouth labelled by days of the deployment. The red dot indicates the location of the mooring. Imagery is sourced from Planet Labs and Sentinel-2. For each day at the time of image collection, the river discharge (Q in $m^3 s^{-1}$), wind speed (Sp in $m s^{-1}$) and direction (Dir in degrees) are labelled.

4.4.2 Inlet morphology and plume spatial variability

Satellite imagery collected over the deployment period displays a spatial overview of the Tukituki River plume throughout the deployment period and highlights the importance of the river inlet geometry in controlling the near-field river plume directionality (Fig. 4.3). The beginning period of the deployment (days 3-17) showed that the inlet had an extended submerged bar directing the plume outflow to the north, with waves breaking along the inlet bar on the southern side. Radial plumes were observed generally all days that were not impacted by the inlet geometry, such as days 29, 33, 42, and 43, as well as during days where the bulk of suspended sediment was transported northward but radial spreading occurred (days 4, 5).

Plume extents from satellite imagery suggests that the freshwater transport as recorded at the mooring may have been reduced until ~day 20 as the near-field plume was directed northward. Two

periods of similar river discharge and wind conditions are examined over multiple tidal cycles with different inlet morphologies, from day 4–8 (Fig. 4.4a) and days 29–33 (Fig. 4.4b). The discharge events had similar peak magnitudes of 270 and 300 $m^3 s^{-1}$ respectively and offshore wind (although differing wind speeds) throughout the entire period. At the start of each event, abrupt transitions to upper layer stratification occurs along with upper layer cross-shelf offshore velocity. The main difference between the two events is the magnitude of tidal variability in the stratification and velocity patterns with greater variability when the inlet was directed north, with cross-shore velocities fluctuating between offshore and onshore for the first event and maintaining offshore flow with greater magnitude for the second. It is possible that during the first event, only buoyancy driven signals are observed, while the second event contains both the buoyancy driven spreading as well as the momentum input from the near-field plume. The upper layer Froude number shows roughly a two-fold increase from days 4–8 compared with days 29–33, with most of the period during days 29–33 the Froude number was greater than 1.

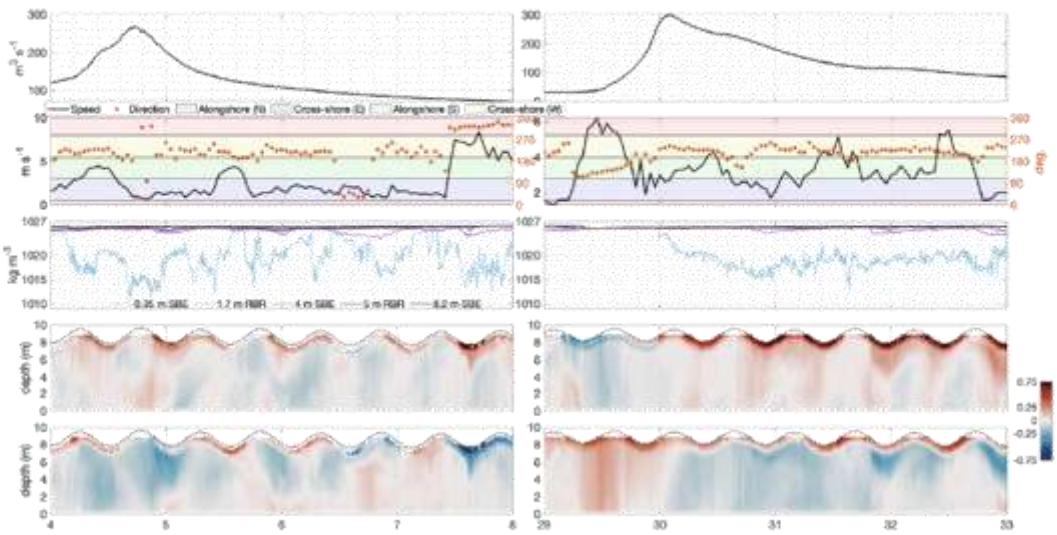

Figure 4.4 Comparison between periods with varying river inlet configurations. The northward directed inlet (left) and the uninhibited inlet (right) are shown under similar discharge and meteorological conditions. The panels include the river discharge, wind speed and direction, density, and cross-shelf and alongshelf velocity.

The timing of satellite data collection did not coincide with the largest wind events but shows a number of modest N wind occurrences (~5 m s^{-1}) where the Ngaruroro/Tūtaekurī/Mokotūāraro plume and the offshore component of the Tukituki plume is directed southward (days 17, 20, 23). Several instances of cross-shore winds with low winds speeds (< 5 m s^{-1}) were additionally captured for onshore winds (days 40 and 42) and offshore winds (days 3, 4, 5, 33, 39 and 43). For all days observed, fronts were present between the plumes of the two rivers which inhibited lateral spreading

from the Tukituki plume northward, and the plume from the Ngaruroro/Tūtaekurī/Mokotūāraro Rivers was not visually observed at the mooring location during the deployment.

4.4.3 Variability with environmental conditions

The relation between environmental conditions and river plume characteristics was assessed through linear correlation analysis between the relevant environmental forcings and main plume properties. Each relevant forcing variable, including the cross-shelf and alongshelf wind, river discharge, tidal height, wave height, and stratification was compared with the river plume response variables that included the cross-shore velocity, alongshore velocity, stratification, and surface density (Fig. 4.5). The cross-shelf wind displayed the highest correlations with the cross-shelf velocity followed by moderate correlations with the alongshelf velocity as well as density stratification. The alongshelf wind in contrast only showed correlations with the alongshelf plume velocity. However, this analysis does not take into account lagged relationships or the dominant timescales of forcing variability, which may show additional patterns regarding river plume response to environmental conditions.

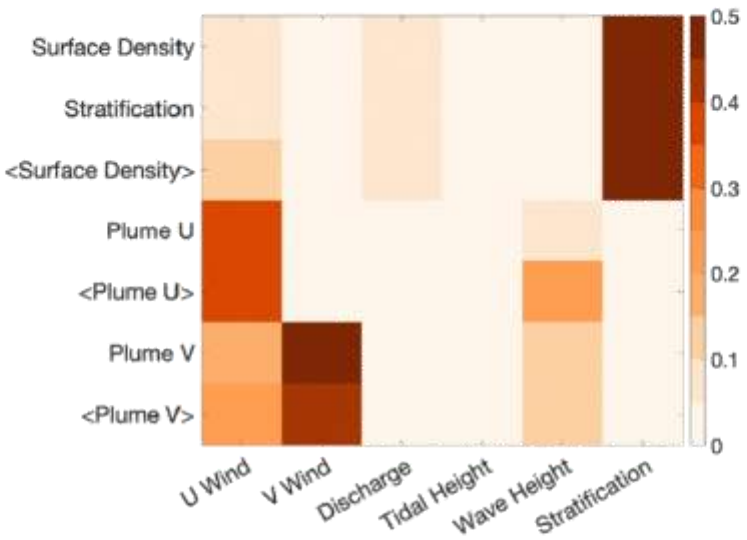

Figure 4.5 The squared linear correlation coefficient (r^2) evaluated between river plume forcing variables (x-axis) and response variables (y-axis). The brackets (< >) denote the use of a tidal filter.

4.4.4 Relation between wind and circulation

The water column velocity was strongly related to wind variability, with differing responses based on the wind direction and stratification. The predominate SW wind direction is directed offshore from the Tukituki River and occurred frequently during the deployment. During SW winds,

surface intensified cross-shore velocity was observed (Fig. 4.2e), and the alongshore velocity was generally two-layer with the surface flowing northward and at depth flowing southward.

During onshore (NE) winds, the offshore directed plume transport was absent in the cross-shore direction and flow was landward. The alongshore flow was northward (when the wind had a slight northward component), likely due to the wind orientation relative to the coastline and showed increased surface shear in comparison to the cross-shore structure, with density stratification still present. The largest decreases in bed density occurred during onshore winds.

One alongshore northward wind (downwelling) event occurred which showed barotropic northward flow and landward cross-shore flow. The plume was likely transported northward away from the mooring location as no stratification was observed. Alongshore southward (upwelling) winds show the surface plume deflecting offshore and to the right, with baroclinic structure observed in both the cross-shore and alongshore directions.

4.4.5 Plume mixing

The vertical structure was used to identify periods of increased mixing throughout the water column and how mixing was related to the interplay of stratification and wind variability. The intensity of turbulence was quantified through the shear squared, the vertical shear of horizontal velocity, defined as $S^2 = (\frac{\partial u}{\partial z})^2 + (\frac{\partial v}{\partial z})^2$. Stresses at the surface and bed drive vertical shear that mix of momentum and buoyancy dependent on the stratification. The surface and bottom boundary layer thicknesses can be described by a critical Ekman thickness which is the depth that mixing from Ekman transport can reach (Lentz and Fewings 2012), which is defined for stratified regions as $\delta = Cu_*/\sqrt{Nf}$ (Moulten et al. 2023). Here C is a constant (1.5), N is the Brunt–Väisälä frequency, and the friction velocity u_* is calculated from the bed and surface shear stress as $u_* = \sqrt{\tau/\rho_0}$. The balance between shear and stratification is represented by the Richardson number, defined as $Ri = g'\rho_z/\rho_0 u_z^2$.

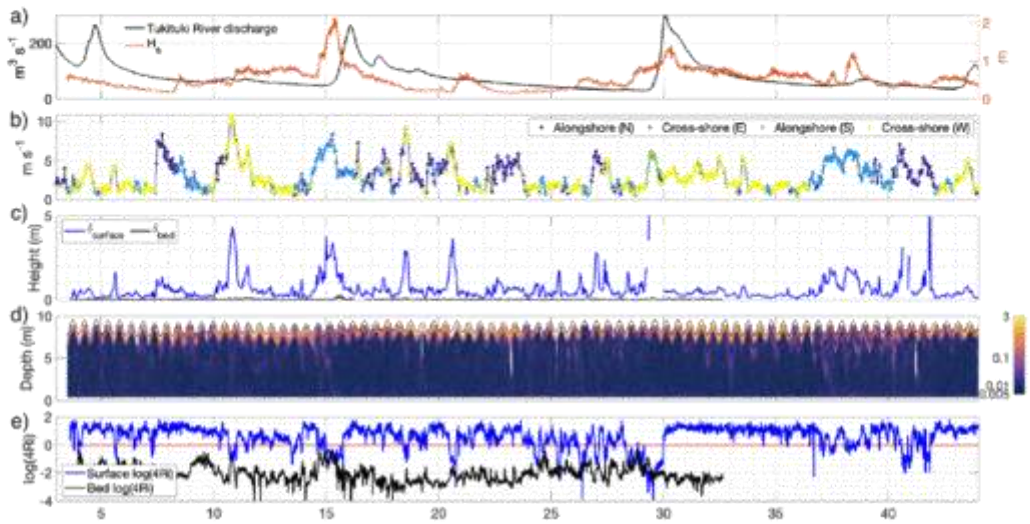

Figure 4.6 Timeseries of mixing related values. a) Tukituki River discharge (black) and significant wave height (orange). b) Wind speed and direction (right axis). c) Critical Ekman depth (m) for the surface (blue) and bottom (black). d) Shear-squared velocity (s^{-2}). e) Richardson number evaluated at the surface (between 0.35 and 1.7 m from the surface) and the closer to the bed (between 5 and 8.2 m from the surface).

The estimated critical Ekman depth at the surface over the deployment ranges from 0.2–4 m below the water surface, with wind events over 1–2-day time frames increasing the depth (Fig. 4.6c). The shear-squared consistently shows highest values in the upper 1 m of the water column (Fig. 4.6d) either at the top of the measured region or ~0.5 m below, with maximum values between 0.5–3 s^{-2} at the surface, and typical values at depth less than 0.03 s^{-2}. Enhanced shear-squared commonly propagates downward into the water column following ebb tide and reaches the bed on few occasions.

The balance between turbulent mixing and stratification is assessed through the Richardson number calculated at the surface and bed (Fig. 4.6e) and compared with an established threshold of stability of 0.25 (Horner-Devine et al. 2015). The average surface Ri is 2.4 indicating predominately stable stratification that is frequently interrupted throughout the deployment, while the average bed Ri is 0.005 and does not exceed the stability threshold during the deployment. The periods of surface Ri<0.25 directly correspond with periods of increased δ_s related to increased wind speeds. These periods show decreased magnitudes of surface S^2 but with S^2 elevated downward through the water column. The decreased magnitude of S^2 is likely due to the reduction in stratification and buoyancy induced shear flow.

4.5 Discussion

The observed circulation patterns at the mooring location were primarily dependent on 1) the river inlet geometry, 2) the river discharge magnitude, and 3) the wind speed and direction. In

particular, the wind variability impacted the cross and alongshelf velocity structure and altered the stratification variability significantly over the deployment. In this section, the response of the vertical structure of velocity, density, and mixing to varying winds is further quantified and compared to previous studies.

4.5.1 Characterizing the wind response

The average response of the velocity profiles to the four wind directions is assessed by averaging vertical profiles over the entire deployment period (Fig. 4.7). The cross-shelf velocity (Fig. 4.7a) shows the greatest offshore directed surface magnitude during offshore winds followed by upwelling winds, and weak offshore surface flow during downwelling winds. During onshore winds, the average surface velocity is landward. At depth (5–6 m from the bed), the average cross-shore velocity is landward for all wind directions with weak speeds. The alongshore winds drive the highest surface alongshore velocities in their respective directions, while offshore wind drives a surface northward velocity and onshore wind drives a surface southward velocity (Fig. 4.7b). The average of the subtidal velocities showed similar patterns as Fig. 4.7.

These results are similar to previous studies that documented increased cross-shore plume velocity during upwelling and downwelling winds (Fong and Geyer 2001, Horner Devine et al. 2015). However, the greatest offshore directed flow occurs during offshore winds on average, which has not been commonly reported (Horner-Devine et al. 2015). Given that the mooring location recorded the near-field plume for roughly half of the deployment, signifying a time-variation of the Rossby number, it is likely that during times where inertia dominates (in the near-field plume), the cross-shelf velocity is less prone to Ekman dynamics and cross-shelf winds can enhance the cross-shelf plume velocity.

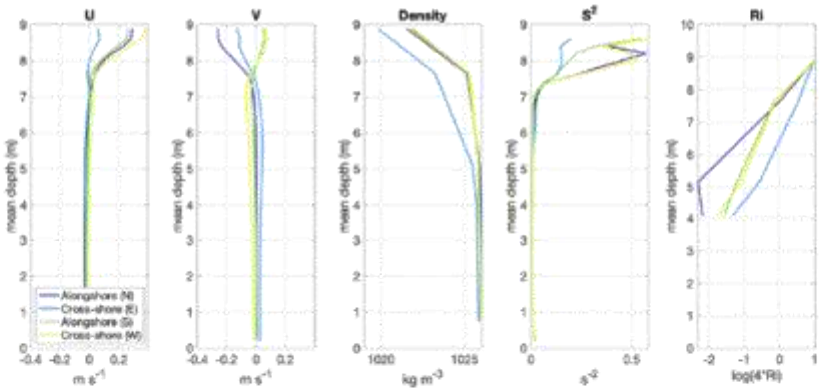

Figure 4.7 Average velocity profiles with to respect to wind direction over the entire deployment. The wind directions are relative to the coastline orientation (shown in Fig 4.2). The y-axis plots the mean depth (m) of the sigma coordinates.

Density profiles are similar for all wind directions with high stratification at the surface, except for onshore winds which show lower density at the surface CTD and throughout the water column (Fig. 4.7c). Closer inspection of the variability between onshore winds and density (Fig. 4.2) shows that density decreases with depth and the plume thickness increases (Fig. 4.7c). Shear-squared profiles show the largest surface shear during offshore and upwelling winds, with lower magnitudes during downwelling and onshore winds (Fig. 4.7d). The mean profiles of Ri show upper water column stable stratification for all wind directions, with higher values at depth again seen for onshore winds (Fig. 4.7e).

4.5.2 Mixing response

The highest shear conditions during the deployment occurred when magnitude of cross-shore plume velocity is the strongest, which corresponded to times of offshore and upwelling winds. The variation of the Richardson number also varies with the wind conditions but does not solely vary with the wind speed or the shear intensity, as the near-surface Ri shows scatter when directly compared with the Ekman depth for Ri values less than 0.25, and additionally does not show a clear relation with wind direction (Fig. 4.8).

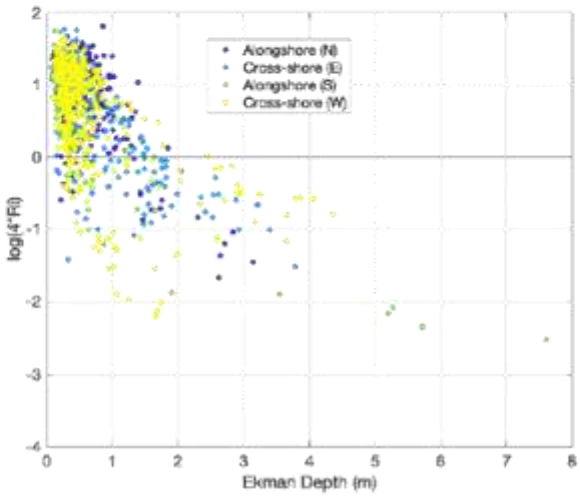

Figure 4.8 The calculated surface Ekman depth (m) compared with the Richardson number (near-surface), coloured by wind direction.

4.5.3 Cross-shore sediment transport

The upper water column suspended sediment concentration ranged from 5-125 mg l^{-1} and was primarily related to variability in the river discharge, while the near bed suspended sediment concentration varied on the order of 1000's of mg l^{-1} and was related to both the river discharge and wave variability (Fig. 4.9a,b). The impact of the observed cross-shelf circulation on the sediment

transport is assessed by comparison with the raw echo magnitude (Fig. 4.9c), the measured SSC values throughout the water column (Fig. 4.9d), and the computed cross-shelf sediment flux at three locations in the water column (Fig. 4.9e,f). In the surface plume layer, the SSC is highly episodic, linked with variations in the river discharge, and is small during non-event time periods. The discharge event on day 16 recorded the highest SSC values at the mooring while the day 4 and day 30 discharge events reached much smaller fractions of the river SSC (~40 mg l^{-1}).

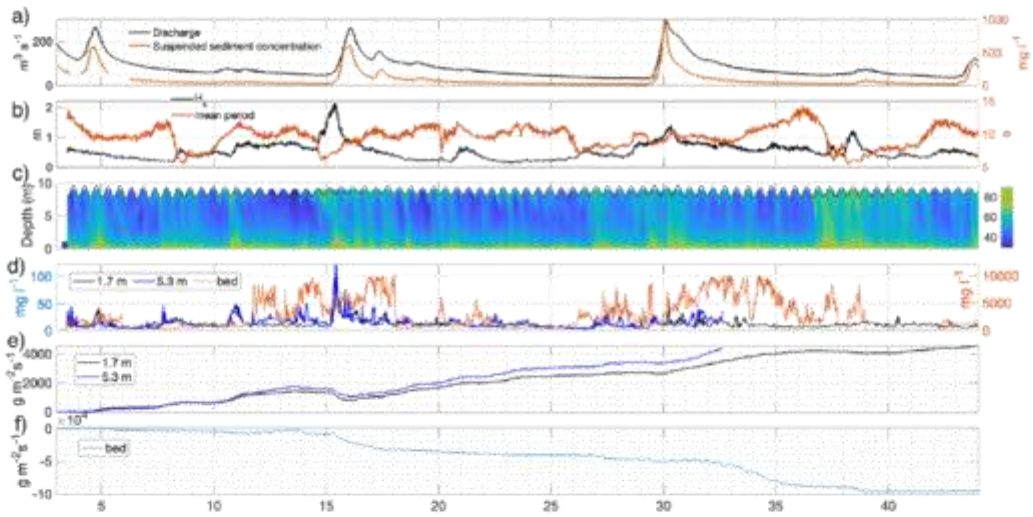

Figure 4.9 Timeseries of suspended sediment concentration and sediment fluxes. a) Tukituki river discharge and suspended sediment concentration. b) Significant wave height and period. c) Echo magnitude (from 0 to 100). d) Suspended sediment concentrations (mg l^{-1}, note that the bed measurement is on the right axis). e) The cumulative near surface cross-shelf sediment fluxes (g $m^{-2}s^{-1}$) and f) the cumulative near bed cross-shelf sediment flux (g $m^{-2}s^{-1}$).

Elevated surface SSC values are followed by subsurface increases in echo intensity (Fig. 4.9c) indicating sediment deposition to the bed. High echo intensity is present from the bed throughout the deployment, which elevates through the water column during increases in wave height. The cumulative cross-shore sediment fluxes for the surface layers show offshore directed transport for the deployment apart from the discharge event on day 16 when onshore winds directed the surface layer landward.

In contrast, the cross-shore transport at the bed was landward for the entire deployment (Fig. 4.9f) and the flux magnitude was an order of magnitude greater than the cross-shore surface flux. For all wind directions, the average near bed cross-shelf velocity is landward (Fig. 4.7a), while the average near bed alongshelf velocity is strongest for cross-shore winds; southward for offshore winds and northward for onshore winds (Fig. 4.7b). Previous work suggests that muddy deposits are

primarily located greater than 10 m depth (White 1994). The circulation at the mooring location suggests that suspended sediment is consistently transported landward at depth, and north or south depending on the water column circulation. Given that the predominant wind direction is offshore which induces a southward alongshore current (Fig. 4.7b), sediment is likely transported southward for a majority of the time.

4.5.4 Scale dependence of river plume

The Tukituki River has smaller time and space scales than the majority of river plumes investigated elsewhere (Horner-Devine et al. 2015, MacCready et al. 2010, Hetland 2010). Smaller plumes have been shown to be less impacted by rotation (Cole et al. 2019), impacted by tidal processes (Basdurak et al. 2020, Spicer et al. 2021), and potentially be influenced by cross-shore winds (Kakoulaki et al. 2014). In this study, radial plumes are observed in satellite imagery with no bulge formation and there was no alongshelf oriented tidal modulation of a low discharge (~10 $m^3 s^{-1}$) river plume as in Basdurak et al. (2020).

Here, oceanward cross-shore winds were found to impact the cross-shelf velocity structure throughout the deployment in addition to upwelling winds, suggesting that the Tukituki River plume may be an intermediate sized river plume with unique characteristics. It is likely that the measurements collected here reflect the time varying properties of the near-field and midfield plume where rotation has varying magnitudes of relative importance. However, these measurements also signify that cross-shore winds, in particular oceanward directed winds, can accelerate the river plume oceanward at speeds greater than during upwelling winds. In addition, the magnitude of shear-squared observed here is relatively high in comparison to reported values from other river plumes, with values measured here of 0.5-3 s^{-2}. Horner-Devine et al. (2015) reports high shear values in the near-field plume on the order of 1 s^{-2}. It would be beneficial for future studies to integrate these results into a river plume classification to add to the existing classification performed by Horner-Devine et al. (2015).

4.6 Conclusion

A deployment offshore of the Tukituki River captured a large range of conditions including multiple discharge events, wind events from a range of directions, and moderate swell conditions. The instrument location was positioned in the near-field river plume for roughly half of the time which is a region of the river plume that has not been sampled comprehensively in past studies. Satellite imagery revealed that the inlet morphology substantially varied over the deployment period which influenced the directionality of the near-field river plume.

The response to varying wind magnitude and direction was characterised in terms of the vertical structure of velocity, stratification, and intensities of shear-driven mixing. Variations in the

wind direction resulted in distinct vertical profiles of cross-shore and alongshore velocity, with similar results as compared with previous studies for upwelling and downwelling winds, but with stronger than expected relations with onshore and offshore winds. The shear-driven mixing of the river plume was found to be strongly related to the wind stress. Finally, the impact of the cross-shelf circulation on the cross-shelf sediment transport was assessed through computing fluxes throughout the water column. It was found that throughout the deployment period the upper water column transported river derived sediment oceanward, but at near the bed, high landward transport of sediment occurred due to the high sediment concentrations found there due to resuspension combined with the persistent landward near bed flow. Together, these results add a conceptual framework for small mountainous river systems and the sediment transport resultant from river plume circulation.

Chapter 5: General Conclusions

5.1 Main findings of thesis

This thesis set out to describe the dynamics of small mountainous river plumes and detail how suspended sediment from these rivers is transited across the inner shelf on multiple spatial scales, from observations of the near-field plume of the Tukituki River to Bay-wide remote sensing observations, and time scales, from individual discharge events to multi-year periods. Particular emphasis was placed on understanding the drivers of river plume variability, including directionality, mixing, and the transport of suspended sediment. The thesis determined the main drivers of circulation and sediment transport patterns in Hawke Bay, as well as provided globally-relevant information regarding small mountainous river plume circulation, mixing, and the transport of suspended sediment across the inner shelf.

The thesis combined multiple different methodologies with datasets, including the wealth of spatiotemporal information available from satellite remote sensing (Chapter 2), detailed information from numerical ocean modelling (Chapter 3), and highly detailed observations of these processes (Chapter 4). These methods produced new insights regarding **1.** circulation in Hawke Bay, **2.** suspended sediment transport from small mountainous river plumes, and **3.** the relation between wind and plume dynamics in small mountainous river plumes, as elucidated in more detail below.

1. Hawke Bay circulation

The circulation in Hawke Bay was found to be heavily influenced by buoyancy input from rivers (Chapter 1), creating density stratification over broad regions of the Bay, with commonly outward-directed radial plumes and buoyancy-driven coastal currents that generally occur in the northern Bay (Fig. 5.1). Similar to past estimates of circulation (e.g. Ridgeway and Stanton 1969), outflow occurs on average at each headland of the Bay (Fig. 5.1), although no strong inflow in the middle of the Bay is observed as was previously suggested (Ridgeway and Stanton 1969). The Wairarapa coastal current is present offshore of the Bay throughout the year, allowing cooler, denser water (relative to the East Cape Current) to be transported into the Bay. The time dependent circulation in the Bay is heavily dependent on wind conditions and the river discharge. Throughout the nearshore of the Bay, the alongshore velocity patterns were driven primarily by wind forcing, while cross-shore velocity was more influenced by buoyancy input from rivers.

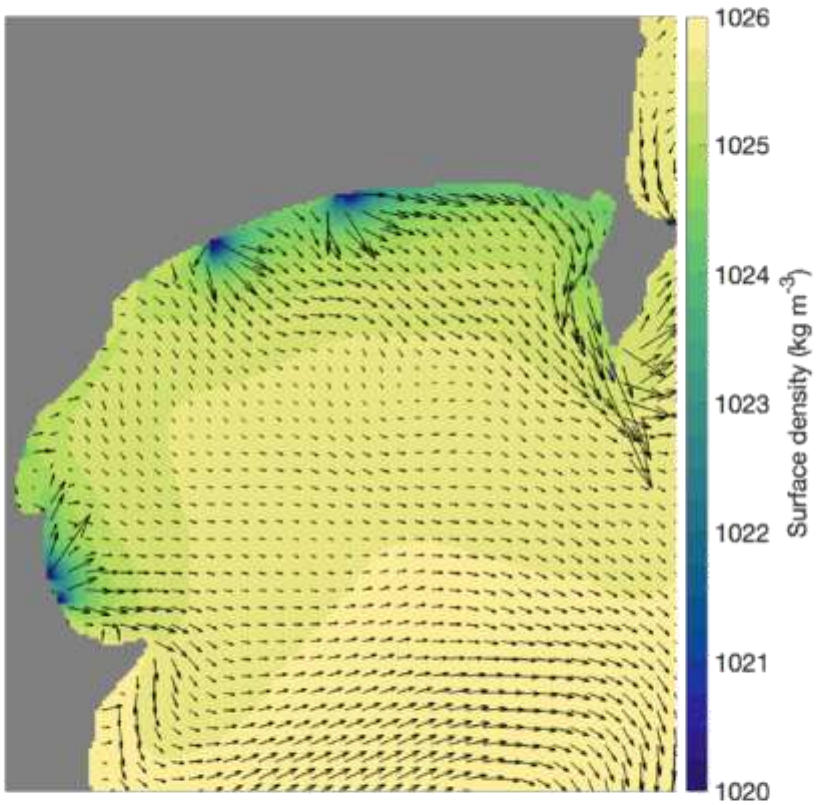

Figure 5.1 The mean surface density and circulation from 2017 to 2019. Mean surface density (coloured; kg m^{-3}) and surface currents (black arrows) in Hawke Bay from 2017 to 2019.

2. Sediment transport in Hawke Bay

The sediment transport in Hawke Bay is initially driven by surface advection from river plumes, with common length scales of surface transport ranging from 2 to 6 km from river inlets, determined from remote sensing (Fig. 5.2). The surface sediment concentration was found to be most linked to temporal variations in river discharge, with secondary impacts from wave resuspension. Wind is important for directing river plumes and was not shown to impact sediment resuspension at the surface. Similar to studies on other rivers, a strong dependence of transport distances on varying particle sizes was found (e.g. Geyer et al. 2004). Fine silt and clay sediments were found to be dispersive throughout the Bay, while coarse silt and aggregated material was only able to be transported a few kilometers from the river mouths through river plumes.

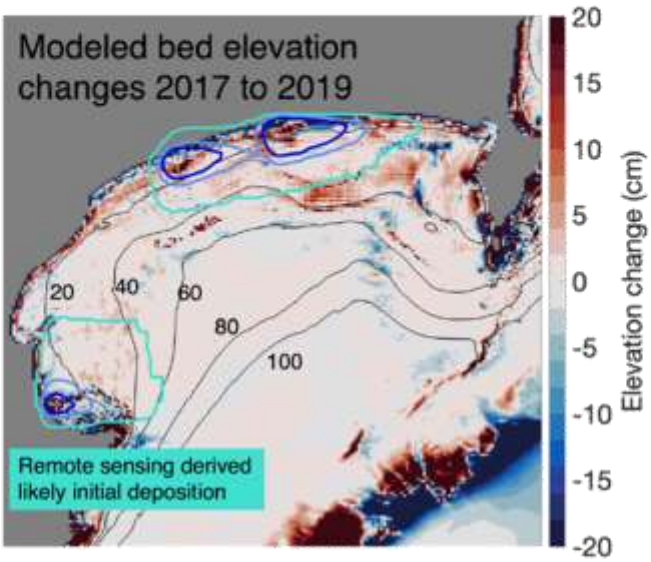

Figure 5.2 The bed sediment deposition from the numerical model (cm) over the period of 2017 to 2019. Depth contours are shown in 20 m intervals. In blue contours, the probabilities of occurrence of the 5 mg l^{-1}TSS value are shown, sourced from Chapter 2.

While sediment from the rivers can settle nearshore if there are small wave heights, the bed stress in the nearshore commonly exceeds thresholds for fine sediment resuspension. Discharge events were shown to produce deposition rates in the range of 1 to 10 cm, however, most fine sediment was transported to depths greater than 40 m over longer time periods. For example, the regions of likely initial sediment deposition (Chapter 2) are broadly representative of longer term sediment accumulation regions (Chapter 3) in offshore depths outside areas of high bed stress. Measurements from offshore of the Tukituki River (Chapter 4) highlight that the near bed velocity is often flowing landward, in opposition to the surface plume layer, which can transport sediment sourced from river plumes and resuspended sediment landward.

3. River plume relation with wind variability

Wind was found to set river plume directionality and is an important component for river plume mixing throughout the Bay, observed from remote sensing, observations, and numerical modelling. The dominant wind direction is from the SW, although the wind displays a broad range of directionality (Fig 5.3), and due to the varying coastline orientation at the major river inlets (Fig. 5.3), a wind direction that is directed offshore in the southern region of the Bay would be directed along the coastline towards the Mahia Peninsula for the northern region, for example. From the remote sensing results (Chapter 2) and the numerical model (Fig. 5.3; Chapter 3), river plumes transport was shown to correspond linearly with wind directions, and the buoyancy flux varied with wind speed (Chapter

3). Offshore of the Tukituki River, the observations (Chapter 4) showed distinct responses of the cross-shore and alongshore velocity profiles, stratification, and mixing to upwelling, downwelling, and cross-shelf winds. The vertical structure observed in the Tukituki River plume is likely found throughout the other rivers in the Bay, but with different probabilities of occurrence due to the varying coastline orientation throughout the Bay.

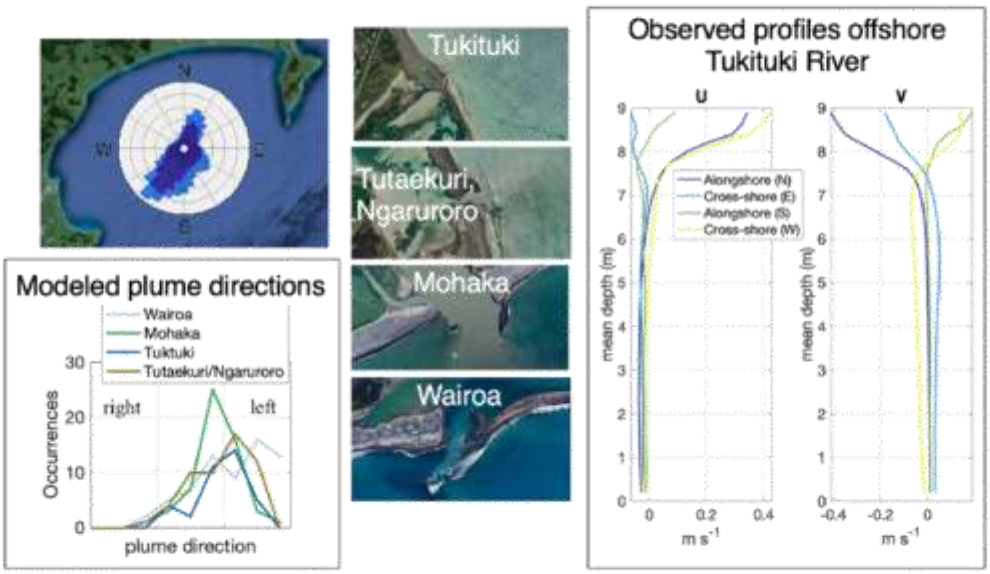

Figure 5.3 The relation between wind and river plume characteristics throughout Hawke Bay. The upper left shows the wind rose from Napier Airport, the bottom left shows modelled river plume directions. The middle panels show the major rivers inlet orientations, and the right plot shows the observed vertical profiles of cross-shore and alongshore velocity in relation to varying wind directions as measured offshore of the Tukituki River.

5.2 Limitations of current work

This thesis used multiple methodologies to take advantage of differing approaches, although each methodology has limitations related either the method itself or the feasibility to be completed during this thesis. The remote sensing analysis would benefit from a TSS algorithm that was created with observations that included a higher range of TSS, as the model shows that the surface SSC can be in range the hundreds of mg l^{-1} during discharge events.

The numerical model showed that the sediment size is a key determinant in setting transport distances from rivers. However, the grain sizes used in Chapter 3 represent the best estimate of characteristic particle sizes in the Bay based on limited measurements. Additional measurements on grain size in rivers, in the Bay, and observations of aggregated particles would add certainty in determining transit patterns from rivers. Additionally, the numerical model simulated river outflows as point sources to the coastal ocean and did not resolve the dynamics of estuaries. This likely induced

greater fresh water delivery to the coast than in nature at times when there is a salt intrusion into the estuaries. The model also did not accurately simulate the momentum flux from rivers as the inlet width is typically much smaller than the model grid size of 500 m. This additions would make the numerical model more realistic but likely would not change the main conclusions of this thesis, as these are derived from multiple lines of evidence.

5.3 Relevance of thesis

Both the terrestrial and marine environment of the Hawkes Bay region can be severely impacted by flood events as exemplified by the devastating effects of Cyclone Gabrielle in 2023, showing the importance of understanding the underlying circulation and sediment transport patterns in small mountainous river systems. The knowledge base generated by this thesis will help inform management strategies and the potential threat to marine ecosystems from sediment loading and seafloor disturbance during discharge events. Locally, this thesis added substantially to our understanding of the characteristics of coastal processes in Hawke Bay, but also informed understanding of small mountainous river systems globally, the characterisation of surface sediment transport from river plumes from remote sensing, and relations between varying wind directions and river plume vertical structure.

References

Albuquerque, J., Antolínez, J.A., Gorman, R.M., Méndez, F.J. and Coco, G., 2021. Seas and swells throughout New Zealand: A new partitioned hindcast. Ocean Modelling, 168, p.101897.

Atkin, E., 2022. Report of Survey: Tukituki River and Entrance. eCoast report prepared for the University of Waikato and the Hawkes Bay Regional Council.

Aurin, D., Mannino, A. and Franz, B., 2013. Spatially resolving ocean color and sediment dispersion in river plumes, coastal systems, and continental shelf waters. Remote Sensing of Environment, 137, pp.212-225.

Basdurak, N.B., Largier, J.L. and Nidzieko, N.J., 2020. Modeling the dynamics of small-scale river and creek plumes in tidal waters. Journal of Geophysical Research: Oceans, 125(7), p.e2019JC015737.

Bever, A.J., McNinch, J.E. and Harris, C.K., 2011. Hydrodynamics and sediment-transport in the nearshore of Poverty Bay, New Zealand: Observations of nearshore sediment segregation and oceanic storms. Continental Shelf Research, 31(6), pp.507-526.

Bever, A.J. and Harris, C.K., 2014. Storm and fair-weather driven sediment-transport within Poverty Bay, New Zealand, evaluated using coupled numerical models. Continental Shelf Research, 86, pp.34-51.

Bostock, H., Jenkins, C., Mackay, K., Carter, L., Nodder, S., Orpin, A., Pallentin, A. and Wysoczanski, R., 2019. Distribution of surficial sediments in the ocean around New Zealand/Aotearoa. Part B: continental shelf. New Zealand Journal of Geology and Geophysics, 62(1), pp.24-45.

Booij, N.R.R.C., Ris, R.C. and Holthuijsen, L.H., 1999. A third-generation wave model for coastal regions: 1. Model description and validation. Journal of geophysical research: Oceans, 104(C4), pp.7649-7666.

Bradford, J.M., 1980. Hydrology, plankton and nutrients in Hawke Bay, September 1976. New Zealand Oceanographic Institute.

Chappell, P.R. 2013. The climate and weather of Hawke's Bay. NIWA Science and Technology Series 58, 44 pp.

Chiswell, S.M., 2002. Wairarapa coastal current influence on sea surface temperature in Hawke Bay, New Zealand. New Zealand Journal of Marine and Freshwater Research, 36(2), pp.267-279.

Cole, K.L. and Hetland, R.D., 2016. The effects of rotation and river discharge on net mixing in small-mouth Kelvin number plumes. Journal of Physical Oceanography, 46(5), pp.1421-1436.

Constantin, S., Doxaran, D., Derkacheva, A., Novoa, S. and Lavigne, H., 2018. Multi-temporal dynamics of suspended particulate matter in a macro-tidal river Plume (the Gironde) as observed by satellite data. Estuarine, Coastal and Shelf Science, 202, pp.172-184.

de Souza, J.M., Suanda, S.H., Couto, P.P., Smith, R.O., Kerry, C. and Roughan, M., 2022. Moana Ocean Hindcast–a 25+ years simulation for New Zealand Waters using the ROMS v3. 9 model. EGUsphere, 2022, pp.1-34.

Dogliotti, A.I., Ruddick, K. and Guerrero, R., 2016. Seasonal and inter-annual turbidity variability in the Río de la Plata from 15 years of MODIS: El Niño dilution effect. Estuarine, Coastal and Shelf Science, 182, pp.27-39.

Eyles, G. and Fahey, B., 2006. The Pakuratahi land use study. Hawkes Bay Regional Council Report 3861.

Feng, L., Hu, C. and Li, J., 2018. Can MODIS land reflectance products be used for estuarine and inland waters?. Water Resources Research, 54(5), pp.3583-3601.

Fong, D.A. and Geyer, W.R., 2001. Response of a river plume during an upwelling favorable wind event. Journal of Geophysical Research: Oceans, 106(C1), pp.1067-1084.

Gangloff, A., Verney, R., Doxaran, D., Ody, A. and Estournel, C., 2017. Investigating Rhône River plume (Gulf of Lions, France) dynamics using metrics analysis from the MERIS 300m Ocean Color archive (2002–2012). Continental shelf research, 144, pp.98-111.

Gerbi, G.P., Chant, R.J. and Wilkin, J.L., 2013. Breaking surface wave effects on river plume dynamics during upwelling-favorable winds. Journal of physical oceanography, 43(9), pp.1959-1980.

Geyer, W.R., Hill, P., Milligan, T. and Traykovski, P., 2000. The structure of the Eel River plume during floods. Continental Shelf Research, 20(16), pp.2067-2093.

Geyer, W.R., Hill, P.S. and Kineke, G.C., 2004. The transport, transformation and dispersal of sediment by buoyant coastal flows. Continental Shelf Research, 24(7-8), pp.927-949.

Godoi, V.A., Bryan, K.R. and Gorman, R.M., 2016. Regional influence of climate patterns on the wave climate of the southwestern Pacific: The New Zealand region. Journal of Geophysical Research: Oceans, 121(6), pp.4056-4076.

Grabowski, R.C., Droppo, I.G. and Wharton, G., 2011. Erodibility of cohesive sediment: The importance of sediment properties. Earth-Science Reviews, 105(3-4), pp.101-120.

Haidvogel, D.B., Arango, H., Budgell, W.P., Cornuelle, B.D., Curchitser, E., Di Lorenzo, E., Fennel, K., Geyer, W.R., Hermann, A.J., Lanerolle, L. and Levin, J., 2008. Ocean forecasting in terrain-following coordinates: Formulation and skill assessment of the Regional Ocean Modeling System. Journal of computational physics, 227(7), pp.3595-3624.

Hale, R.P. and Ogston, A.S., 2015. In situ observations of wave-supported fluid-mud generation and deposition on an active continental margin. Journal of Geophysical Research: Earth Surface, 120(11), pp.2357-2373.

Harris, C.K., Sherwood, C.R., Signell, R.P., Bever, A.J. and Warner, J.C., 2008. Sediment dispersal in the northwestern Adriatic Sea. Journal of Geophysical Research: Oceans, 113(C11).

Hersbach, H., Bell, B., Berrisford, P., Hirahara, S., Horányi, A., Muñoz-Sabater, J., Nicolas, J., Peubey, C., Radu, R., Schepers, D. and Simmons, A., 2020. The ERA5 global reanalysis. Quarterly Journal of the Royal Meteorological Society, 146(730), pp.1999-2049.

Hetland, R.D., 2005. Relating river plume structure to vertical mixing. Journal of Physical Oceanography, 35(9), pp.1667-1688.

Hetland, R.D. and Hsu, T.J., 2013. Freshwater and sediment dispersal in large river plumes. Biogeochemical Dynamics at Large River-Coastal Interfaces: Linkages with Global Climate Change, edited by: Bianchi, TS, Allison, MA, and Cai, W.-J., Springer, New York, USA, pp.55-85.

Hickey, B.M., Kudela, R.M., Nash, J.D., Bruland, K.W., Peterson, W.T., MacCready, P., Lessard, E.J., Jay, D.A., Banas, N.S., Baptista, A.M. and Dever, E.P., 2010. River influences on shelf ecosystems: introduction and synthesis. Journal of Geophysical Research: Oceans, 115(C2).

Hicks, D.M., Shankar, U., McKerchar, A.I., Basher, L., Lynn, I., Page, M. and Jessen, M., 2011. Suspended sediment yields from New Zealand rivers. Journal of Hydrology (New Zealand), pp.81-142.

Hill, P.S., Milligan, T.G. and Geyer, W.R., 2000. Controls on effective settling velocity of suspended sediment in the Eel River flood plume. Continental shelf research, 20(16), pp.2095-2111.

Horner-Devine, A.R., Hetland, R.D. and MacDonald, D.G., 2015. Mixing and transport in coastal river plumes. Annual Review of Fluid Mechanics, 47, pp.569-594.

Hunter, E.J., Chant, R.J., Wilkin, J.L. and Kohut, J., 2010. High-frequency forcing and subtidal response of the Hudson River plume. Journal of Geophysical Research: Oceans, 115(C7).

Kakoulaki, G., MacDonald, D. and Horner-Devine, A.R., 2014. The role of wind in the near field and midfield of a river plume. Geophysical Research Letters, 41(14), pp.5132-5138.

Kerry, C., Roughan, M. and De Souza, J., 2023. Characterising the variability of boundary currents and ocean heat content around New Zealand using a multi-decadal high-resolution regional ocean model. Journal of Geophysical Research: Oceans, p.e2022JC018624.

Kirk, J.T., 1994. Light and photosynthesis in aquatic ecosystems. Cambridge university press.

Kniskern, T.A., Kuehl, S.A., Harris, C.K. and Carter, L., 2010. Sediment accumulation patterns and fine-scale strata formation on the Waiapu River shelf, New Zealand. Marine Geology, 270(1-4), pp.188-201.

Komar, P.D., 2010. Shoreline evolution and management of Hawke's Bay, New Zealand: tectonics, coastal processes, and human impacts. Journal of Coastal Research, 26(1 (261)), pp.143-156.

Kuehl, S.A., Alexander, C.R., Blair, N.E., Harris, C.K., Marsaglia, K.M., Ogston, A.S., Orpin, A.R., Roering, J.J., Bever, A.J., Bilderback, E.L. and Carter, L., 2016. A source-to-sink perspective of the Waipaoa River margin. Earth-Science Reviews, 153, pp.301-334.

Kumar, N. and Feddersen, F., 2017. The effect of Stokes drift and transient rip currents on the inner shelf. Part II: With stratification. Journal of Physical Oceanography, 47(1), pp.243-260.

Kumar, N., Feddersen, F., Suanda, S., Uchiyama, Y. and McWilliams, J., 2016. Mid-to inner-shelf coupled ROMS–SWAN model–data comparison of currents and temperature: Diurnal and semidiurnal variability. Journal of Physical Oceanography, 46(3), pp.841-862.

Lee, Z., Pahlevan, N., Ahn, Y.H., Greb, S. and O'Donnell, D., 2013. Robust approach to directly measuring water-leaving radiance in the field. Applied Optics, 52(8), pp.1693-1701.

Lehmann, M.K., Gurlin, D., Pahlevan, N., Alikas, K., Conroy, T., Anstee, J., Balasubramanian, S.V., Barbosa, C.C., Binding, C., Bracher, A. and Bresciani, M., 2023. GLORIA-A globally representative hyperspectral in situ dataset for optical sensing of water quality. Scientific Data, 10(1), p.100.

Lemagie, E. and Lerczak, J., 2020. The evolution of a buoyant river plume in response to a pulse of high discharge from a small midlatitude river. Journal of Physical Oceanography, 50(7), pp.1915-1935.

Lentz, S.J. and Fewings, M.R., 2012. The wind-and wave-driven inner-shelf circulation. Annual review of marine science, 4, pp.317-343.

Many, G., Bourrin, F., de Madron, X.D., Ody, A., Doxaran, D. and Cauchy, P., 2018. Glider and satellite monitoring of the variability of the suspended particle distribution and size in the Rhône ROFI. Progress in oceanography, 163, pp.123-135.

McKee, B.A., Aller, R.C., Allison, M.A., Bianchi, T.S. and Kineke, G.C., 2004. Transport and transformation of dissolved and particulate materials on continental margins influenced by major rivers: benthic boundary layer and seabed processes. Continental Shelf Research, 24(7-8), pp.899-926.

McSweeney, S.L., Kennedy, D.M., Rutherfurd, I.D. and Stout, J.C., 2017. Intermittently Closed/Open Lakes and Lagoons: Their global distribution and boundary conditions. Geomorphology, 292, pp.142-152.

Milligan, T.G., Hill, P.S. and Law, B.A., 2007. Flocculation and the loss of sediment from the Po River plume. Continental Shelf Research, 27(3-4), pp.309-321.

Milliman, J.D. and Syvitski, J.P., 1992. Geomorphic/tectonic control of sediment discharge to the ocean: the importance of small mountainous rivers. The journal of Geology, 100(5), pp.525-544.

Moghimi, S., Özkan-Haller, H.T., Akan, Ç. and Jurisa, J.T., 2019. Mechanistic analysis of the wave-current interaction in the plume region of a partially mixed tidal inlet. Ocean Modelling, 134, pp.110-126.

Moriarty, J.M., Harris, C.K. and Hadfield, M.G., 2015. Event-to-seasonal sediment dispersal on the Waipaoa River Shelf, New Zealand: A numerical modeling study. Continental Shelf Research, 110, pp.108-123.

Moulton, M., Suanda, S.H., Garwood, J.C., Kumar, N., Fewings, M.R. and Pringle, J.M., 2023. Exchange of plankton, pollutants, and particles across the nearshore region. Annual Review of Marine Science, 15, pp.167-202.

Murphy, A.H., 1988. Skill scores based on the mean square error and their relationships to the correlation coefficient. Monthly weather review, 116(12), pp.2417-2424.

Nechad, B., Dogliotti, A., Ruddick, K. and Doxaran, D., 2016, May. Particulate backscattering and suspended matter concentration retrieval from remote-sensed turbidity in various coastal and riverine turbid waters. In Living Planet Symposium, Proceedings of the conference held (pp. 9-13).

Norris, T., 2019. Sediment monitoring using automatic ISCO samplers for State of the Environment reporting in Hawke's Bay. Report from the Hawkes Bay Regional Council. HBRC Report No. RM19-245-5398.

O'Callaghan, J., 2019. Spatial mapping of subsurface oxygen depletion in Hawke Bay. NIWA client report number 2019213WN.

O'Callaghan, J.M. and Stevens, C.L., 2017. Evaluating the surface response of discharge events in a New Zealand Gulf-ROFI. Frontiers in Marine Science, 4, p.232.

Olabarrieta, M., Warner, J.C. and Kumar, N., 2011. Wave-current interaction in Willapa Bay. Journal of Geophysical Research: Oceans, 116(C12).

Pantin, H.M., 1966. Sedimentation in Hawke Bay No. Bulletin 171 New Zealand Department of Science and Industrial Research.

Pawlowicz, R., Di Costanzo, R., Halverson, M., Devred, E. and Johannessen, S., 2017. Advection, surface area, and sediment load of the Fraser River plume under variable wind and river forcing. Atmosphere-Ocean, 55(4-5), pp.293-313.

Paquet, F., Proust, J.N., Barnes, P.M. and Pettinga, J.R., 2009. Inner-forearc sequence architecture in response to climatic and tectonic forcing since 150 ka: Hawke's Bay, New Zealand. Journal of Sedimentary Research, 79(3), pp.97-124.

Ridgway, N. M., 1960. Surface water movements in Hawke Bay, New Zealand, New Zealand Journal of Geology and Geophysics 3:253-261.

Ridgway N. M. and Stanton B. R., 1969. Some hydrological features of Hawke Bay and nearby shelf waters, New Zealand Journal of Marine and Freshwater Research 3: 545-559

Rodriguez, A.R., Giddings, S.N. and Kumar, N., 2018. Impacts of nearshore wave-current interaction on transport and mixing of small-scale buoyant plumes. Geophysical Research Letters, 45(16), pp.8379-8389.

Rong, Z., Hetland, R.D., Zhang, W. and Zhang, X., 2014. Current–wave interaction in the Mississippi–Atchafalaya river plume on the Texas–Louisiana shelf. Ocean Modelling, 84, pp.67-83.

Saldías, G.S., Sobarzo, M., Largier, J., Moffat, C. and Letelier, R., 2012. Seasonal variability of turbid river plumes off central Chile based on high-resolution MODIS imagery. Remote Sensing of Environment, 123, pp.220-233.

Smolarkiewicz, P.K. and Margolin, L.G., 1998. MPDATA: A finite-difference solver for geophysical flows. Journal of Computational Physics, 140(2), pp.459-480.

Soulsby, R.L. and Whitehouse, R.J., 1997, January. Threshold of sediment motion in coastal environments. In Pacific Coasts and Ports' 97: Proceedings of the 13th Australasian Coastal and Ocean Engineering Conference and the 6th Australasian Port and Harbour Conference; Volume 1 (pp. 145-150). Christchurch, NZ: Centre for Advanced Engineering, University of Canterbury.

Spicer, P., Cole, K.L., Huguenard, K., MacDonald, D.G. and Whitney, M.M., 2021. The effect of bottom-generated tidal mixing on tidally pulsed river plumes. Journal of Physical Oceanography, 51(7), pp.2223-2241.

Stevens, C.L., O'Callaghan, J.M., Chiswell, S.M. and Hadfield, M.G., 2021. Physical oceanography of New Zealand/Aotearoa shelf seas–a review. New Zealand Journal of Marine and Freshwater Research, 55(1), pp.6-45.

Suanda, S.H., Feddersen, F., Spydell, M.S. and Kumar, N., 2018. The effect of barotropic and baroclinic tides on three-dimensional coastal dispersion. Geophysical Research Letters, 45(20), pp.11-235.

Thrush, S.F., Hewitt, J.E., Cummings, V.J., Ellis, J.I., Hatton, C., Lohrer, A. and Norkko, A.J.F.I.E., 2004. Muddy waters: elevating sediment input to coastal and estuarine habitats. Frontiers in Ecology and the Environment, 2(6), pp.299-306.

Traykovski, P., Geyer, W.R., Irish, J.D. and Lynch, J.F., 2000. The role of wave-induced density-driven fluid mud flows for cross-shelf transport on the Eel River continental shelf. Continental shelf research, 20(16), pp.2113-2140.

Walsh, J.P. and Nittrouer, C.A., 2009. Understanding fine-grained river-sediment dispersal on continental margins. Marine Geology, 263(1-4), pp.34-45.

Warner, J.C., Sherwood, C.R., Signell, R.P., Harris, C.K. and Arango, H.G., 2008. Development of a three-dimensional, regional, coupled wave, current, and sediment-transport model. Computers & geosciences, 34(10), pp.1284-1306.

Warrick, J.A., Xu, J., Noble, M.A. and Lee, H.J., 2008. Rapid formation of hyperpycnal sediment gravity currents offshore of a semi-arid California river. Continental Shelf Research, 28(8), pp.991-1009.

White, J.L., 1994. Coastal Processes. Nearshore Suspended Sediment in Hawke Bay. Report to the Hawke Bay Regional Council. Technical Services Department, Hawkes Bay Regional Council, TS, 94(3).

Wright LD, Nittrouer CA., 1995. Dispersal of river sediments in coastal seas: six contrasting cases. Estuaries. Sep;18:494-508.

Wright, L.D., Thom, B.G. and Higgins, R.J., 1980. Wave influences on river-mouth depositional process: examples from Australia and Papua New Guinea. Estuarine and coastal marine science, 11(3), pp.263-277.

Wu, X., Feddersen, F., Giddings, S.N., Kumar, N. and Gopalakrishnan, G., 2020. Mechanisms of Mid-to Outer-Shelf Transport of Shoreline-Released Tracers. Journal of Physical Oceanography, 50(7), pp.1813-1837.

Yu, X., Lee, Z., Shang, Z., Lin, H. and Lin, G., 2021. A simple and robust shade correction scheme for remote sensing reflectance obtained by the skylight-blocked approach. Optics Express, 29(1), pp.470-486.

Assessing the effectiveness of trees for landslide mitigation in Hawke's Bay

Prepared for: Hawke's Bay Regional Council June 2024

Hawkes Bay Regional Council Publication No. 5660

HAWKES BAY
REGIONAL COUNCIL
TE KAUNIHERA Ā-ROHE O TE MATAU-A-MĀUI

ISSN 2703-2051 (Online)
ISSN 2703-2043 (Print)

(06) 835 9200
0800 108 838
Private Bag 6006 Napier 4142
159 Dalton Street . Napier 4110

Environmental Science

Assessing the effectiveness of trees for landslide mitigation in Hawke's Bay

Prepared for: Hawke's Bay Regional Council June 2024

Hawkes Bay Regional Council Publication No. Report number 5660

Reviewed By:

Dr Ashton Eaves – Senior Land Scientist

Approved By:

Sam French – Science Manager

ISSN 2703-2051 (Online)
ISSN 2703-2043 (Print)

Manaaki Whenua
Landcare Research

Assessing the effectiveness of trees for landslide mitigation in Hawke's Bay

Prepared for: Hawke's Bay Regional Council

June 2024

Assessing the effectiveness of trees for landslide mitigation in Hawke's Bay

Contract Report: LC4479

Anatolii Tsyplenkov, Hugh Smith

Manaaki Whenua – Landcare Research

Reviewed by:	*Approved for release by:*
Andrew Neverman Researcher – Geomorphology Manaaki Whenua – Landcare Research	John Triantafilis Portfolio Leader – Managing Land & Water Manaaki Whenua – Landcare Research

Disclaimer

This report has been prepared by Landcare Research New Zealand Ltd for Hawke's Bay Regional Council. If used by other parties, no warranty or representation is given as to its accuracy and no liability is accepted for loss or damage arising directly or indirectly from reliance on the information in it.

Contents

Summary v
1 Introduction 1
2 Background 1
3 Objectives 2
4 Methods 2
4.1 Farm selection 2
4.2 Tree influence model on slope stability (TIMSS) 4
4.3 Landslide susceptibility modelling 7
4.4 Landslide-to-stream connectivity modelling 8
4.5 Coupling landslide susceptibility and connectivity 9
4.6 Effectiveness of trees on farms 11
4.7 Farm-scale landslide sediment delivery to streams 11
5 Results 12
5.1 Landslide susceptibility and connectivity 12
5.2 Farm-scale landslide sediment delivery 13
5.3 Effectiveness of trees on farms 17
6 Conclusions and recommendations 20
7 Acknowledgements 20
8 References 21

Appendix – Summary statistics of pastoral areas within the 50 farms selected for further analysis. 23

Summary

Project and client

- Hawke's Bay Regional Council (HBRC) contracted Manaaki Whenua – Landcare Research (MWLR) to assess the effectiveness of individual trees for reducing the occurrence of rainfall-induced shallow landslides on farms in the region.
- As part of this project, HBRC asked MWLR to estimate the magnitude of reductions in the number of shallow landslides and the amount of landslide sediment delivered to streams that might have been achieved by the presence of individual trees in pastoral areas during Cyclone Gabrielle.
- The work on assessing the effectiveness of trees for shallow landslide mitigation was completed under the Extreme Weather Recovery Advice Fund (contract ID C09X2303).

Objectives

The project had the following objectives.

- Model the reduction in the number of rainfall-induced shallow landslides due to the presence of individual trees on pastoral land during Cyclone Gabrielle for 50 farms in the Hawke's Bay region.
- Model the reduction in landslide-derived sediment load delivered to the stream network due to the presence of trees in pasture areas on the selected farms during Cyclone Gabrielle.
- Produce combined shallow landslide susceptibility and connectivity raster maps for the selected farms.

Methods

- The influence of individual trees on farm-scale landslide erosion and sediment loads was modelled for (a) the baseline scenario, whereby existing trees in pastoral areas were removed; (b) the contemporary tree cover scenario. The analysis used a tree map produced for HBRC by MWLR as part of the HBRC–MWLR LiDAR partnership project (2022–2024) and a landslide inventory for Cyclone Gabrielle from the GNS-led mapping project (see Leith et al. 2023).
- The selection of farms for analysis focused on pastoral areas on farms that experienced high rainfall during Cyclone Gabrielle but varied levels of landsliding. The AgriBase data set was used to identify farm boundaries, and the New Zealand Land Cover Database (LCDB v5.0, 2018) was used to retrieve the farm-pasture polygons.
- The existing statistical model representing the influence of individual trees on landslide susceptibility (Spiekermann et al. 2021, 2022a) was updated using available data on individual trees and a LiDAR-derived digital elevation model (DEM) for pastoral areas with landslide scar area data from semi-automated mapping in northern Hawke's Bay by Betts et al. (2023).
- Using the shallow landslide susceptibility and morphometric connectivity model framework from Spiekermann et al. 2022a and Tsyplenkov et al. 2023, we estimated sediment delivery to streams by shallow landslides for the two scenarios.

- The difference in landslide occurrence between the two scenarios was used to estimate the reduction in landslide erosion and sediment delivery to streams associated with the presence of individual trees on pastoral land.

Results

- Cyclone Gabrielle triggered 20,392 shallow landslides across all the selected farms. The corresponding gross shallow landslide erosion was estimated to be 2.54×10^6 t, while an estimated 0.17×10^6 t (6.6%) of landslide-derived sediment reached the stream network.
- With trees removed from pastoral areas, we estimated that 22,257 shallow landslides could have been triggered by Cyclone Gabrielle. That count resulted in gross landslide erosion of 2.77×10^6 t with an estimated 0.18×10^6 t (6.5%) of sediment delivered to the stream network.
- Farm-scale modelling revealed that existing tree cover may have prevented an additional 1,865 landslides occurring (8.4%), or, when expressed as gross landslide erosion, 0.23×10^6 t of eroded material.
- The presence of trees in pastoral areas achieved an estimated median 7% reduction in landslide numbers across the 50 farms. When expressed as sediment yield, this equated to a median 10% decrease in landslide erosion, irrespective of whether sediment was delivered to the stream network.
- The existing tree cover on pastoral land led to an estimated 9% reduction in landslide sediment delivery to streams when summed across all farms. This proportional reduction equates to approximately 16,150 t of sediment that was prevented from reaching the stream network due to the influence of trees in stabilising land and reducing the occurrence of landslides during Cyclone Gabrielle.

Conclusions and recommendations

- Our analysis showed that existing tree cover in pastoral areas prevented an estimated 1,865 additional landslides across all farms, with a median 7% reduction in landslide count. This equates to a median 10% decrease in sediment yield delivered to streams. In areas with trees near streams and on susceptible slopes, sediment delivery reductions of up to 24% were estimated.
- The main driver of the reductions in sediment delivery was tree density in pastoral areas highly susceptible to landslides, where landslide runout was likely to connect with the stream network. This area has already been reduced from 5.7% to 4.7% across all farms due to existing trees.
- Further reductions in future landslide sediment delivery to streams could be achieved through additional tree planting targeting pasture areas that are highly susceptible and highly likely to produce landslides that connect to streams. These areas have been identified in the farm-scale landslide susceptibility and connectivity maps accompanying this report.

1 Introduction

Cyclone Gabrielle triggered a large number of shallow landslides across the Hawke's Bay region, resulting in extensive land damage and substantial sediment deposition in downstream environments. In response to this event, Hawke's Bay Regional Council (HBRC) engaged Manaaki Whenua – Landcare Research (MWLR) to assess the effectiveness of existing trees in reducing the occurrence of rainfall-induced shallow landslides on selected farms in the region.

The present report adopts a data-driven, statistical modelling approach designed to quantify the impact of individual trees in pastoral areas on landslide susceptibility and the spatial probability of landslide-derived sediment reaching streams. The analysis uses a tree map produced for HBRC by MWLR as part of the HBRC–MWLR LiDAR partnership project (2022–2024). The model was applied to farms exhibiting a range of landslide susceptibility, tree cover, and landslide damage from Cyclone Gabrielle, facilitating a comparative assessment of the effectiveness of individual trees in reducing landslides under varying conditions.

The findings from this report will help HBRC to communicate to stakeholders the influence of existing trees in pastoral areas on the incidence of landslides triggered by the cyclone. The insights gained may also help target future tree planting to areas most susceptible to landslides and where landslides are most likely to contribute sediment to streams. This information is crucial for enhancing land management practices and limiting the future occurrence of shallow landslides in the region.

2 Background

Between 12 and 16 February 2023 an extreme rainfall event, referred to as Cyclone Gabrielle, affected much of the northern North Island of New Zealand, causing widespread damage. It was a severe event that required a national-level response. States of emergency were declared for seven regions of New Zealand. Along with surface, coastal, and river flooding, the event triggered more than 140,000 landslides, delivering significant amounts of sediment to downstream receiving environments (Leith et al. 2023).

Recent work by Spiekermann et al. (2022a, 2022b) proposed a data-driven model framework to quantify the effectiveness of trees for mitigating rainfall-induced shallow landslide erosion. The approach is based on coupling a landslide susceptibility model with a morphometric, landslide-to-stream connectivity model. The landslide susceptibility model included high-resolution, spatially explicit representation of the influence of individual trees at the landscape scale.

This model framework provides a basis for estimating reductions in the number of shallow landslides and the amount of landslide sediment delivered to streams that may have been achieved by the presence of trees in pastoral areas on farms in Hawke's Bay during Cyclone Gabrielle.

3 Objectives

The project had three objectives.

- Model the reduction in the number of rainfall-induced shallow landslides due to the presence of individual trees on pastoral land during Cyclone Gabrielle for 50 farms in the Hawke's Bay region.
- Model the reduction in landslide-derived sediment load delivered to the stream network due to the presence of trees in pasture areas during Cyclone Gabrielle on the selected farms.
- Produce combined shallow landslide susceptibility and connectivity raster maps for the selected farms.

4 Methods

Using the shallow landslide susceptibility and connectivity model framework from Spiekermann et al. 2022a and Tsyplenkov et al. 2023, we estimated sediment delivery to streams by shallow landslides for:

- a treeless scenario, where existing individual trees within pastoral areas on the selected farms were removed, called the 'baseline' scenario;
- an existing trees scenario, comprising the contemporary tree cover derived from the 2020/21 regional LiDAR survey, called the 'real' scenario.

We also compared the model's spatial predictions with interim landslide mapping data for Cyclone Gabrielle (data accessed on 1 November 2023) in the Hawke's Bay region (Leith et al. 2023). Our focus was farms that experienced high rainfall during Cyclone Gabrielle but varied levels of landsliding. The difference in landslide occurrence reflects, in part, the presence of trees and landscape susceptibility. Comparing the model results for the two scenarios allowed us to assess the extent to which the presence of individual trees on pastoral land reduced landslide occurrence and sediment delivery to streams.

4.1 Farm selection

Using geospatial information on farm boundaries and pastoral land cover, we selected 50 farms that were susceptible to landslide occurrence where landslide source points were mapped and the maximum 48 h rainfall during Cyclone Gabrielle uniformly exceeded 150 mm across the farm polygon (a typical threshold for landslide triggering; Basher et al. 2020). The selection procedure was as follows.

1. AgriBase (Sanson 2005) farm polygons were intersected with 'pasture' land (i.e. 'low' and 'high' producing grassland classes) from the New Zealand Land Cover Database (LCDB v5.0, 2018). Given the focus on the effectiveness of individual trees in pastoral land, we removed areas on the farm with continuous forest or scrub cover.
2. The resulting farm-pasture polygons from step 1 were filtered based on:

- at least 95% of the farm-pasture polygon area intersected mapping grids containing Cyclone Gabrielle landslide data (from the GNS-led mapping project, see Leith et al. 2023)
- at least 95% of the farm-pasture polygon area received at least 150 mm of rain in 48 h (from the HBRC 48 h rainfall map for Cyclone Gabrielle)
- mean rainfall was ≥250 mm in 48 h per farm-pasture polygon
- the area of discontinuous farm-pasture polygon was ≥1 km²
- landslide density was ≥10 scars/km².

First, we used the AgriBase layer to subset farms into specific classes. Polygons with the 'farm_type' attribute equal to 'MTW', 'NEW', 'OTH', 'SLY', 'URB', 'NAT', 'FOR', 'NOF', 'UNS', 'LIF' were omitted. These polygons represent plantation forests, urban areas and infrastructure, and scrub areas. The subsetted AgriBase layer was then united with the LCDB polygons to create polygons containing both farm-type and land-cover classes. For further analysis, only polygons identified in LCDB as 'High Producing Exotic Grassland' and 'Low Producing Grassland' were selected to represent pastoral areas.

The rainfall threshold of 150 mm in 48 h over >95% of each farm-pasture polygon area was chosen to ensure that most pasture areas on the farm experienced rainfall that exceeded a typical threshold for initial landslide triggering (Basher et al. 2020). The additional criterion of mean rainfall ≥ 250 mm in 48 h allowed us to further subset the polygons to those with higher rainfall that may trigger a higher density of landslides for subsequent analysis. This approach was designed to reduce the chance that a relative lack of landslides on any farm was due to insufficient storm rainfall.

The second constraint on farm selection was the overlap with landslide mapping grids containing Cyclone Gabrielle landslide data needed for model validation (Leith et al. 2023). As of 1 November 2023 only 19% of the region had been mapped (see Figure 1). This included 103,989 landslides of different movement types and materials. More than 86% of mapped landslides were soil or debris material, approximately 1% were rockfalls, and 6% contained woody debris. In terms of movement type, most landslides (98.2%) were slides or flows. For the purposes of this research, landslides classified as rockfalls were excluded from further analysis.

Additional preprocessing steps applied to the landslide inventory included the removal of scar (source area) duplicates and scars mapped without landslide deposits. Also, scar points located within the LiDAR-derived stream network (see section 4.4 for details) were considered stream bank failures and were excluded. Overall, 2.2% of mapped landslides were removed from the initial data set for the above-mentioned reasons.

The selection procedure produced 50 farm-pasture polygons for high-resolution modelling, with areas that ranged from 1 to 11.5 km² (2.9 km² median). The selected farm-pasture polygons span a large range of rainfall and landslide densities (cf. Appendix). On average, the farm-pasture polygons received 354 mm of rainfall, ranging from 253 mm for farm No. 21 to 519 mm for farm No. 39. Across all 50 farms a total of 20,392 landslides were triggered by Cyclone Gabrielle. Landslide densities ranged from 11 scars/km² (farm No. 42) to 300 scars/km² (farm No. 40), with an average of 113 scars/km². An average

existing tree density on LCDB-mapped pastoral land was 695 trees/km² and ranged from 114 trees/km² to 2,201 trees/km².

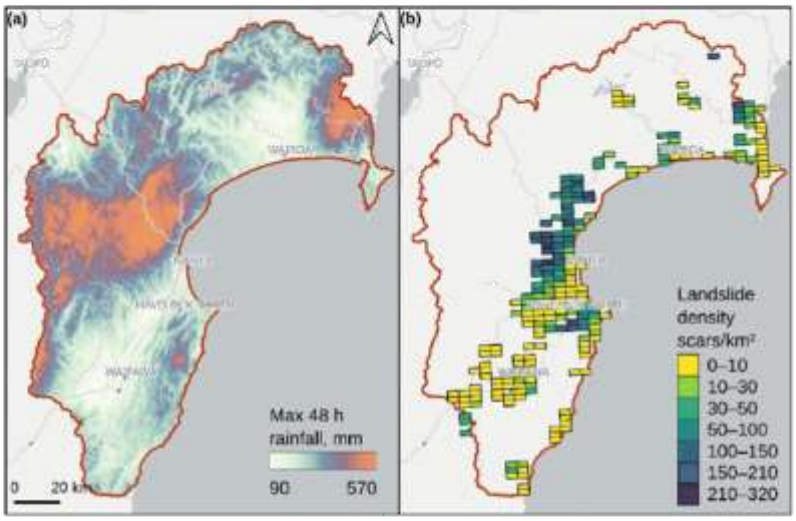

Figure 1. Hawke's Bay region overview: (a) maximum cumulative rainfall for 48 h during Cyclone Gabrielle (source: HBRC); (b) Cyclone Gabrielle landslide densities within mapping grids (source: GNS-led mapping project, Leith et al. 2023).

4.2 Tree influence model on slope stability (TIMSS)

We calibrated the statistical model representing the influence of individual trees on landslide susceptibility (Spiekermann et al. 2021, 2022a, 2022b, 2023) using available data on individual trees, landslide scar areas, and the LiDAR DEM for pastoral areas. The spatial data on individual trees was produced as part of the HBRC–MWLR LiDAR partnership project (2022–2024), where trees were delineated from the LiDAR-derived DEM and canopy height model using the PyCrown algorithm (Zörner et al. 2018). The minimum tree detection height and radius were 0.5 m.

The $TIMSS$ calibration required high-resolution landslide scar area (polygon) data to quantify the extent to which the area of landslide-eroded land was influenced by proximity to individual trees. For this we used landslide scar-mapping data from the March 2022 storm events in northern Hawke's Bay (Betts et al. 2023) and a multi-temporal landslide data set from Wairarapa (Spiekermann et al. 2021, 2022b), given that equivalent scar polygon data from high-resolution mapping are not available for Cyclone Gabrielle. This step improved the applicability of the original $TIMSS$ model to Hawke's Bay by using data from the region.

The $TIMSS$ represents the average influence of an individual tree on slope stability and has the following attributes (Spiekermann et al. 2023).

- Values are spatially distributed as a function of distance from the tree (trunk).
- Contributions of neighbouring trees to slope stability are considered additive.

- Local hydrological and mechanical effects are represented implicitly.

The original approach by Spiekermann et al. (2021) was developed for four different tree species (poplar, willow, kānuka, conifer, and eucalyptus). However, since no species data were available in the Hawke's Bay data set, we calibrated the model using a combined $TIMSS$ (i.e. one tree influence model on slope stability for all tree species). On the one hand, this approach does not allow for a detailed study of the impact of a specific tree type on slope stability (Spiekermann et al. 2022a); on the other hand, it enables calibration of $TIMSS$ with an increased number of tree data points (Spiekermann et al. 2021).

Combining the Wairarapa and northern Hawke's Bay data sets produced a database of 88,948 landslide scar polygons. To create the $TIMSS$, first we selected only those trees that stand at a distance of at least 15 m from other trees to isolate the influence of individual trees on slope stability for the purpose of model calibration (Spiekermann et al. 2021). Then we kept only those trees that were located on pastoral land by intersecting with LCDB v5.0 2018 'pasture' polygons (see section 4.1 for definition). In addition, trees were excluded if located on slopes where landslides were considered less likely to occur, defined as slopes below 17.5° (Spiekermann et al. 2021). This threefold selection procedure resulted in a data set comprising 160,429 individual trees.

Two final steps were involved in the calculation of the $TIMSS$. First, the landslide scar polygons were gridded at a 1 m resolution to create a binary grid of eroded soil surface and non-landslide eroded areas. Next, for each tree we calculated the number of landslide-eroded and stable (i.e. non-landslide) pixels within a radius from 0 to 40 m (r). Thus, for each tree we calculated the tree influence with a precision of 1 m, expressed as a fraction of eroded pixels of all land around the tree. The fraction of landslide eroded area as a function of distance from the tree $f(r)$ could then be calculated for the whole data set by aggregating by r.

A non-linear least-squares logistic regression model was used to fit $f(r)$. The logistic growth function was defined as:

$$f(r) = \frac{b_c}{1+e^{\frac{xmid-r}{scal}}} \quad (1)$$

where b_c is a parameter representing the asymptote; $xmid$ is a parameter representing the r value at the inflection point of the curve; and $scal$ is the scale parameter on the input axis. Thus, the $TIMMS$ was defined as the proportional reduction in landslide-eroded area, expressed as:

$$TIMSS = b_c - f(r) = 1 - \frac{1}{1+e^{\frac{xmid-r}{scal}}} \quad (2)$$

where $TIMSS$ is the mitigation at a given pixel for an individual tree.

When applied spatially, the influence of more than one tree is assumed to be additive, and the upper limit on the number of trees contributing to slope stability at a given pixel is assumed to be four (Spiekermann et al. 2021). The $TIMSS$ was thus a two-dimensional representation of biophysical erosion and sediment control at 1 m resolution (see Figure 2).

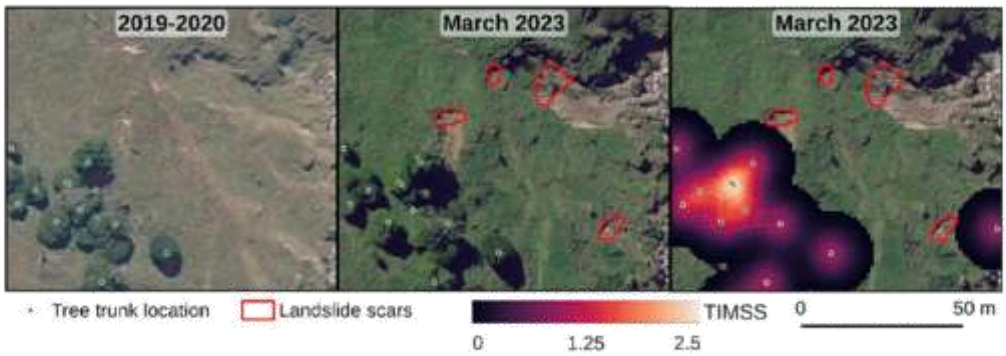

Figure 2. Illustration of spatial application of the $TIMSS$. Multiple landslides occurred during the Cyclone Gabrielle, which can be seen on March 2023 imagery, compared to previous one. Although trees contribute to slope stability, they do not always prevent landslide erosion – a reflection of a multivariate problem. Note that the influence of more than one tree at a given location is assumed to be additive, which is why values exceed 1.

The results of the $TIMSS$ recalibration are shown in Figure 3. The points in Figure 3(a) are the measured mean values of fractions of eroded soil at each 1 m increment away from individual trees. Figure 3(b) shows the results of the normalised reduction in eroded soil (eq. 2). Where the layout of trees is such that more than one tree contributes to slope stability at a given location, the influence on slope stability is assumed to be additive. Therefore, $TIMSS$ values can exceed 1 when applied spatially (see Figure 2). The normalised tree influence on slope stability decreased rapidly with increasing r, dropping to 0.5 at 6 m (Figure 3(b)). The maximum effective distance was 13 m.

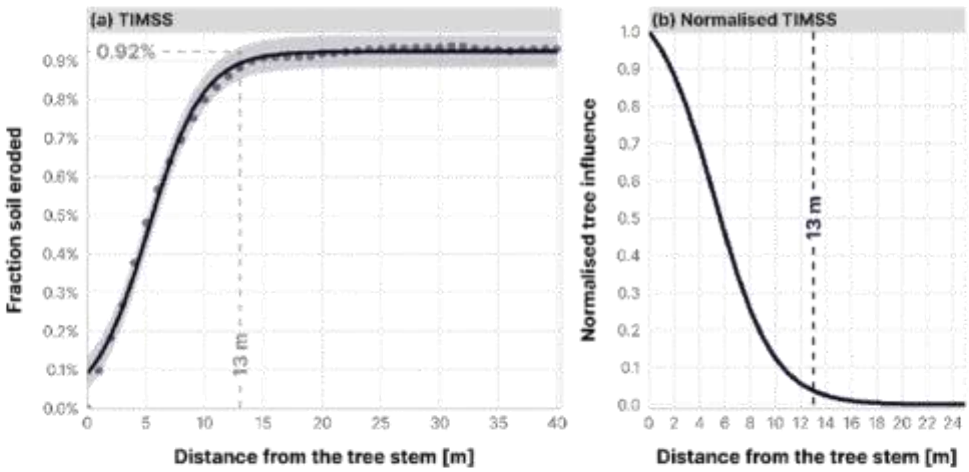

Figure 3. (a): Mean fraction of eroded soil by distance from tree, fitted using a non-linear logistic regression model with a 95% confidence band. (b): normalised mean tree influence for an individual tree, as a reduction in eroded soil. Vertical lines show the maximum effective distance of 13 m.

4.3 Landslide susceptibility modelling

The $TIMSS$-based landslide susceptibility model was applied following the method described in Spiekermann et al. 2022b using a combined shallow landslide inventory based on mapping from high-resolution imagery in northern Hawke's Bay and Wairarapa (Spiekermann et al. 2021; Betts et al. 2023). The inventory consisted of *ca.* 58,000 rainfall-induced shallow landslides on pastoral land. Binary logistic regression (BLR) is frequently used for statistical landslide susceptibility modelling because it represents the probability of a binary response variable, which corresponds to the absence or presence of landslides (Smith et al., 2023). We used a 1:1 balanced sample design, with an equal number of landslide presence and randomly generated landslide absence points.

To develop the statistical model of landslide susceptibility, key predictor variables of shallow landslide erosion were generated from existing terrain and lithology data sets. The initial selection of predictor variables was based on a geomorphological understanding of physical processes that might influence slope stability, supported by the findings of recent studies of landslide susceptibility in New Zealand (Spiekermann et al. 2022; Smith et al. 2023). Therefore we included: the topographic variables of slope, gradient and aspect (northernness, easternness); tree cover using $TIMSS$; and top rock lithology from the New Zealand Land Resources Inventory (Newsome et al. 2008). BLR modelling was performed using the tidymodels framework (Kuhn & Wickham 2020), and the terra package (Hijmans 2023) was used for spatial model predictions, both of them within the open-source statistical software R 4.4.0 (R Core Team 2024).

To test model prediction performance, we used k-fold ($k = 10$) cross-validation (CV). Samples were randomly partitioned into 10 folds, whereby 9 folds were used to train the model and the remaining fold used to test the predictive ability of the model using selected performance metrics. This procedure was repeated until each of the 10 folds had been used for model testing. To ensure the performance measures were not influenced by a particular data partitioning, this process was repeated five times. Moreover, we used 100 balanced bootstraps (with an equal number of absence and landslide points), each with a different set of randomly selected absence points for the five repeats of k-fold CV.

Model classification performance was evaluated using receiver operating characteristic curves and calculation of the area under the receiver operating characteristic curve ($AUROC$) using the yardstick R-package (Kuhn et al. 2023). A good $AUROC$ score is considered to be between 0.8 and 0.9, while an excellent score is greater than 0.9 (Obuchowski 2003). We also estimated an F_1 score, which is a confusion matrix metric widely used in the binary classification of balanced data sets (Chicco & Jurman 2020). The F_1 is defined as the harmonic mean of precision and recall:

$$F_1 = \frac{2 \times TP}{2 \times TP + FP + FN}, \quad (3)$$

where true positives (TP) are the correct predictions, while false negatives (FN) and false positives (FP) are the incorrect predictions. The F_1 ranges from 0 to 1, where $F_1 = 1$ corresponds to perfect classification. Usually, classification with an F_1 score higher than 0.7 is considered 'good' (Chicco & Jurman 2020).

The model that corresponded to the median $AUROC$ value of 0.91 and F_1 of 0.85 was selected and used for spatial prediction. We classified the spatial probabilities of the landslide susceptibility map into three classes based on thresholds related to the percentage of observed landslides falling within each susceptibility class. Class thresholds were determined by ranking the landslides used to fit the model by their probability values in decreasing order (Spiekermann et al. 2022). The 'high' class contains 80% of the mapped landslides, which have probabilities ≥ 0.60, while the 'moderate' class corresponds to a further 15% of landslides (probabilities ≥ 0.38 to <0.60), and the remaining 5% of landslides fall into the class 'low' (probabilities < 0.38).

4.4 Landslide-to-stream connectivity modelling

Morphometric landslide-to-stream connectivity was trained based on a LiDAR-derived 5 m DEM using a binary logistic regression model (Spiekermann et al. 2022a; Tsyplenkov et al. 2023). Connectivity was expressed as a spatial probability (range 0–1), where areas with values close to 1 have a higher likelihood of connecting to a stream network, while areas close to zero have a low likelihood of connection. The DEM-derived stream network (using a D8 flow accumulation algorithm and a 10 ha channel initiation threshold; refer to Smith et al. 2024) was merged with a derived national layer comprising river and lake polygons, which was used to represent wide river channels and waterbodies (Smith & Betts 2021).

The BLR model was fitted using spatial covariate data for connected and disconnected landslide source areas (mapped with centroid points), obtained from mapping areas that intersect with available LiDAR coverages in the Hawke's Bay, Gisborne, and Greater Wellington regions. The combined landslide source and deposit inventory presently comprises approximately 41,000 landslides, where 8.5% of them are connected to the stream network. Our results revealed a strong dependency of connectivity on the overland flow distance to the stream network ($DownDist$). Results obtained from this single-variable model exhibited similar predictive performance compared to more complex, multi-variable models (Tsyplenkov et al. 2023).

We cross-validated the BLR model within the tidymodels R-package infrastructure (Kuhn & Wickham 2020) using the following procedure.

1. Balanced bootstrap resampling was performed with replacement, ensuring that every bootstrap had an equal amount of connected and disconnected landslides.
2. Each bootstrap resample was further split into training and testing data sets, and the model was fitted to the training data set.
3. The testing data set was used to evaluate the model performance with a set of metrics described in section 4.3.

The whole procedure was repeated and produced 100 different models, with their corresponding parameter estimates and model metrics. The model with the highest $AUROC$ value was used for predictions. In the present version, the BLR model achieved a median $AUROC$ of 0.87 in cross-validation.

We classified spatial probabilities predicted with the BLR model into three classes (high, moderate, and low). As with the landslide susceptibility classes, the thresholds used to define each connectivity class were determined by ranking the connected landslides used to fit the model by their probability values in decreasing order. 'High' connectivity corresponds to 80% of the mapped landslides, which have probability values ≥ 0.58. 'Moderate' corresponds to a further 15% of the mapped landslides, which have probability values between ≥0.18 to <0.58, while 'low' relates to the remaining 5% of landslides, with values < 0.18.

We also estimated the class-specific sediment delivery ratio (SDR, dimensionless) based on Cyclone Gabrielle landslide mapping. In the absence of data on landslide-eroded volumes or areas for estimating SDRs, it was necessary to rely on count data using point-based landslide mapping (Leith et al. 2023). SDR_{ij} describes the proportion of all mobilised material entering the stream network for the ith connectivity class and jth farm. SDR_{ij} was calculated for each connectivity class i (high, moderate, and low) based on the estimated volume of connected scars from class i (LCV_{ij}) per farm j relative to the total estimated landslide scar volume in class i per farm j (LV_{ij}), following Spiekermann et al. (2022a).

$$SDR_{ij} = \frac{LCV_{ij}}{LV_{ij}} \times DR \quad (4)$$

To compute SDRs, we assumed that shallow landslides had a mean depth of 1 m based on studies reporting shallow landslide depths in hill country terrain (Crozier 1996; Reid & Page 2003; Betts et al. 2017). Data on landslide source areas were unavailable, so we used the median landslide area from landslide polygon mapping across northern Hawke's Bay following the March 2022 storm events (Betts et al. 2023). The median landslide scar area was 89 m^2 based on 35,710 landslides mapped within pastoral areas. The delivery rate (DR) was set to 0.5 for the stream network, which indicates that, on average, connected landslides deliver approximately 50% of mobilised sediment to the stream (Reid & Page 2003; Spiekermann et al. 2022a).

4.5 Coupling landslide susceptibility and connectivity

We integrated spatial predictions of landslide susceptibility and connectivity. First, we reclassified the continuous susceptibility and connectivity probability rasters into classes using thresholds described above. An intersection of the two reclassified spatial predictions resulted in an initial matrix of nine joint classes describing both the likelihood of landslides occurring in the future and the potential for sediment to be delivered to the stream network. We named the classes accordingly (i.e. the intersection of high susceptibility and high connectivity classes produced 'High LS / High Con' corresponding to a class where landslides are likely to occur and reach the stream network). To avoid ambiguous situations where high connectivity exists while the landslide susceptibility is low, we merged all connectivity classes in the low susceptibility zone into one, referred to as 'Low LS' (see Figure 4).

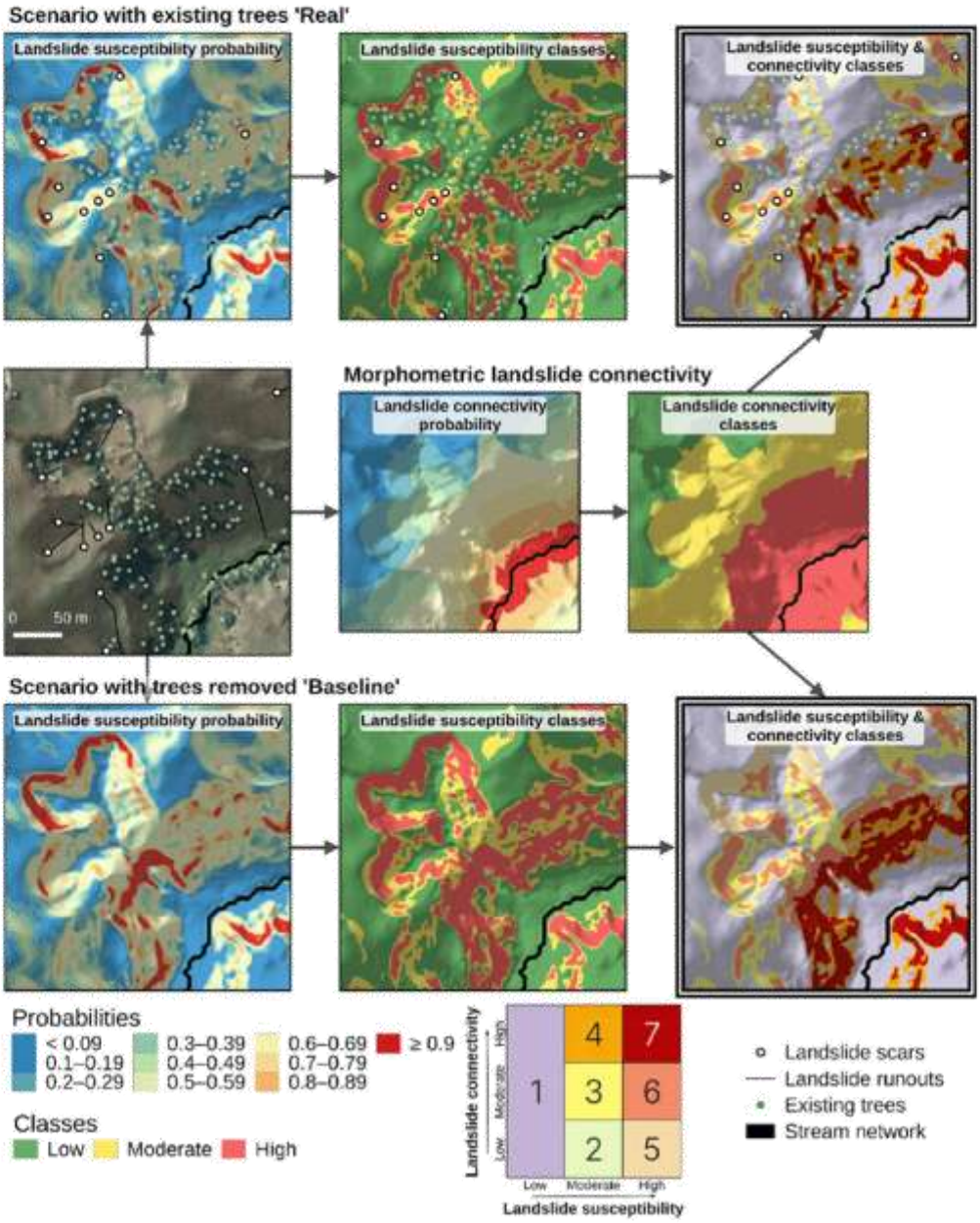

Figure 4. Scheme illustrating the integration of class-based shallow landslide susceptibility and connectivity model outputs for two scenarios: 'baseline' with trees removed and 'real' with existing trees.

4.6 Effectiveness of trees on farms

Based on the $TIMSS$ calibration described in section 4.2, landslide susceptibility modelling was performed for farms selected in section 4.1. This produced estimates of the influence of existing trees in pastoral areas on landslide susceptibility at 1 m resolution ('real' scenario). For comparison, the existing trees were removed from pastoral areas, and landslide susceptibility was estimated for a treeless reference condition ('baseline' scenario). The difference between these two layers (existing trees vs treeless reference) provided the basis for quantifying the influence of existing trees on landslide susceptibility at the farm scale. This difference is expressed in terms of a change in the number of landslides (N) per farm, based on the mapped landslide spatial density (scars/km^2) corresponding to different susceptibility classes, and the change in sediment delivery to streams (SY) per farm.

4.7 Farm-scale landslide sediment delivery to streams

We estimated the average reduction in sediment load delivered to the stream network that can be attributed to the presence of individual trees in pastoral areas for the selected farms during Cyclone Gabrielle. Combining tree-level susceptibility modelling (section 4.3) and a morphometric landslide connectivity model (section 4.4) allowed us to estimate how the presence of individual trees influences both landslide susceptibility and connectivity at the farm scale.

Reductions in shallow landslide erosion and sediment delivery were based on estimated changes in event sediment yield (SY, t/km^2) between the baseline and real scenarios. To estimate the reduction in landslide sediment yield per farm, we used the Cyclone Gabrielle landslide density per joint susceptibility and connectivity class (described in section 4.5) per farm to estimate the total number of landslides per farm, based on the change in joint class area following the removal of trees in the baseline scenario. The total number of landslides per farm under the baseline scenario was estimated by multiplying the class-specific landslide densities by the class areas for each farm.

The median landslide area (A, 89 m^2) and a landslide depth (D, 1 m) derived from earlier work in the absence of data from Cyclone Gabrielle were used to estimate the farm-specific event sediment yield (SY_j) for both scenarios (i.e. SY_{baseline} and SY_{real}):

$$SY_j = \frac{\sum_{n=1}^{i} SDR_{ij} \times N_{ij} \times A \times D \times \rho}{P_j}, \quad (5)$$

where P_j is the pastoral area for the jth farm (km^2); SDR_{ij} and N_{ij} are the sediment delivery ratio and landslide number (respectively) for every joint class i and farm j (see section 4.5); and ρ is soil bulk density, equal to 1.4 t/m^3 (Spiekermann et al. 2022). The reduction in landslide sediment yield ($SY_{\text{reduction}}$, %) for the event was estimated as:

$$SY_{\text{reduction}} = 100 \times \frac{SY_{\text{real}} - SY_{\text{baseline}}}{SY_{\text{baseline}}} \quad (6)$$

5 Results

5.1 Landslide susceptibility and connectivity

The interim landslide mapping data available for Cyclone Gabrielle in the Hawke's Bay region (Leith et al. 2023) was not used in training the susceptibility and connectivity models, which means these data provide a basis for independently assessing the class-based susceptibility and connectivity maps (see Figure 4). We found that most (63%) Gabrielle-triggered shallow landslides occurred in the high susceptibility class, while 24% occurred in the moderate class, and 13% in low.

The proportion of Gabrielle-triggered landslides connected to streams with source areas (mapped using points) located in the high connectivity class area equated to 54%, while 25% of the connected landslides occurred in the moderate class and 21% in the low class. The farm average proportion of connected landslides in the high connectivity class was 67%, moderate was 18%, and low was 15%.

The median estimated SDR value for the high connectivity class was 0.14, for moderate it was 0.04, and for low it was 0.01, based on the Gabrielle landslide mapping data for each farm (Figure 5). The highest SDR values were observed at those farms where most landslides were triggered in the high connectivity class and landslide runout reached the stream network. For example, at farm No. 7, 39 out of 57 landslides in the high connectivity class were connected to streams. In contrast, the lowest SDR values were observed at farms where there were no connected landslides mapped; for example, at farm No. 11 none of the 84 mapped landslides reached the stream network.

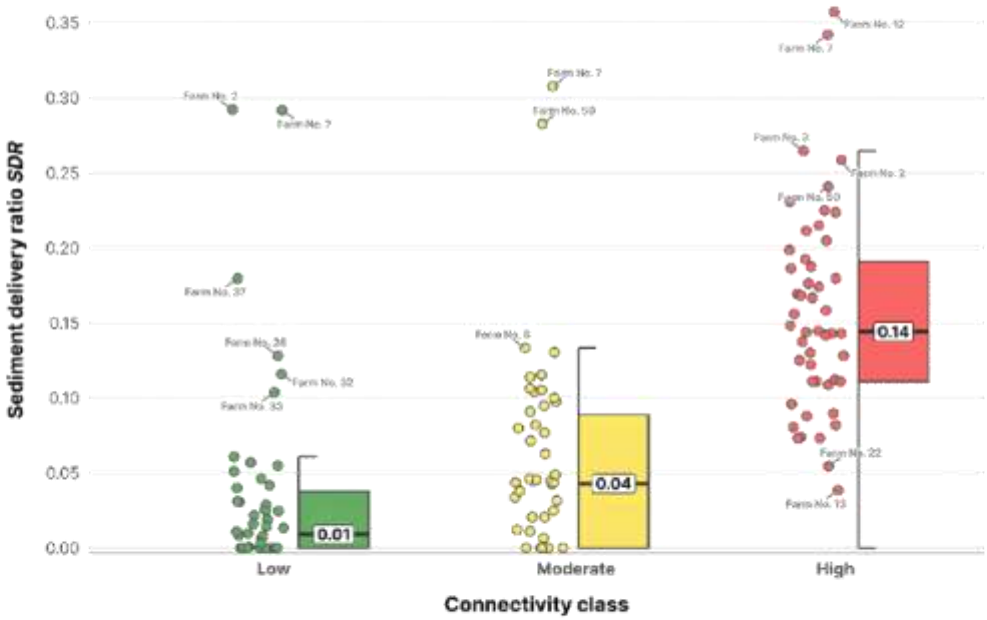

Figure 5. Distributions of estimated farm and class-specific SDRs based on the Cyclone Gabrielle landslide mapping data (Leith et al. 2023). SDR was estimated according to Equation 4, with the 10 ha digital stream network as the connectivity target.

5.2 Farm-scale landslide sediment delivery

Cyclone Gabrielle triggered 20,392 shallow landslides across all the selected farms. The corresponding gross landslide erosion was estimated to be 2.54 × 10^6 t, while an estimated 0.17 × 10^6 t of landslide-derived sediment reached the stream network. Across the selected farms, on average 7.5% of eroded material reached the stream network, ranging from 0 to 32%.

The estimated farm-scale sediment yield delivered to the stream network from shallow landslides ranged from 0 to 3,707 t/km², with a median of 723 t/km² for the real scenario (Figure 6). The highest SY_{real} was observed at farm No. 6, where 314 landslides were mapped and the corresponding SY_{real} was 3,707 t/km². The lowest SY_{real} was observed at farm No. 11, with 84 landslides mapped and an SY_{real} of 0 t/km², since no landslides were connected to the stream network (Table 1).

With trees removed from pastoral areas (i.e. the baseline scenario), we estimated that 22,257 shallow landslides (8.4% more) could have been triggered by Cyclone Gabrielle across the modelled farms. That count resulted in gross landslide erosion of 2.77 × 10^6 t with an estimated 0.18 × 10^6 t delivered to the stream network. The increase in landslides corresponds to a farm $SY_{baseline}$ delivered to the stream network ranging from 0 to 4,173 t/km², with a median of 813 t/km².

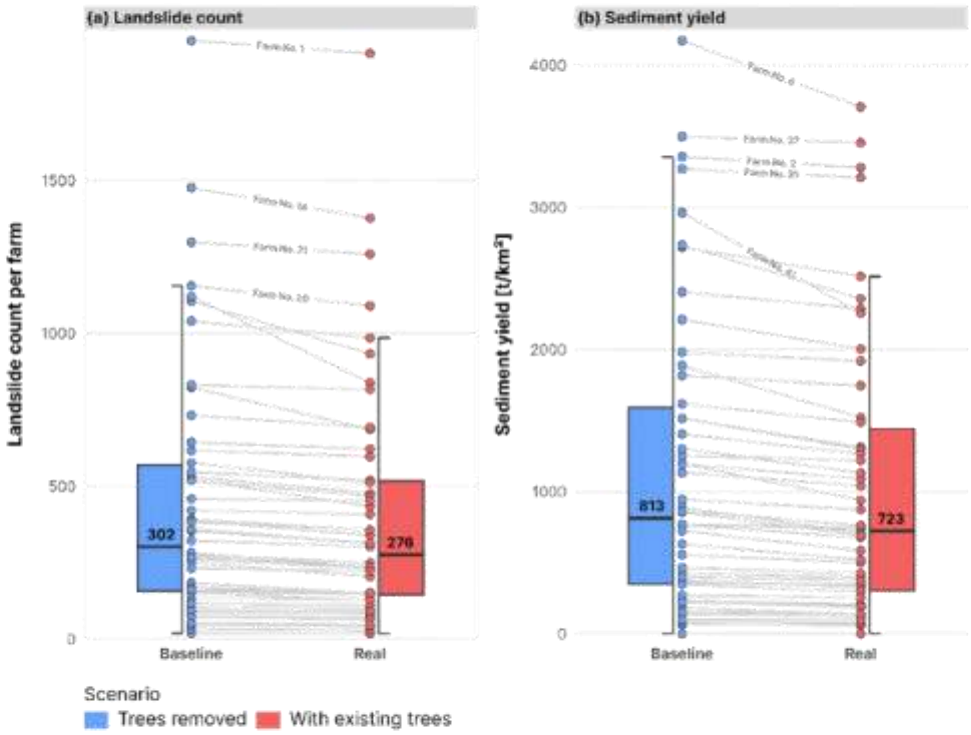

Figure 6. Estimated reduction in landslide number (a) and sediment yield (b) across the selected farms between the two scenarios: baseline with trees removed and real with existing trees.

Table 1. Summary of the two modelled scenarios: baseline (with trees removed) and real (with existing trees) across the 50 selected farms, expressed as landslide number per farm, landslide spatial density per farm, landslide sediment yield delivered to the stream network per farm, and estimated proportional reduction in landslide number and sediment yield, based on comparison of the baseline and real scenarios.

HBFID	Landslide number per farm		Landslide density per farm (scars/km²)		Landslide sediment yield per farm (t/km²)		Reduction (%)	
	Baseline	Real	Baseline	Real	Baseline	Real	Landslide number	Sediment Yield
41	1,121	838	372	278	2,964	2,255	25	24
23	184	149	82	67	180	140	19	22
44	282	235	224	186	1,197	939	17	22
40	823	686	359	300	889	708	17	20
35	522	434	143	119	1,887	1,522	17	19
19	577	511	129	114	724	585	11	19
24	1,105	933	300	253	855	694	16	19
27	360	314	100	88	632	521	13	17
30	260	233	97	87	223	186	10	17
15	250	204	88	71	235	196	19	16
45	151	128	143	121	348	295	15	15
49	52	46	40	35	225	192	11	15
43	33	28	32	27	141	121	14	14
34	387	339	122	107	1,516	1,297	13	14
32	268	235	225	198	2,735	2,358	12	14
18	530	477	140	126	1,516	1,313	10	13
50	72	64	50	45	1,303	1,131	11	13
12	18	17	16	15	377	328	7.4	13
36	519	468	96	87	862	763	9.7	11

HBFID	Landslide number per farm		Landslide density per farm (scars/km²)		Landslide sediment yield per farm (t/km²)		Reduction (%)	
	Baseline	Real	Baseline	Real	Baseline	Real	Landslide number	Sediment Yield
6	353	314	212	189	4,173	3,707	11	11
25	276	249	81	73	763	678	9.6	11
3	158	151	45	43	557	501	4.4	10
26	161	145	96	87	1,406	1,265	10	10
39	169	148	94	82	231	208	13	9.8
13	322	302	51	48	66	60	6.1	9.8
28	391	356	188	171	2,211	2,004	9	9.4
48	161	151	36	34	154	140	6.4	9.3
5	732	692	160	151	1,194	1,091	5.4	8.7
14	1,477	1,377	153	143	465	426	6.7	8.5
17	383	357	133	124	1,135	1,041	6.7	8.3
20	1,155	1,090	216	203	1,618	1,488	5.7	8
22	115	110	105	100	368	338	4.7	8
7	157	145	69	64	2,721	2,514	7.5	7.6
10	1,040	985	135	128	945	874	5.3	7.5
8	101	98	59	57	427	396	3.3	7.3
16	158	151	106	101	399	374	4.6	6.1
46	231	223	33	31	270	255	3.5	5.5
33	545	519	182	173	2,405	2,286	4.8	4.9
9	421	408	148	143	1,817	1,747	3.1	3.9
21	1,298	1,259	169	164	765	738	3	3.5
29	644	622	107	103	771	746	3.3	3.3

HBFID	Landslide number per farm		Landslide density per farm (scars/km²)		Landslide sediment yield per farm (t/km²)		Reduction (%)	
	Baseline	Real	Baseline	Real	Baseline	Real	Landslide number	Sediment Yield
38	616	597	144	139	1,982	1,919	3.2	3.2
4	74	73	52	51	358	347	2	3
1	1,958	1,916	170	166	1,252	1,221	2.1	2.4
42	44	43	11	11	79	77	2.7	2.4
2	132	129	105	103	3,356	3,281	2.3	2.2
47	91	90	28	28	97	95	1.6	2.1
31	831	817	207	203	3,271	3,211	1.7	1.8
37	458	452	168	166	3,499	3,455	1.3	1.3
11	89	84	44	41	—*	—*	5.3	—*

* None of the mapped landslides on farm No. 11 reached the stream network during Cyclone Gabrielle; therefore, the sediment yield for both scenarios has not been estimated.

5.3 Effectiveness of trees on farms

Our modelling across the 50 farms showed that, under the treeless baseline scenario, only 5.7% (9.6 km^2) of the total pastoral area on the farms is both highly susceptible to shallow landsliding and has high potential for sediment delivery to the stream network (i.e., 'High LS / High Con'). However, due to the actual tree cover (real scenario), this class is reduced to 4.7% of the total area. The class reduction resulted in the prevention of an additional 1,865 landslides occurring (8.4%), or, when expressed as gross landslide erosion, 0.23 × 10^6 t of eroded material.

The existing tree cover on pastoral land led to an estimated 9% reduction in landslide sediment delivery to streams when summed across all farms. This proportional reduction equates to approximately 16,150 t of sediment that was prevented from reaching the stream network due to the influence of trees in stabilising land and reducing the occurrence of landslides during Cyclone Gabrielle.

The presence of trees in pastoral areas achieved a median 7% estimated reduction in landslide numbers across the 50 farms. When expressed as SY, this equated to a median 10% decrease (Figure 7). Based on the individual farm results, we can see that the presence of trees produced up to a 24% reduction in landslide sediment delivery to the stream network. This result was achieved where trees occurred in areas that were highly susceptible and where landslides were highly likely to connect to the stream network (i.e. steep slopes proximal to the stream network).

At farms with an SY reduction greater than or equal to 15%, the individual tree density (defined as trees that stand at least 13 m from other trees, see Figure 3) ranged from 145 to 241 trees/km^2, with an average of 193 trees/km^2. For farms with a lower observed reduction (<5%), the average individual tree density was 85 trees/km^2, ranging from 32 to 160 trees/km^2.

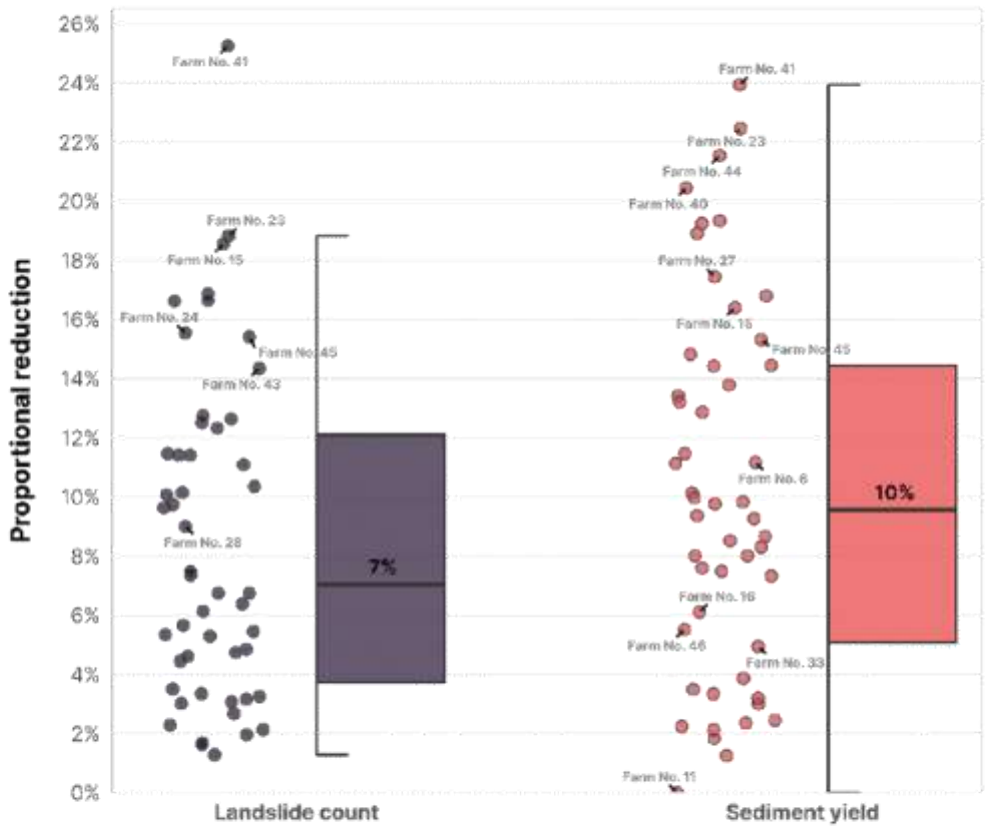

Figure 7. Proportional reduction (%) in landslide number and sediment yield delivered to the stream network across the selected farms in the two scenarios: baseline, with trees removed, and real, with existing trees.

Pearson r correlation analysis showed a moderate (r = 0.51) but statistically significant (p < 0.001) positive correlation between the estimated maximum 48 h rainfall during Cyclone Gabrielle and farm-scale landslide density. That provides evidence that more landslides were triggered with increasing rainfall intensity, which is consistent with previous findings (e.g. Smith et al. 2023).

Our analysis revealed that it is not only the number of trees located in areas highly susceptible to landslide occurrence that might influence sediment delivery to streams, but also the location of those highly susceptible zones within a farm. The pastoral hillslopes of farm No. 49 (Figure 8) illustrate this. According to our estimation, SY reduced from 225 t/km² in the baseline scenario to 192 t/km² in the real scenario. This 15% reduction in yield was largely achieved because trees in pastoral areas on this farm occur in proximity to the stream network. Moreover, the presence of trees in pastoral areas of this farm produced a 24% reduction in the 'High LS / High Con' class area.

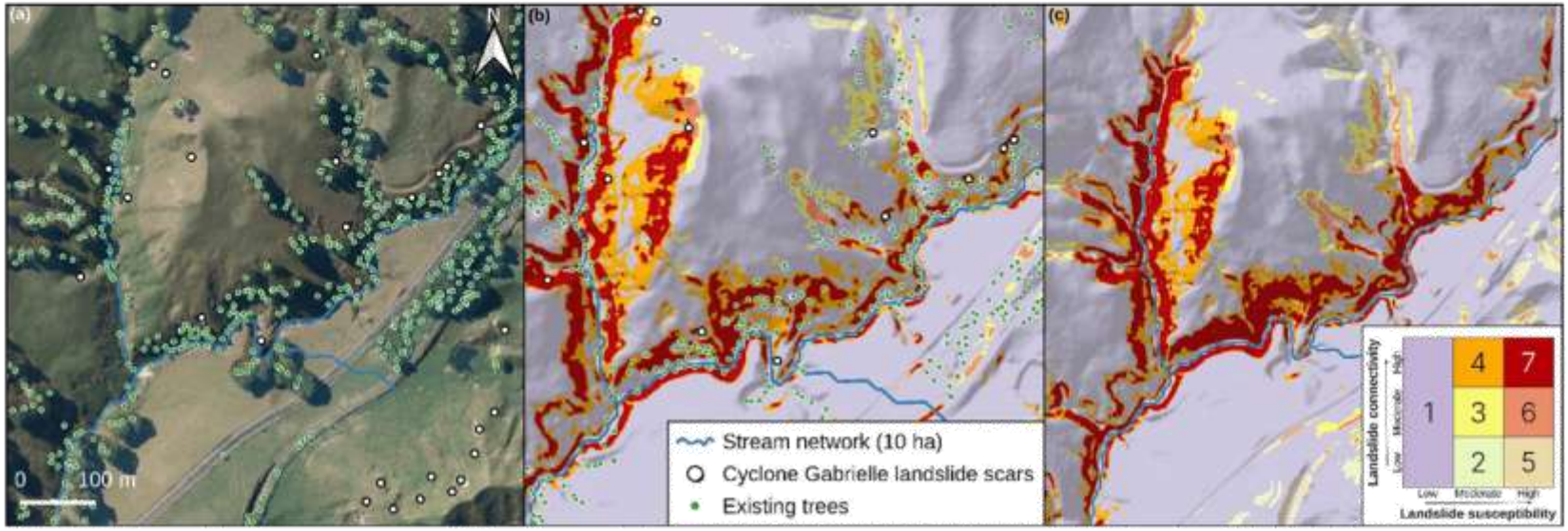

Figure 8. The influence of individual trees on the spatial extent of areas highly susceptible to landslide occurrence and connectivity to streams: (a) satellite imagery of farm No. 49, showing the location of existing trees and mapped landslide scars after Cyclone Gabrielle (landslide data from Leith et al. 2023); (b) modelled shallow landslide susceptibility and connectivity for the real scenario (i.e. with existing trees); (c) modelled shallow landslide susceptibility and connectivity for the baseline scenario (i.e. with trees removed). Note the reduction in 'High LS / High Con' areas from (c) to (b).

6 Conclusions and recommendations

The present report estimates the magnitude of reductions in the number of shallow landslides and landslide sediment delivered to streams that may have been achieved by the presence of individual trees on pastoral areas in the Hawkes Bay region during Cyclone Gabrielle. We focused on 50 farms that experienced high rainfall but variable levels of landsliding, and modelled two scenarios: baseline, with all existing trees removed, and real, with existing tree cover.

Our analysis revealed that existing tree cover prevented the additional occurrence of 1,865 landslides (or 0.23×10^6 t of eroded material) across all modelled farms, with a median farm-scale reduction in landslide count of 7%. When expressed as a sediment yield delivered to the stream network, the reduction equates to a median 10% decrease. Where trees were located in close proximity to the stream network and on susceptible slopes, farm-scale reductions in sediment delivery to streams of up to 24% were estimated. Our modelling suggested that existing tree cover prevented approximately 16,150 t of landslide-derived sediment from reaching the stream network during Cyclone Gabrielle across the selected farms.

We found that the main driver of the reductions in sediment delivery was tree density in pastoral areas highly susceptible to landslides where landslide runout was likely to connect with the stream network. Due to the presence of existing trees, this area has already been reduced from 5.7% to 4.7% across the selected farms. Further reductions in future landslide sediment delivery to streams may be achieved through additional tree planting targeting pasture areas that are highly susceptible and highly likely to produce landslides that connect to streams. These areas have been identified in the farm-scale landslide susceptibility and connectivity maps accompanying this report.

Future applications of the $TIMSS$-based landslide susceptibility and connectivity model framework could extend to a larger number of farms and focus on estimating reductions in landslide sediment delivery to streams that might be achieved using targeted approaches to tree planting. This could include testing scenarios involving different tree densities or planting patterns, including the targeted planting of spaced trees to pasture areas based on the high-resolution landslide susceptibility and connectivity maps.

7 Acknowledgements

This work was funded by the New Zealand Ministry of Business, Innovation & Employment (MBIE) through the Extreme Weather Recovery Advice Fund (contract ID C09X2303). We acknowledge staff from Hawke's Bay Regional Council, particularly Ashton Eaves and Kathleen Kozyniak, for discussions leading to this work and for the provision of spatial data. We are grateful to GNS Science for early access to the Cyclone Gabrielle landslide inventory. We thank Andrew Neverman for reviewing the report.

8 References

Basher L, Spiekermann R, Dymond J, Herzig A, Hayman E, Ausseil A-G 2020. Modelling the effect of land management interventions and climate change on sediment loads in the Manawatu-Whanganui region. New Zealand Journal of Marine and Freshwater Research 54: 490–511.

Betts H, Basher L, Dymond J, Herzig A, Marden M, Phillips C 2017. Development of a landslide component for a sediment budget model. Environmental Modelling & Software 92: 28–39. https://doi.org/10.1016/j.envsoft.2017.02.003

Betts H, Smith HG, Neverman AJ, Tsyplenkov A 2023. Wairoa shallow landslide and debris deposit mapping following storm events in March 2022. Manaaki Whenua – Landcare Research contract report LC4331 for Hawke's Bay Regional Council.

Chicco D, Jurman G 2020. The advantages of the Matthews correlation coefficient (MCC) over F1 score and accuracy in binary classification evaluation. BMC Genomics 21(1): 6. https://doi.org/10.1186/s12864-019-6413-7

Crozier M 1996. Runout behaviour of shallow, rapid earthflows. Zeitschrift Für Geomorphologie. Supplementband 105: 35–48.

Hijmans RJ 2023. terra: Spatial data analysis. https://CRAN.R-project.org/package=terra

Kuhn M, Vaughan D, Hvitfeldt E 2023. yardstick: Tidy characterizations of model performance. https://CRAN.R-project.org/package=yardstick

Kuhn M, Wickham H 2020. Tidymodels: a collection of packages for modelling and machine learning using tidyverse principles. https://www.tidymodels.org

Leith K, McColl S, Robinson T, Massey C, Townsend D, Rosser B, et al. 2023. Reflections on the challenges of mapping >100,000 landslides triggered by Cyclone Gabrielle. Geoscience Society of New Zealand Annual Conference 2023, Abstracts 164A, 280.

Newsome PFJ, Wilde RH, Willoughby EJ. 2008. Land Resource Information System Spatial Data Layers: Data Dictionary. Landcare Research New Zealand Ltd, Palmerston North. http://digitallibrary.landcareresearch.co.nz/cdm/ref/collection/ p20022coll14/id/67.

Obuchowski NA 2003. Receiver operating characteristic curves and their use in radiology. Radiology 229(1): 3–8. https://doi.org/10.1148/radiol.2291010898

R Core Team 2024. R: a language and environment for statistical computing. Vienna, R Foundation for Statistical Computing. https://www.R-project.org/

Reid LM, Page MJ 2003. Magnitude and frequency of landsliding in a large New Zealand catchment. Geomorphology 49(1–2): 71–88. https://doi.org/10.1016/S0169-555X(02)00164-2

Sanson RL 2005. The AgriBase farm location database. Proceedings of the New Zealand Society of Animal Production 65: 93–96.

Smith HG, Betts H 2021. Memorandum on implementing a national index for susceptibility to streambank erosion. Manaaki Whenua – Landcare Research contract report LC3998 for the Ministry for the Environment.

Smith HG, Neverman AJ, Betts H, Herzig A 2024. Improving understanding and management of erosion with LiDAR. Manaaki Whenua – Landcare Research contract report for Hawke's Bay Regional Council.

Smith HG, Neverman AJ, Betts H, Spiekermann R 2023. The influence of spatial patterns in rainfall on shallow landslides. Geomorphology 437: 108795. https://doi.org/10.1016/j.geomorph.2023.108795

Spiekermann R, McColl S, Fuller I, Dymond J, Burkitt L, Smith HG 2021. Quantifying the influence of individual trees on slope stability at landscape scale. Journal of Environmental Management 286: 112194. https://doi.org/10.1016/j.jenvman.2021.112194

Spiekermann R, Smith HG, McColl S, Burkitt L, Fuller I 2022a. Development of a morphometric connectivity model to mitigate sediment derived from storm-driven shallow landslides. Ecological Engineering 180: 106676. https://doi.org/10.1016/j.ecoleng.2022.106676

Spiekermann RI, Smith HG, McColl S, Burkitt L, Fuller I 2022b. Quantifying effectiveness of trees for landslide erosion control. Geomorphology 396: 107993. https://doi.org/10.1016/j.geomorph.2021.107993

Spiekermann RI, van Zadelhoff F, Schindler J, Smith HG, Phillips C, Schwarz M 2023. Comparing physical and statistical landslide susceptibility models at the scale of individual trees. Geomorphology 440: 108870. https://doi.org/10.1016/j.geomorph.2023.108870

Tsyplenkov A, Smith HG, Betts H, Neverman AJ 2023. Data-driven shallow landslide connectivity analysis to reduce sediment delivery to streams. Geoscience Society of New Zealand Annual Conference 2023: Abstracts 164A, 280.

Zörner J, Dymond J, Shepherd J, Wiser S, Jolly B 2018. LiDAR-based regional inventory of tall trees – Wellington, New Zealand. Forests 9(11): 1–16. https://doi.org/10.3390/f9110702

Appendix – Summary statistics of pastoral areas within the 50 farms selected for further analysis.

HBFID	Farm-pasture area (km²)	Mean 48 h rainfall during Cyclone Gabrielle (mm)	Fraction of farm area mapped by Leith et al. (2023)	Number of landslides	Landslide density (scars/km²)	Spaced tree density (trees/km²)
1	12	257	100%	1,916	166	47
2	1.2	347	100%	129	103	58
3	3.5	337	100%	151	43	56
4	1.4	336	100%	73	51	47
5	4.6	364	100%	692	151	74
6	1.7	407	100%	314	189	115
7	2.3	382	100%	145	64	116
8	1.7	322	100%	98	57	68
9	2.9	331	100%	408	143	88
10	7.7	302	100%	985	128	94
11	2	325	100%	84	41	74
12	1.1	321	100%	17	15	35
13	6.3	351	100%	302	48	92
14	9.7	278	100%	1,377	143	159
15	2.9	269	100%	204	71	99
16	1.5	348	100%	151	101	91
17	2.9	421	99%	357	124	196
18	3.8	349	100%	477	126	170
19	4.5	357	100%	511	114	152
20	5.4	416	99%	1,090	203	119
21	7.7	253	100%	1,259	164	82
22	1.1	290	100%	110	100	62
23	2.2	427	97%	149	67	143
24	3.7	496	100%	933	253	159
25	3.4	329	100%	249	73	162
26	1.7	320	100%	145	87	86
27	3.6	368	100%	314	88	97
28	2.1	425	100%	356	171	201
29	6	279	100%	622	103	153
30	2.7	373	100%	233	87	161
31	4	333	97%	817	203	95
32	1.2	436	100%	235	198	354
33	3	352	100%	519	173	162

HBFID	Farm-pasture area (km^2)	Mean 48 h rainfall during Cyclone Gabrielle (mm)	Fraction of farm area mapped by Leith et al. (2023)	Number of landslides	Landslide density (scars/km^2)	Spaced tree density (trees/km^2)
34	3.2	387	100%	339	107	174
35	3.6	289	96%	434	119	164
36	5.4	347	99%	468	87	194
37	2.7	431	100%	452	166	95
38	4.3	452	100%	597	139	115
39	1.8	519	100%	148	82	113
40	2.3	457	100%	686	300	243
41	3	480	100%	838	278	176
42	4.1	296	98%	43	11	29
43	1	364	100%	28	27	119
44	1.3	386	100%	235	186	211
45	1.1	342	100%	128	121	148
46	7.1	349	98%	223	31	145
47	3.3	270	98%	90	28	40
48	4.5	275	100%	151	34	99
49	1.3	270	100%	46	35	133
50	1.4	275	100%	64	45	112

TE MAHERE TAONGA O
TE PAPA RĒHIA O TE WHANGA
AHURIRI REGIONAL PARK MASTERPLAN
DRAFT ISSUE FOR PUBLIC ENGAGEMENT

STORMWATER

Increase the resilience of the City's stormwater infrastructure network by maintaining and enhancing attenuation on the site as part of a series of initiatives to reduce the impacts of rainfall events on the urban areas of Napier.

WATER QUALITY

Improve the quality of water discharged from the City's urban waterways noting these form part of the municipal stormwater network.

MAURI

To return the mauri back to Te Whanga, enhance and preserve mahinga kai and improve harmony with Papatūānuku.

ECOLOGICAL EXCELLENCE

Promote the re-establishment of native habitat values throughout the site and its interface with Te Whanga and the Taipo Stream.

NATURAL ENVIRONMENT

To maintain a predominantly natural environment.

SIGNIFICANT INFRASTRUCTURE

Recognise the functional need of regionally significant infrastructure.

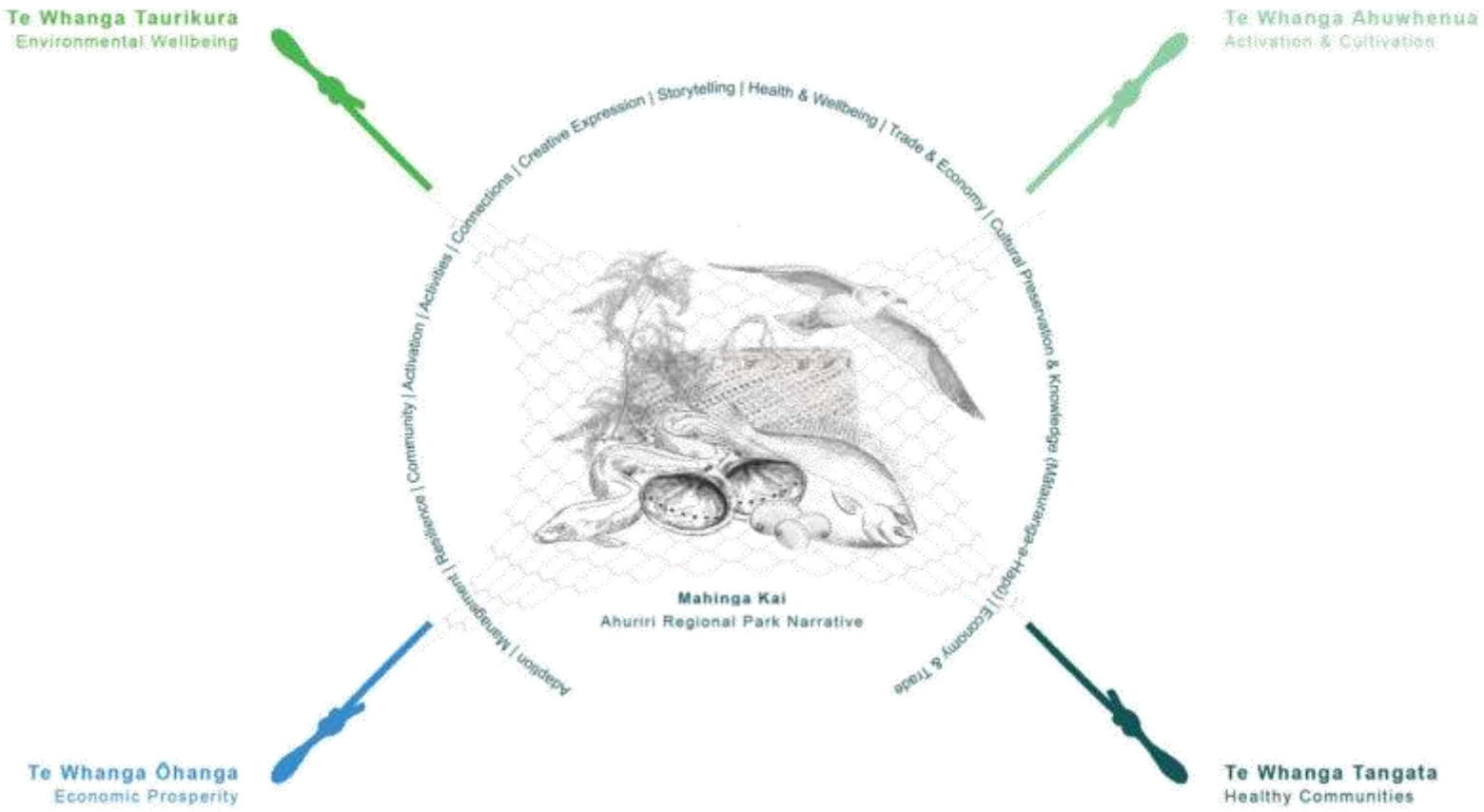
Te Whanga Taurikura
Environmental Wellbeing
Te Whanga Ahuwhenua
Activation & Cultivation
Connections | Creative Expression | Storytelling | Health & Wellbeing | Trade & Economy | Cultural Preservation & Knowledge (Mātauranga-a-Hapū) | Economy & Trade
Adaption | Management | Resilience | Community | Activation | Activities
Mahinga Kai
Ahuriri Regional Park Narrative
Te Whanga Ōhanga
Economic Prosperity
Te Whanga Tangata
Healthy Communities

TE WHANGANUI-A-OROTU
AHURIRI REGIONAL PARK 2050 - CORE PROGRAMS

TE WHANGANUI A OROTU
AHURIRI REGIONAL PARK 2050 - FUTURE POTENTIAL PROGRAMS

TE WHANGANUI A GROTU
TAIPO STREAM
PUPIPU STREAM
Toilets
Wayfinding and Cultural Story telling nodes
Existing waterway link to wetland south of stop bank maintained
Existing Blokart Hawkes Bay Facility
Proposed vehicle access
Pedestrian/ cycleway
CORE REGIONAL PARK PROGRAMS
1 Lagoon Farm Treatment Wetlands (Delivered as separate project)
2 Plant production nursery for on-site use
3 Ahuriri Regional Park Waharoa | Entrance
4 Te Wao Nui | Regenerating Forest
5 Regenerating Native Wetland
6 Naturalisation of existing drain channel
7 Trail connections to existing cycleway
8 Island nodes
9 Landmark pou and interactive wetland play zone
10 Ahuriri Regional Park Visitor Hub
11 Discovery + Learning | Play + Sculptural Park
12 Manuka Plantation
13 Pa Harakeke flax collection
14 South Marsh Waka Landing stop and stay area with Lookout platforms and Picnic facilities
15 Taipo Confluence Waka Landing & lookout tower
16 Flexible use amphitheatre space
17 Wool shed Multi use Community Events Centre
18 Community Foraging Zone and Trails
19 Regional Park Eco Camp - short stay guests
20 Pump station Waka Landing & Visitor Kiosk
Boffa Miskell
www.boffamiskell.co.nz
0
300m
1:10,000 @ A3
AHURIRI REGIONAL PARK MASTERPLAN
DRAFT MASTERPLAN - CORE PARK PROGRAMS

TE WHANGANUI A OROTU
YARGE STREAM
PORIRUA STREAM
Toilets
Wayfinding and Cultural Story telling nodes
Existing waterway link to wetland south of stop bank maintained
Existing Blokart Hawkes Bay Facility
Proposed vehicle acces
Pedestrian/ cycleway
POTENTIAL FUTURE PROGRAMS
(Developed with public + private partnerships and NGOs)
A Expansion to Plant nursery for commercial, retail & educational capacity
B Expansion area for active recreational activities
C Whare Pora | Cultural Weaving & Education Centre space
D Freedom camping area
E Accomodation/ Health Retreat Facility
F Development of complementary commercial use area
G Predator Proof Fence (indicative potential alignment only)
H Eco-Sanctuary Main Entrance
I Freshwater research and demonstration ponds (e.g. Tuna | eel, kōura | freshwater crayfish)
J Salt water research and demonstration ponds (e.g. Papaka | Crab, Patiki | Flounder, Purimu | Cockles)
K Whare Wananga | Learning & Research Hub
L Te Whanganui-a-Orotu Landmark Gateway Pedestrian/Cycle Bridge.
M Restoring historic bridge connection to north bank
Boffa Miskell
www.boffamiskell.co.nz
0
300m
1:10,000 @ A3
AHURIRI REGIONAL PARK MASTERPLAN
DRAFT MASTERPLAN - POTENTIAL FUTURE PROGRAMS

CORE REGIONAL PARK PROGRAMS

1. Lagoon Farm Treatment Wetlands (Delivered as separate project)
2. Plant production nursery for on-site use
3. Ahuriri Regional Park Waharoa | Entrance
4. Te Wao Nui | Regenerating Forest
5. Regenerating Native Wetland
6. Naturalisation of existing drain channel

0 250m
1:7,500 @ A3

SYDNEY PARK TREATMENT PONDS

TE KUKUMAI O TOA WETLAND, PORIRUA (PORIRUA CITY COUNCIL)

PYRAMIDA HILLS CULTURAL HERITAGE PARK, TAURANGA

PEKAPEKA WETLANDS, HASTINGS

CORE REGIONAL PARK PROGRAMS

- 7 Trail connections to existing cycleway
- 8 Island nodes
- 9 Landmark pou and interactive wetland play zone
- 10 Ahuriri Regional Park Visitor Hub

0 250m
1:7,500 @ A3

PAPAMOA HILLS CULTURAL HERITAGE PARK, TAURANGA

PUNAKAIKI VISITOR CENTRE, PUNAKAIKI

TE KAIKOHO NATURE PRECINCT, HAMILTON

POU AO-NUKU AO-WAIKA, TAURPO

CORE REGIONAL PARK PROGRAMS

11. Discovery + Learning | Play + Sculptural Park
12. Manuka Plantation
13. Pa Harakeke flax collection
14. South Marsh Waka Landing stop and stay area with Lookout platforms and Picnic facilities
15. Taipo Confluence Waka Landing & lookout tower

POUWHENUA, PAKOWHAI

VIEWING TOWER VECHT RIVER ATELIERBEIN, ATELIERBEIN ARCHITECTEN

BAY OF ISLANDS WAKA TOUR

CORE REGIONAL PARK PROGRAMS

- (16) Flexible use amphitheatre space
- (17) Wool shed Multi use Community Events Centre
- (18) Community Foraging Zone and Trails
- (19) Regional Park Eco Camp - short stay guests
- (20) Pump station Waka Landing & Visitor Kiosk

0 500m
1:15,000 @ A3

BOWL OF BROOKLANDS, NEW PLYMOUTH

MATARAWA VILLAGE FARMERS MARKET

YE PARAPARA | HAMILTON GARDENS, HAMILTON

ROLLING HUTS, METHOW VALLEY, WASHINGTON STATE, US

MAKAHIKA OUTDOOR PURSUIT CENTRE, LEVIN

POTENTIAL FUTURE PROGRAMS

- Expansion to Plant nursery for commercial, retail & educational capacity
- Expansion area for active recreational activities
- Whare Pore | Cultural Weaving & Education Centre space
- Freedom camping area
- Accommodation/ Health Retreat Facility
- Development of complementary commercial use area

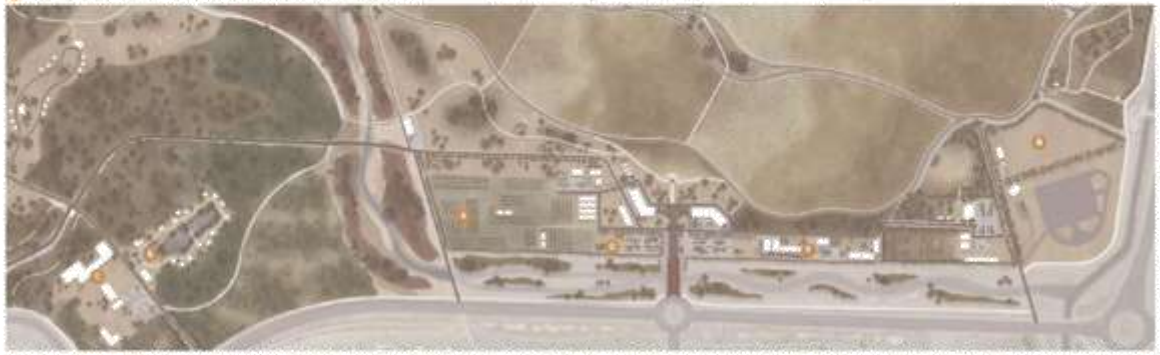

0 250m
1:7,500 @ A3

TAKAANGA (THE LEARNING CENTRE, WAITAKI - HB ARCHITECTURE

POTENTIAL FUTURE PROGRAMS

- Predator Proof Fence (indicative potential alignment only)
- Eco-Sanctuary Main Entrance
- Freshwater research and demonstration ponds (e.g. tuna | eel, kōura | freshwater crayfish)
- Salt water research and demonstration ponds (e.g. Papaka | Crab, Paliki | Flounder, Purimu | Cockles)
- Whare Wānanga | Learning & Research Hub
- Te Whanganui-a-Orotu Landmark Gateway Pedestrian/Cycle Bridge
- Restoring historic bridge connection to north bank

TE ARAPEKAPEKA BRIDGE, WAIKATO

AHURIRI REGIONAL PARK MASTERPLAN

PERSPECTIVE - TAIPO STREAM WAKA LANDING & WATCHTOWER

AHURIRI REGIONAL PARK MASTERPLAN

PERSPECTIVE - PUMPSTATION WAKA LANDING & VISITOR KIOSK

AHURIRI REGIONAL PARK MASTERPLAN

PERSPECTIVE - REGENERATING FOREST & NATURAL WETLANDS

AHURIRI REGIONAL PARK MASTERPLAN
PERSPECTIVE - TREATMENT WETLAND ISLANDS

AHURIRI REGIONAL PARK MASTERPLAN
PERSPECTIVE - VISITOR CENTRE AERIAL

AHURIRI REGIONAL PARK MASTERPLAN

DIAGRAM - PROGRAMMING

AHURIRI REGIONAL PARK MASTERPLAN

DIAGRAM - ECOTONES

AHURIRI REGIONAL PARK MASTERPLAN

DIAGRAM - HYDROLOGY

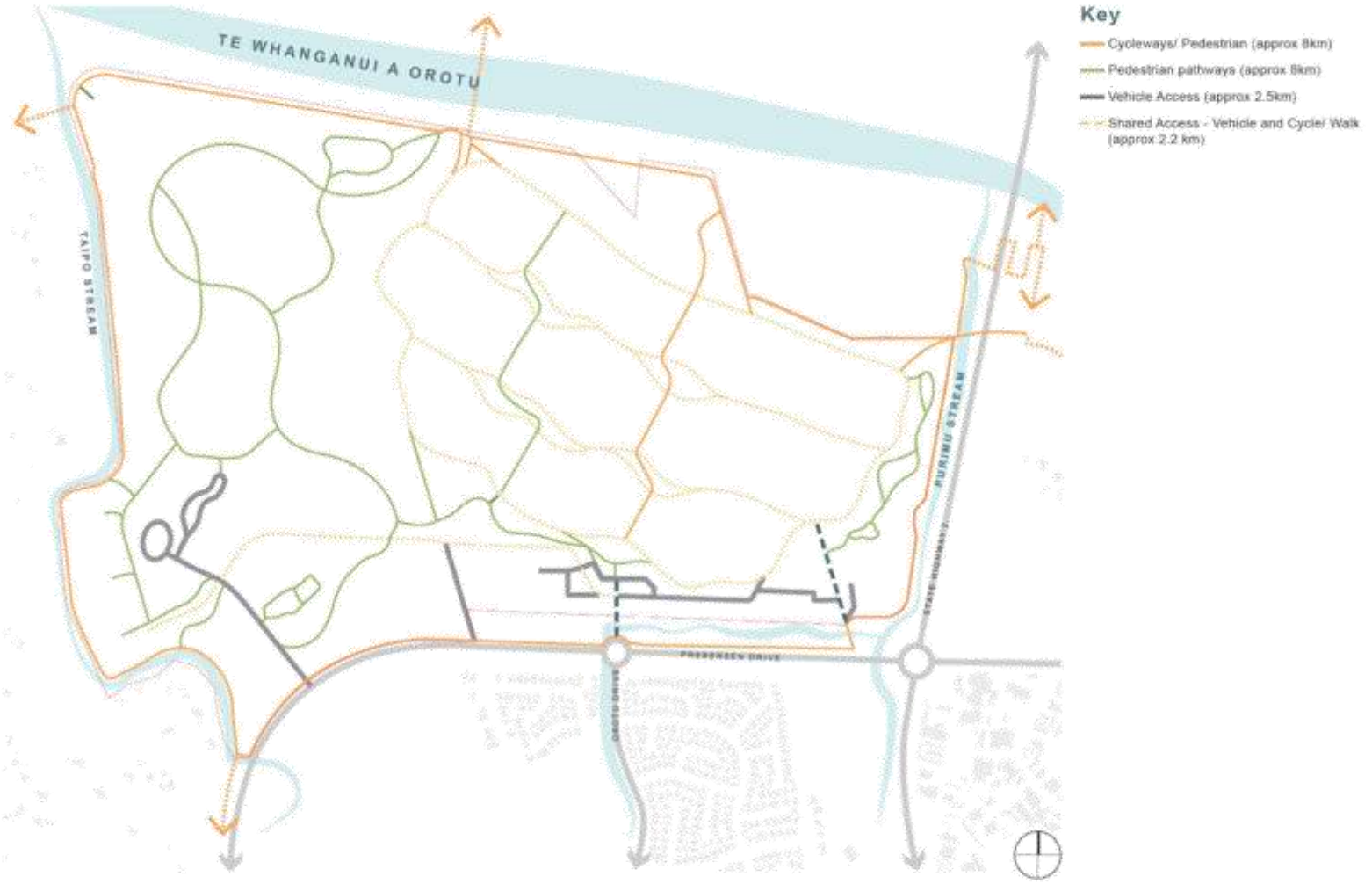

AHURIRI REGIONAL PARK MASTERPLAN

DIAGRAM - CIRCULATION

AHURIRI REGIONAL PARK MASTERPLAN

DIAGRAM - CREATIVE ARTS & WAYFINDING

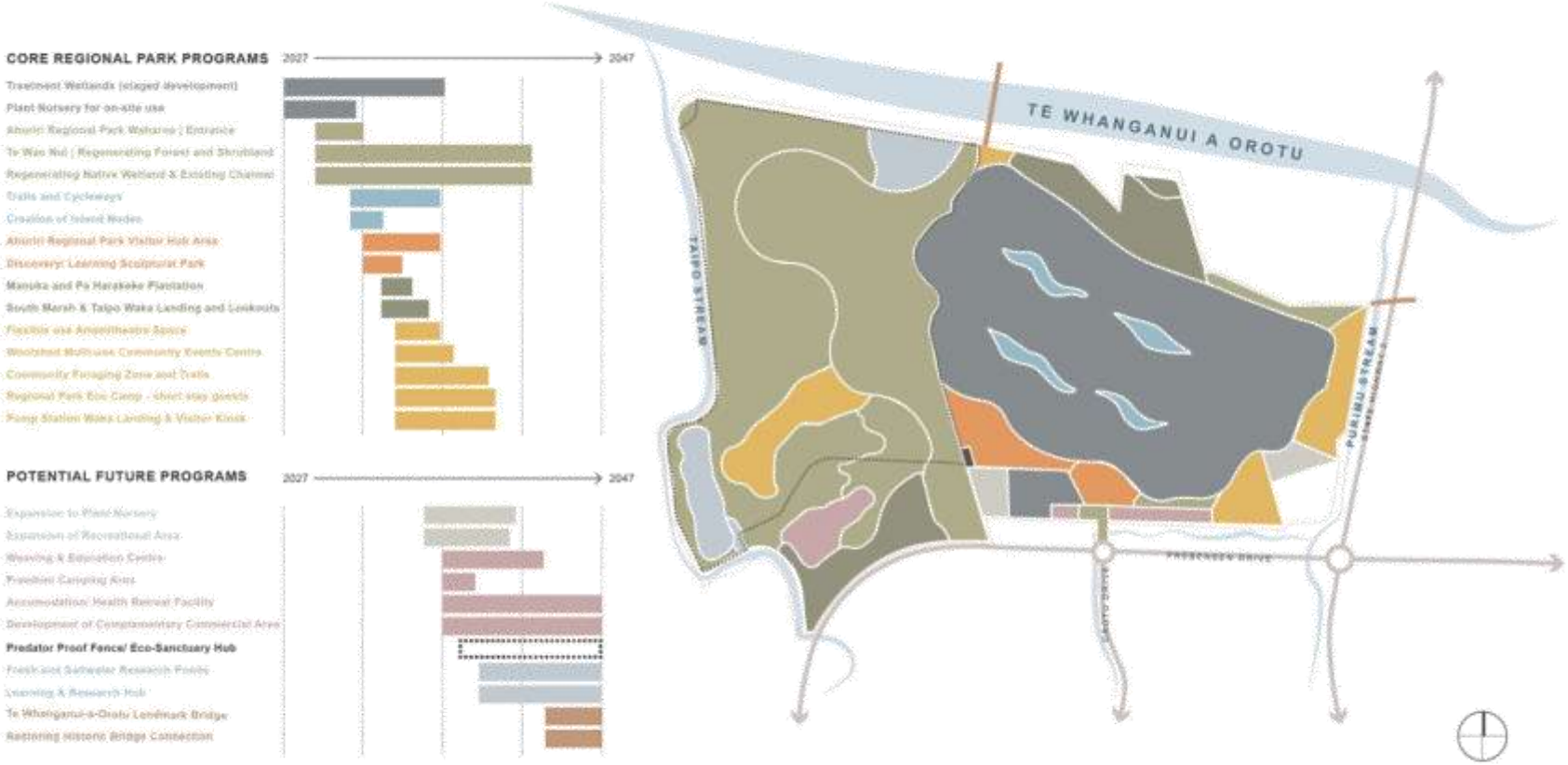

AHURIRI REGIONAL PARK MASTERPLAN
INDICATIVE STAGING

Regional shallow landslide connectivity modelling and topographic wetness analysis

Prepared for: Hawke's Bay Regional Council November 2024

Hawkes Bay Regional Council Publication No. 5673

HAWKES BAY
REGIONAL COUNCIL
TE KAUNIHERA Ā-ROHE O TE MATAU-A-MĀUI

ISSN 2703-2051 (Online)
ISSN 2703-2043 (Print)

HAWKES BAY
REGIONAL COUNCIL
TE KAUNIHERA Ā-ROHE O TE MATAU-A-MĀUI

(06) 835 9200
0800 108 838
Private Bag 6006 Napier 4142
159 Dalton Street . Napier 4110

Environmental Science

Regional shallow landslide connectivity modelling and topographic wetness analysis

Prepared for: Hawke's Bay Regional Council November 2024

Hawkes Bay Regional Council Publication No. Report number 5673

Reviewed By:
Dr Ashton Eaves – Senior Land Scientist

Approved By:
Dr Haley Ataera – Science Manager

ISSN 2703-2051 (Online)
ISSN 2703-2043 (Print)

Manaaki Whenua
Landcare Research

Regional shallow landslide connectivity modelling and topographic wetness analysis

Prepared for: Hawke's Bay Regional Council

November 2024

Regional shallow landslide connectivity modelling and topographic wetness analysis

Contract Report: LC4550

Anatolii Tsyplenkov, Hugh Smith

Manaaki Whenua – Landcare Research

Reviewed by:	*Approved for release by:*
Andrew Neverman Researcher – Geomorphology Manaaki Whenua – Landcare Research	Jo Cavanagh Acting Portfolio Leader – Managing Land & Water Manaaki Whenua – Landcare Research

Disclaimer

This report has been prepared by Landcare Research New Zealand Ltd for Hawke's Bay Regional Council. If used by other parties, no warranty or representation is given as to its accuracy and no liability is accepted for loss or damage arising directly or indirectly from reliance on the information in it.

Contents

Summary v
1 Introduction 1
2 Background 1
3 Objectives 3
4 Methods 3
4.1 Landslide-to-stream connectivity modelling 3
4.2 Coupling landslide susceptibility and connectivity 5
4.3 Validation with Cyclone Gabrielle data 5
4.4 Topographic wetness index (TWI) 6
5 Results 7
5.1 Landslide-to-stream connectivity 7
5.2 Topographic wetness index (TWI) 9
6 Conclusions 10
7 Acknowledgements 10
8 References 11

Summary

Project and client

- Hawke's Bay Regional Council (HBRC) contracted Manaaki Whenua – Landcare Research (MWLR) to produce morphometric landslide-to-stream connectivity layers for rainfall-induced shallow landslides to improve understanding and management of erosion in the Hawke's Bay region.
- As part of this project, HBRC asked MWLR to estimate the topographic wetness index (TWI) to support land use planning in the region.

Objectives

The project had the following objectives.

- Model the rainfall induced shallow landslide-to-stream connectivity in the Hawke's Bay region at 5 m resolution.
- Produce a combined shallow landslide susceptibility and connectivity class-based raster map for the Hawke's Bay region.
- Estimate the TWI for the region based on the light detection and ranging (LiDAR)–derived digital elevation model (DEM).

Methods

- Using the landslide morphometric connectivity binary logistic regression (BLR) model framework from Spiekermann et al. (2022) and Tsyplenkov et al. (2023),[1] we estimated shallow landslide-to-stream connectivity for the Hawke's Bay region.
- Predictive performance of the BLR model was assessed using cross-validation. Model classification (i.e. connected versus unconnected landslide scars) was evaluated using receiver operating characteristic curves (ROC) and calculating the area under curve (AUC) based on 100 model iterations.
- Following (2023) Ministry for the Environment guidance for critical source areas we estimated TWI based on the LiDAR-derived DEM at 5 m horizontal resolution.

[1] Spiekermann RI, Smith HG, McColl S, Burkitt L, Fuller IC 2022. Development of a morphometric connectivity model to mitigate sediment derived from storm-driven shallow landslides. Ecological Engineering. 180: 106676. https://doi.org/10.1016/j.ecoleng.2022.106676
Tsyplenkov A, Smith HG, Betts H, Neverman A 2023. Data-driven shallow landslide connectivity analysis to reduce sediment delivery to streams. In: Frontin-Rollet GE, Nodder SD (eds) Geoscience Society of New Zealand Annual Conference 2023: Abstracts Volume GSNZ Miscellaneous Publication 164A. Pp. 250–250.

Results

- Region-wide predictions of shallow landslide-to-stream connectivity were produced with probability- and class-based scales, while the TWI was estimated across the region and supplied as a raster layer.
- The Cyclone Gabrielle landslide data provided an independent validation of the mapped connectivity classes. We found that 62% of all Gabrielle-related landslides that connected to streams had source areas located within the 'High' connectivity class area, while 21% occurred in the 'Moderate' class and 17% in the 'Low' class.
- The class-based landslide-to-stream connectivity raster was combined with the previously supplied class-based shallow landslide susceptibility layer where all forestry land mapped in the New Zealand Land Cover Database (LCDB v5.0) had been converted to grass cover for analysis. The resulting combined class-based layer may be used to identify areas that are both highly susceptible to landsliding and likely to generate runout that reaches the stream network.

Conclusions

- The combined regional shallow landslide susceptibility and connectivity layer provides land managers with high resolution spatial information that may be used to support future land use planning and to better target tree planting to those areas of pastoral land most susceptible to instability and likely to deliver sediment to streams.
- The high-resolution TWI estimates based on the LiDAR-derived DEM may be used to identify critical source areas to support land and water planning in the region.

1 Introduction

Hawke's Bay Regional Council (HBRC) engaged Manaaki Whenua – Landcare Research (MWLR) to produce morphometric landslide-to-stream connectivity layers for rainfall-induced shallow landslides and to estimate the topographic wetness index (TWI) to support future land use planning in the region.

The present report adopts a data-driven, statistical modelling approach designed to assess the spatial probability of runout from a shallow landslide reaching the stream network. The results of this model were used in conjunction with the regional shallow landslide susceptibility layer previously produced for HBRC (Smith et al. 2024). The combination of spatial information on landslide susceptibility and landslide-to-stream connectivity may be used to identify at high resolution (5 m) those areas that are both highly susceptible to landslides and highly likely to deliver sediment to streams in the future.

In response to the Ministry for the Environment's (MfE) guidance on critical source areas (Ministry for the Environment 2023), HBRC also requested we compute the topographic wetness index (TWI) for the region using a light detection and ranging (LiDAR)–derived 5 m digital elevation model (DEM). The TWI provides a spatial estimate of areas prone to saturation and generation of surface runoff (Beven & Kirkby 1979).

We computed the topographic wetness index using the 5 m LiDAR-derived DEM and produced a raster layer containing TWI values that may be used to identify critical source areas across the region.

2 Background

The HBRC have previously commissioned work to produce a regional rainfall-induced shallow landslide susceptibility layer (Smith et al. 2024). Statistical landslide susceptibility modelling by Smith et al. (2024) used data from over 116,000 shallow landslide scars (source areas) and was based on LiDAR-derived topographic inputs as well as land cover and rock type data.

Region-wide predictions of shallow landslide susceptibility were produced as raster layers at 5 m resolution with probability- and class-based scales for contemporary land cover (see Figure 1) and for land cover where all forestry land mapped in the New Zealand Land Cover Database (LCDB v5.0) has been converted to grass cover for the purpose of analysis. This forestry-to-grass conversion provided a common reference condition for comparing the inherent susceptibility of forestry and pastoral land.

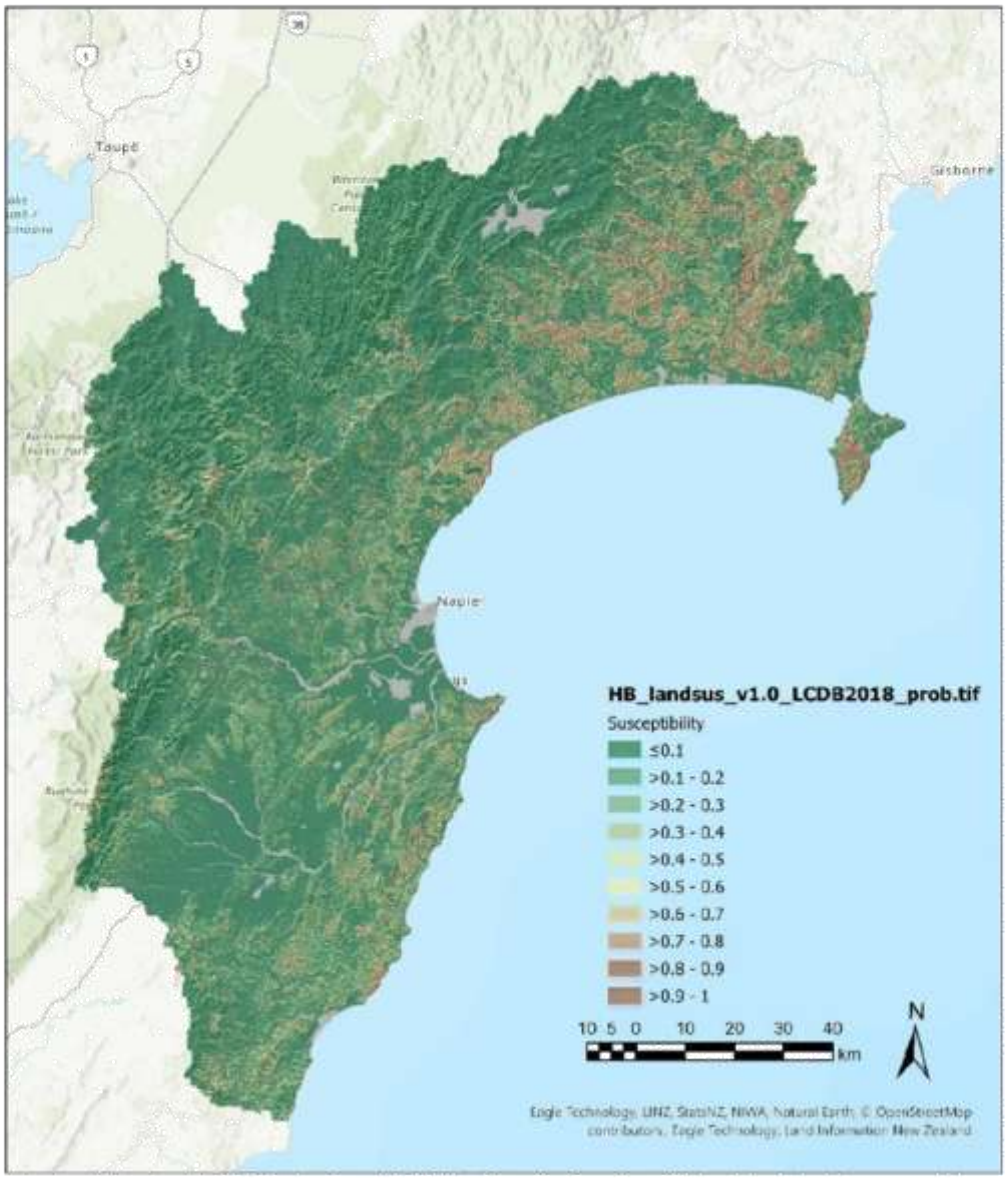

Figure 1. Shallow landslide susceptibility (probability scale) for the Hawke's Bay region based on the LiDAR-derived 5 m digital elevation model (DEM) and 2018 land cover from LCDB v5.0 (Source: Reproduced from Smith et al. 2024, Fig. 10).

Recent work by MWLR proposed a data-driven model framework to estimate spatial probability of a landslide reaching the stream network. The framework is based on statistical models developed by MWLR as part of the Smarter targeting of erosion control (STEC) MBIE Endeavour programme (2018–2023). Initial work by Spiekermann et al. (2022) described an earlier version of the connectivity model. Subsequently, this modelling

approach was further developed using an expanded landslide data set (Tsyplenkov et al. 2023; Tsyplenkov et al. 2024[2]).

We use spatial outputs from the shallow landslide susceptibility and morphometric, landslide-to-stream connectivity models to produce a combined class-based layer that expresses both landslide susceptibility and landslide-to-stream connectivity.

3 Objectives

The project had the following objectives.

- Model the rainfall induced shallow landslide-to-stream connectivity in the Hawke's Bay region at 5 m resolution.
- Produce a combined shallow landslide susceptibility and connectivity class-based raster map for the Hawke's Bay region.
- Estimate the TWI for the region based on the light detection and ranging (LiDAR)–derived digital elevation model (DEM).

4 Methods

4.1 Landslide-to-stream connectivity modelling

Morphometric landslide-to-stream connectivity was predicted based on a LiDAR-derived 5 m DEM using a binary logistic regression model (Spiekermann et al. 2022; Tsyplenkov et al. 2023). Connectivity was expressed as a spatial probability (range 0–1), where areas with values close to 1 have a higher likelihood of connecting to a stream network, while areas close to 0 have a low likelihood of connection. Connectivity analysis requires a digital representation of the stream network and other receiving environments such as lakes. For this purpose, the DEM-derived stream network (using a D8 flow accumulation algorithm and a 10 ha channel initiation threshold; refer to Smith et al. 2024) was merged with a derived national layer comprising river and lake polygons, which was used to represent wide river channels and waterbodies (Smith & Betts 2021).

The binary logistic regression (BLR) model was fitted using spatial covariate data for connected and unconnected landslides obtained from mapping areas that intersect with available LiDAR coverages in the Hawke's Bay, Gisborne, and Greater Wellington regions. The combined landslide source and deposit inventory used for modelling presently comprises approximately 41,000 landslides, where 8.5% of them are connected to the

[2] At date of writing this paper is still under review, so is not included in the main reference list: Tsyplenkov A, Smith HG, Betts H, Neverman A 2024. Data-driven shallow landslide connectivity analysis to reduce sediment delivery to streams. Global and Earth Surface Processes Change: (in review)

stream network. Additional landslide data may be obtained and used to further refine the model in the future.

Covariate data available for potential selection and inclusion in the connectivity model included a range of DEM-derived morphometric variables as well as land cover and rock type classes. An automated LASSO (least absolute shrinkage and selection operator) procedure was used to select variables and estimate model coefficients. Overall, we tested 11 different models of various complexity and more than 45 connectivity predictors, describing the landslides morphology, underlying geology and land cover, and terrain morphometry. Our results revealed a strong dependency of connectivity on the overland flow distance to the stream network ($DownDist$). Results obtained from a single-variable model based on the $DownDist$ exhibited similar predictive performance compared to more complex, multi-variable models (Tsyplenkov et al. 2023; Tsyplenkov et al. 2024[3]). Therefore the $DownDist$-based single variable model was chosen for regional predictions.

We cross-validated the BLR model within the tidymodels R-package infrastructure (Kuhn & Wickham 2018) using the following procedure.

1. Balanced bootstrap resampling was performed with replacement, ensuring that every bootstrap had an equal number of connected and unconnected landslides.
2. Each bootstrap resample was further split into training and testing data sets, and the model was fitted to the training data set.
3. The testing data set was used to evaluate the model performance with a set of metrics described below

Model classification performance was evaluated using receiver operating characteristic curves and calculation of the area under the receiver operating characteristic curve (AUC) using the yardstick R-package (Kuhn et al. 2017). A good AUC score is considered to be between 0.8 and 0.9, while an excellent score is greater than 0.9 (Obuchowski 2003).

The whole procedure was repeated and produced 100 different models, with their corresponding parameter estimates and model metrics. The model with the highest AUC value was used for predictions. In the present version, the BLR model achieved a median AUC of 0.87 in cross-validation.

We classified spatial probabilities predicted with the BLR connectivity model into three classes ('High', 'Moderate', and 'Low'). Thresholds used to define each connectivity class were determined by ranking the connected landslides used to fit the model by their probability values in decreasing order. 'High' connectivity corresponds to 80% of the mapped landslides, which have probability values ≥ 0.58. 'Moderate' corresponds to a further 15% of the mapped landslides, which have probability values between ≥0.18 to <0.58, while 'Low' relates to the remaining 5% of landslides, with values <0.18.

[3] See footnote 2 for citation.

4.2 Coupling landslide susceptibility and connectivity

To visualise and interpret spatial patterns in connectivity we need to consider the spatial variation in landslide susceptibility (Smith et al. 2021). For this purpose, we used the previously supplied (Smith et al. 2024) shallow landslide susceptibility layer ('HB_landsus_v1.0_forestrytograss_class.tif') where forestry land covers (i.e. 'Exotic Forest' and 'Forest – Harvested') mapped in the New Zealand Land Cover Database (LCDB v5.0) 2018 class have been converted to grass cover for the purpose of spatial analysis. This provides a common reference condition (i.e. removes woody cover) for assessing the inherent susceptibility of these areas independent of the time-varying influence of forest cover. The Erosion susceptibility classification (ESC) in the National Environmental Standards for Commercial Forestry (NES-CF) also assesses susceptibility by assuming land is under permanent pasture cover (Ministry for Primary Industries 2017).

To integrate spatial predictions of landslide susceptibility and connectivity first we reclassified the continuous connectivity probability raster into classes using thresholds described above (see Section 4.1). An intersection of the two reclassified spatial predictions (susceptibility and connectivity) resulted in a matrix of nine joint classes describing both the likelihood of landslides occurring in the future and the potential for landslide sediment to be delivered to the stream network. We named the classes accordingly (i.e. the intersection of high susceptibility and high connectivity classes produced 'High LS / High Con' corresponding to a class where landslides are likely to occur and reach the stream network). To avoid ambiguous situations where high connectivity exists while the landslide susceptibility is low, we merged all connectivity classes in the low susceptibility zone into a single class, referred to as 'Low LS'.

4.3 Validation with Cyclone Gabrielle data

We also compared the connectivity model's spatial predictions with interim landslide mapping data for Cyclone Gabrielle (data accessed on 1 November 2023) in the Hawke's Bay region (Leith et al. 2023). The Gabrielle landslide data were not used in training the model and thus these data may be used to provide an independent validation of the class-based map.

The interim landslide mapping data for Cyclone Gabrielle covers approximately 19% of the Hawke's Bay region (as of 01 November 2023). The inventory contains 104,229 landslide scars points and 110,886 landslide runout lines. The preprocessing and data quality checks were as follows. First, we removed all landslide scar points which had no associated runout mapped (and vice versa). Secondly, we defined the landslide terminus points as the most downslope point on the landslide runout lines. Finally, for both scar and runout terminus points we extracted the elevation from the 1 m LiDAR DEM and removed those data where the mapped landslide source point was located below the runout terminus point. As a result of this procedure, approximately 2.7% of the original landslide inventory was removed, and 101,400 scars were left and used for validation.

4.4 Topographic wetness index (TWI)

The TWI concept was initially proposed by Beven and Kirkby (1979). The TWI integrates the water supply from upslope catchment area and downslope water drainage for each cell in a DEM (Kopecký et al. 2021). Therefore, TWI has two main components:

$$TWI = \ln \frac{SCA}{\tan \beta}, \quad (1)$$

where SCA is a specific catchment area in m²/m; and β is local slope in radians. The SCA accounts for accumulated water, whereas the local slope β accounts for the local gravitational force moving the accumulated water downwards. In NZ, the TWI has been proposed by as a basis for delineating critical source areas (Ministry for the Environment 2023).

However, the MfE 2023 document does not mention the recommended flow accumulation algorithm for SCA estimation. Previous studies (Grabs et al. 2009; Kopecký et al. 2021; Riihimäki et al. 2021) showed that Equation 1 is very sensitive to the SCA parameter, and the resulting TWI can vary significantly across flow accumulation algorithms. Therefore, in the current report, we adapted the workflow (see Figure 2) from Kopecky et al. (2021), who found it to produce the most reliable and robust results for predicting soil moisture with TWI. We used Quinn's (1991) multiple flow accumulation algorithm to retrieve SCA, and the slope was estimated using the 3rd-order bivariate Taylor polynomial method described by Florinsky (2016). All procedures were performed in the standalone Whitebox Tools (Lindsay 2016) using the LiDAR-derived DEM resampled to 5 m horizontal resolution.

The DEM-derived stream network, which was created using a D8 flow accumulation algorithm and a 10 ha channel initiation threshold (refer to Smith et al. 2024), was burned into the DEM before the TWI estimation.

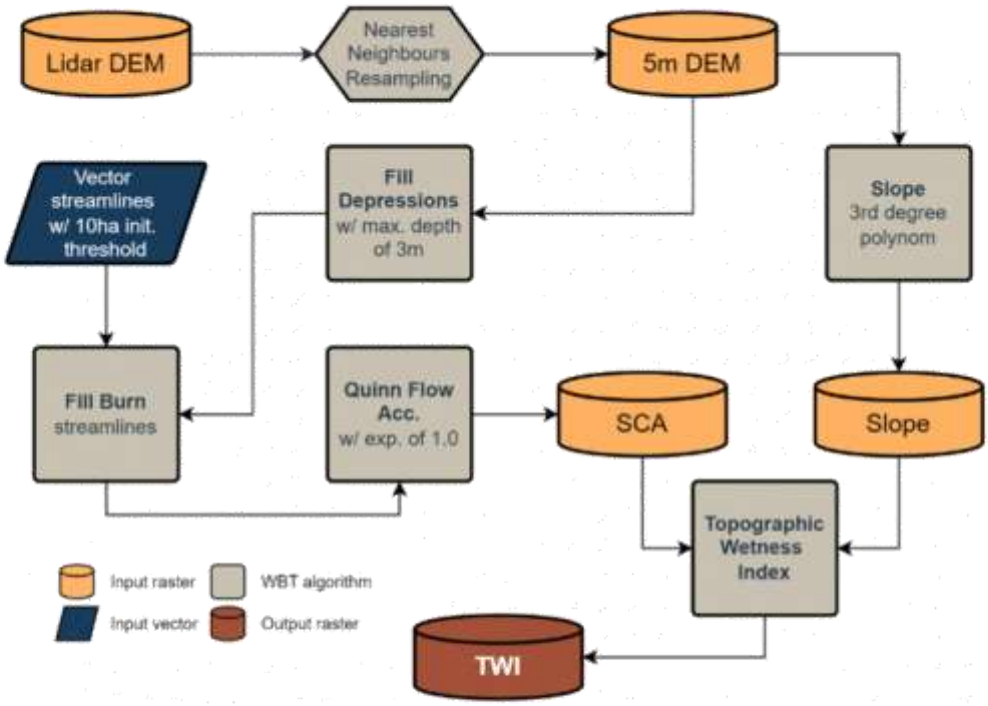

Figure 2. Whitebox Tools (WBT) workflow used in the current report to estimate topographic wetness index (TWI) for Hawke's Bay at 5 m horizontal resolution. Names of the WBT algorithms are in bold.

5 Results

5.1 Landslide-to-stream connectivity

The combined shallow landslide susceptibility and landslide-to-stream connectivity layer is shown in Figure 3. Most land (72%, see Table 1) within the Hawke's Bay region lies in the first class – 'Low LS'. The 'High LS / High Con' class occupies 539 km^2 or 3.42% of the region. 'High LS / High Con' together with 'High LS / Mod Con' and 'Mod LS / High Con' classes outline most of the land prone to both landslide occurrence and landslide sediment delivery to streams. These three classes (i.e. classes 4, 6 and 7 in Table 1 and Figure 3) cover c.10% of the region and are most extensive in northern Hawke's Bay.

Cyclone Gabrielle triggered at least 101,400 landslides in the Hawke's Bay region according to interim landslide mapping data (Leith et al. 2023). Of these scars, 10.7% were connected to a 10 ha digital stream network combined with lakes and river polygons. Since the Cyclone Gabrielle landslide mapping data was not used in training the connectivity model, these data provided a basis for independently assessing the class-based connectivity map.

We found that most (62%) Gabrielle-related landslides that connected to streams had source areas (mapped using centroid points) located within the 'High' connectivity class area, while 21% were in the 'Moderate' class, and 17% in the 'Low' class.

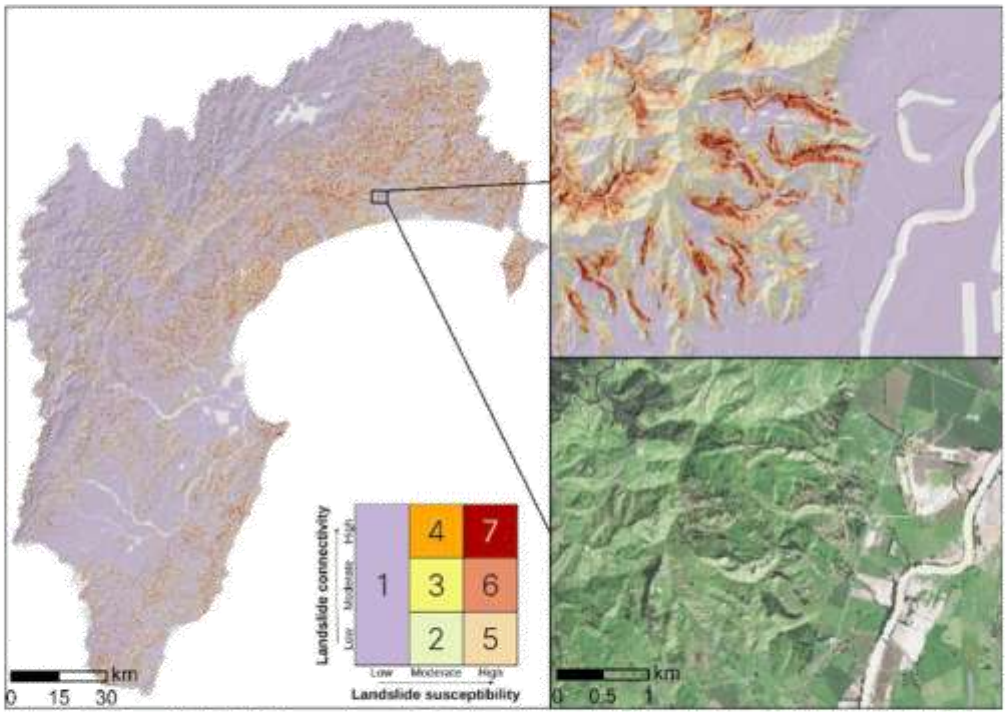

Figure 3. Spatial distribution of combined shallow landslide susceptibility and landslide-to-stream connectivity classes for the Hawke's Bay region. Class colours shown in key in main image.

Table 1. Area of land within each class (1–7) based on the combined shallow landslide susceptibility and landslide-to-stream connectivity layer for the Hawke's Bay region

Class	Area (km^2)	Area (%)
1. Low LS	11,364	72
2. Mod LS / Low Con	745	4.73
3. Mod LS / Mod Con	556	3.53
4. Mod LS / High Con	643	4.09
5. High LS / Low Con	479	3.04
6. High LS / Mod Con	377	2.39
7. High LS / High Con	539	3.42
No Data[1]	1,042	6.62
Total	**15,745**	**100**

[1] Rivers, lakes, urban and built-in areas.

5.2 Topographic wetness index (TWI)

The TWI ranged from 0–34, with a mean of 4.95 and median of 4.44 (Figure 4). Higher TWI values correspond to more saturation-prone areas. We found 99% of TWI values to lie in the range 0.9–24. The highest TWI values occurred in lowland areas, floodplains and wetlands, while the lowest occurred in upslope areas and close to ridges (Figure 5).

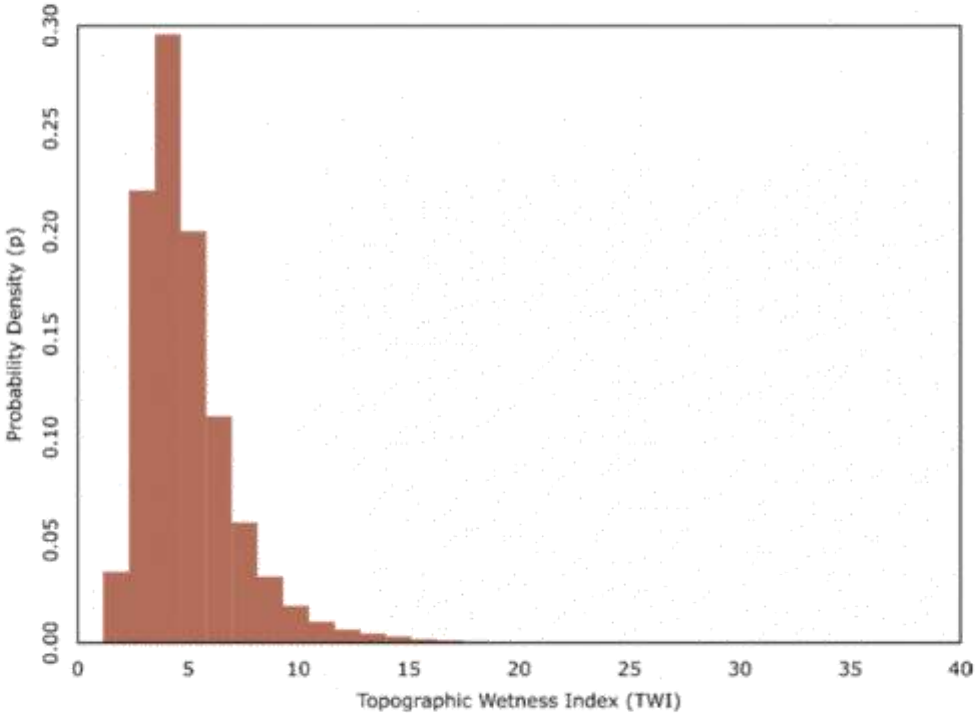

Figure 4. Probability density function of TWI values in the Hawke's Bay region.

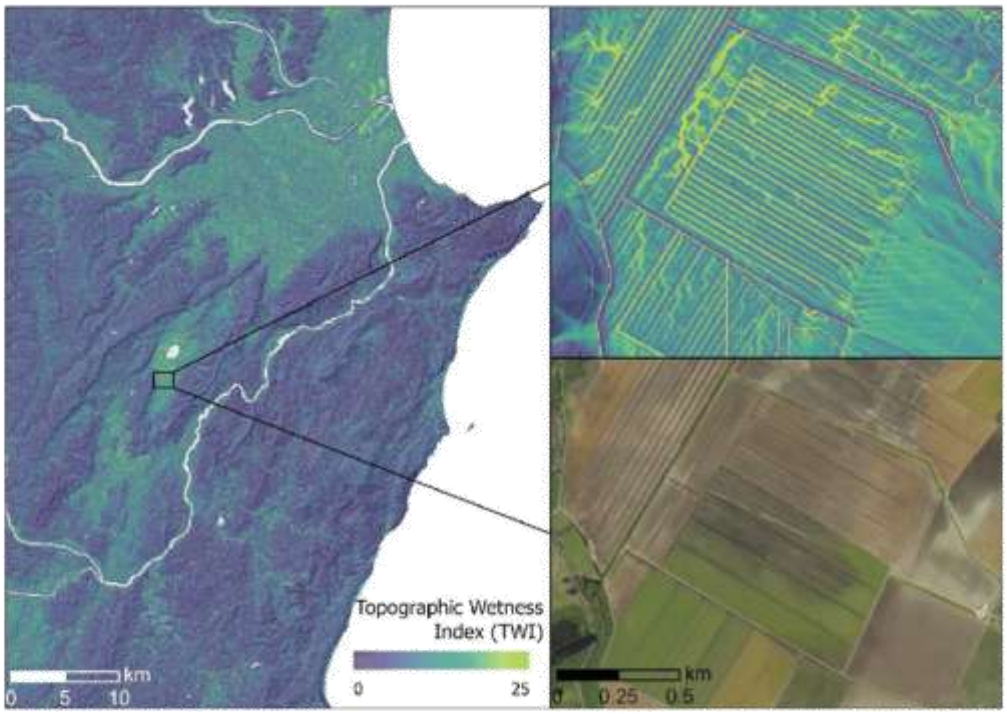

Figure 5. Overview of the TWI spatial distribution across the Hawke's Bay region.

6 Conclusions

The present report estimated rainfall-induced shallow landslide-to-stream connectivity across the Hawke's Bay region using a statistical model. Combined with previous shallow landslide susceptibility modelling, we produced a joint class-based landslide susceptibility and landslide-to-stream connectivity raster map. The statistical model used to predict connectivity performed well in cross-validation, achieving a median AUC of 0.87. The spatial pattern in connectivity classes also showed reasonable agreement with the spatial distribution of mapped stream-connected shallow landslides following Cyclone Gabrielle.

The TWI was estimated for the region using the LiDAR-derived 5 m DEM and may be used to identify critical source areas to support land and water planning.

7 Acknowledgements

We acknowledge Hawke's Bay Regional Council (HBRC) for funding this work. We specifically acknowledge and thank Ashton Eaves and Kathleen Kozyniak from HBRC for their advice and discussions leading to this work. We are grateful to GNS Science for early access to the Cyclone Gabrielle landslide inventory.

8 References

Beven KJ, Kirkby MJ 1979. A physically based, variable contributing area model of basin hydrology / Un modèle à base physique de zone d'appel variable de l'hydrologie du bassin versant. Hydrological Sciences Bulletin 24(1):43–69.

Florinsky IV 2016. Digital terrain analysis in soil science and geology. 2nd edn. London, Academic Press.

Grabs T, Seibert J, Bishop K, Laudon H 2009. Modeling spatial patterns of saturated areas: A comparison of the topographic wetness index and a dynamic distributed model. Journal of Hydrology 373(1):15–23.

Kopecký M, Macek M, Wild J 2021. Topographic wetness index calculation guidelines based on measured soil moisture and plant species composition. Science of The Total Environment 757: 143785. https://doi.org/10.1016/j.scitotenv.2020.143785

Kuhn M, Vaughan D, Hvitfeldt E 2017. yardstick: tidy characterizations of model performance. Version 1.3.1. https://doi.org/10.32614/CRAN.package.yardstick (accessed 11 September 2024).

Kuhn M, Wickham H 2018. tidymodels: easily install and load the 'tidymodels' packages. Version 1.2.0. https://doi.org/10.32614/CRAN.package.tidymodels (accessed 11 September 2024).

Leith K, McColl S, Robinson T, Massey C, Townsend D, Rosser B, Smith H, Wolter A, Jones K, Barrell D, et al. 2023. Reflections on the challenges of mapping >100,000 landslides triggered by Cyclone Gabrielle. In: Frontin-Rollet GE, Nodder SD (eds) Geoscience Society of New Zealand Annual Conference 2023: Abstracts Volume GSNZ Miscellaneous Publication 164A. Pp. 142–142.

Lindsay JB 2016. Whitebox GAT: a case study in geomorphometric analysis. Computers & Geosciences 95: 75–84.

Ministry for Primary Industries (MPI) 2017. Plantation forestry erosion susceptibility classification risk assessment for the National Environmental Standards for Plantation Forestry. Wellington, Ministry for Primary Industries.

Ministry for the Environment (MfE) 2023. Critical source areas. Guidance for intensive winter grazing. Wellington, Ministry for the Environment.

Obuchowski NA 2003. Receiver operating characteristic curves and their use in radiology. Radiology 229(1): 3–8.

Quinn P, Beven K, Chevallier P, Planchon O 1991. The prediction of hillslope flow paths for distributed hydrological modelling using digital terrain models. Hydrological Processes. 5(1): 59–79.

Riihimäki H, Kemppinen J, Kopecký M, Luoto M 2021. Topographic wetness index as a proxy for soil moisture: the importance of flow-routing algorithm and grid resolution. Water Resources Research 57(10): e2021WR029871. https://doi.org/10.1029/2021WR029871

Smith HG, Betts H 2021. Memorandum on implementing a national index for susceptibility to streambank erosion. Manaaki Whenua – Landcare Research contract report LC3998.

Smith HG, Neverman A, Betts H, Herzig A 2024. Improving understanding and management of erosion with LiDAR. Manaaki Whenua – Landcare Research Contract Report LC4466.

Smith HG, Spiekermann R, Betts H, Neverman AJ 2021. Comparing methods of landslide data acquisition and susceptibility modelling: Examples from New Zealand. Geomorphology. 381: 107660. https://doi.org/10.1016/j.geomorph.2021.107660

Spiekermann RI, Smith HG, McColl S, Burkitt L, Fuller IC 2022. Development of a morphometric connectivity model to mitigate sediment derived from storm-driven shallow landslides. Ecological Engineering. 180: 106676. https://doi.org/10.1016/j.ecoleng.2022.106676

Tsyplenkov A, Smith HG, Betts H, Neverman A 2023. Data-driven shallow landslide connectivity analysis to reduce sediment delivery to streams. In: Frontin-Rollet GE, Nodder SD (eds) Geoscience Society of New Zealand Annual Conference 2023: Abstracts Volume GSNZ Miscellaneous Publication 164A. Pp. 250–250.

Ūawa Catchment Working Group

Land Overlay 3B and Transition Advisory Group (TAG)

12 November 2024

Purpose of this paper

The purpose of this paper is to provide information on the Transition Advisory Group (TAG) formed to support transition of Land Overlay 3B (LO3B) to permanent vegetation cover.

1. Recap: Land Overlay 3B (LO3B)

Council has been focusing on identifying the worst eroding land across the region for transitioning to permanent vegetation cover. This connects directly to one of the Ministerial Inquiry into Land Use (MILU) report recommendations to identify land that carries 'extreme erosion susceptibility' (purple zone). The report argues for this land to be returned to permanent forest. If we can accurately identify these high-risk areas, gain support from our communities and work out pathways to transition, we have the potential to address a large part of our region's erosion problem. The remaining highly productive land will continue to provide valuable primary produce.

We are currently calling this spatial layer 'Land Overlay 3B', as an extension of our current land overlay framework (in the TRMP).

What we are working towards is the combination of three types of spatial information:

- Landslide susceptibility layer
- Morphometric connectivity model – an extension of the susceptibility layer
- Gully erosion layer

This combined information will form the basis of LO3B mapping.

Landslide susceptibility and morphometric connectivity

A lot of research was done in the aftermath of cyclone Gabrielle. Part of this work involved the mapping of land across the region vulnerable to landslide susceptibility. This was done by Dr Hugh Smith at Manaaki Whenua / Landcare Research. The data was made available to Council last year[1].

In December 2023, Council engaged Manaaki Whenua to develop a 'morphometric connectivity model' that aligns with the landslide susceptibility layer. The model

[1] Gisborne Morphometric Landslide Susceptibility and Connectivity

identifies the spatial probability of those landslides reaching waterways and used a LiDAR-derived Digital Elevation Model.

These spatial probabilities were aggregated into seven classes corresponding to likelihood of landslide susceptibility and likelihood of connectivity:

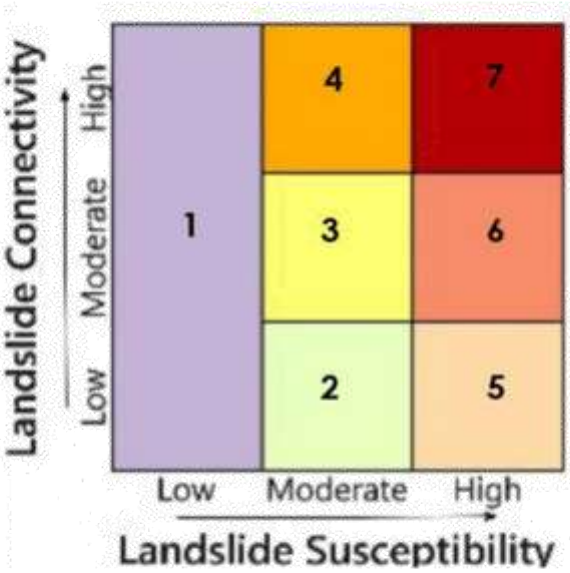

Class	Description
1	Low Landslide Susceptibility
2	Mod LS / Low Connectivity
3	Mod LS / Mod Connectivity
4	Mod LS / High Connectivity
5	High LS / Low Connectivity
6	High LS / Mod Connectivity
7	High LS / High Connectivity

The final output (combining susceptibility and connectivity) was completed in mid-March this year.

Given the model covers a range of probabilities across the region, we've been considering how to set the threshold for defining the LO3B layer. After discussion and exploring the data on GIS, we are looking to combine classes 4 and 7 as the basis for engagement.

Both carry high risk of sediment connecting to waterways and we believe this is a good way to demonstrate the critical relationship between land-use and the receiving environment.

Unsurprisingly, these two classes both tend to be found along waterways where the risk of erosion entering the receiving environment is highest.

Gully erosion layer

Gully erosion is another significant erosion type in this region. Recent research by Dr Mike Marden has indicated that the current area of hill country affected by gully erosion is only 5% less than what it was 60 years ago. That is a small reduction despite the various remediation efforts since the 1960s.

We will look to include actively eroding gullies within the LO3B layer, in addition to the shallow landslide and connectivity layer.

Currently Dr Marden is working with MPI to develop an updated gully erosion GIS database for the region.

2. Transition Advisory Group (TAG)

In August 2024, Council formed a Transition Advisory Group (TAG) to consider options and tools for on-the-ground implementation to transition Land Overlay 3B (LO3B) land out of existing land use and into permanent vegetation cover.

The purpose of the Transition Advisory Group (TAG) is for members with local expertise and knowledge to inform and assist Council in identifying options for transition land identified as LO3B from existing land uses to a permanent vegetative cover.

The TAG consists of members from a range of diverse background:

- Tangata whenua
- Forestry interests
- Pastoral farming interests
- Indigenous vegetation expertise
- Community interests
- Council staff

The TAG meets monthly, with the first meeting held in August 2024. The TAG is scheduled to wrap up in April 2025.

Key output – Transition guide

Members are tasked to contribute their expertise and knowledge to develop a transition guide. This document will outline site-specific steps for transition and includes scenarios and case studies across Tairāwhiti and other parts of Aotearoa that align with our region's geology and/or landscape.

The aim of the transition guide is to provide landowners, farmers and foresters the best, site-specific guidance they need to help reduce soil erosion and improve water quality, which in turn will enhance land, aquatic and marine biodiversity.

The draft transition guide is expected to be distributed more widely for comments and feedback once a draft document is completed. A draft table of contents is provided in **Appendix 1** of this paper.

3. Next Steps

Gaining community-wide support for change

Beyond the TAG, Council will socialise LO3B and the Transition guidance document with the wider community. The strength of transition will be in widespread support for the idea in principle and commitment from landowners to implement on-the-ground actions. Staff will look to broaden the conversation in 2025 through catchment planning as well as the review of the Tairāwhiti Resource Management Plan.

Resourcing regional transformation

A critical part of this work is to explore funding avenues and mechanisms to enable effective and comprehensive transition across the region. There are several avenues to

explore including the ETS, biodiversity credits, and the potential for cross-sector funding initiatives such as the MAHI pilot at Te Kautuku[2].

Work in this space is currently underway.

Catchment planning

LO3B is vitally connected to catchment planning. Catchments provide a more meaningful and achievable scale to deliver change. Tangata whenua, landowners and communities are closely connected within catchments and can coordinate to deliver change.

Importantly, work at this scale will be closely connected to the environmental outcomes and Long-Term Visions that our communities will set for each of the seven catchment areas of Tairāwhiti. LO3B will help to achieve the aspirations set within catchment plans by reducing sediment and slash migration, improving riparian habitat and in-stream conditions, and moderating stormwater runoff.

Council staff are exploring the potential of freshwater farm and forestry plans as a way of working with landowners to identify practical measures to implement LO3B. Part of this work involves exploring the application of a digital dashboard that can provide catchment-scale information to support transition. This kind of work is underway in the Te Arai and Waimatā catchments.

[2] https://toha.network/tekautuku

Appendix 1: Draft Table of Contents of Transition Guide

1. **Introduction**
   1.1. Scope
   1.2. Purpose
   1.3. Guide layout
2. **Chapter 1: Objectives and transition outcomes**
   2.1. The issue we are addressing
   2.2. The key things to achieve
   2.3. The intended outcome
   2.4. How TAG initiative sit in the matrix of other regulatory and non-regulatory sustainable land use programmes
3. **Chapter 2: Potential land use scenarios for transition**
   3.1. The most likely starting points – a limited typology of existing scenarios
   3.2. In each scenario includes information on how much land is contained, the future intentions or motivations of the landowners
   3.3. Images
4. **Chapter 3: Land use transition planning**
   4.1. Where available, reference industry or sector plans
   4.2. The issues and challenges associated with transitioning
5. **Chapter 4: Transition budget, resourcing and timeframes**
   5.1. Estimation of the funding, management, people resource and time needed to start and complete transition
6. **Chapter 5: Barriers to land use transition**
   6.1. Identifying and resolving challenges to undertake land use transition
7. **Chapter 6: Transition implementation**
   7.1. Putting the plan into action
8. **Chapter 7: Funding opportunities and incentives**
   8.1. The funding options or incentives currently available
   8.2. How the funding options or incentives may be operationalised or administered
9. **Appendix 1: Transition case studies**
10. **Acknowledgements**